CYCLODEXTRIN-BASED ROTAXANES: AN APPROACH TO PROTECTION OF A CHROMOPHORE

A thesis submitted to the Board of the Faculty
of Physical Sciences in partial fulfilment of the
requirements for the degree of

Doctor of Philosophy

in

The University of Oxford

by

Carol Ann Stanier

of Wolfson College, Oxford
and the Dyson Perrins Laboratory, Oxford.

January 2002.

Carol Stanier
Wolfson College

January 2002

Cyclodextrin-based rotaxanes: an approach to protection of a chromophore

A series of novel [2]rotaxanes of general formula **1** has been synthesised, exploiting the hydrophobic effect to cause binding inside α- or β-cyclodextrin cavities, and making use of Suzuki coupling to stopper the rotaxane.

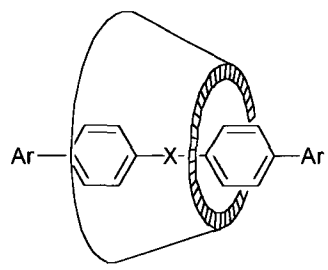

1

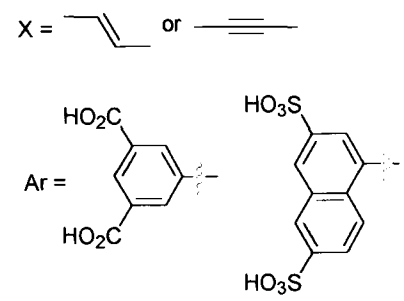

The size complementarity of the dumbbell and cyclodextrin units was investigated. The rotaxanes were characterised by use of 2D NMR techniques and, in one case, by X-ray crystallography.

The reactivity of one such rotaxane (α-cyclodextrin, stilbene core and carboxylic acid stoppered) was investigated by comparison with the corresponding dumbbell. The presence of the cyclodextrin was shown to have a protective influence towards some reactants.

The absorption and emission properties of these rotaxanes were compared. We have demonstrated an increase in the fluorescence quantum yield by up to a factor of three.

The photo-induced isomerisation of all the stilbene-based rotaxanes and dumbbells synthesised was surveyed; in one case it was found that encapsulation had completely prevented this isomerisation. A quantitative investigation of the proportions and extinction coefficients of the *trans* and *cis* isomers of one rotaxane in the photostationary state was undertaken, and the quantum yields of switching deduced. The rate of photodegradation and the ultimate products of this were investigated. The major photoproduct in both cases arose through photo-induced hydration of the stilbene double bond.

The final chapter is concerned with attempts to synthesise rotaxanes by reaction of a 1,3,5-triazine with an azo dye (**2**).

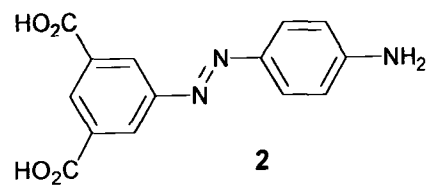

2

Related rotaxanes have been successfully prepared in the past[1-3], however in this instance the attempts did not result in significant amounts of rotaxane formation. This was rationalised by the shorter length of the dye.

The thesis as a whole illustrates the stabilisation of chromophores that is possible through the formation of rotaxanes.

[1] M. R. Craig, *Angew. Chem. Int. Ed.* 2001, *40*, 1071 - 1074.
[2] M. R. Craig, DPhil Thesis, Dyson Perrins Laboratory, University of Oxford (Oxford), 2001.
[3] S. J. Alderman, Part II Thesis, Dyson Perrins Laboratory, University of Oxford (Oxford), 2001.

Acknowledgements

I would like to take this opportunity to express my gratitude to a few people, without whom this thesis may not have been written at all, or may have been considerably less well written.

First of all, thanks must go to Dr Harry Anderson, for all his enthusiasm and patience throughout my DPhil, also to the whole Anderson group, past and present, for keeping me sane(ish). I would also like to thank Dr Aidan Lavery and Prof. Peter Gregory for agreeing to supervise my project from Avecia and Dr Clive Foster for the same and for his interest and input (and for singing worse than me).

Thanks go to all the ex-Suzuki chemists; Dr Pete Taylor (who may have escaped but will never be forgotten), Mike Hall (for proving that even cowboys can get chemistry to work), and particularly Mike O'Connell for so many things, including stealing my glassware, nicking my starting materials and making plasticine animals. Also to many other rotaxane chemists including Dr Mikey C. (for knowing everything about rotaxanes in my first year, everything about writing-up in my fourth year, and being a true friend), Dr Jonathan Buston (for not running away when I mentioned 'diazomethane' and instilling some sense into me), Mark Bass (who suffered for science even more than I did but was less stressed by it), Dr Jasper Michels (for making me look comparatively sane and for teaching me the Dutch for 'ostrich') and even the Munchkin for providing entertainment and chocolate (but not for painting the lab red).

Thank you to Dr Iain Blake for persuading me not to give up in the early days. Thanks also to James Matthews (computer expert extraordinaire) for performing surgery on my computer and enabling me to finish my DPhil by not dropping me off the climbing wall at any point. Tom Screen and Alex Krivokapic also deserve a mention for going through the final year hell at around the same time as me.

Many thanks to all the DP technical staff including Dr Robin Alpine for the super-speedy mass spectra, and Drs Tim Claridge and Barbara Odell for obtaining the necessary information from the tiniest amount of NMR samples.

Cheers also to Reb for providing the necessary northern influence and to Rach for the 'girly' chats. And a big thank you to my parents for all their support (moral, emotional and financial), despite not really understanding why this was so important to me.

Thank you to everyone who has done any proof-reading (most of you already mentioned for other things) or just listened to me stress over the past few months. Or years.

Contents

Abbreviations and Terminology used in this Thesis

Ac	acetyl
APCI	Atmospheric Pressure Chemical Ionisation
aq.	aqueous
Bu	butyl
cat.	catalytic
COSY	Correlated Spectroscopy
CPK	Corey-Pauling-Koltun (space filling models, designed to represent actual relative atom sizes)
DMF	dimethyl formamide
DMSO	dimethyl sulfoxide
EI	Electron ionisation
EPSRC	Engineering and Physical Sciences Research Council
eq.	equivalents
ESI	Electrospray
Et	ethyl
FAB	Fast atom bombardment
h	hour(s)
HSQC	Heteronuclear Single Quantum Coherence (^{1}H to heteroatom through bond correlation experiment)
LDA	lithium diisopropyl amide
MALDI-TOF	Matrix-Assisted Laser Desorption Ionisation – Time of Flight
M	mol l^{-1}
Me	methyl

mol.	moles
n-BuLi	*n*-butyl lithium
NMR	Nuclear Magnetic Resonance
NMWCO	nominal molecular weight cut-off
NOE	Nuclear Overhauser Effect
NOESY	Nuclear Overhauser Effect spectroscopy
Ph	phenyl
ROESY	rotating Overhauser Effect spectroscopy
THF	tetrahydrofuran
TLC	thin-layer chromatography
TM-α-cyclodextrin	2,3,6-tri-O-methyl α-cyclodextrin
UV/Vis	Ultraviolet/Visible Absorption
w.r.t.	with respect to
α-CD	α-cyclodextrin
β-CD	β-cyclodextrin

All stilbenes are *E* unless otherwise specified.

41⊂α-CD denotes a rotaxane comprised of dumbbell **41** encapsulated by α-cyclodextrin.

Chapter 1; Introduction to the encapsulation of chromophores

The properties of a molecule depend upon its environment. Control of the immediate environment gives rise to interesting and useful modifications of physical and chemical properties. An approach to this control is by encapsulation of the molecule as a 'guest' inside a 'host' species. Encapsulation may result from either a host-guest interaction resulting in reversible binding (binding constants usually of the order 10^3-10^4 M^{-1}) or an irreversibly bound species such as a rotaxane. A rotaxane is an encapsulated molecule, which is not covalently bonded to the macrocycle but is unable to escape, due to large stoppers at either end (see Figure 1.1). First of all, we will concentrate on how the chemical and physical properties of the guest are affected by encapsulation.

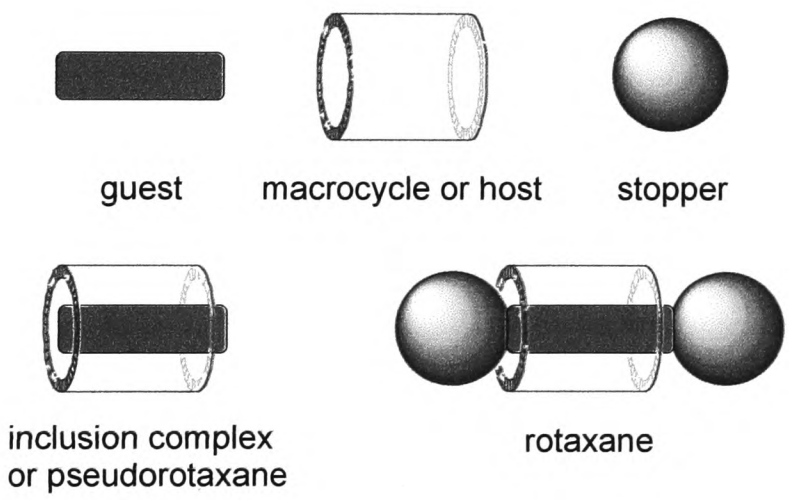

Figure 1.1. *Components of pseudorotaxanes and rotaxanes.*

The properties which will be considered here can be loosely divided into the categories of physical and chemical characteristics of the encapsulated molecule. Physical properties which can be altered by encapsulation include interaction with light (absorption and emission spectra), and magnetic fields (NMR spectra). Solubility and aggregation can also be greatly affected by encapsulation and

conformational changes can be induced or prevented. Changes in the chemical properties of the guest molecule usually result from the kinetic stabilisation of high energy states. The inter- and intramolecular reactivity can also be affected.

The reason for looking at this field is to assess why these changes in behaviour occur and how they can best be put to use. Much attention has been paid to binding and encapsulation in recent years. There has been much synthetic work to prepare varied macrocycles such as cyclodextrins[1], cyclophanes[2], linked calixarenes[3] and the more exotic, such as the 'tennis balls' of Rebek[4]. Many guests have been shown to bind inside these macrocycles, primarily in water but also in other solvents and in the solid state. These complexes have in some cases been characterised in great detail and uses for the bound complex have been suggested. This is a growing field and much work is required to fully understand the ways in which encapsulation affects the properties of molecules.

The aim of this thesis is to describe the synthesis of rotaxanes by use of cyclodextrins as the macrocycle, and to investigate the reactivity of chromophores encapsulated in these macrocycles. This includes a comparison of the physical and chemical properties of the rotaxanes with those of the unencapsulated equivalents.

1.1. Physical Properties

In the majority of published examples, the changes in physical behaviour upon encapsulation have been used merely to prove that encapsulation has occurred. This is especially true for characteristics such as NMR and UV/Vis absorption spectra.

1.1.1. NMR

NMR is probably the most powerful tool available to the synthetic organic chemist, and there has been much work published on the effects of encapsulation in this area. Many papers detail only the NMR spectrum of the encapsulated species, leaving the reader to guess at the changes which have occurred on binding. However, as might be expected, encapsulation does induce specific changes in the NMR spectrum. These consist primarily of changes in chemical shift due to an alteration in environment and changes in relaxation rate due to through space interactions (the Nuclear Overhauser effect). Protons inside an aromatic macrocycle may experience a ring current and so shift upfield, however, the presence of a ring current is not essential to enable chemical shift changes on binding to be observed. This can be seen in the work of Hamai[5] on inclusion complexes of azulene (see Figure 1.2). Some protons are more shielded than others; here the H-2 and H-6 are shifted less upfield than the others. This is taken to mean that the β-cyclodextrin sits mainly on the central part of the molecule, so that the environment for H-2 and H-6 is less changed upon encapsulation than for the other protons. The peaks in these spectra also broaden on encapsulation, this is explained by the rate of exchange between free and bound species.

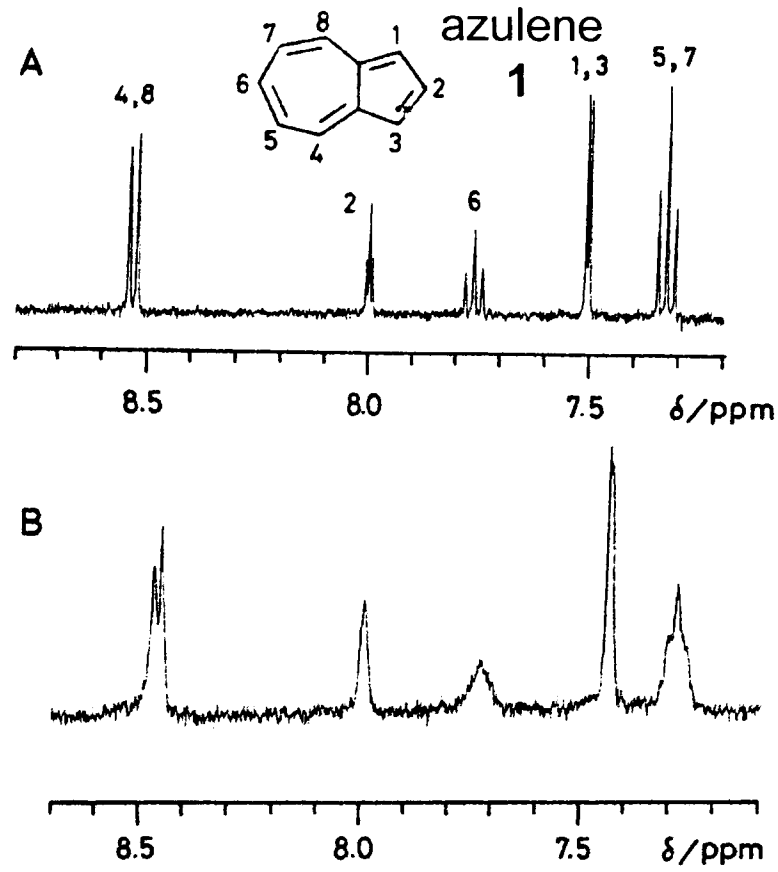

Figure 1.2.[5] *^{1}H NMR of azulene (spectrum A) in D_2O and (spectrum B) in D_2O containing 5×10^{-3} mol l^{-1} β-cyclodextrin.*

Schneider[6] also described complexation-induced shifts in the ^{1}H NMR spectrum of naphthalene derivatives. He used these to conclude which part of the guest was bound, assuming that little difference in chemical shift implies that the environment of that proton has not been greatly altered.

Hoshi's[7] work on binding of benzoic acids with β-cyclodextrin (Figure 1.3) gave a detailed insight into the magnitude of ^{13}C chemical shift change on encapsulation, as well as developing methods to calculate this.

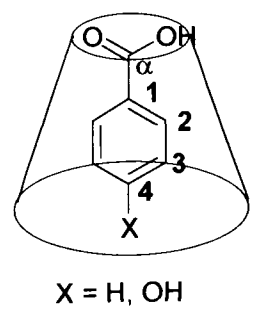

Figure 1.3. *Hoshi's encapsulation of benzoic acids.*

Table 1.1. *Change in chemical shift upon encapsulation.*

Carbon no.	ppm shift of benzoic acid on encapsulation	ppm shift of *p*-hydroxybenzoic acid on encapsulation
α	-1.7	-1.65
1	-1.18	-0.78
2	1.59	1.70
3	-0.76	-0.57
4	0.93	0.72

From the values in Table 1.1 it can be concluded that not all parts of the acid experience the same shielding effect. However, detailed assignment of the position of the macrocycle relative to its guest cannot be performed using this information alone. A useful addition to this would be details of the NOEs, such as those described by Anderson[8] for interactions between a dumbbell and macrocycle.

Another effect caused by encapsulation of a small molecule within a large macrocycle is an alteration in tumbling rates of the molecule in solution. This may affect the sign and magnitude of observed NOEs and relaxation times.

The majority of differences in NMR spectra on encapsulation are easily explained, although prediction of these phenomena is somewhat less facile. Changes in the environment of an atom, whether they are solvation changes or conformational ones induced by the macrocycle upon the guest, may affect the NMR spectrum. However in cases such as these, where there are no covalent bonds between host and guest, often the only way to ascertain reliably the relative orientations of the molecules is

by use of NOEs. This is especially important where one or both of the components is asymmetrical.

1.1.2. Absorption properties

The UV/Vis absorption spectrum is a useful method of deciding whether or not binding or encapsulation has occurred. This is due to the large changes which can be seen in some cases. These changes are probably due to differences in the solvation environment of the chromophore, as well as to extended lifetime of the excited state. Newkome and Moorefield[9] have recently reported a visible change in the colour of phenolphthalein (**2** and **3**)(Scheme 1.1) upon binding of this dye by a dendrimer based on β-cyclodextrin.

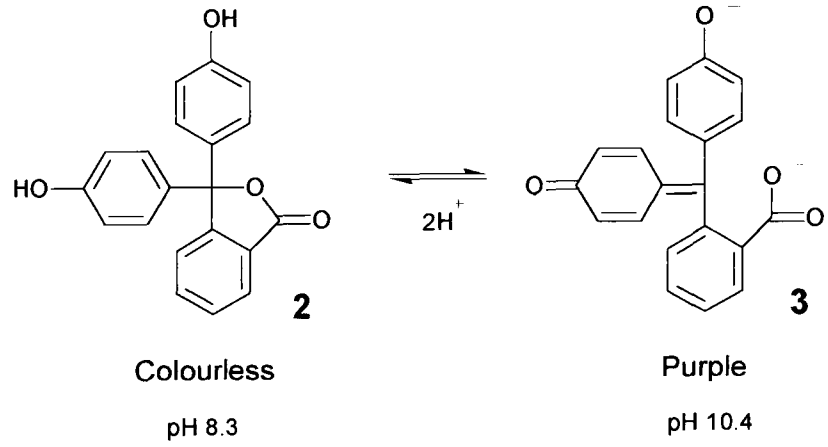

Scheme 1.1. *Phenolphthalein.*

Phenolphthalein (**2** and **3**) is normally used as an indicator due to this dramatic colour change on deprotonation. However, it is claimed here to change colour from purple (equivalent to an absorbance at 552 nm) to colourless upon encapsulation by the cyclodextrin dendrimer. Displacement of the phenolphthalein with adamantanes (known to bind strongly to such receptors) caused a further change back to the purple. The authors claim that the colour change is unlikely to be due to

deprotonation within the cavity, this being a hydrophobic environment, and is simply a shift of absorption to a lower wavelength, probably as a result of the less polar environment in which the chromophore now finds itself. Such dramatic changes in absorption wavelength are however uncommon in this field, and these results are also open to other interpretations such as a change in pKa upon encapsulation or the preferential binding of only **3**, the colourless lactone.

Jung's[10] work on azo dye aggregates also shows a bathochromic shift on encapsulation by α-cyclodextrin from 380 nm to 390 nm, and 520 nm to 540 nm, respectively.

Sanchez and de Rossi[11] describe not only a hypsochromic shift of the maximum wavelength in the absorption spectrum of azobenzene derivatives on binding, but also a reduction in the molar extinction coefficient.

There are many examples of a shift in absorption on encapsulation. These changes in wavelength of absorption maxima probably result from solvation effects (solvatochromism). It is commonly known that measurement of UV/Vis spectra in less polar solvents can produce a shift of absorption to shorter wavelength; the hydrophobic environment provided by the majority of these macrocyles on encapsulation can be considered to be analogous to this.

1.1.3. Emission properties

Fluorescence properties can be altered in similar ways to UV/Vis absorption properties by encapsulation. Thus emission wavelengths can be shifted, and fluorescence yield can be increased[12] or, in rare cases, reduced. The increase in fluorescence quantum yield is likely to be a result of the protection of the excited species which can be afforded by encapsulation. Dan[13] found fluorescence

enhancement of a squaraine (**4**) when bound in a 2:1 inclusion complex with β-cyclodextrin.

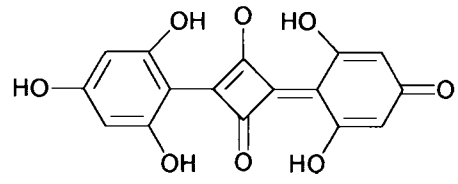

4

The emission yield was seen to increase by up to 90 times on encapsulation in water. This was attributed to a decrease in rotational freedom resulting from the binding, and also to the removal of water from the immediate environment of the fluorophore, which would normally quench fluorescence.

Bergmark's studies of coumarins[14], and Hoshino and Imamura's[15] studies of the binding of benzene derivatives by β-cyclodextrin, also lead to the conclusion that exclusion of water from the hydrophobic cavity of the host provided a great contribution to the increase in fluorescence on encapsulation; where water was included in the complex with the fluorophore (achieved by using a larger host molecule), fluorescence efficiency decreased. Exclusion of water resulted in a greater emission intensity.

An example of an increase in fluorescence efficiency that has been used as a classroom demonstration[16] is that of ANS (**5**) (aminophenylnaphthalene sulfonic acid) and hydroxypropyl-β-cyclodextrin (seen in Figure 1.4.).

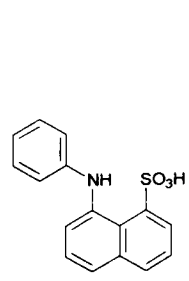

5

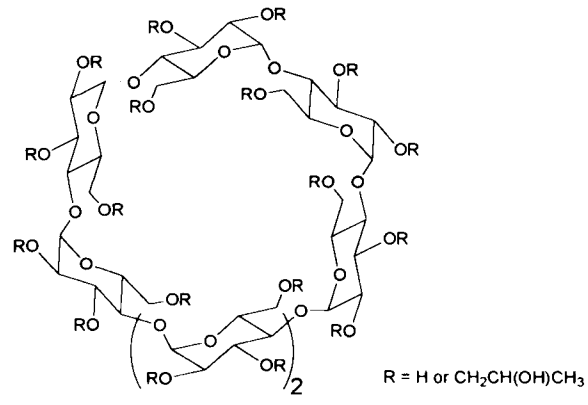

Figure 1.4. *The components for a visible demonstration of fluorescence enhancement.*

The ANS has a very low fluorescence quantum efficiency, but the huge increase in efficiency on addition of the cyclodextrin solution is clearly visible in the presence of a UV lamp. The resultant emitted light is blue shifted from the green emission of the unencapsulated ANS. This may be qualitative, but the change observed is a clearly visible one, implying that the quantitative change upon encapsulation is very large.

A more complex system is that described by Swager[17] in which the fluorescence of a chromophore is changed both in wavelength (from 396 nm to 520 nm) upon encapsulation, and in shape (loss of vibrational structure). This is attributed to exiplex formation between macrocycle and dumbbell unit. The system is depicted in Figure 1.5.

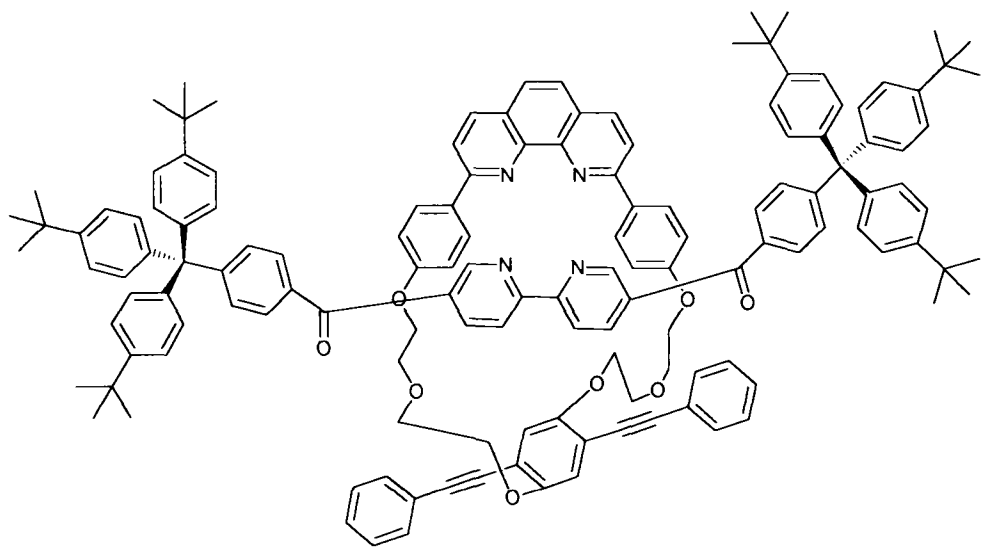

Figure 1.5. *Swager's rotaxane exiplex.*

Most papers referring to fluorescence spectra describe enhancement of fluorescence. This may be because of a protection factor; encapsulation may prevent solvent molecules or other quenchers from reaching the excited chromophore, thereby reducing the chance of non-radiative decay. Enhancement of fluorescence is, of course, also a more useful alteration to the original properties of the encapsulated molecule.

1.1.4. Solubility

Encapsulation tends to make the guest more soluble in solvents which can dissolve the host macrocycle, although this is rarely commented upon in the literature.

Anderson[8] reports that the first ever rotaxane of an azo dye is more soluble in most solvents than the free azo dye itself. Stoddart[18] also reports that the rotaxane of 4,4'-bipyridyl using dendritic stoppers and a crown ether as the macrocycle is soluble in organic solvents of relatively low polarity (purification is performed using dichloromethane and ethanol) despite the double positive charge on the central bipyridyl section. This is a potentially useful property of encapsulation which does not seem to have been greatly investigated.

1.1.5. Aggregation

Dan and Willner[19] performed a study of the effect of encapsulation on the aggregation in solution of various dyes, including thionin (**6**).

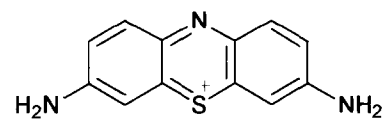

Thionin **6**

This phenomenon was followed by monitoring the UV/Vis spectrum, however the effects seen are attributable to aggregation properties as well as to direct changes in the absorption upon encapsulation.

Thionin is normally found in solution as dimers or polyaggregates, which are in equilibrium with the monomeric form. Concentration also affects the extent of aggregation, higher concentration leading to higher aggregation. The monomer of thionin is luminescent, whilst dimerisation causes intramolecular quenching of this

luminescence. The monomer also absorbs visible light at a higher wavelength than that of the dimer (598 nm and 558 nm respectively). A titration of β-cyclodextrin against the UV/Vis absorbance or fluorescence shows clearly the shift of equilibrium from the dimer to the monomer as more β-cyclodextrin is added. This can be seen in Figures 1.6 and 1.7 respectively.

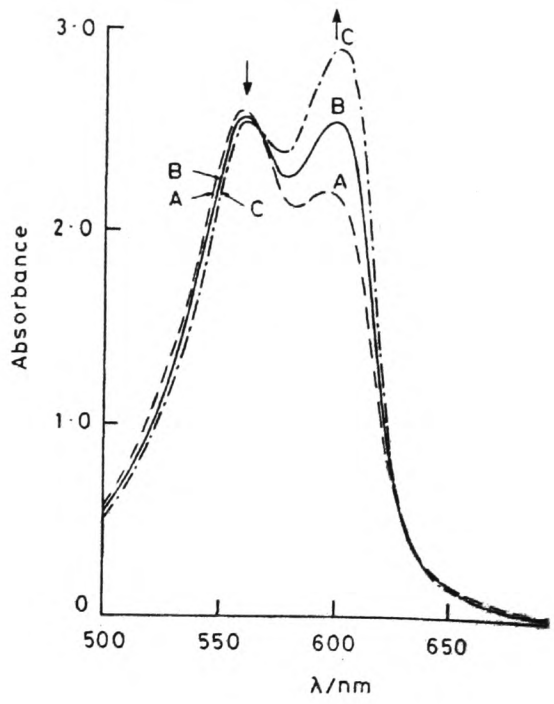

Figure 1.6[19]. *Effect of β-cyclodextrin on the aggregation of thionin (**6**), (concentration of thionin = 8.1 × 10⁻⁴ M); A, without addition of β-cyclodextrin; B, with β-cyclodextrin = 1.2 × 10⁻³ M; and C with β-cyclodextrin = 2.7 × 10⁻³ M.*

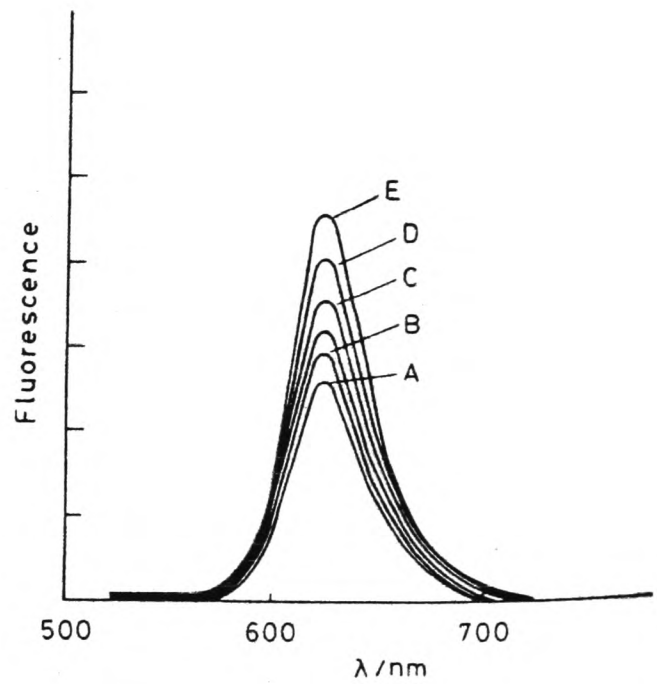

Figure 1.7[19]. *Effect of β-cyclodextrin on the emission spectrum of thionin (**6**), excitation at 595 nm, (concentration of thionin = 4.5 × 10⁻⁶ M); A, without addition of β-cyclodextrin; B, with β-cyclodextrin = 1.66 × 10⁻⁴ M; C with β-cyclodextrin = 3.1 × 10⁻⁴ M; D with β-cyclodextrin = 8.3 × 10⁻⁴ M; E with β-cyclodextrin = 1.9 × 10⁻³ M.*

Degani[20] has also shown a predomination of unaggregated dye over di-aggregate, only in the presence of β-cyclodextrin. In this case the dye employed was Rhodamine B (**7**).

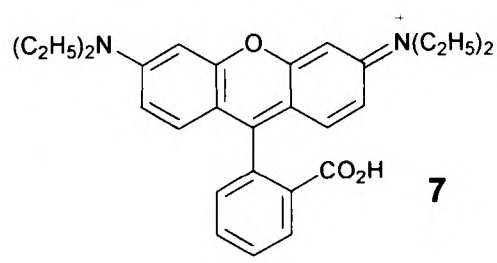

7

Encapsulation effectively removes the monomer from solution, thereby shifting the equilibrium towards the monomer. This increases the fluorescence yield substantially. The authors describe little difference between the spectra of bound and unbound monomer - this implies that this is a potentially useful way of preventing aggregation even in a concentrated solution of the dye.

In contrast to the last examples, Sato[21] saw enhanced dimerisation in studies of cyanines binding in β- or γ-cyclodextrin, probably due to the larger cavity in these macrocycles. Hirai[22] also saw formation of a 2:1 complex on encapsulation of 3 dyes, methylene blue, methyl orange and crystal violet with γ-cyclodextrin. However in this case the dimerisation enhanced, rather than quenched, the fluorescence.

Jung and co-authors[10] have synthesised and characterised a system designed to drastically increase the aggregation present in the system. This is portrayed in Scheme 1.2.

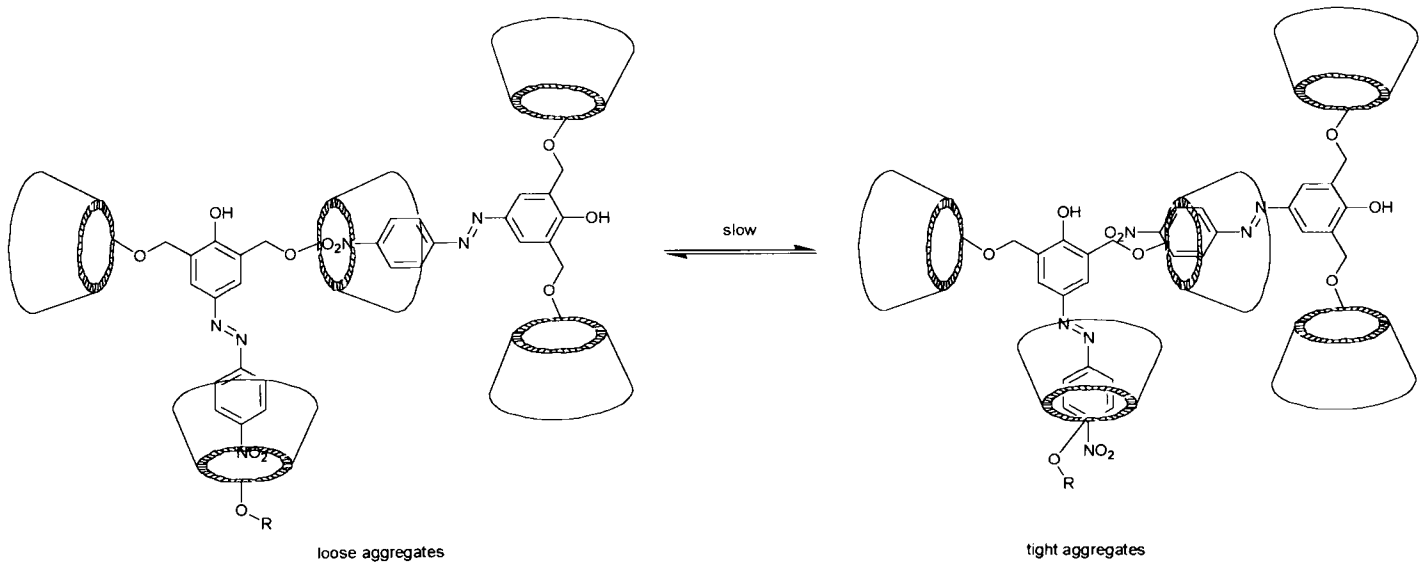

Scheme 1.2. *Jung's azo-based aggregate system.*

This is an example of supramolecular self assembly induced by the binding properties of a small part of the assembly.

1.1.6. Conformation

Takeshita[23] has shown that the *antiparallel* : *parallel* ratio of **8** to **9** is considerably increased upon addition to a solution of β- or γ-cyclodextrin. The ratio, which is normally 64 : 36 *antiparallel* : *parallel*, is raised linearly with addition of the macrocycles to give a maximum of just under 90 % *antiparallel* with β-cyclodextrin and just below 80 % with γ-cyclodextrin. This is explained by the formation of a complex of **8** and **9** with the cyclodextrin which encourages formation of the *antiparallel* conformer. This can then react upon irradiation to give a closed ring. The system is shown in Scheme 1.3.

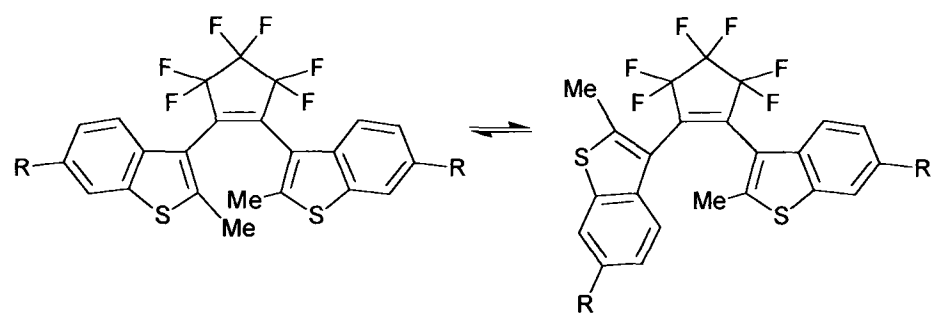

Antiparallel **8** ⇌ Parallel **9**

Scheme 1.3. *Parallel and anti-parallel conformers used in the work of Takeshita.*

The authors irradiated the mixtures at 313 nm and measured the relative quantum yields of cyclised product. These are presented in Table 1.2.

Table 1.2. *Quantum yields of cyclisation reaction with different host molecules.*

Species present in solution	Quantum yield of reaction on irradiation
8 / **9**	0.38
8 / **9** + α-cyclodextrin	0.37
8 / **9** + β-cyclodextrin	0.58
8 / **9** + γ-cyclodextrin	0.53

The lack of change upon addition of α-cyclodextrin proves that the observed alteration is due to encapsulation; α-cyclodextrin is too small to encapsulate **8** or **9** and thus no preferential formation of the *antiparallel* conformer is seen.

Another example of the stabilisation of one conformer over another by encapsulation is seen in the work of Sueishi and Nishimura[24]. Here the effect of cyclodextrins upon the thermal isomerisation of spiropyrans is investigated.

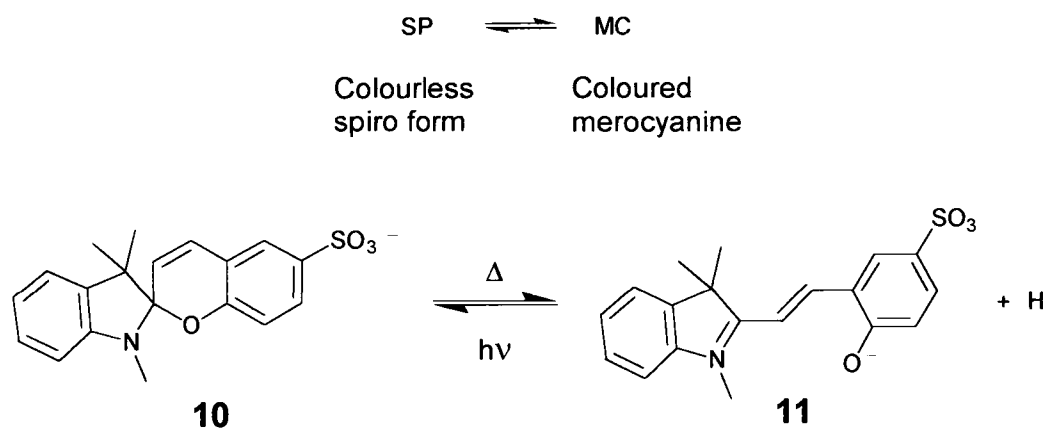

Scheme 1.4. *Isomerisation of spiropyran to merocyanine.*

As β-cyclodextrin is added to a solution in water of the spiropyran-merocyanine shown in Scheme 1.4, the spiropyran form (**10**) is stabilised, thus driving the equilibrium fully over to this form. This can be seen in the absorption spectrum of the solution.

1.2. Chemical properties

There are probably less examples of the change in chemical behaviour of a molecule on encapsulation than those demonstrating physical changes. This is due to the relative youth of this area of research. Most examples of chemical difference after encapsulation are an indirect result of a change in the physical properties such as the

solvation or available space. Also discussed here are several less general observations, in which each example needs to be considered carefully.

1.2.1. Reactivity of functional groups

Ohara[25] and Chênevert[26] investigated the effects of encapsulation upon the Fries rearrangement of phenoxy esters (Scheme 1.5).

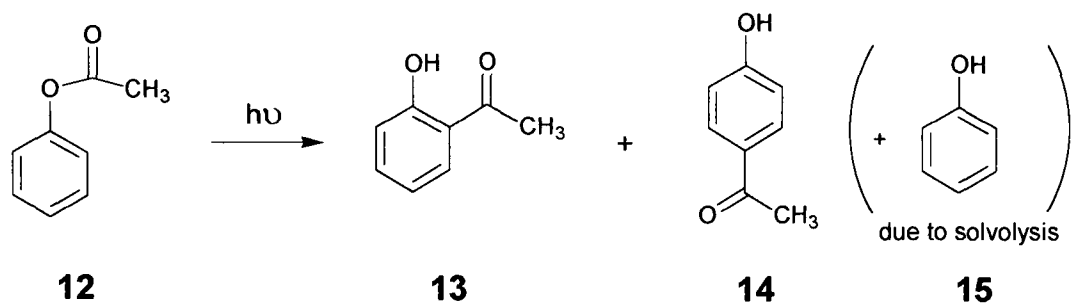

Scheme 1.5. *Fries rearrangement of benzyl esters inside β-cyclodextrin.*

The light-induced reaction is understood to proceed *via* an intra-molecular mechanism[27, 28], although the Lewis acid catalysed alternative may be partially inter-molecular. Irradiation in the presence of β-cyclodextrin resulted in a changed *ortho* : *para* ratio (see Table 1.3).

Table 1.3. *Ratio[§] of products on irradiation in the presence of different cyclodextrins.*

In aqueous solution	% conversion	% *ortho* **13**	% *para* **14**	% phenol **15**	*para* : *ortho* ratio
12	12.0	25.7	25.7	48.6	1 : 1
12 + glucose	25.2	32.4	32.6	35.0	1 : 1
12 + β-cyclodextrin	41.0	11.2	69.0	19.8	6.2 : 1

[§] All ratios determined on the crude reaction mixture by GC analysis.

Chênevert suggested that this is due to the formation of an inclusion complex. Although there is clearly some form of catalysis by the sugar units as shown by the enhanced conversion in the presence of glucose, this cannot fully explain the results seen. Evidently the presence of β-cyclodextrin favours the formation of the *para* over the *ortho* product. This could be due to the available space within the host cavity. It is possible that the hydrophobicity or polarity of the medium (in this case the host cavity) is also an important factor, as solvent polarity can often have a marked effect upon product distribution where rearrangement occurs or unstable intermediates are generated.

A good example of work in which reactivity of an encapsulated molecule is hindered by the host is that of Vögtle[29], in which a cyclophane considerably slows the reaction of an encapsulated rod-like guest (in this case the guest is non-covalently bound into the macrocycle in the form of a rotaxane, **16**) towards such

reagents as bromine, hydrogen and triethylamine. The reactions are summarised in Scheme 1.6.

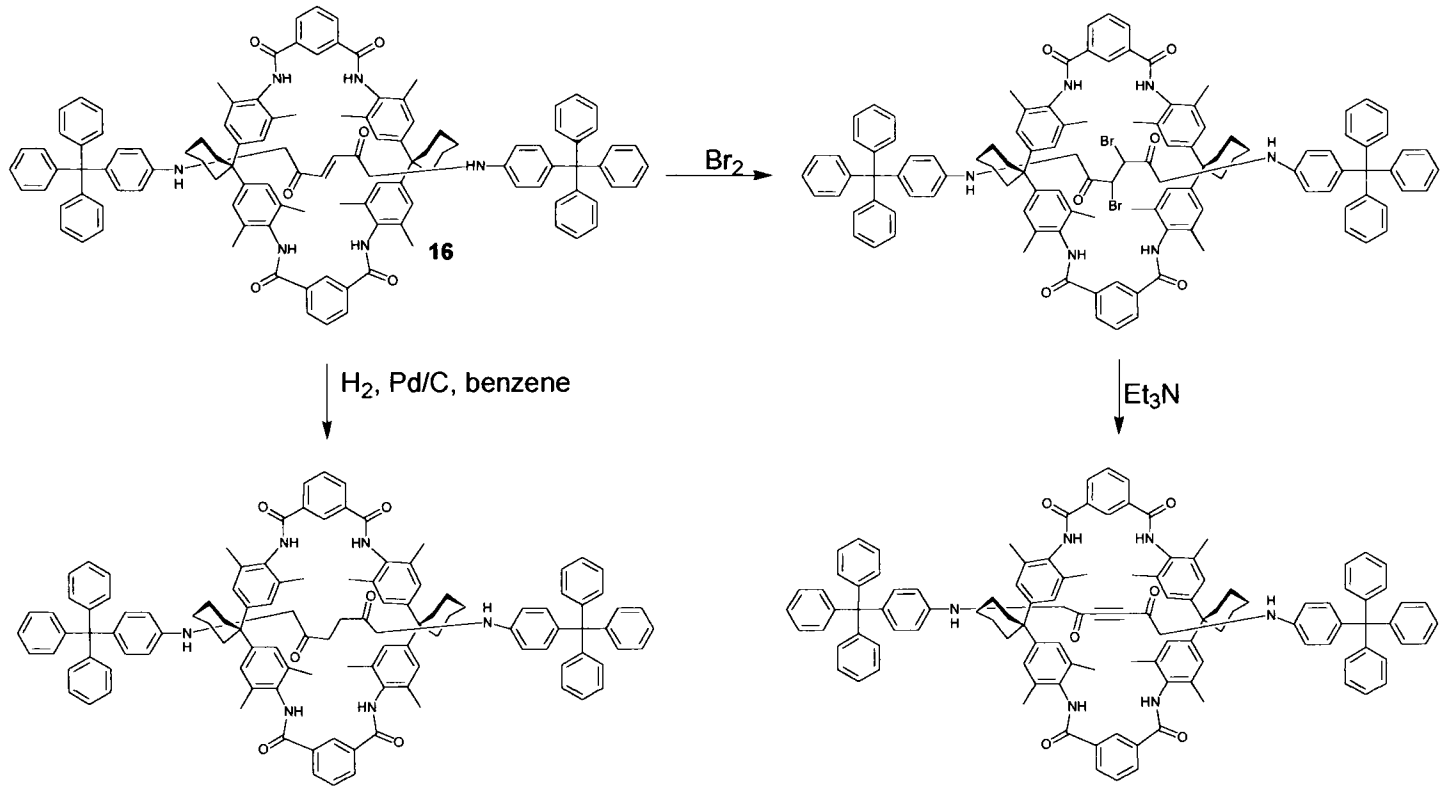

Scheme 1.6. *Vögtle's work[29] on the reactivity of a non-covalently bound 'axle'.*

However, the reactivity of **16** is not completely prevented by encapsulation; the cyclophane clearly does not provide enough steric bulk to exclude the possibility of reactive encounters. For example, in the hydrogenation reaction, the rate is slowed by a factor of up to seven, depending on the exact dumbbell unit used.

This example does demonstrate that use of a host species may significantly protect the encapsulated molecule from external reactive agents. Previous work in Oxford[30, 31] has also investigated the slowing of reaction rate by rotaxane formation.

The reactivity of a molecule can be changed in different ways by encapsulation. It is possible to raise the reactivity towards intramolecular reactions and towards other reactive species.

A good example of how an encapsulated molecule can be made more reactive towards other reactants is shown in the work of Rebek[4, 32, 33]. These papers describe

a 'tennis ball' shaped cavity which has been shown to be employable as a 'miniature reaction chamber'. Other suggested uses include a potential for use as a drug delivery system. The 'tennis ball' is formed from two components held together by hydrogen bonding.

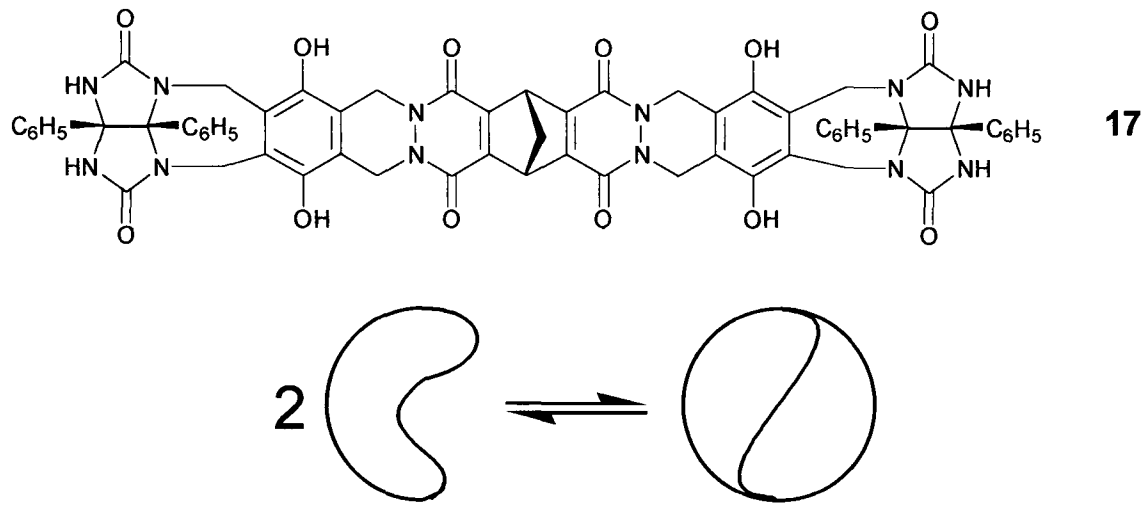

17

Figure 1.8. *Rebek's 'tennis ball' capsule.*

This molecular capsule (**17**) can considerably increase the rate of Diels-Alder reaction between benzoquinone (**18**) and 1,3-cyclohexadiene (**19**), shown in Scheme 1.7.

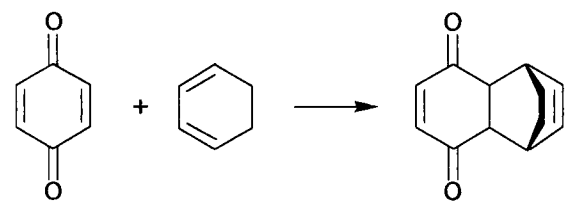

18 **19** **20**

Scheme 1.7. *The Diels-Alder reaction enhanced by encapsulation.*

The rate of reaction is raised from a half-life of 2 days by over two orders of magnitude for reactants at a molar concentration, however, this is not a catalytic reaction. Once formed, the Diels-Alder adduct **20** is unable to leave the hydrophobic cavity in which it was formed. Indeed, the adduct itself is also readily encapsulated once added to a solution of 'tennis ball' **17**. NMR signals show that reaction occurs

once encapsulated. This implies some mediation of the reaction as the transition state must also be encapsulated successfully. Addition of other good guests for this system also slows the reaction rate back to that of the original unencapsulated reaction. The authors attribute this rate enhancement mainly to the much higher effective molarity of diene (**19**) to dienophile (**18**) once encapsulated and estimate this to be about 2.4 M.

An oft-quoted example of how encapsulation can make a reactive species much less reactive towards other molecules is Cram's work on the 'taming' of cyclobutadiene[32].

Cram used carcerands to encapsulate many reactive species. The resulting host-guest complex is called a carceplex, such as that shown in Figure 1.9.

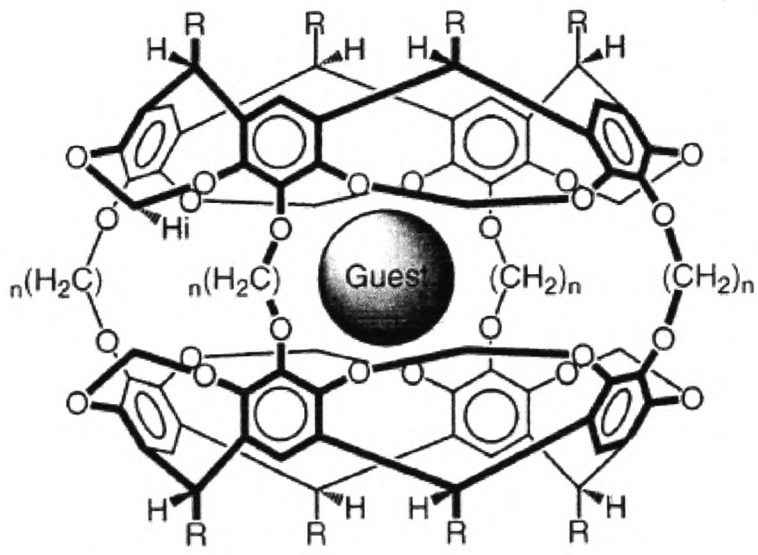

Figure 1.9[32, 34]. *Cram's carceplex*

Carcerands such as this may be used to bind the δ-lactone (**21**).

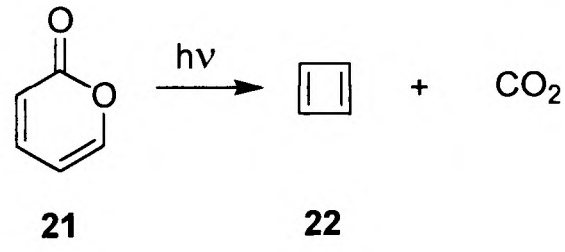

21 **22**

Scheme 1.8. *Encapsulated reaction to 'tame' cyclobutadiene.*

The δ-lactone **21** reacts as depicted in Scheme 1.8. On irradiation, carbon dioxide is lost to form cyclobutadiene[3], **22**. The carbon dioxide is small enough to pass through gaps in the macrocycle, however the reactive diene cannot escape and cannot react with the inside of the calixarene cavity. The macrocycle protects the guest from dimerisation or addition of other reactive molecules to such an extent that NMR shows the complex to be stable for over two weeks in the solid state and over 24 hours in solution.

The same carceplex has also been used to protect dibromomethane from *n*-butyl lithium in solution[34]. A 0.5 mM solution of the carceplex formed with CH_2Br_2 and the carcerand in dry THF was mixed with 300 equivalents of *n*-BuLi at 25 °C, however no reaction occurred. This shows once again that encapsulation has prevented a reaction which would have occurred rapidly if there had been no encapsulation.

Another example of the use of carceplexes for a variety of chemistry is the work of Warmuth[35] on the stabilisation of benzyne (**23**). Benzyne was formed *in situ* as shown in Scheme 1.9.

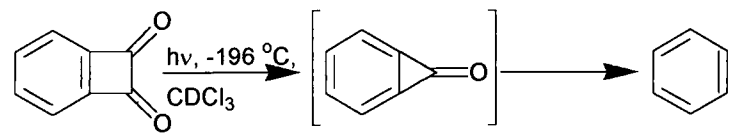

23

Scheme 1.9. *Formation of benzyne from a precursor.*

Once formed, the benzyne was stable for a short time at low temperature (between -196 °C and -75 °C) in deuterochloroform, long enough for a ^{1}H NMR spectrum of benzyne to be obtained.

Work in this field by Mock[36] has produced rotaxanes *via* a reaction which is accelerated by inclusion.

There have also been various literature examples of occasions on which encapsulation can enhance the rate of an intramolecular reaction. Some of the best examples of this come from the field of enzyme mimics, in which molecules such as modified cyclodextrins are utilised to bind and simultaneously catalyse a reaction such as the hydrolysis of an ester. However, this is a whole field of study in itself, and as such this review cannot begin to encompass the vast body of literature on this topic. One classic example is that of Breslow's artificial enzyme[37], portrayed in Figure 1.10.

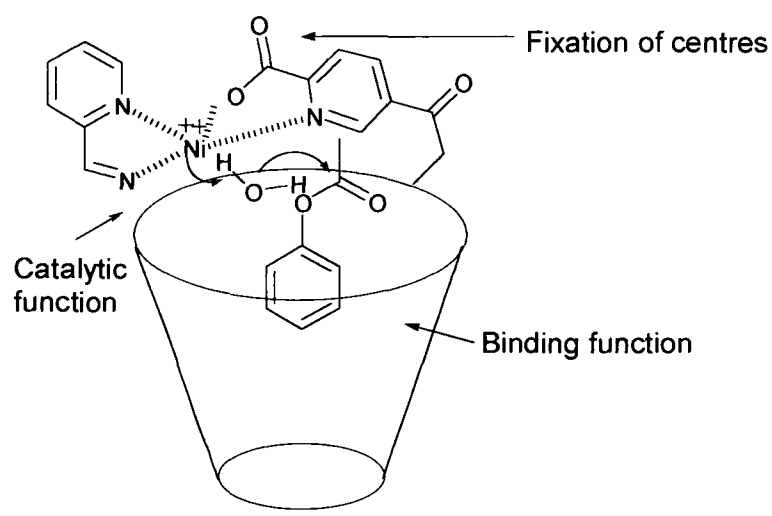

Figure 1.10. *Breslow's artificial enzyme, exhibiting binding and catalytic qualities.*

Here the cyclodextrin macrocycle binds the aromatic ester, while a catalytic side-arm acts upon the bound molecule to enhance the reaction rate.

The previously described work of Takeshita[23] on photocyclisation also gives an example of increased reactivity towards an intramolecular reaction. When the mixture of *antiparallel* and *parallel* conformers (**8** and **9**) was irradiated, the results show clear preference for a specific reaction as a result of encapsulation.

1.2.2. *Cis*⇆*trans* isomerisation

A specific reaction which has received much attention in this field of supramolecular chemistry is the *cis*⇆*trans* isomerisation of a double bond.

Such photochemistry is often monitored by observation of the UV spectrum. A well studied example of this is the photoisomerisation of *trans*→*cis*-azobenzene, shown in Scheme 1.10.

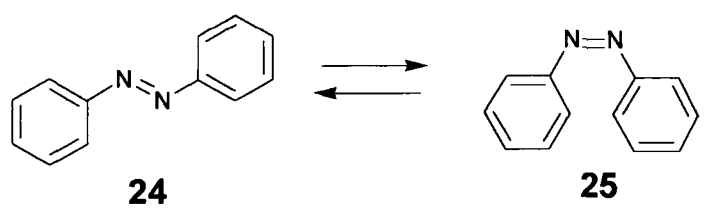

24 **25**

Scheme 1.10. *Trans*⇆*cis isomerisation of azobenzene.*

Addition of α- or β-cyclodextrin has no effect on the UV spectrum of *cis*-azobenzene[38]. The authors attribute this to the fact that, for steric reasons, *cis*-azobenzene (**25**) cannot form a host-guest complex with these macrocycles. However, *trans*-azobenzene (**24**) can be encapsulated within both α- and β-cyclodextrin, red shifting the n→π* and π→π* bands. Inhibition of the *trans*→*cis* isomerisation is also seen on irradiation in the presence of both these cyclodextrins.

Sanchez and de Rossi[11] performed a more detailed study of this subject area, using a variety of azobenzene derivatives. They found that thermal isomerisation was inhibited by presence of β-cyclodextrin. This was attributed to formation of an inclusion complex which hindered rotation of the double bond; the volume required for rotation to *cis*-azobenzene not being attainable within the cyclodextrin cavity.

A related system is that of Fujimoto[39], shown in Scheme 1.11. Here, the azobenzene is actually linked to a cyclodextrin unit.

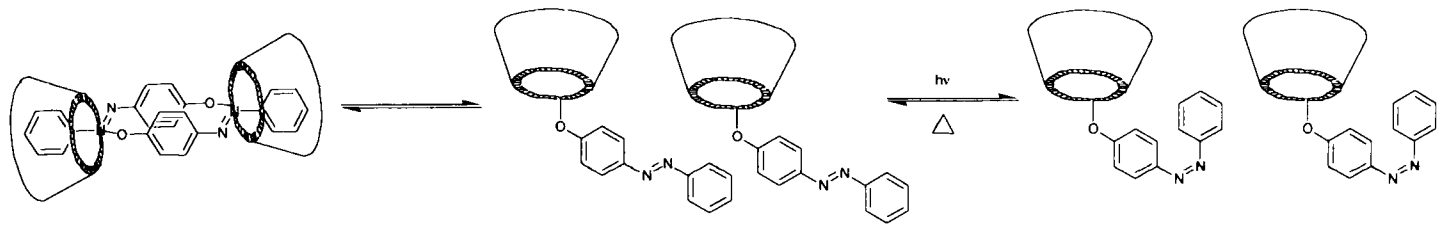

Scheme 1.11. *Fujimoto's[39] photo-switchable 'Janus' rotaxane.*

The azobenzene-cyclodextrin unit forms a dimer only when the azobenzene is in the *trans* form. Stoddart[40] has also exploited the fact that isomerisation of an azobenzene unit changes the shape completely and so may switch binding properties on and off; this work is shown in Scheme 1.12.

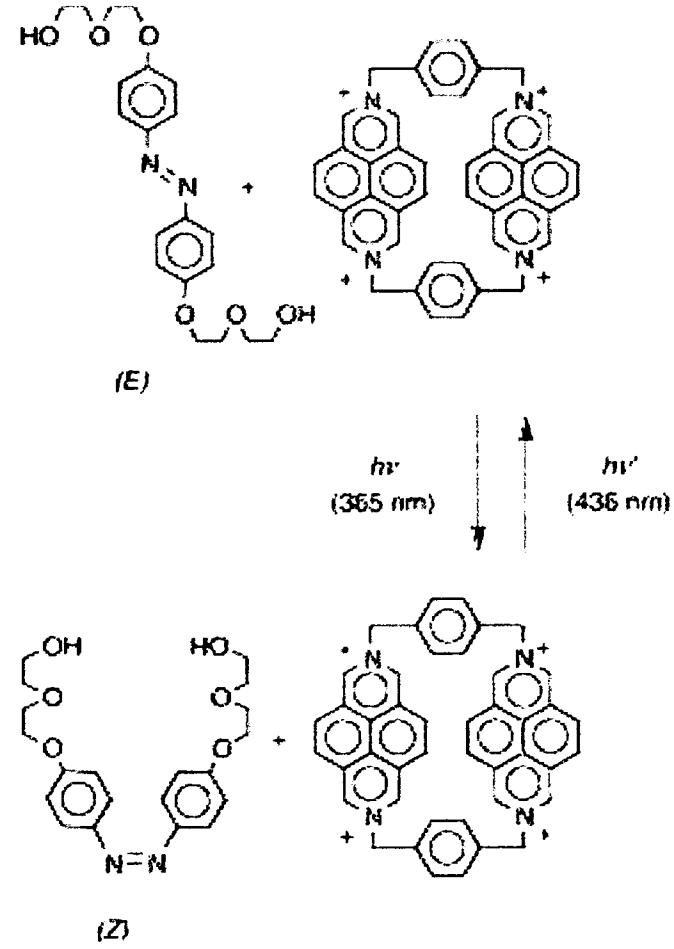

Scheme 1.12[40]. *Stoddart's switchable binding of an azobenzene unit.*

Nakashima[41] also designed a switchable azobenzene-based pseudorotaxane with α-cyclodextrin as the macrocycle. Work in Oxford has proven that this idea is transferable to other systems[42]. Such a structural motif is becoming common in the

new field of molecular switches and many believe that it shows much promise for the construction of molecular machines.

1.2.3. Other photochemistry of stilbenes

Stilbene, like azobenzene, also has a rich photochemistry. It is a similarly suitable shape for binding within cavities and for the formation of rotaxanes, but has only recently been employed for these purposes.

Wenz[43] has investigated the supramolecular control of this photochemistry by inclusion in α-, β-, and γ-cyclodextrins. He found that dimerisation, *cis*⇆*trans* isomerisation or phenanthrene formation can be tuned, depending on which size of cavity is employed. A similar study was carried out by Pitchumani and Srinivasan[44] on styrylpyridines. Kim[45] has enhanced the photodimerisation of a stilbene derivative by inclusion in a cucurbitril cavity.

Wenz[46] has also taken advantage of this property of stilbenes to form and stopper his polyrotaxane using both β- and γ-cyclodextrin. This is depicted in Scheme 1.13.

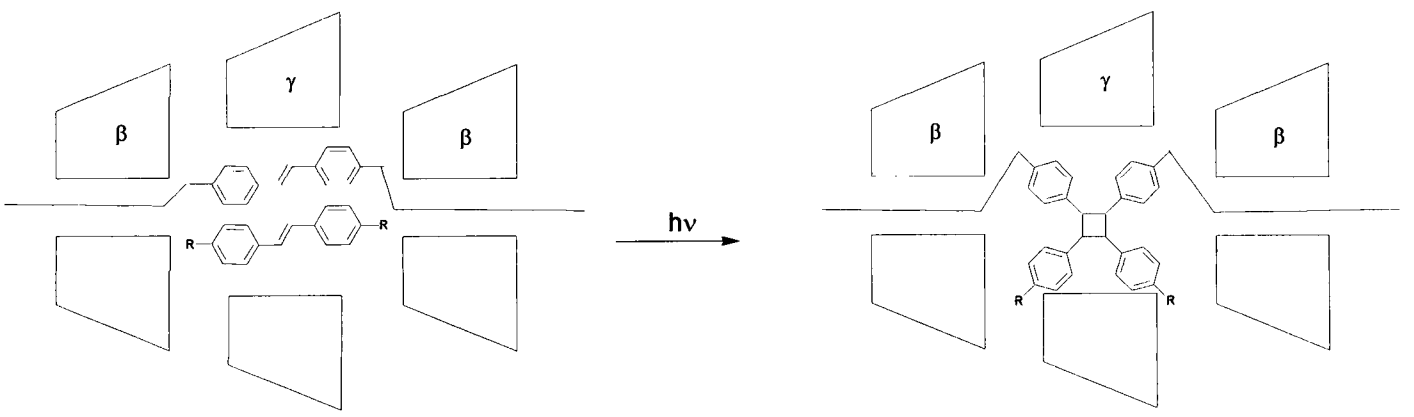

Scheme 1.13. *Photochemical synthesis of Wenz's polyrotaxane.*

The dimer is formed inside γ-cyclodextrin by irradiation, but is too large to pass through β-cyclodextrin once this reaction has occurred; the polymer is therefore trapped inside the chain of cyclodextrins.

More recently, Stoddart[47] has also used this approach to form polyrotaxanes.

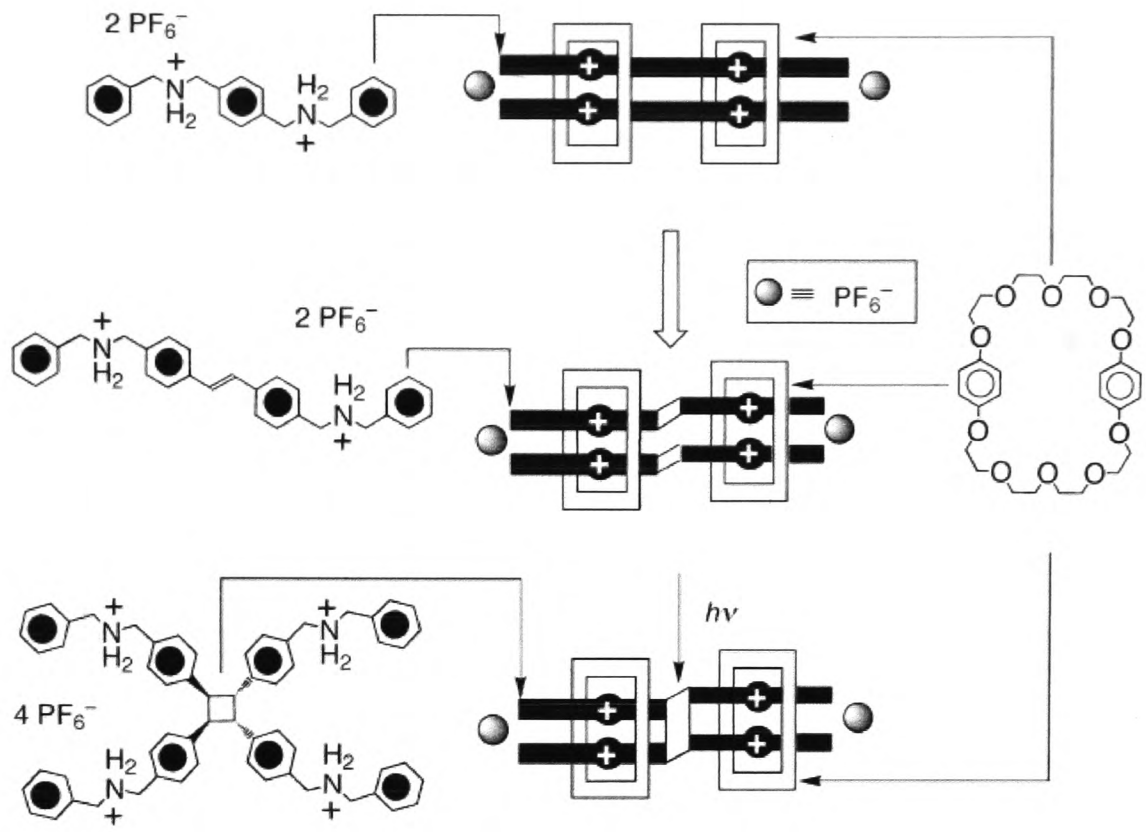

Scheme 1.14. *Stoddart's dimerised stilbene, forming a polyrotaxane.*

The authors claim that the cyclobutane formed in this dimerisation (shown in Scheme 1.14) is stereochemically pure, a feature of the controlling influence of the crown ether macrocycle.

1.3. Methods of encapsulation

As already shown in the previous examples, there are several ways of achieving encapsulation of a guest compound. The simplest approach is a straightforward complexation process which results in an equilibrium of encapsulated and free guest molecule. Many of the examples used to describe changes in properties come under this category. A disadvantage of this method is the fact that the guest molecule is not permanently bound within the host, and thus it is not always clear if these changes are effected exclusively by the encapsulation process. The reversibility may, however, be regarded as advantageous in some circumstances. Changes in

environment such as solvent or temperature may cause a higher degree of unthreading in such complexes.

Another route to encapsulated guest molecules is employed by Cram[34] in the synthesis of his 'cage' molecules (carceplexes). This approach is most effective, as all the bound species is held permanently within the cage. It cannot escape without destruction of the carceplex cage. This approach is perhaps best employed when the guest molecule involved is highly reactive, such as the examples performed with benzyne and cyclobutadiene as the encapsulated species. In such cases, the protective ability of the carceplex is exploited to its full potential, in order to study otherwise unstable compounds. However, this approach is not so useful if we want to make use of the altered properties of the encapsulated compound; the complete protection from the outside environment also means that very little chemistry may be performed upon the guest molecule. Such guests are, on the whole, quite small molecules which may limit their usefulness. In order to be able to make use of this enhancement of properties in materials, it is desirable to produce a species which incorporates both a high degree of protection from the external environment and the potential to exploit the modified reactivity to synthesise new compounds with interesting chemical and physical properties. Rotaxane formation may fulfil this potential.

1.4. Rotaxane synthesis

There are three approaches to the synthesis of rotaxanes documented in the literature; these are depicted in Scheme 1.15.

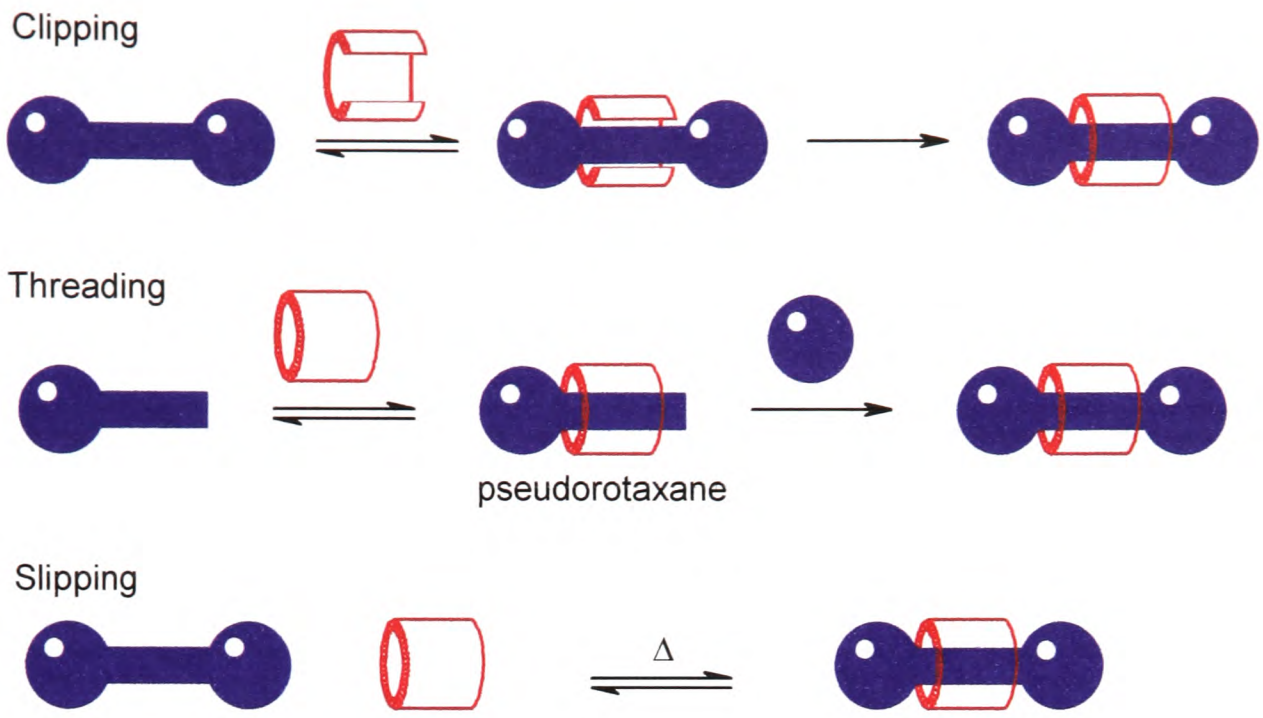

Scheme 1.15. *Methods of rotaxane synthesis*

Clipping is the route in which the dumbbell is synthesised completely, and the macrocycle is then cyclised around the dumbbell unit. This method has been exploited by Stoddart[48]. Slipping is another route in which the dumbbell is first prepared and then subsequently transformed into a rotaxane, in this case by forcing it through a macrocycle, often at high temperature and/or pressure. This has been utilised by Stoddart[49] and Vögtle[50]. The disadvantage of slipping as a route to rotaxane formation is that the reverse reaction may occur when the rotaxane is subjected to the slipping conditions, resulting in unthreading.

Threading is probably the most widely used method of rotaxane formation. This may be due to the fact that it requires less specialised functionalities than the clipping or slipping methods, which both necessitate certain structural motifs in their components. Threading is a much more general technique which can be used in conjunction with any method of achieving encapsulation within the macrocycle, and templating effects *via* hydrogen bonds, ionic interactions and other non-covalent

bonds. Examples of these templated rotaxane formations can be seen in Stoddart's work[51], as well as that of Vögtle[52], Leigh[53] and Sauvage[54].

1.5. Hydrophobic Effects

We chose the hydrophobic effect as our method of rotaxane formation as it allows a wider range of core molecules to be utilised; most organic molecules have some degree of hydrophobicity and this should allow us to tailor the core of the rotaxane to show a difference in physical as well as chemical properties on rotaxane formation. For this reason, we also aimed to synthesise the corresponding dumbbells without the macrocycle, to enable comparisons to be drawn effectively.

The hydrophobic effect[55, 56] is largely understood to be of entropic origin, although it is probable that some enthalpic effects are also grouped under this heading. Water in a nonpolar cavity has less mobility and therefore a lower degree of entropy to that in bulk solution. The organic surfaces of the host and guest molecules will be more polarisable than water and thus organic-organic interactions will result in more favourable Van der Waals contributions than organic-water ones. Release of water by binding an organic guest therefore increases the entropy of the water and improves the enthalpic situation. There is some controversy as to the exact causes of this so-called hydrophobic effect, which will not be discussed further in this work. We are concerned not with the causes of the effect so much as with the results thereof.

The hydrophobic effect causes apolar molecules to aggregate when dissolved in water. This causes, for example, proteins to fold and non-polar guests to bind inside non-polar hosts. The effect is at its strongest in water (hence the name) but may be

observed to a lesser extent in less polar solvents as well. There is no element of recognition to such binding, except the hydrophobicity of guest and host.

Pseudorotaxanes and pseudopolyrotaxanes have been made by use of this effect previously[57, 58], but here we are concerned with the production of stoppered, discrete rotaxanes *via* this method.

1.6. Cyclodextrins

Cyclodextrins are a good choice of macrocycle for this purpose as they have hydrophilic exteriors but the cavity is hydrophobic. They are commercially available and many inclusion complexes of cyclodextrins have already been documented[5, 11, 20, 59, 60]. Cyclodextrins containing six, seven or eight glucose units are available, enabling the cavity size to be tuned to the guest used, and this symmetry also facilitates characterisation, for example, by NMR. The different sizes of macrocycle are outlined in Figure 1.11.

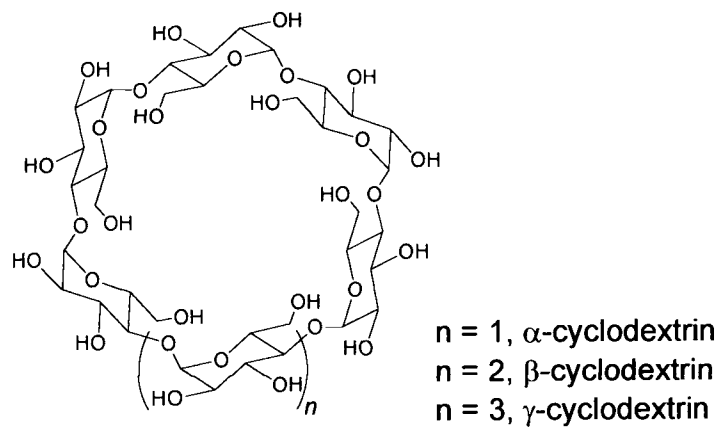

Figure 1.11. *The general structure of cyclodextrins.*

1.7. Previous hydrophobic rotaxanes

Previously in this group, rotaxanes have been prepared which consist of cyclodextrin macrocycles containing azo dyes[8, 61] and cyanine dyes[62]. Polyrotaxanes

such as **26** and pseudopolyrotaxanes such as **27** (shown in Figure 1.12) have also been synthesised in a project[63] parallel to that discussed in this work.

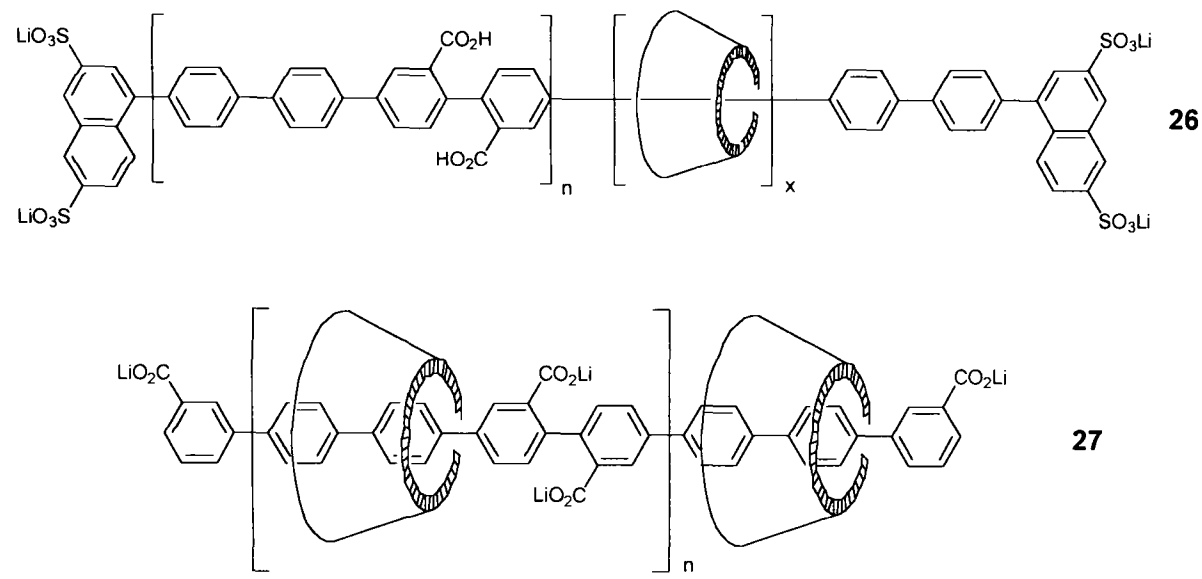

Figure 1.12. *Polyrotaxanes synthesised in Oxford via Suzuki coupling methods and making use of the hydrophobic effect to ensure binding.*

These polyrotaxanes have been shown to have interesting properties and research is ongoing to exploit these for applications in electronic devices.

In this work, we decided to choose fluorescent chromophores whose physical properties could be more thoroughly investigated. Stilbene chromophores are frequently used in commercial applications such as fluorescence brighteners (for paper and in washing powder) and in sunscreens. They are generally highly fluorescent but have a low solubility and are not completely light stable. Diphenylacetylene (tolan) fluorophores are the other class of inclusion molecule chosen here. It is predicted that rotaxane formation using these chromophores should improve fluorescence properties as well as solubility and light stability.

Some attempts to produce further rotaxanes with different azobenzene groups will also be undertaken, in an effort to further the knowledge of this already established area.

As we have chosen to synthesise our rotaxanes in water in order to use the hydrophobic effect, we required a good coupling reaction to enable 'stoppering' of the rod to occur once the cyclodextrin was bound. The reaction in question should fulfil certain criteria:

- Efficiency; since we require good yields of product over semi-reacted species.
- Simplicity, if possible requiring only one step for rotaxane formation from set building blocks.
- The building blocks should be straightforward to prepare and easy to handle.
- A UV/Vis chromophore and / or fluorophore should be present in the building blocks or formed during rotaxane formation, as we wish to compare physical properties of the dumbbell and rotaxane.
- It should work well in water, and reaction with hydroxyl groups should also be avoided, if possible (the cyclodextrin can be protected but this would affect its properties considerably).

It is also preferable that the reaction chosen should already be reasonably well known and understood, with a fair range of reaction conditions and optimum details published. Our work is intended to use known methods for a new purpose; namely to synthesise rotaxanes.

1.8. Conclusions of Chapter 1

This review has attempted to describe important work and key results in the field of molecular encapsulation, focussing on the changes in physical and chemical

characteristics on encapsulation. Relevant examples from the literature have been given.

Differences in NMR spectra after encapsulation have not been well documented. However, it is clear that a change in the environment of a molecule such as that brought about by encapsulation will have a profound effect upon an environment-dependent characteristic such as NMR. These environmental changes may be due to solvation changes within the macrocycle, but in most cases are probably proximity effects of the macrocycle itself. These can be demonstrated by use of NOE experiments.

Encapsulation almost invariably has some effect on the UV/Vis spectrum of chromophores. The form this takes is varied. It is possible to see shifts to both higher and lower wavelength; these may be shifts of only a few nm up to around 50 nm. This is probably due to the relative solvation of the chromophore before and after encapsulation. Changes in the extinction coefficient are also commonplace, although again these can be increases or decreases. Binding can also have an indirect effect upon the UV/Vis spectrum by inducing some more subtle change in the guest molecule (e.g. a deprotonation or conformational change) which in turn has an effect on the UV/Vis absorption spectrum.

In a similar and related way, the fluorescence spectrum is also affected by encapsulation. Emission and wavelengths can be shifted to higher or lower wavelength, and emission intensity can be drastically altered, usually increased, sometimes by many orders of magnitude. Encapsulation by different macrocycles has varying effects, depending on size and chemical nature of the macrocycle.

Host-guest complexation or rotaxane formation generally increases solubility in water or organic solvents. In particular, hydrophobic molecules such as aromatics can be made soluble in water by encapsulation in amphiphilic macrocycles.

How encapsulation affects the aggregation properties depends rather on the relative sizes of guest and binding cavity. If the ratio is such that only one guest can be bound, the aggregation is decreased and monomer units predominate. However if the cavity is larger and two or more molecules can be encapsulated within, this may well increase the degree of aggregation. This facet of molecular encapsulation is a potentially useful one which can be employed in supramolecular assemblies as well as upon monomeric units.

The effect of encapsulation upon conformation is primarily a question of volume; in order to be successfully encapsulated, a molecule must be confinable in the volume of a specific cavity. As it is normally preferable for a molecule in the ground state to be untwisted, this often means occupying a somewhat larger volume and so encapsulation must in this case involve binding of a less favourable conformation, which is unable to revert to the more favoured form without release from the host.

Photochemistry in particular is often changed when a guest molecule is encapsulated. Many light-induced reactions are isomerisations which, as discussed for conformational changes, depend on available volume. Changes in absorbance wavelength on encapsulation may also play a part in the photochemistry possible in a system.

The reactivity of functional groups can be enhanced or reduced by using a cage molecule as a miniature reaction chamber. This can raise effective molarity of two bound components, thereby increasing the rate of reaction. It can also be used to

protect a reactive species from the external reaction mixture, preventing an extremely reactive species such as cyclobutadiene from reaction.

Rotaxane formation is an ideal way of investigating such changes as those described here. We hope to demonstrate enhanced stability towards chemical attack and light, and good optical properties. We have designed a system in order to accomplish this. The following chapters will be concerned with the synthesis and investigation of properties of these rotaxanes.

References for Chapter 1

[1] A. R. Khan, P. Forgo, K. J. Stine, V. T. DSouza, *Chem. Rev.* **1998**, *98*, 1977.

[2] S. B. Ferguson, E. M. Sanford, E. M. Seward, F. Diederich, *J. Am. Chem. Soc.* **1991**, *113*, 5410.

[3] D. J. Cram, M. E. Tanner, C. B. Knobler, *J. Am. Chem. Soc.* **1991**, *113*, 7717.

[4] N. Branda, R. Wyler, J. Rebek, *Science* **1994**, *263*, 1267.

[5] S. Hamai, T. Ikeda, A. Nakamura, H. Ikeda, A. Ueno, F. Toda, *J. Am. Chem. Soc.* **1992**, *114*, 6012.

[6] H.-J. Schneider, T. Blatter, S. Simova, *J. Am. Chem. Soc.* **1991**, *113*, 1996.

[7] M. Sakurai, H. Hoshi, Y. Inoue, R. Chujo, *Chem. Phys. Lett.* **1989**, *163*, 217.

[8] S. Anderson, T. D. W. Claridge, H. L. Anderson, *Angew. Chem. Int. Ed. Engl.* **1997**, *36*, 1310 - 1313.

[9] G. R. Newkome, L. A. Godínez, C. N. Moorefield, *J. Chem. Soc., Chem. Commun.* **1998**, 1821.

[10] J. H. Jung, C. Takesisa, Y. Sahata, T. Kineda, *Chem. Lett.* **1996**, 147.

[11] A. M. Sanchez, R. H. d. Rossi, *J. Org. Chem.* **1996**, *61*, 3446.

[12] R. Corradini, A. Dossena, R. Marchelli, A. Panagai, G. Sartor, M. Saviano, A. Lombardi, V. Pavone, *Chem. Eur. J.* **1996**, *2*, 373.

[13] S. Dan, K. G. Thomas, M. V. George, P. V. Kanut, *J. Chem. Soc. Faraday Trans.* **1992**, *88*, 3419.

[14] W. R. Bergmark, A. Davis, C. York, A. Macintosh, G. Jones, *J. Phys. Chem.* **1990**, *94*, 5020.

[15] M. Hoshino, M. Imamura, *J. Phys. Chem.* **1981**, *85*, 1820.

[16] B. D. Wagner, P. J. MacDonald, M. Wagner, *J. Chem. Educ.* **2000**, *77*, 178 -181.

[17] M. J. MacLachlan, A. Rose, T. M. Swager, *J. Am. Chem. Soc.* **2001**, *123*, 9180 - 9181.

[18] D. B. Amabilino, P. R. Ashton, V. Balzani, C. L. Brown, A. Credi, J. M. J. Fréchet, J. W. Leon, F. M. Raymo, N. Spencer, J. F. Stoddart, M. Venturi, *J. Am. Chem. Soc.* **1996**, *118*, 12012.

[19] P. Dan, I. Willner, *J. Chem. Soc., Perkin Trans. 2* **1984**, 455.

[20] Y. Degani, I. Willner, Y. Haas, *Chem. Phys. Lett.* **1984**, *104*, 497.

[21] K. Kasatani, M. Ohashi, H. Sato, *Carbohydrate Res.* **1989**, *192*, 197.

[22] H. Hirai, N. Toshima, S. Uenoyama, *Bull. Chem. Soc. Jap.* **1985**, *58*, 1156.

[23] M. Takeshita, C. N. Choi, M. Irie, *J. Chem. Soc., Chem. Commun.* **1997**, 2265.

[24] Y. Sueishi, T. Nishimura, *J. Phys. Org. Chem.* **1995**, *8*, 335.

[25] M. Ohara, K. Wanatabe, *Angew. Chem., Int. Ed. Engl.* **1975**, *14*, 820.

[26] R. Chênevert, N. Voyer, *Tetrahedron Lett.* **1984**, *40*, 5007.

[27] J. March, *Advanced Organic Chemistry*, 4th ed., John Wiley and Sons, New York, **1992**.

[28] M. R. Sandner, E. Hedaya, D. J. Trecker, *J. Amer. Chem. Soc.* **1968**, *90*, 7249-7254.

[29] A. H. Parham, B. Windisch, F. Vögtle, *Eur. J. Org. Chem.* **1999**, 1233 - 1238.

[30] M. R. Craig, DPhil Thesis, Dyson Perrins Laboratory, University of Oxford (Oxford), **2001**.

[31] M. R. Craig, M. G. Hutchings, T. D. W. Claridge, H. L. Anderson, *Angew. Chem. Int. Ed.* **2001**, *40*, 1071 - 1074.

[32] J. Kang, J. Rebek, *Nature* **1997**, *385*, 50.

[33] J. C. Sherman, *Tetrahedron* **1995**, *51*, 3395.

[34] D. J. Cram, M. E. Tanner, R. Thomas, *Angew. Chem., Int. Ed. Engl.* **1991**, *30*, 1024.

[35] R. Warmuth, *Angew. Chem. Int. Ed. Engl.* **1997**, *36*, 1347 - 1350.

[36] W. L. Mock, T. A. Irra, J. P. Wepsiec, M. Adhya, *J. Org. Chem.* **1989**, *54*, 5302 - 5308.

[37] I. Tabushi, *Tetrahedron* **1984**, *40*, 269.

[38] P. Bortolus, S. Monti, *J. Phys. Chem.* **1987**, *91*, 5046.

[39] T. Fujimoto, A. Nakamura, Y. Inoue, Y. Sakata, T. Kaneda, *Tetrahedron Lett.* **2001**, 7987 - 7989.

[40] V. Balzani, A. Credi, F. Marchioni, J. F. Stoddart, *Chem. Commun.* **2001**, 1860 - 1861.

[41] H. Murakami, A. Kawabuchi, K. Kotoo, M. Kunitake, N. Nakashima, *J. Am. Chem. Soc.* **1997**, *119*, 7605 - 7606.

[42] S. J. Alderman, Part II Thesis, Dyson Perrins Laboratory, University of Oxford (Oxford), **2001**.

[43] W. Herrmann, S. Wehrle, G. Wenz, *Chem. Commun.* **1997**, 1709 - 1710.

[44] H. S. Banu, A. Lalitha, K. Pitchumani, C. Srinivasan, *Chem. Commun.* **1999**, 607 - 608.

[45] S. Y. Jon, Y. H. Ko, S. H. Park, H.-J. Kim, K. Kim, *Chem. Commun.* **2001**, 1938 - 1939.

[46] W. Herrmann, M. Schneider, G. Wenz, *Angew. Chem. Int. Ed. Engl.* **1997**, *36*, 2511 - 2514.

[47] D. G. Amirsakis, M. A. Garcia-Garibay, S. J. Rowan, J. F. Stoddart, A. J. P. White, D. J. Williams, *Angew. Chem. Int. Ed.* **2001**, *40*, 4256 - 4261.

[48] P. T. Glink, A. I. Oliva, J. F. Stoddart, A. J. P. White, D. J. Williams, *Angew. Chem. Int. Ed.* **2001**, *40*, 1870 - 1875.

[49] M. Asakawa, P. R. Ashton, R. Ballardini, V. Balzani, M. Belohradsky, M. T. Gandolfi, O. Kocian, L. Prodi, F. M. Raymo, J. F. Stoddart, M. Venturi, *J. Am. Chem. Soc.* **1997**, *119*, 302 - 310.

[50] F. Vögtle, O. Safarowsky, C. Heim, A. Affeld, O. Braun, A. Mohry, *Pure and Applied Chemistry* **1999**, *71*, 247-251.

[51] S. J. Cantrill, D. A. Fulton, M. C. T. Fyfe, J. F. Stoddart, A. J. P. White, D. J. Williams, *Tetrahedron Lett.* **1999**, *40*, 3669.

[52] G. M. Hübner, J. Gläser, C. Seel, F. Vögtle, *Angew. Chem. Int. Ed.* **1999**, *38*, 383.

[53] F. G. Gatti, D. A. Leigh, S. A. Nepogodiev, A. M. Z. Slawin, S. J. Teat, J. K. Y. Wong, *J. Am. Chem. Soc.* **2001**, *123*, 5983 - 5989.

[54] N. Armaroli, V. Balzani, J. P. Collin, P. Gavina, J. P. Sauvage, B. Ventura, *J. Am. Chem. Soc.* **1999**, *121*, 4397.

[55] W. Blokzijl, J. B. F. N. Engberts, *Angew. Chem. Int. Ed. Engl.* **1993**, *32*, 1545 - 1579.

[56] H. J. Schneider, R. Kramer, S. Simova, U. Schneider, *J. Am. Chem. Soc.* **1988**, *110*, 6442 - 6448.

[57] H. Ogino, *J. Am. Chem. Soc.* **1981**, *103*, 1303-1304.

[58] M. Ceccato, P. L. Nostro, P. Baglioni, *Langmuir* **1997**, *13*, 2436 - 2439.

[59] J. Szejtli, *Chem. Rev.* **1998**, *98*, 1743 - 1754.

[60] A. Harada, *Acc. Chem. Res.* **2001**, *34*, 456 - 464.

[61] M. R. Craig, M. G. Hutchings, T. D. W. Claridge, H. L. Anderson, *Chem. Commun.* **1999**, 1539.

[62] J. E. H. Buston, J. R. Young, H. L. Anderson, *Chem. Commun.* **2000**, 905 - 906.

[63] P. N. Taylor, M. J. O'Connell, L. A. McNeill, M. J. Hall, R. T. Aplin, H. L. Anderson, *Angew. Chem. Int. Ed.* **2000**, *39*, 3456 - 3460.

Chapter 2; Synthesis and characterisation of new rotaxanes

2.1. Approach to rotaxane synthesis

The method of rotaxane synthesis we chose was designed to utilise known chemistry to prepare novel compounds. For this we exploited the hydrophobic effect to bind the core within an amphiphilic macrocycle. Use of the hydrophobic effect enabled rotaxanes to be formed without the need for the complex structural motifs often needed for templated reactions. We chose cyclodextrins as the macrocycles because they are very water-soluble and yet have hydrophobic cavities. They have been shown to bind many organic molecules well in water[1]. They are also commercially available, cheap, and easy to modify[2], should this be required. For the stoppering reaction, Suzuki coupling proved to be a convenient means of combining the water-soluble components to form rotaxanes. Scheme 2.1 shows the general requirements for such a coupling. The boronic acid binds inside the cyclodextrin due to the hydrophobic effect, and palladium catalysed coupling is then used to 'stopper' the pseudorotaxane and turn it into a rotaxane, by reaction with sterically demanding aryl iodides.

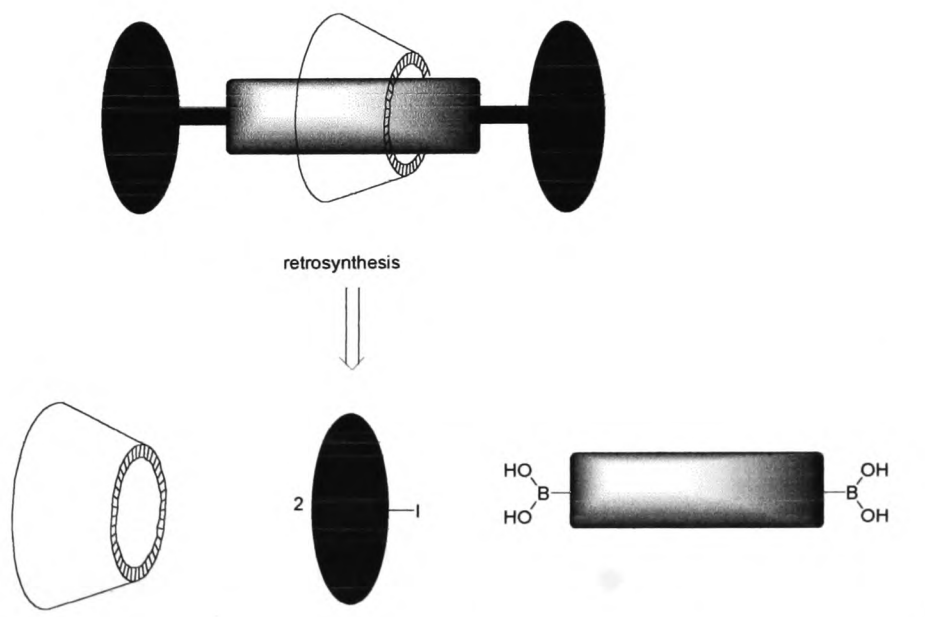

Scheme 2.1. *General retrosynthesis of Suzuki coupled rotaxanes.*

In choosing the particular dumbbell units to be incorporated into the rotaxanes, it was necessary to bear in mind the synthetic accessibility of both the iodide and boronic acid components, and the availability of their corresponding precursors. At the same time, conjugated dumbbells with interesting chemical and photochemical properties would give us more insight into potential changes in properties upon encapsulation. The target molecules were therefore chosen to include stilbene and tolan functionalities.

2.2. Synthesis of the building blocks

The core of all these target molecules requires common building blocks **28 - 31,** which can be coupled using Suzuki methods in the presence of a palladium (0) catalyst (and α- or β-cyclodextrin in the rotaxane synthesis) to give an aromatic core.

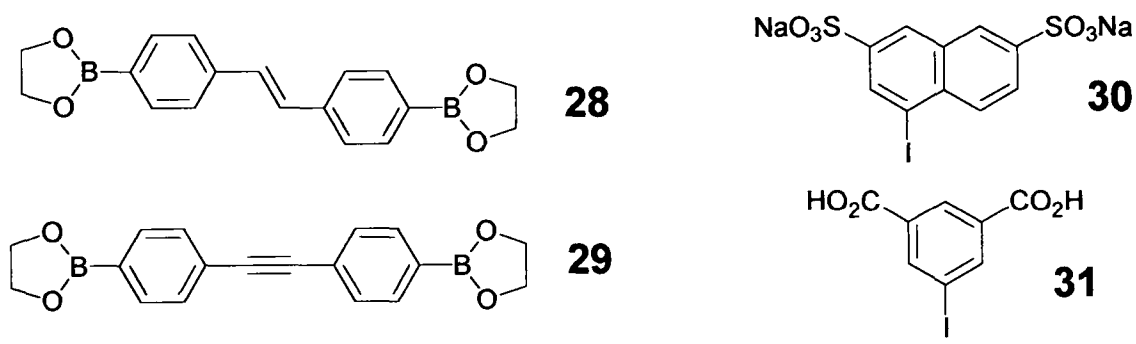

Figure 2.1. *Target starting materials.*

α-Cyclodextrin has an internal diameter of about 0.57 nm[1], and the cavity of β-cyclodextrin is about 0.78 nm across. Therefore, stopper group **30** should be large enough to hold both α- and β-cyclodextrin on to the hydrophobic core, whereas CPK models suggested that stopper group **31** should be a stopper for only α-cyclodextrin.

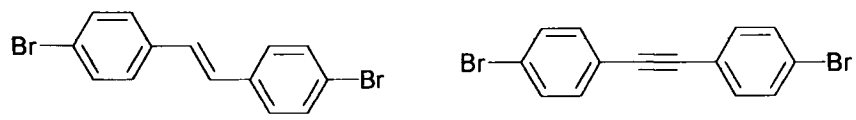

32 **33**

A straightforward preparation of the boronate esters **28** and **29** can be achieved from the corresponding dibromo compounds **32** and **33**. **32** can be disconnected in two ways, the first method consisting of a Wittig-Horner-Emmons coupling (Scheme 2.2).

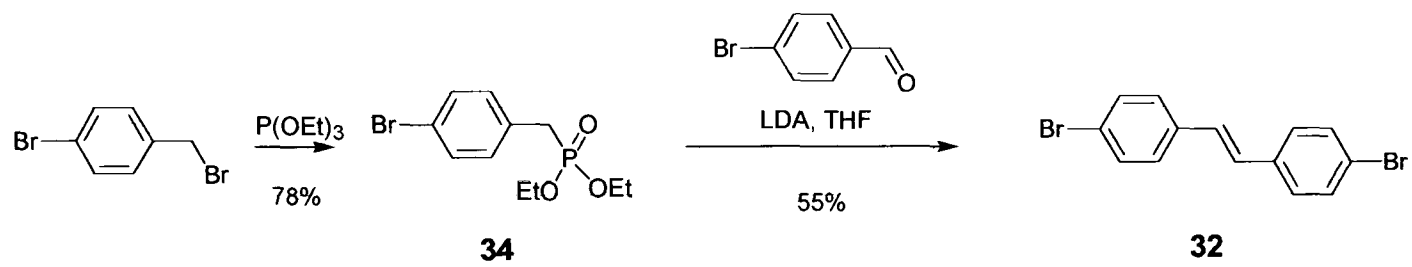

Scheme 2.2. *Preparation of dibromostilbene 32 from 4-bromobenzyl bromide.*

The phosphonate **34** was formed in good yield *via* an Arbusov style reaction, according to literature precedent[3]. Formation of the dibromostilbene **32**[4] was difficult to achieve cleanly, despite *in situ* preparation of the LDA and careful monitoring of the temperature. Flash chromatography gave pure **32** in 55 % yield on a half-gram scale, but this method proved difficult to scale up. For this reason, another method was sought.

The second method[5] is outlined in Scheme 2.3. Both the chemistry and purification proved to be much simpler, although the yields were lower than those from the Wittig route. However, this route could be performed on up to 15 g of starting material, enabling us to synthesise large amounts of the necessary dibromides, and it uses cheaper starting materials. The acetylenic core **33** can also be made from the same tetra bromo intermediate **35**[6], making this route even more time efficient.

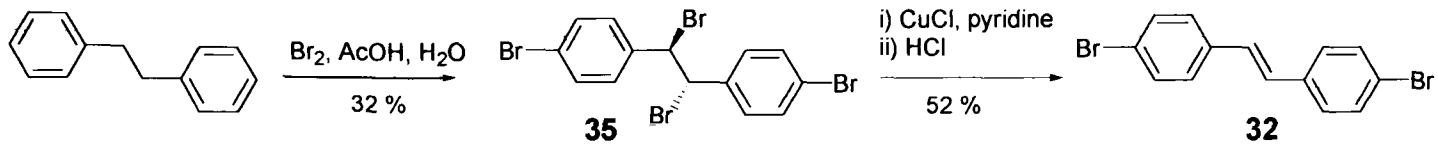

Scheme 2.3. *Alternative route to the dibromide* ***32****.*

Bromination of dibenzyl gave a mixture of 4,4- and 2,4- substituted components, however removal of the desired **35** from the reaction mixture was simple, as it was insoluble even in hot acetic acid. Subsequent purification proved impractical due to the extreme insolubility of **35**. For this reason, the tetrabrominated compound **35** was used without further purification. Elimination of bromine gave stilbene **32** which had a higher solubility, thus the impurities from the previous step could more easily be removed at this point.

The tetrabromide **35** and dibromide **32** were characterised by NMR and mass spectrometry techniques; both were in good agreement with the expected structures. The melting points were also close to the literature values.

Synthesis of the diboronic acid **36** and subsequent protection as the ester **28** was achieved following standard procedures[7], shown in Scheme 2.4.

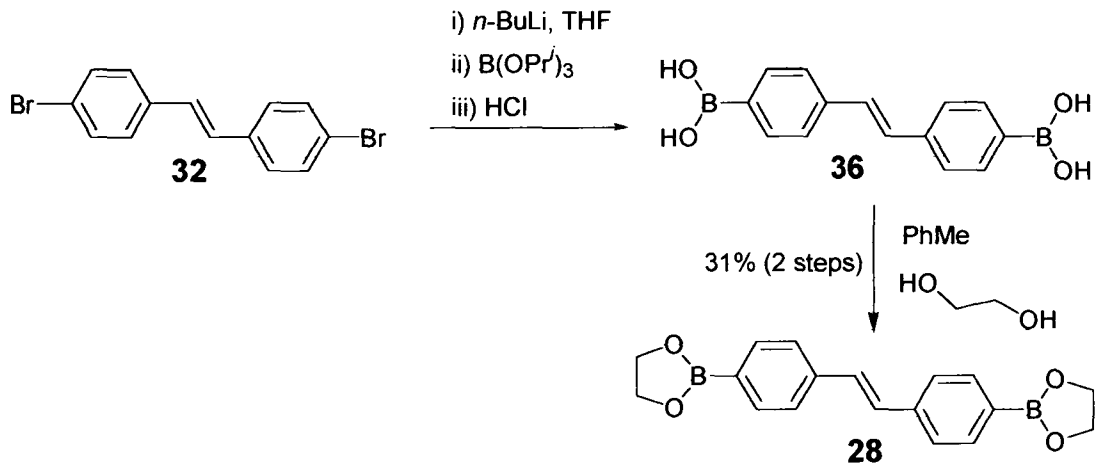

Scheme 2.4. *Synthesis of the boronate ester* ***28****.*

Although boronic acids are active in Suzuki coupling, these are often difficult to handle and purify, being gel-like and displaying much aggregation in solution. They

also readily form anhydrides[8, 9], which can complicate measurement of exact quantities. For this reason, we prepared the cyclic boronate esters **28** and **29**, which are crystalline, air-stable for many months, and not prone to water loss. The acid was formed by hydrolysis of the initially formed diisopropyl ester, which is quite labile and therefore not suitable for storage purposes. The yield over the two steps is poor; probably the first step is the yield limiting one as varied amounts of ethanediol resulted in no great difference in the final yield. These esters are hydrolysed under the basic Suzuki reaction conditions to give the active boronate salts of **36** and **37** *in situ*.

The acetylenic boronate ester **29** was made similarly from the dibromide **33** (Scheme 2.5) which was obtained from the tetrabromo[6] precursor **35** by sodium ethoxide promoted elimination.

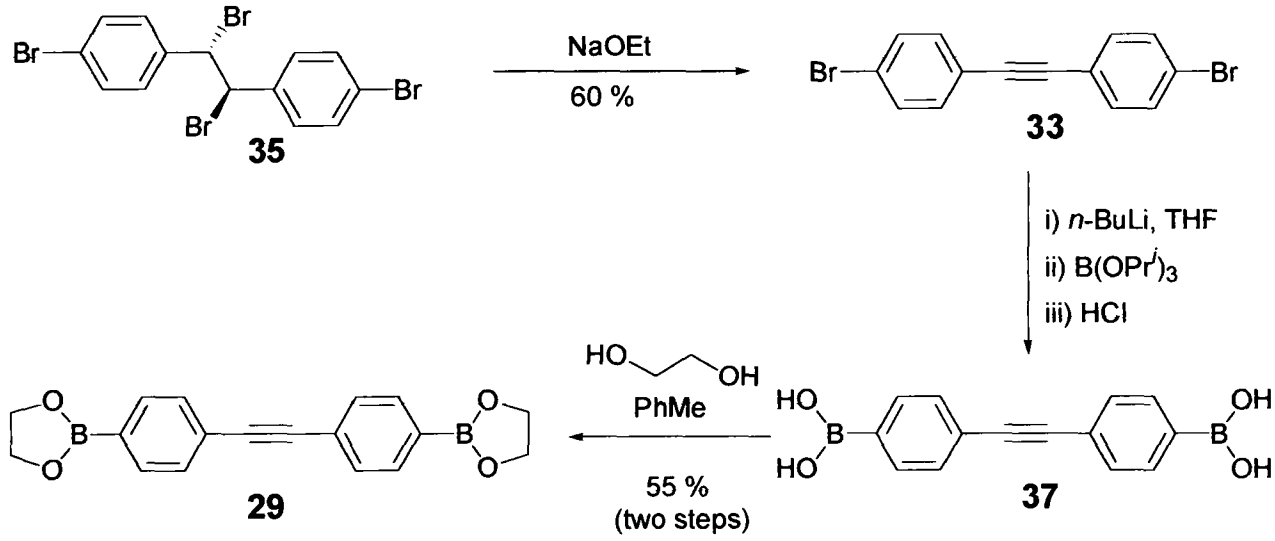

Scheme 2.5. *Synthesis of the tolan dibromide **33** and subsequently the boronate ester **29**, from the tetrabrominated intermediate **35**.*

The dibromodiphenylacetylene **33** was prepared from the tetrabromo intermediate **35** by elimination of 2 equivalents of hydrogen bromide using freshly prepared sodium ethoxide as base. The crystalline dibromotolan **33** was then reacted using the

same conditions as previously used for preparation of **28** to give the boronate ester **29** in a good yield.

Both diboronates **28** and **29** were fully characterised by NMR, mass spectrometry, elemental analyses and UV/Vis techniques. Although the stilbene boronic acid **36** has been synthesised previously[7], **28** and **29** had not appeared in the literature before this work. All data found is in agreement with that expected of such compounds.

The stoppers were chosen because they confer the desired water solubility and are easily prepared from common amines by de-diazoniation chemistry.

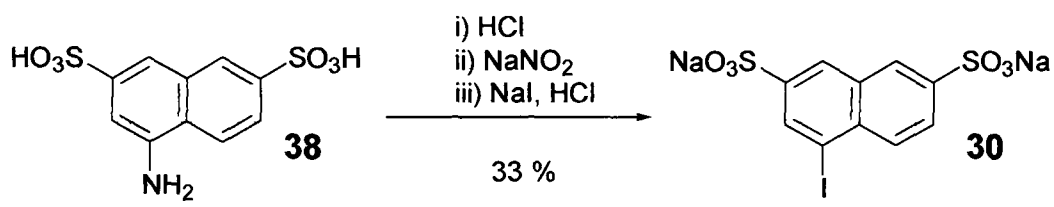

Scheme 2.6. *Reaction of Freund's acid* ***38*** *to form the stopper* ***30****.*

Freund's acid (1-amino-3,6-naphthalenedisulfonate disodium salt) **38**, kindly donated by Dr M. G. Hutchings of DyStar UK Ltd., was easily converted to the iodide **30** (portrayed in Scheme 2.6). Excess iodine, which was still present in the solid, was then removed by sublimation under vacuum with heating, and the solid subsequently purified by recrystallisation from water. This method of iodine removal was found to be the most time efficient of several methods tried. Use of liquid-liquid extraction or repeated recrystallisations reduced yields considerably and was thus abandoned in favour of the sublimation procedure.

Iodoisophthalic acid **31** was synthesised by a similar route[10] and was kindly provided by James D. Kelly.

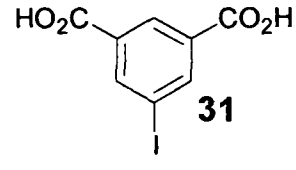

The dicarboxylic acid stopper (**31**) is much smaller than the naphthalene disulfonate stopper (**30**); probably large enough to stopper only α-cyclodextrin and not β-cyclodextrin. However purification of this stopper and its derivative rotaxanes has thus far proven to be simpler than was the case with the naphthalene disulfonates, due to the variation in solubility at different pH of the carboxylic acids.

2.3. Synthesis of the rotaxanes

Palladium-mediated coupling of an aryl halide (usually iodide or bromide, although the use of chlorides has been reported recently[11]) with an arylboronic acid has been used extensively since its discovery by Suzuki[12] in 1981. This type of chemistry is suitable for use in water. Indeed, water is often added to organic solvents such as DMF[13, 14] to facilitate the coupling of water-insoluble compounds *via* this cross-coupling. Suzuki chemistry has already been employed to synthesise water-soluble polymers[15, 16] and various components for use in medicinal chemistry[17, 18], thereby proving its versatility in addition to considerably expanding the knowledge of this recently discovered field. The breadth of knowledge was a deciding factor in the choice of coupling reaction for rotaxane formation.

In water, and in the presence of cyclodextrins, our group has found the Suzuki coupling reaction works extremely well[19, 20]. In parallel with this work, others in Oxford have used this method of coupling to form polypseudorotaxanes and polyrotaxanes[21]. This work aims to expand upon these topics by synthesis of discrete monomer versions of these polymers, in order to facilitate an investigation of exactly how encapsulation affects the properties of the dumbbell.

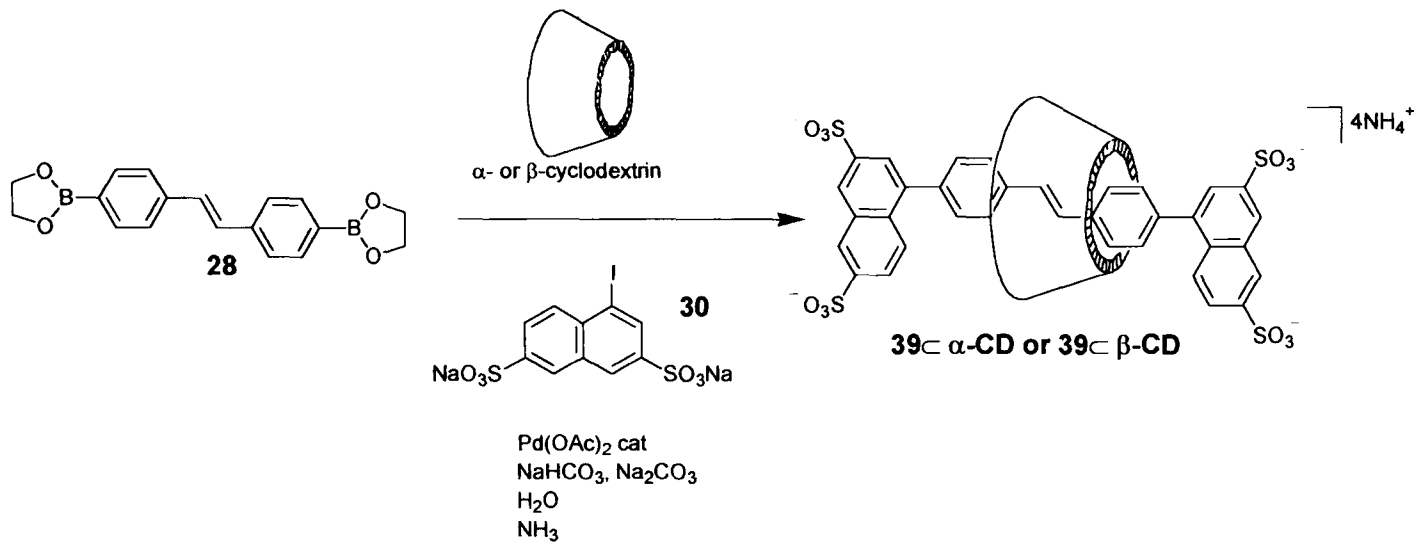

Scheme 2.7. *Conditions for Suzuki coupling to form rotaxanes.*

The rotaxanes **39⊂α-CD** - **43⊂β-CD** (shown in full in Section 2.4) were all synthesised according to Scheme 2.7. The starting materials, catalyst, and base were dissolved in degassed water, giving a black or dark brown, highly fluorescent solution of crude rotaxane. All reactions were carried out in the absence of air, as oxygen has been shown to oxidise the palladium catalyst. The catalyst we used is somewhat unusual in that no phosphine ligands are added, as in the majority of cases. However, there is precedent for use of such a catalyst[14, 22]. Addition of ligands was not necessary for the synthesis, as it can be seen that good yields can be achieved even without ligands, and in most cases the colloidal palladium formed by reduction of the palladium acetate is readily removable during purification of the crude rotaxanes. The necessary reduction of Pd(II) to Pd(0), given the lack of other reductants present, is thought to be by a stoichiometric amount of the boronic acid[23]. This small percentage of unincorporated diboronic acid seems critical in the synthesis of polymers[21] due to premature termination of the growing polymer chains. In the case of these 'monomers' it proved unnecessary to account for the slight shortfall of boronic acid used, perhaps because of the lower percentage of catalyst employed (1 – 2 % instead of 5 % for the polymers).

Reasonably large excesses of the cyclodextrin seem to be required; this complicates the purification of the sulfonated rotaxanes somewhat, as both the bound cyclodextrin (in the form of a rotaxane) and the unbound cyclodextrin are very soluble in water. A suitable way to remove the excess macrocycle was by the use of cationic resin ion-exchange chromatography. Although this does not allow complete purification of the rotaxane, it does cleanly remove all uncharged species such as unused boronate ester and, more importantly, the cyclodextrin. At low and neutral pH, negatively charged species are retained by the resin, allowing uncharged species to be washed away. This also acts as a fine filter to remove colloidal palladium that could not be removed at the previous filtration stage. This procedure allowed analysis of the crude mixture by NMR, which had not been possible until this point due to the large excess of cyclodextrin present. Pure rotaxanes were obtained by a simple method of precipitation out of a small volume of water with a less polar solvent such as 2-propanol, ethanol or acetone.

2.4. Summary of all rotaxanes synthesised

The rotaxanes that have been successfully synthesised and characterised are shown below:

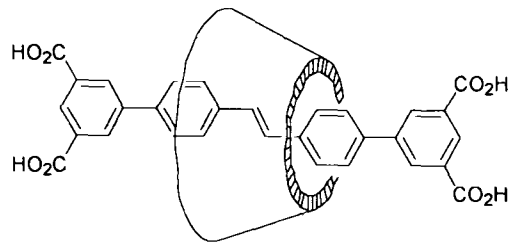

α-cyclodextrin (73 %); **40**⊂ α-**CD**

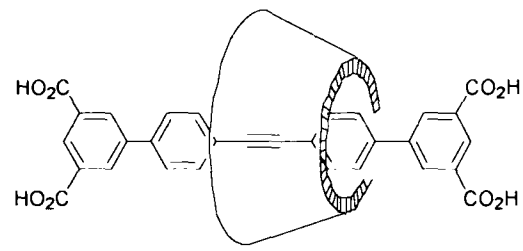

α-cyclodextrin (50 %); **41**⊂ α-**CD**

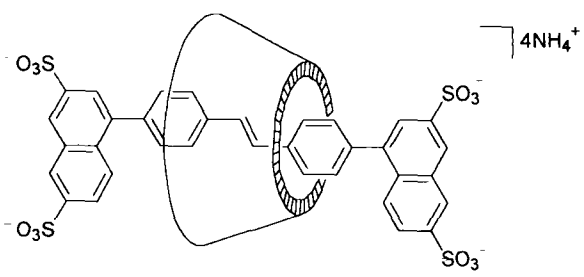

α-cyclodextrin (25 %); **39**⊂ α-**CD**

β-cyclodextrin (14 %); **39**⊂ β-**CD**

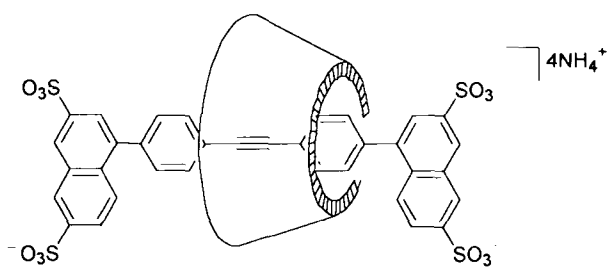

α-cyclodextrin (31 %); **42**⊂ α-**CD**

β-cyclodextrin (16 %); **42**⊂ β-**CD**

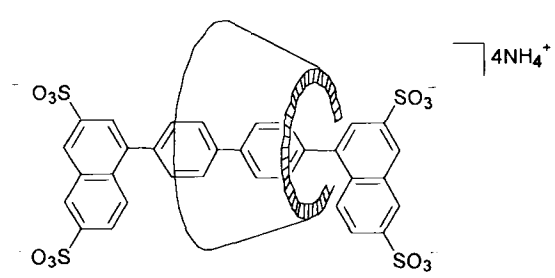

β-cyclodextrin (4 %); **43**⊂ β-**CD**

Rotaxane **43**⊂β-**CD** was synthesised by Michael J. Hall and purified and characterised by Peter N. Taylor[21]. Rotaxane **41**⊂α-**CD** was prepared by Michael J. O'Connell[20].

Yields shown are optimised. The variation in yields reflects in part the ease of purification; in general the sulfonates **39**⊂α-**CD** and **42**⊂α-**CD** - **43**⊂β-**CD** required more extensive purification, resulting in greater losses. However, the trends in yields do also reflect the binding affinities of the various boronates for the two cyclodextrins. This was investigated in the optimisation process.

2.5. Optimisation of threading conditions

In order to optimise the reaction conditions, a series of test reactions were carried out, to ascertain the crude yield of rotaxane *vs.* dumbbell. This was done by ion-exchange chromatography of the crude reaction mixtures, which were then investigated by 250 MHz ^{1}H NMR. Ion exchange removed only any excess cyclodextrin or salts present in the reaction mixture (as explained in 2.3), but did not change the ratio of dumbbell to rotaxane or any other negatively charged organic species (such as half-formed dumbbell which might on occasion be present). The ratio of integrals of cyclodextrin : aromatic protons gave an indication of the relative amounts of rotaxane to other aromatic impurities.

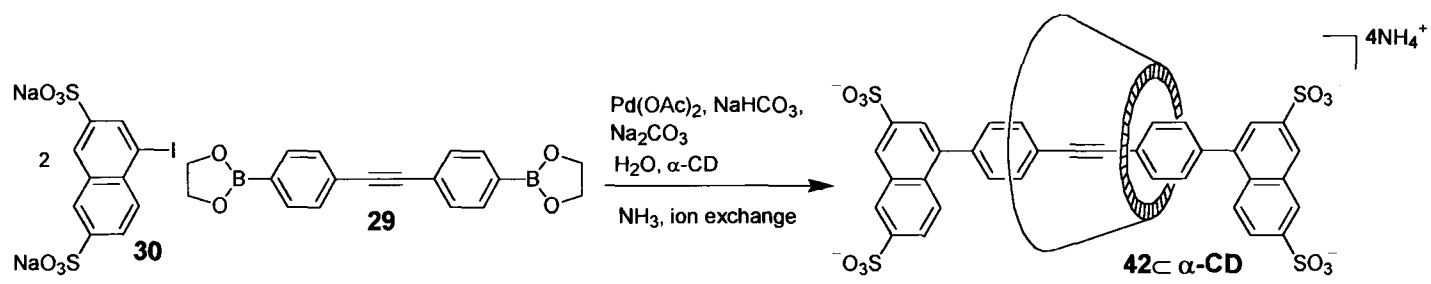

Scheme 2.8. *Rotaxane formation reaction used in the optimisation of conditions study.*

The reaction chosen for these studies was the formation of the α-cyclodextrin rotaxane (**42⊂α-CD**, portrayed in Scheme 2.8), having the naphthalene disulfonate stopper and acetylenic core. The ratios of rotaxane to other aromatic species are shown in the table below as % threading of the cyclodextrins, determined using the post ion-exchange reaction mixture. Where not otherwise stated, conditions were kept as similar as possible. Reaction times were 15 h each.

Table 2.1. *Summary of findings from the optimisation of rotaxane* ***42⊂α-CD*** *synthesis conditions*[§].

Temperature (°C)	Eq. α-cyclodextrin w.r.t. boronic acid **29**	Concentration of reactants (mol l^{-1})	% threading (^{1}H NMR)[$]
85	6.6	0.026	100
85	18	0.026	50
45	6.6	0.026	95
25	2	0.026	100
45	2	0.026	90
45	2	0.052	77

[§]All reactions carried out with 2.0 eq. **30**, 7.6 eq. $NaHCO_3$, 7.6 eq. Na_2CO_3 and 2 mol % $Pd(OAc)_2$. Subsequent ion-exchange on cationic resin with 1 × 250 cm^3 pH1 acetic acid (aq.), 2 × 250 cm^3 water and 2 × 250 cm^3 1 % NH_3 (aq.).

[$]For the specified rotaxane formation this was calculated as follows: Integral of non-anomeric cyclodextrin envelope (4.1 – 3.5 ppm)/36 × 18 = *x*. where *x*/integral of aromatic envelope (8.5 – 7.5) = threading ratio, 36 being the number of non-anomeric protons and 18 being the number of aromatic protons on the rod.

Noting that the error in using NMR integrals in this way is *ca.* ±10 %, it can be seen from these results that

i. A very large excess of cyclodextrin such as that required for saturation of the reaction mixture with α-cyclodextrin is detrimental, probably because it inhibits the coupling reaction.

ii. The number of equivalents of cyclodextrin needed increases with temperature.

iii. Increased concentration of the reagents also seems to hinder the reaction.

These observations can be interpreted to show that optimum conditions for reaction would seem to be 45 °C and using *ca.* 6 eq. of α-cyclodextrin. Though there are conditions giving similar yields at 85 °C and 25 °C, it seemed that a little heating was required for the reaction to commence, whereas the use of excessive heat could result in other, unwanted reactions. The mid-range temperature was therefore chosen for the preparative reactions.

It should be kept in mind whilst interpreting these data that there are some severe limitations in the measurements made. Most importantly, overall yield and amount of rotaxane present in the crude reaction mixture are not necessarily directly linked, as these studies do not take into account the potential difficulties in removal of different types of impurities. They can serve as a guide to producing 'pure crude' rotaxanes but it must be stressed that the achievement of the best possible yield may involve further adaptation of the method employed here.

One of the most likely side reactions is protodeboronation *i.e.* loss of the boronate ester group which would severely inhibit rotaxane formation. This is thought to occur at a faster rate at higher temperatures[24], in addition to being catalysed by many solvents[25] and also many coupling catalysts[26-28].

Previous work within the Anderson group[20] has shown that after a few hours at 85 °C under nitrogen, protodeboronation makes no significant contribution, being only 3 - 4 %. After 20 - 25 h the amount of protodeboronated species was found to become more significant at 8 - 9 %. By this time, we expect the Suzuki coupling

reaction to be completed, so this boron loss is not expected to play a large part in inhibition of the main coupling reaction.

2.6. Comparison of size factors in threading

Another path of investigation was the efficiency of threading which was observed using varied rods and cyclodextrins. This should give an idea of the size complementarity involved, as well as the relative binding affinities.

This investigation was done in a similar way to the previous one, by utilising the NMR integrals observed. They give an interesting insight into the binding exploited in rotaxane formation, which could not be directly observed through titration as the unstoppered boronic acid also forms complexes with cyclodextrins[29] in which the chromophore is not encapsulated. These render all attempts at UV and NMR titrations unusable[30]. All reactions were carried out over 15 h at 85 °C, 0.026 mol l^{-1} boronic acid and 6.6 eq. cyclodextrin, with the naphthalene stopper **30**. The elevated temperature may minimise any aggregation effects between boronic acid molecules, thereby allowing the size complementarity to be explored more easily. The results of the study are listed in Table 2.2.

Table 2.2. *Summary of findings from the size-factors study*[§].

Rotaxane formed	Rod	Cyclodextrin	% Threading[$] (^{1}H NMR)
-	Biphenyl	α	No rotaxane formed
43⊂β-CD	Biphenyl	β	30
39⊂α-CD	Stilbene	α	60
39⊂β-CD	Stilbene	β	64
42⊂α-CD	Acetylene	α	100
42⊂β-CD	Acetylene	β	66

[§]All reactions carried out with 2.0 eq. **30**, 0.026 mol l^{-1} boronic ester, 6.6 eq. cyclodextrin, 7.6 eq. $NaHCO_3$, 7.6 eq. Na_2CO_3 and 2 mol % $Pd(OAc)_2$ at 85 °C Subsequent ion-exchange on cationic resin with 1 × 250 cm^3 pH1 acetic acid (aq.), 2 × 250 cm^3 water and 2 × 250 cm^3 1 % NH_3 (aq.).

[$]This was calculated as follows: Integral of non-anomeric cyclodextrin envelope (4.1 – 3.5 ppm)/*c* × a = *x*. where *x*/integral of aromatic envelope (8.5 – 7.5) = threading ratio, *c* being the number of non-anomeric protons and *a* being the number of aromatic protons on the rod.

Rotaxane formation was not seen on combination of α-cyclodextrin and the biphenyl boronate ester. From this observation, along with the formation of rotaxane **43⊂β-CD**, we can conclude that the biphenyl unit does not bind at all favourably inside the smaller α-cyclodextrin. Possibly it does not fit at all. This suggests that biphenyl > stilbene > acetylene in terms of size and rigidity, both of which are important in binding, and is consistent with the results seen in azo-dye rotaxanes[31]. The other experiments shown also support this idea; biphenyl gives only 30 % crude rotaxane formation with β-cyclodextrin, as opposed to around 65 % for both the

other, smaller boronate esters. Binding within α-cyclodextrin improves with a smaller size of rod. The acetylenic core appears to thread particularly well within α-cyclodextrin; it seems that here the size complementarity is excellent. This is supported by the proven high affinity of α-cyclodextrin for aliphatic acetylenes over alkanes[32].

2.7. Synthesis of the dumbbells

To investigate the changes in properties resulting from encapsulation, it was necessary to synthesise the unencapsulated forms of all the aromatic cores. The synthesis proceeded in an identical fashion as the rotaxane synthesis, and is shown in Scheme 2.9.

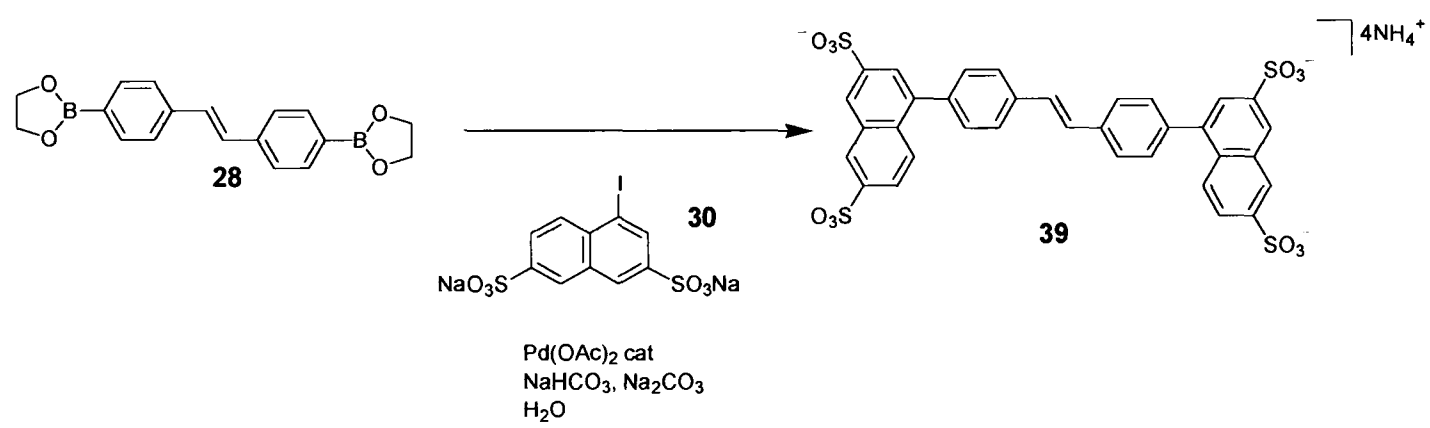

Scheme 2.9. *Synthesis of the dumbbells* ***39*** *to* ***43****.*

After initial difficulties in the synthesis and purification of the dumbbells, it was found that it was advantageous not to purify these mixtures *via* ion-exchange chromatography. The reason behind this is not clear, as tests indicate that the dumbbells are not retained by the ion-exchange resin. It is possible that the long exposure to bright laboratory lights on the ion-exchange column resulted in photoisomerisation and degradation in the case of the dumbbells (see Chapter 5). At the time, however, this was not well understood. After these initial hurdles had been

overcome, the majority of the dumbbells could be isolated, albeit in generally lower yields than for the equivalent rotaxanes.

In most cases it was possible to purify the dumbbells by precipitation, to give sodium salts of the sulfonic acid (**39**, **43**). Only for the purification of **42** was a silica column always required. It is possible that the acetylenic boronate ester does not react well under these conditions, despite giving good yields in the case of the rotaxanes. This is borne out by work carried out by Michael J. O'Connell[30], in which he found that it was not possible to form **41** by this route at all, and the only route found for the synthesis of **41** involved hydrolysis of the macrocycle from the corresponding rotaxane **41⊂α-CD**.

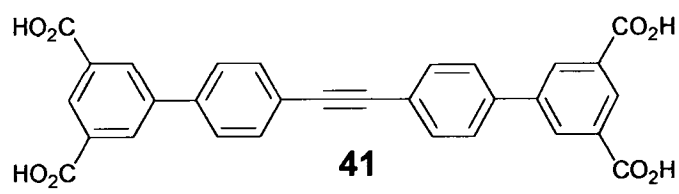

41

Given the satisfactory yields in the acetylenic rotaxanes **41⊂α-CD**, **42⊂α-CD**, and **42⊂β-CD**, it appears that solubility may be a major factor. In the case of the rotaxanes, the boronic acid component is solubilised by encapsulation with the cyclodextrin, enabling a clean reaction to occur. However, it seems unlikely that solubility can be the only factor, as the reaction mixtures appeared to be solutions or at least partially dissolved. Aggregation of the hydrophobic tolan boronate **29** in solution could prevent or hinder its intended reaction with aryl iodides **30** and **31.** Measurement of this quantity is not simple. As discussed in Section 2.5, titrations were not informative in the case of cyclodextrins and these boronate species.

The remaining dumbbells **39** to **43** were prepared by the described methods:

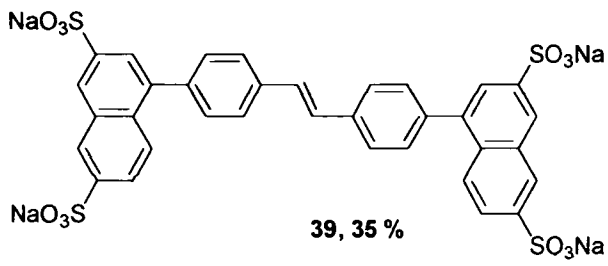

39, 35 %

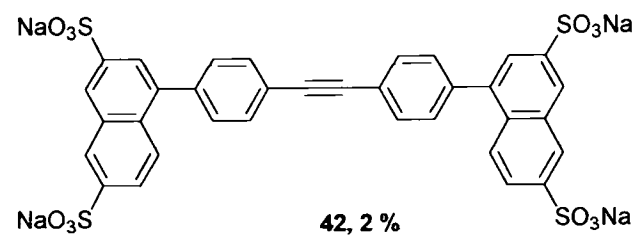

42, 2 %

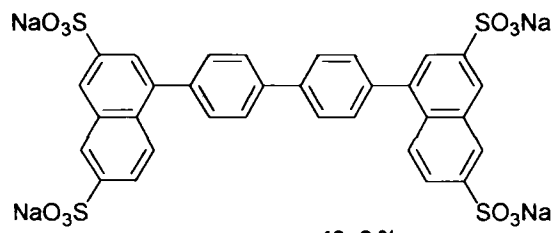

43, 2 %

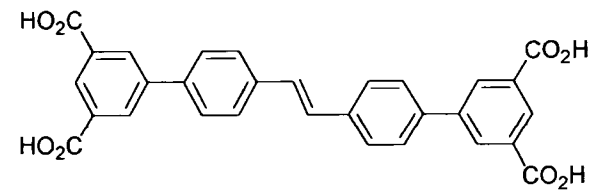

40, 71 %

Dumbbell **43** was synthesised by Peter N. Taylor.

All dumbbells were characterised by NMR and mass spectrometry.

2.8. Characterisation of the rotaxanes

Full assignment of the stilbene isophthalic acid rotaxane **40⊂α-CD** ^{1}H and ^{13}C NMR spectra was carried out using 2D techniques.

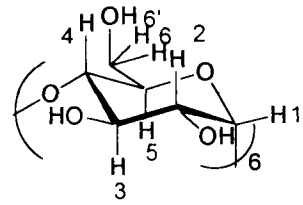

Figure 2.2. *Numbering system for the cyclodextrin glucose unit.*

The ^{1}H NMR spectrum of α-cyclodextrin has been fully assigned previously, however inclusion of a guest molecule can influence the environment[33] and hence the chemical shift of the macrocycle protons. For this reason, we carried out assignment of the sugars, albeit using previous data as an aid.

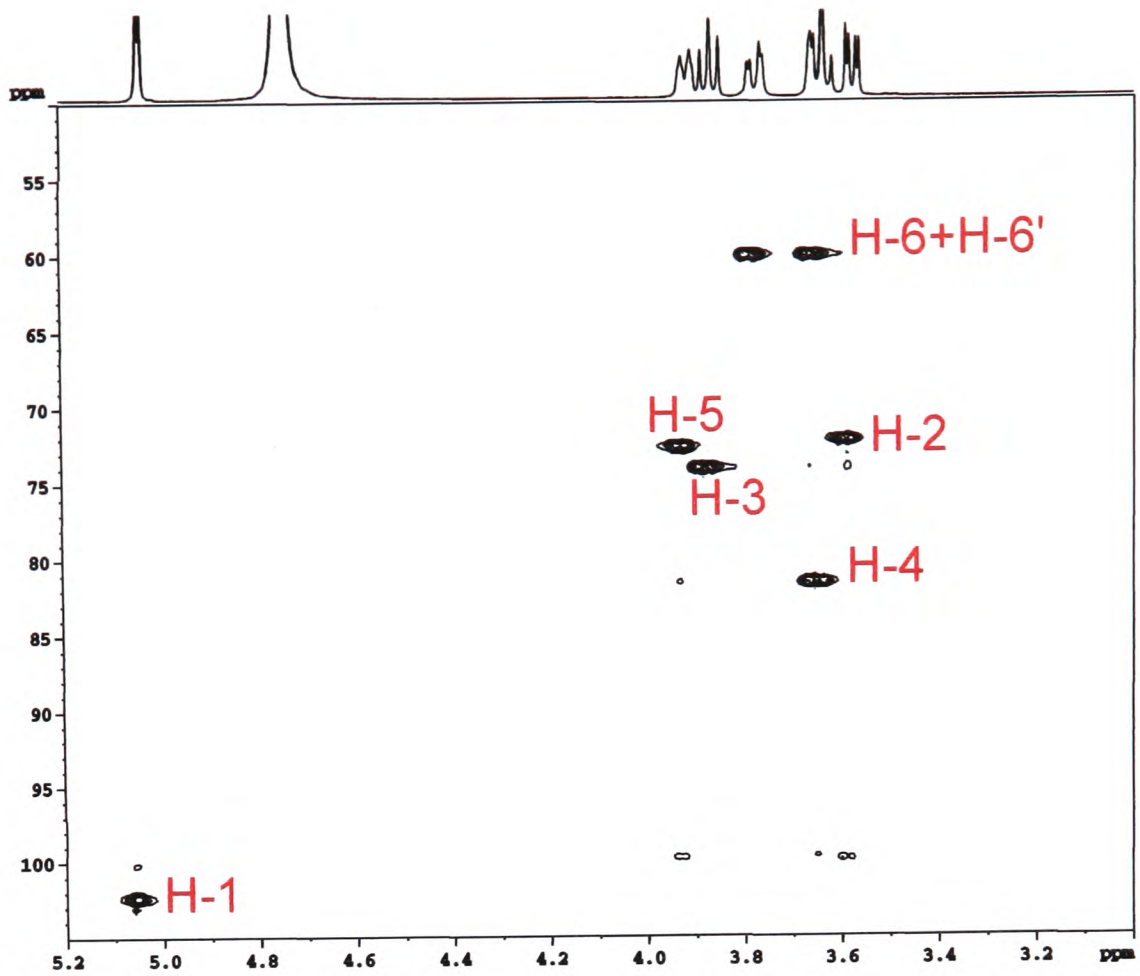

Figure 2.3. *HSQC of the cyclodextrin region of rotaxane* ***40⊂α-CD*** *with assignments, recorded in* D_2O *at 500 MHz .*

The anomeric proton (H-1) is always the most easily discernable from its chemical shift of typically 5.0 ppm; the well resolved coupling patterns were most useful in distinguishing the other protons. H-2 is a double doublet, split by both H-1 and H-3. H-3 and H-4 appear as triplets, being strongly coupled to their axial partners. H-5 appears as a complex multiplet, split by H-4, H6 and H-6'. The H-6 have different chemical environments as they are diastereotopic, but are readily identified from the HSQC spectrum (Figure 2.3) as they both exhibit one-bond coupling to the same carbon. The HSQC was then used to assign the ^{13}C spectrum as well (not shown).

2.8.1. Changes in NMR spectra upon encapsulation

Encapsulation of small molecules has been shown to have a marked effect upon their NMR spectra in some cases. This is naturally more pronounced when the

macrocycle used is aromatic and possesses a ring current[34]. However changes have also been seen in non-aromatic macrocyclic systems[33, 35, 36].

We were therefore interested in the comparison of spectra from a series of rotaxanes. The aromatic regions of the spectra of dumbbell **39** and rotaxanes **39⊂α-CD** and **39⊂β-CD** are depicted in Figure 2.4.

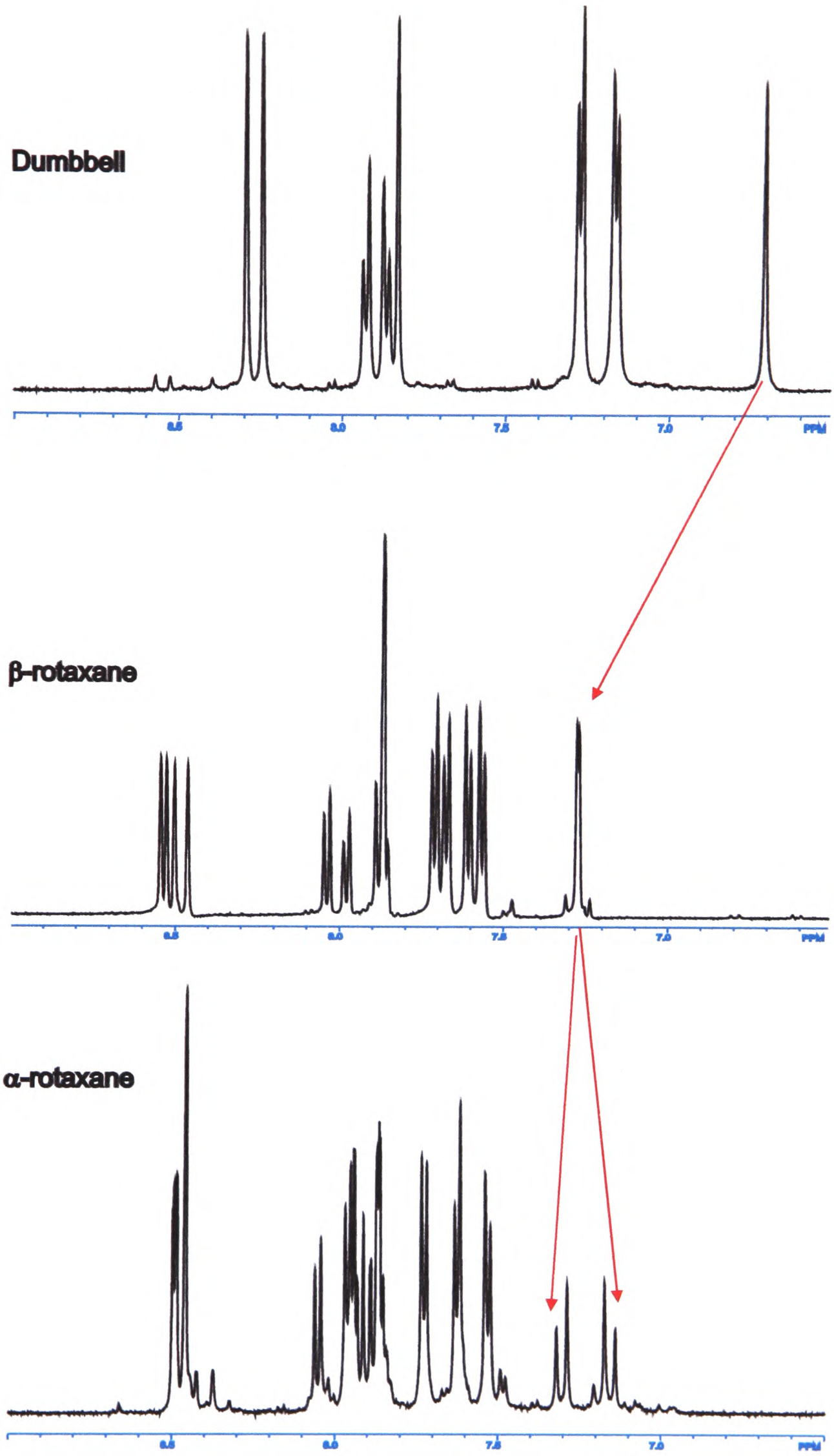

Figure 2.4. *Comparison of the aromatic regions of* ***39****,* ***39⊂α-CD****, and* ***39⊂β-CD****, all recorded in* D_2O *at 500 MHz. The alkene proton changes most notably.*

This figure (2.4) clearly shows the difference in the spectra upon encapsulation. The desymmetrisation of the dumbbell core caused by encapsulation with an asymmetrical molecule results in doubling of the signals in both cases; this is to be expected, as protons which were chemically identical in the dumbbell **39** are in different environments with respect to the cyclodextrin in **39⊂α-CD** and **39⊂β-CD**. The change in chemical shift of the stilbene proton on transition from the dumbbell (6.72 ppm) to both rotaxanes (7.27 ppm) is particularly apparent; in this respect, the size of the cyclodextrin does not appear to make much difference. However, the smaller cavity of α-cyclodextrin does have a pronounced effect on the splitting pattern observed. On transition from the larger β-cyclodextrin to α-cyclodextrin, the average apparent chemical shift (7.27 ppm) and coupling constants (16.6 Hz) remain similar but the disparity in chemical shift increases. There are many differences throughout the aromatic regions of the three compounds, however the changes in the alkene protons are most pronounced. Other changes include a downfield shift of the entire aromatic envelope. The biphenyl protons produce a complex pattern, especially in the case of the rotaxane with α-cyclodextrin **39⊂α-CD**, where the two ends of the dumbbell have more different chemical environments. On the whole, it is still possible to trace these back to the original, unencapsulated unit, although seen on its own, the spectrum of **39⊂α-CD** seems incredibly complex.

2.8.2. Position of Cyclodextrin

In order to assign the position of the cyclodextrin relative to the dumbbell backbone, it was necessary to exploit through-space interactions by use of 1D NOE spectra and

a 2D NOESY (Figures 2.5. and 2.6.), in addition to a single bond proton-carbon correlation experiment.

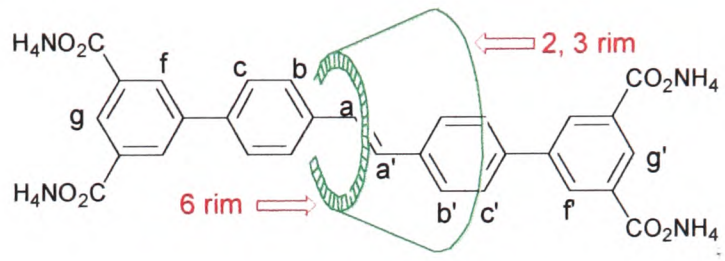

40⊂ α-CD

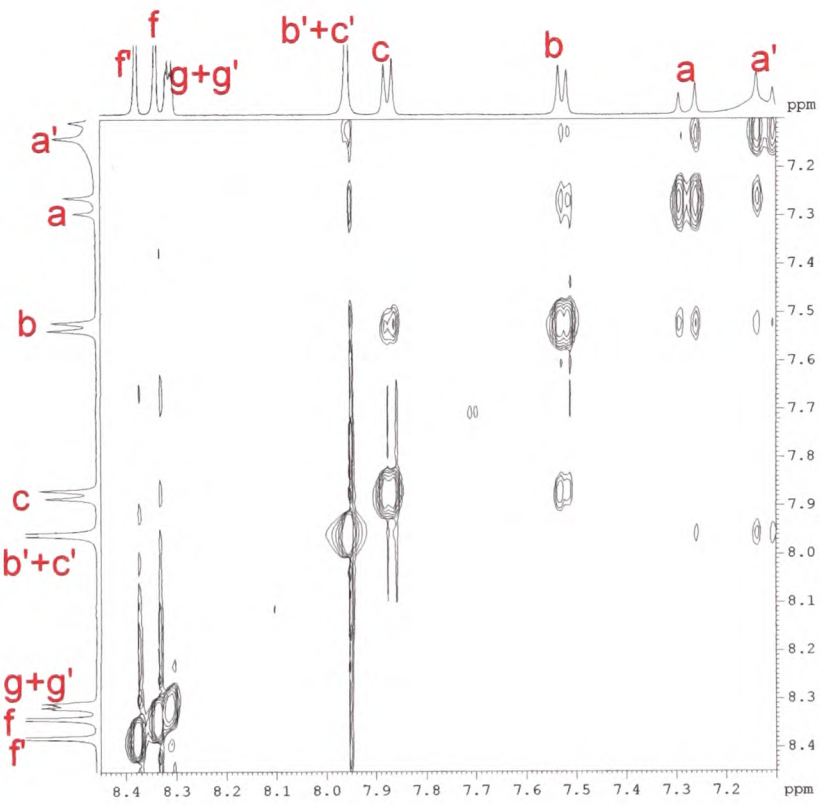

Figure 2.5. *Expansion of the aromatic region of the NOESY with assignments of the protons, recorded in D_2O at 500 MHz.*

Figure 2.5 shows the aromatic-aromatic proton long range interactions, which enabled the assignment of which protons were in which 'half' of the dumbbell. Initially an arbitrary assignment (*x* or *x'*) must be given to one proton, and all other protons are assigned relative to this one. We started with the alkene protons *a* and *a'* which have typical chemical shifts (7.1 – 7.3 ppm) of benzylic alkenes, and which can be immediately identified from their high coupling constant (15.5). Cross-peaks

from *a* to *b* and *a'* to the overlapping *b'+c'* peaks can be seen. The stopper protons appear at higher chemical shift, as expected for *meta* substituted benzene carboxylates.

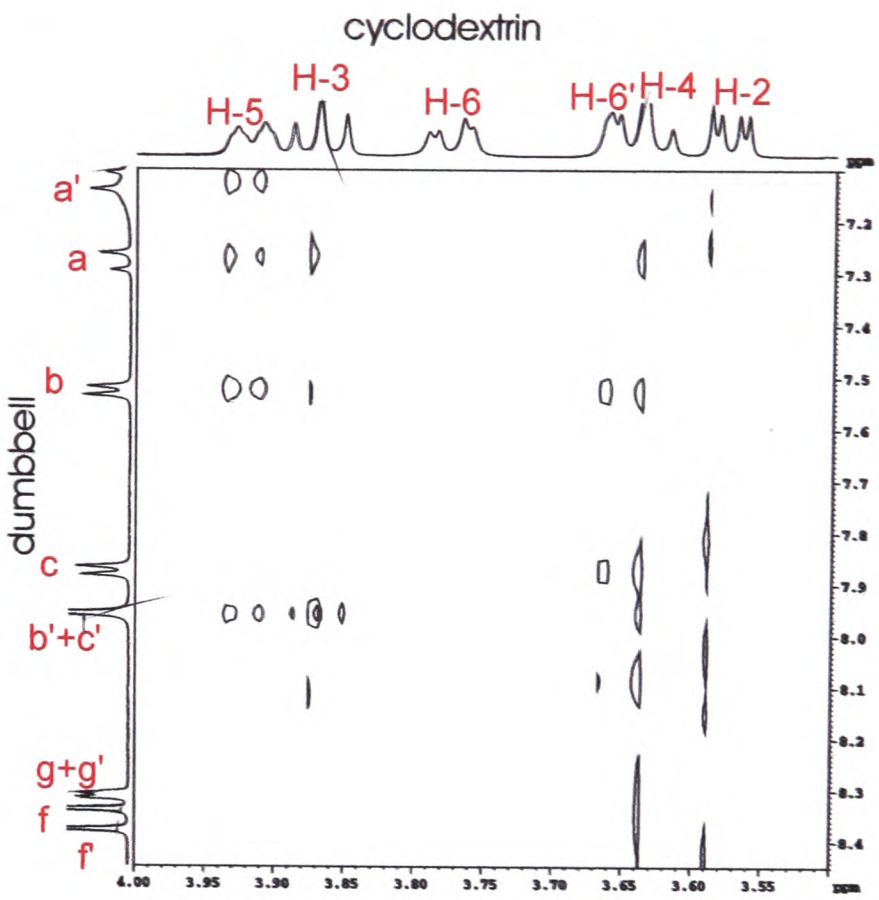

Figure 2.6. *Expansion of NOESY spectrum of the rotaxane* ***40⊂α-CD*** *with assignments, showing the cyclodextrin-dumbbell interactions.*

Table 2.3. *Summary of NOEs seen in the rotaxane* ***40⊂α-CD*** *between aromatic core and cyclodextrin components.*

	f	c	b	a	a'	b'	c'	f'
3				W	W	W	S	W
5		M	W	M	M	S	S	
6/6'		M	W	W	W	W	W	

S = strong interaction, M = medium strength interaction, W = weak interaction.

The fact that NOEs are observed between the dumbbell and cyclodextrin unit implies that they must be held in quite close proximity to each other. The wide range

of near protons observed, however, cannot be accounted for by any single conformation which could be adopted by the molecule. This indicates a large degree of mobility of the cyclodextrin unit, despite the tight fit.

There does appear to be a slight preference for the cyclodextrin binding towards one end of the dumbbell, with the wide 2,3 rim closer to one stopper than the narrower rim is to the other stopper moiety.

2.8.3. Crystal structure of the rotaxane 40⊂α-CD

In order to investigate whether this preference was also seen in the solid state, crystals of the free acid **40⊂α-CD** were grown. This was achieved by heating one end of an NMR tube containing an aqueous, undissolved sample of **40⊂α-CD** to 40 °C, and allowing the rest of the tube to be air-cooled. This created a temperature gradient which slowly dissolved **40⊂α-CD** at the heated end of the tube. This then slowly crystallised in the cooler part of the tube.

Experience within the Anderson group suggests that cyclodextrin-based rotaxanes are difficult to crystallise. When such rotaxanes crystallise at all, it is often with large degrees of disorder, making it virtually impossible to solve any crystallographic data which may be obtained. Indeed, surveys of the literature revealed that although crystal structures of cyclodextrin inclusion complexes had previously been solved[37-41], as had non-cyclodextrin based rotaxanes[42-44], no crystal structure of a cyclodextrin based rotaxane had ever been published. The crystal structure of **40⊂α-CD**, solved by William Clegg[45] using synchrotron X-rays at Daresbury station 9.8, can be seen in Figure 2.7. Data can be found in Appendix 2.1.

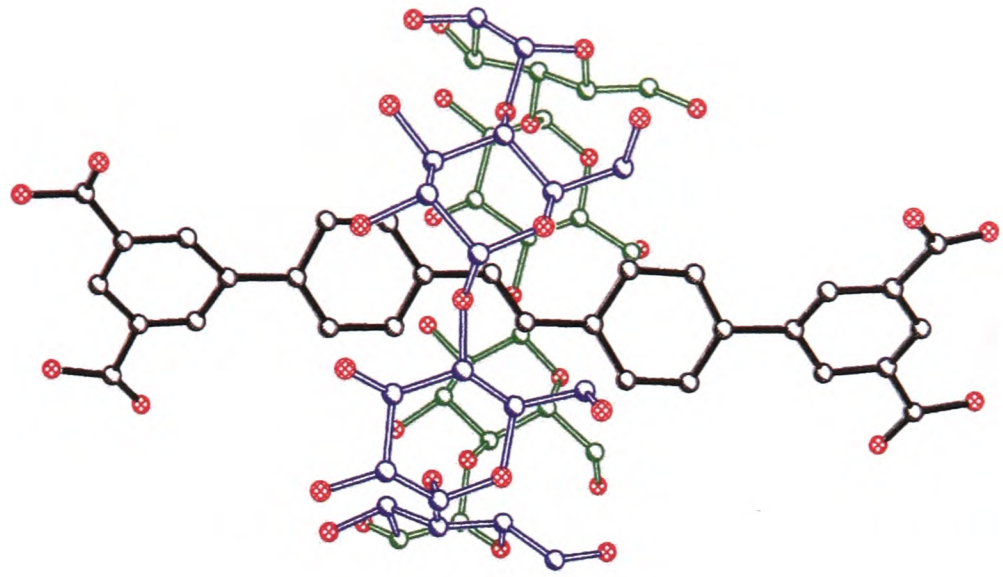

Figure 2.7. *Side view of* ***40⊂α-CD*** *from the crystal structure.*

In this system there is a large amount of disorder resulting in a relatively high R-factor (0.168). This is probably due to the large amount of water present in the crystal. The side view clearly shows the position of the cyclodextrin upon the dumbbell unit in the solid state; over the alkene. The biphenyl rings are twisted by 29^{o} and 24^{o} at the 6-rim side and 2,3-rim sides respectively, however the rest of the stilbene is essentially planar. This proves that the dumbbell is not put under any significant strain upon encapsulation. Despite this, however, the end-on view (Figure 2.8) demonstrates the distortion present in the system.

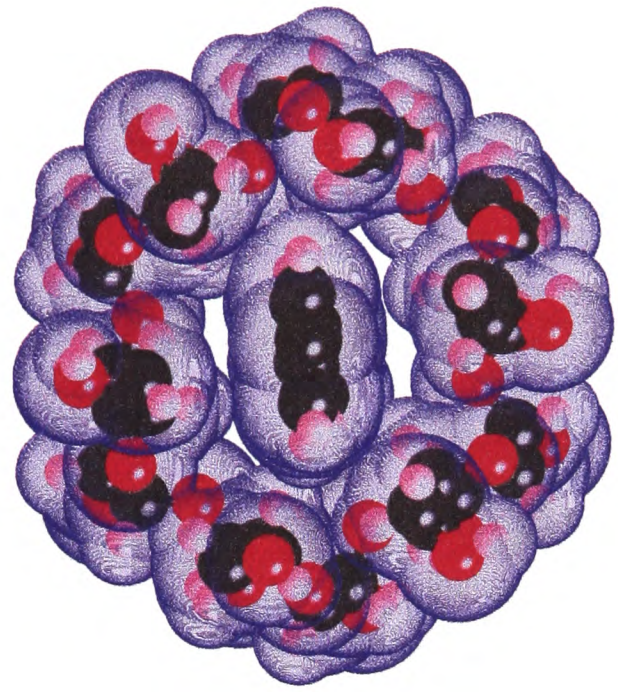

Figure 2.8. *End-on view of* ***40⊂α-CD*** *in crystal structure viewed from the 6-rim end, stopper units are removed for clarity.*

This view emphasises the distension of the cyclodextrin molecule necessary to encompass the aromatic core. The longest transannular distance (H5 to H5) is 5.3 Å, whereas others are 4.3 Å and 4.0 Å. This indicates that the cyclodextrin has a high degree of flexibility as, despite the deformity required, the rotaxane formation is high yielding (73 %). Furthermore, ^{1}H and ^{13}C NMR spectra in D_2O show only one environment for each of the 6 glucose units, implying that the cyclodextrin spins in a free and dynamic manner about the dumbbell core. This is fast on the NMR timescale at room temperature.

2.9. Conclusions of Chapter 2

A range of building blocks have been synthesised with the aim of producing a range of rotaxanes and their corresponding dumbbells *via* Suzuki coupling. This range has then, for the most part, been successfully synthesised in moderate to good yield. The reaction conditions have been optimised in terms of temperature and concentration used, and ideal conditions of 45 °C, 6 equivalents of cyclodextrin, and concentration

of boronic acid of 26 mM have been established. The size complementarities between macrocycle and dumbbell have also been investigated; here it was discovered that acetylene units display the best size complementarity for α-cyclodextrin, while β-cyclodextrin shows only medium to poor complementarity for all dumbbells tested. The rotaxanes prepared have been characterised, in particular by the use of NMR techniques. Comparison of ^{1}H NMRs within a series (consisting of a dumbbell **39** and two rotaxanes, **39⊂α-CD** and **39⊂β-CD**) has been carried out, showing significant changes in chemical shift and splitting upon encapsulation. The through-space interactions have also been fully investigated for one of the rotaxanes, **40⊂α-CD**. These are important as they show incontrovertibly that the cyclodextrin is non-covalently bonded onto the dumbbell.

A crystal structure of rotaxane **40⊂α-CD** has been determined; this is the first reported crystal structure of a cyclodextrin-based rotaxane.

References for Chapter 2

[1] J. Szejtli, *Chem. Rev.* **1998**, *98*, 1743.

[2] A. R. Khan, P. Forgo, K. J. Stine, V. T. D'Souza, *Chem. Rev.* **1998**, *98*, 1977 - 1996.

[3] S. D. Taylor, C. L. Kotoris, A. N. Dinaut, M. J. Chen, *Tetrahedron* **1998**, *54*, 1691 - 1714.

[4] R. S. Mali, P. G. Jagtap, *Synth. Commun.* **1991**, 841.

[5] J. I. G. Cadogan, P. W. Inward, *J. Chem. Soc.* **1962**, 4170 - 4178.

[6] H. J. Barber, R. Slack, *J. Chem. Soc.* **1944**, 612 - 614.

[7] H. Suenaga, K. Nakashima, M. Mikami, H. Yamamoto, T. D. James, K. R. A. S. Sandanayake, S. Shinkai, *Recl.Trav. Chim. Pays-Bas* **1996**, *115*, 44 - 48.

[8] J. G. Coutts, H. R. Goldschmid, O. C. Musgrave, *J. Chem. Soc. C* **1970**, 488 - 493.

[9] F. M. Hawthorne, *J. Org. Chem.* **1958**, *23*, 1579 - 1580.

[10] A. Grahl, *Chem. Ber.* **1895**, *28*, 85.

[11] A. F. Littke, G. C. Fu, *Angew. Chem. Int. Ed.* **1998**, *37*, 3387 - 3388.

[12] N. Miyaura, T. Yanagi, A. Suzuki, *Synth. Commun.* **1981**, *11*, 513.

[13] I. P. Beletskaya, *Pure and Appl. Chem* **1997**, *69*, 471 - 476.

[14] J. P. Genet, M. Savignac, *J. Organomet. Chem.* **1999**, *576*, 305 - 317.

[15] F. E. Goodson, T. I. Wallow, B. M. Novak, *Macromolecules* **1998**, *31*, 2047 - 2056.

[16] A. D. Child, J. R. Reynolds, *Macromolecules* **1994**, *27*, 1975 - 1977.

[17] D. Ma, Q. Wu, *Tetrahedron Lett.* **2001**, *42*, 5279 - 5281.

[18] J. M. A. Humphrey, James B.; Chamberlin, A. Richard., *J. Am. Chem. Soc.* **1996**, *118*, 11759-11770.

[19] M. J. Hall, Part II Thesis, Dyson Perrins Laboratory, University of Oxford, Oxford, **2000**.

[20] M. J. O'Connell, Part II Thesis, Dyson Perrins Laboratory, University of Oxford, Oxford, **2000**.

[21] P. N. Taylor, M. J. O'Connell, L. A. McNeill, M. J. Hall, R. T. Aplin, H. L. Anderson, *Angew. Chem., Int. Ed.* **2000**, *39*, 3456-3460.

[22] N. A. Bumagin, V. V. Bykov, I. P. Beletskaya, *Izv. Akad. Nauk., SSSR Ser. Khim.* **1989**, 2394.

[23] M. M. Mañas, M. Perez, R. Pleixats, *J. Org. Chem.* **1996**, *61*, 2346.

[24] E. W. Abel, W. Gerrard, M. F. Lappert, *J. Chem. Soc.* **1958**, 1451.

[25] T. Wanatabe, N. Miyaura, A. Suzuki, *Synlett* **1992**, *3*, 207.

[26] H. G. Kuivila, J. F. Reuwer, J. A. Mangravite, *J. Am. Chem. Soc.* **1964**, *86*, 2666.

[27] H. R. Snyder, J. A. Kuck, J. R. Robinson, *J. Am. Chem. Soc.* **1938**, *60*, 121.

[28] J. R. Johnson, M. G. V. Campen, *J. Am. Chem. Soc.* **1938**, *60*, 121.

[29] T. D. James, K. R. A. S. Sandanayake, S. Shinkai, *Angew. Chem., Int. Ed. Engl.* **1996**, *35*, 1911 - 1922.

[30] M. J. O'Connell, H. L. Anderson, *unpublished work.*

[31] S. Anderson, T. D. W. Claridge, H. L. Anderson, *Angew. Chem., Int. Ed. Engl* **1997**, *36*, 1310 - 1313.

[32] J. Huuskonen, J. E. H. Buston, N. D. Scotchmer, H. L. Anderson, *New J. Chem.* **1999**, *23*, 1245.

[33] H.-J. Schneider, F. Hacket, V. Rüdiger, H. Ikeda, *Chem. Rev.* **1998**, *98*, 1755-1786.

[34] A. Collet, in *Compr. Supramol. Chem., Vol. II* (Ed.: F. Vögtle), Elsevier, Oxford, **1996**, pp. 325-365.

[35] M. Sakurai, H. Hoshi, Y. Inoue, R. Chujo, *Chem. Phys. Lett.* **1989**, *163*, 217.

[36] S. Hamai, T. Ikeda, A. Nakamura, H. Ikeda, A. Ueno, F. Toda, *J. Am. Chem. Soc.* **1992**, *113*, 7717.

[37] A. Arduini, R. Ferdani, A. Pochini, A. Secchi, F. Ugozzoli, *Angew. Chem., Int. Ed.* **2000**, *39*, 3453-3456.

[38] S. Makedonopoulou, I. M. Mavridis, *Acta Crystallogr., Sect. B: Struct. Sci.* **2000**, 322-331.

[39] K. A. Udachin, L. D. Wilson, J. A. Ripmeester, *J. Am. Chem. Soc.* **2000**, *122*, 12375 - 12376.

[40] K. Harata, *Bull. Chem. Soc. Jpn.* **1979**, *52*, 2451-2459.

[41] M. Crisma, R. Fornasier, F. C. N. R. Marcuzzi, *Carbohydr. Res.* **2001**, *333*, 145-151.

[42] S. Anderson, W. Clegg, H. L. Anderson, *Chem. Commun.* **1998**, 2379 - 2380.

[43] S. J. Cantrill, M. C. T. Fyfe, A. M. Heiss, J. F. Stoddart, A. J. P. White, D. J. Williams, *Chem. Commun.* **1999**, 1251-1252.

[44] F. G. Gatti, D. A. Leigh, S. A. Nepogodiev, A. M. Z. Slawin, S. J. Teat, J. K. Y. Wong, *J. Am. Chem. Soc.* **2001**, *123*, 5983-5989.

[45] C. A. Stanier, M. J. O'Connell, W. Clegg, H. L. Anderson, *Chem. Commun.* **2001**, 493 - 494.

Chapter 3; Chemical Reactivity of the Rotaxane

3.1. Introduction

This chapter describes the work undertaken to investigate the relative reactivity of the encapsulated and unencapsulated chromophores. In addition to this, reaction of the whole rotaxane will be investigated. Although many studies of inclusion complexes have shown that chemical reactivity of a guest molecule can be either enhanced or greatly reduced by surrounding it with a host, these studies have rarely been extended to 'permanent' complexes such as rotaxanes or catenanes. An example of one such 'permanent' complex is a carcerand inclusion complex[1], in which a single molecule of cyclobutadiene could be shielded from the external chemical environment by inclusion inside a cage molecule. Another example is the work of Vögtle (shown in Scheme 3.1[2]), in which a less sterically demanding macrocycle than a cyclodextrin retarded bromination rate of an encapsulated alkene.

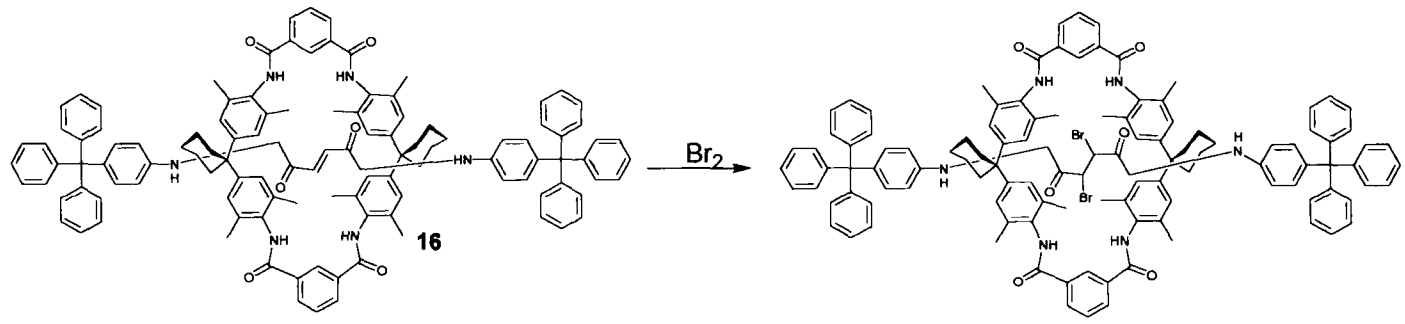

Scheme 3.1. *Vögtle's work on bromination of a rotaxane.*

Previous work in Oxford[3] has shown that encapsulation by rotaxane formation enhanced the stability of an azo dye with respect to both reductive and oxidative bleaching. Many studies[1, 4-6] have shown that encapsulation by a host molecule can reduce the reactivity of the guest; we aim to demonstrate this by the use of a reactive dumbbell component.

These studies centre around the different reactivities of rotaxane **40⊂α-CD** and dumbbell **40**.

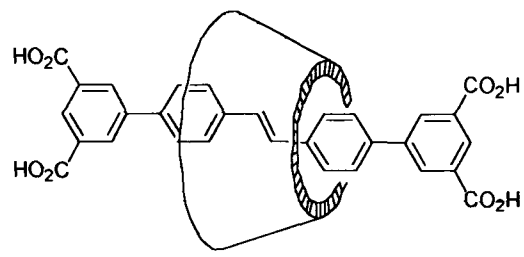

40⊂ α-CD

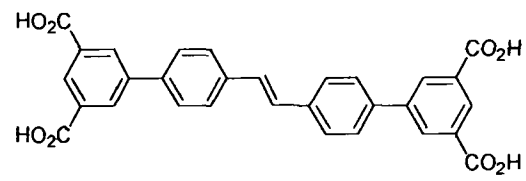

40

This rotaxane and dumbbell pair (shown above) could be synthesised on the largest scale, which enabled more test reactions, and introduced the possibility of characterisation of the reaction products. The stilbene chromophore has a rich and varied chemistry and it is possible to envisage many different potential reactions, including electrophilic or nucleophilic attack on the alkene, oxidations including cleavage of the alkene, electrophilic substitution on the biphenyl rings, cycloadditions involving the alkene and many others. The potential reactivity of the cyclodextrin must also be considered in the design of any test reactions. In general, cyclodextrins are stable to basic or reducing conditions, but they may be cleaved by strongly oxidising or strongly acidic reagents.

3.2. Electrophilic attack on the alkene

By analogy to the work of Vögtle[2], initial attempts at reaction of the alkene core focussed on electrophilic bromination. Vögtle's work was carried out in organic solvents, however we chose to attempt a similar conversion in water, due to the aqueous solubility of these rotaxanes and dumbbells. It should be noted that electrophilic addition of a species of the type X-Y (e.g. BrOH) to the stilbene will desymmetrise the dumbbell unit, forming two chiral centres and leading to the possibility of two different orientations of the cyclodextrin with respect to the core.

3.2.1. Bromination of dumbbell 40

The conditions for bromination were first tested on the dumbbell (Scheme 3.2). This strategy was adopted because we were hoping to prove that the inherent reactivity of the stilbene had been masked by encapsulation. The first step to proving this was the confirmation that reaction could occur in the absence of the cyclodextrin.

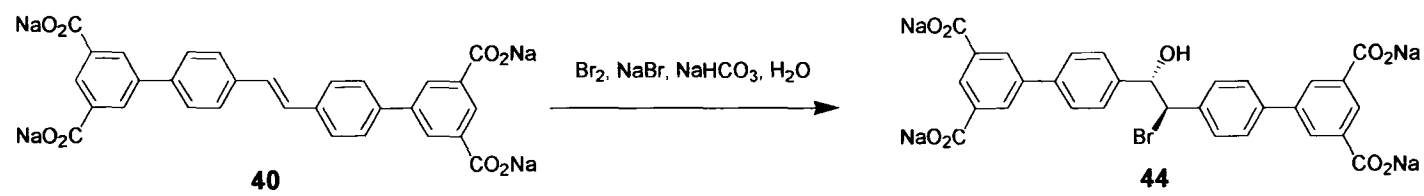

Scheme 3.2. *Bromination of the dumbbell* ***40****.*

We chose to use a mixture of bromine and sodium bromide to act as a water-soluble donor of Br^+. This created an acidic solution in which the carboxylate was insoluble, so sodium bicarbonate was added to buffer the mixture. The reaction was monitored by UV/Vis spectroscopy. After a few hours, there was a noticeably lower absorption at 340 nm (the stilbene peak) in comparison to the absorption at 265 nm, attributed to the biphenyl units. The reaction was deemed to be complete when no absorption at 340 nm could be detected.

The crude reaction mixture contained mass fragments consistent with the desired product (Calculated for bromination product: 559 $[M\text{-}CO_2H]^-$), Found: 561). The pure compound **44** proved impossible to isolate. However, this work illustrates that these reaction conditions are suitable for bromination of the stilbene.

3.2.2. Bromination of rotaxane 40⊂α-CD

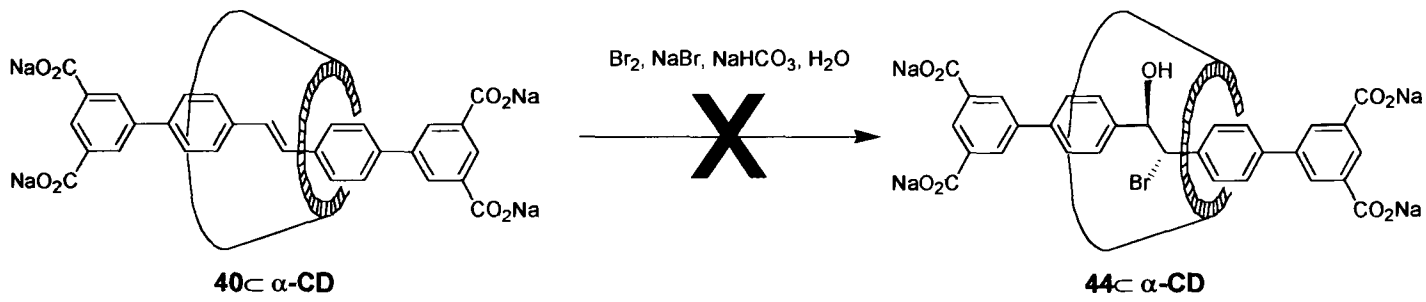

40⊂ α-CD **44⊂ α-CD**

Scheme 3.3. *Attempted bromination of the rotaxane* ***40⊂α-CD*** *and expected product.*

Bromination of the rotaxane **40⊂α-CD** was tested using identical conditions to those used with the dumbbell (Scheme 3.3). Initial monitoring by UV/Vis spectroscopy suggested that the reaction may indeed have been successful, as destruction of the stilbene chromophore was seen with time, indicated by a steady reduction in the absorption at 347 nm. However, upon work up by ultrafiltration to remove salts and fragments of small molecular weight, the ^{1}H NMR was complex. Electrospray mass spectrometry (negative mode) revealed that the cyclodextrin was still attached to the dumbbell core. The mass of the molecular ion was 18 a.m.u. less than that expected for **44⊂α-CD**, but still contained bromine, as demonstrated by the isotope pattern. This led us to propose a reaction between the cyclodextrin and dumbbell components, leading to **45**.

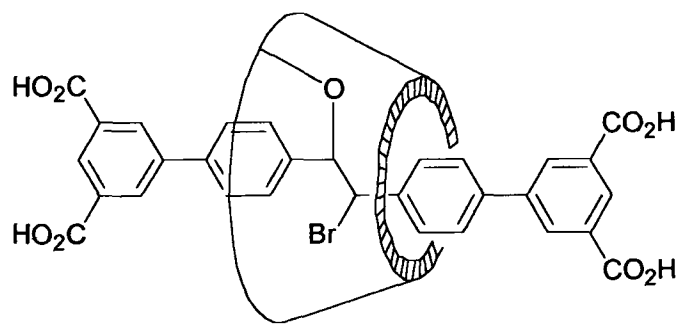

45

The formation of **45** would proceed *via* a bromonium ion intermediate, however the high effective molarity of cyclodextrin hydroxyls in close proximity to the bromonium intermediate implies that these may act as the nucleophiles instead of

the expected hydrolysis. It should also be taken into consideration that the cyclodextrin hydroxyls have a lower pKa than that of water (the most acidic is the hydroxyl in the 2 position[7] with a pKa of 12.3). This means that the attacking species is more likely to be the conjugate base, the cyclodextrin hydroxide. An analogy can also be drawn between the proposed product **45** and work by Vögtle[8], in which he described **46** (Figure 3.1) and such species as '[1]rotaxanes'.

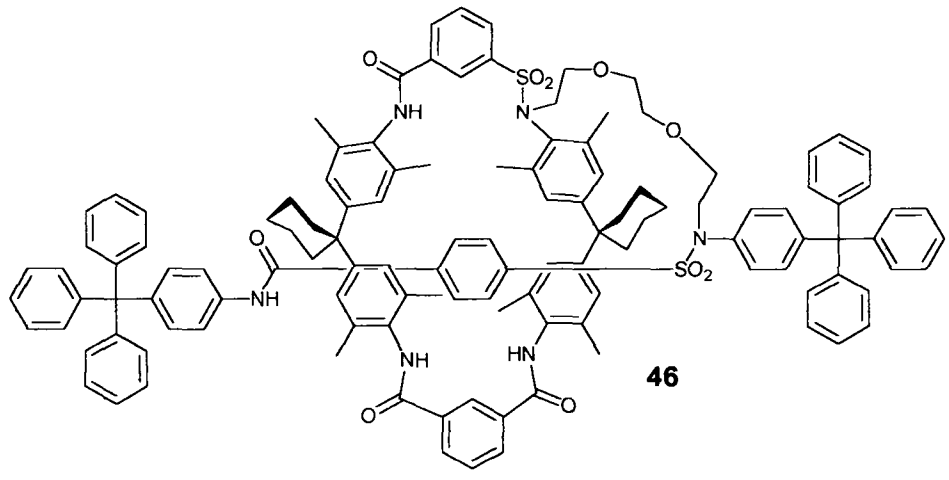

46

Figure 3.1. *Vögtle's [1]rotaxane[8], also prepared from a [2]rotaxane starting material.*

It is to be expected that **45** would appear complicated in the ^{1}H and ^{13}C NMR spectra, due to the fact that tethering the cyclodextrin prevents the previous free, rapid spinning of the macrocycle around the dumbbell core. Each sugar unit of the α-cyclodextrin would appear different in the NMR, making assignments extremely difficult. This may potentially be further complicated by the presence of two different isomers, with different orientations of the cyclodextrin relative to the core, which is desymmetrised by bromination. Given the fact that there are three chemically different hydroxyl groups (2, 3, and 6 positions, shown in Figure 3.2), all of which could act as nucleophiles, it is clear that there are many different potential isomers of **45**.

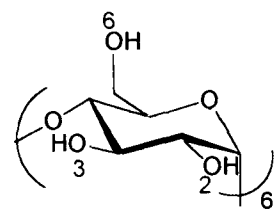

Figure 3.2. *α-Cyclodextrin, showing the different positions of hydroxyl groups.*

The 2 position is the most easily deprotonated, however CPK models indicate that the 6 hydroxyl is better placed to attack from a steric respect. Even supposing that the reaction mixture were uncontaminated by other species, it is unlikely that purification would be possible, as all species would be very similar. Work continued with the crude mixture, in the hope of identifying some of the species present.

2D NMR techniques did throw some light on this matter. HSQC correlations between protons at 5.65 – 5.33 ppm (shown in red in Figure 3.3) and carbons at 50 ppm indicated the presence of a benzylic alcohol or ether of the form shown in Figure 3.3.

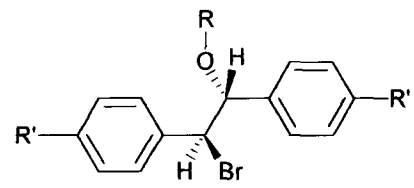

Figure 3.3. *Suggested structure from HSQC.*

Unfortunately, subjecting α-cyclodextrin to the bromination conditions in place of the rotaxane **40⊂α-CD** showed by ^{1}H NMR that the cyclodextrin itself is not completely stable to these conditions and may fragment. This could also account for some of the complex signals in the ^{1}H NMR, although the extensive ultrafiltration in the work-up would have removed all but the largest of such fragments. For this reason, this initial area of study was abandoned and other, less destructive reagents sought.

3.2.3. Epoxidation of dumbbell 40

Epoxidation is another common reaction of alkenes. The choice of epoxidising agent was governed by two factors: firstly, the dumbbell unit must react with the epoxidising agent and secondly, the epoxidising agent must not react with the cyclodextrin, in order to avoid the problems seen in the bromination studies. The first of these two criteria proved to be the greater problem in this case, as many standard epoxidising agents such as hydrogen peroxide and peracetic acid had no effect upon the dumbbell unit. *meta*-Chloroperbenzoic acid was not tested, being insoluble in water. Recent work on dimethyl dioxirane[9, 10] suggested that this might be effective and this proved to be the case.

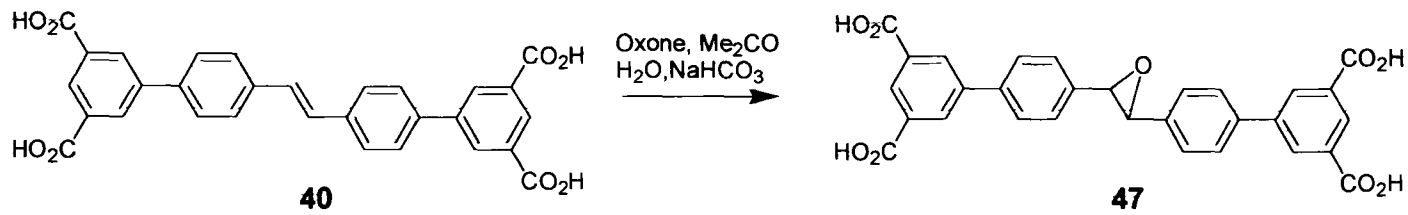

40 **47**

Scheme 3.4. *Epoxidation of the dumbbell* ***40*** *with dimethyl dioxirane.*

Dimethyl dioxirane is formed *in situ* from the action of oxone (a highly oxidising potassium salt; $2KHSO_5.KHSO_4.K_2SO_4$) on acetone. The reaction, shown in Scheme 3.4, appears to work best in basic solution, which is ideal for the solubility of these compounds. However, dimethyl dioxirane does decompose to acetone on standing over long periods of time, or when the temperature is raised above 5 °C. It was therefore important to check for the presence of oxidant in the reaction mixture by use of starch-iodine paper, topping up the oxone as necessary, in addition to monitoring the reaction by UV/Vis spectroscopy.

Destruction of the stilbene chromophore was seen, in much the same manner as observed during the bromination reaction (reduction in absorption at 340 nm). The crude ^{1}H NMR indicated the presence of more than one aromatic species suggesting that, although reaction had occurred, it had not done so cleanly. MALDI-TOF mass spectrometry revealed that the epoxide **47** was present. However, there was also some diol present in the mixture, presumably resulting from addition of hydroxide to the epoxide, and some other species which appeared to be double bond cleavage products such as aldehydes (calculated mass ion for aldehyde: 258.2, found: many peaks around 284 – 255). Purification again proved to be problematic but as it was clear that the dimethyl dioxirane had reacted with the dumbbell **40** in the expected fashion, the more important issue was the investigation of the rotaxane under these epoxidation conditions.

3.2.4. Attempted epoxidation of rotaxane 40⊂α-CD

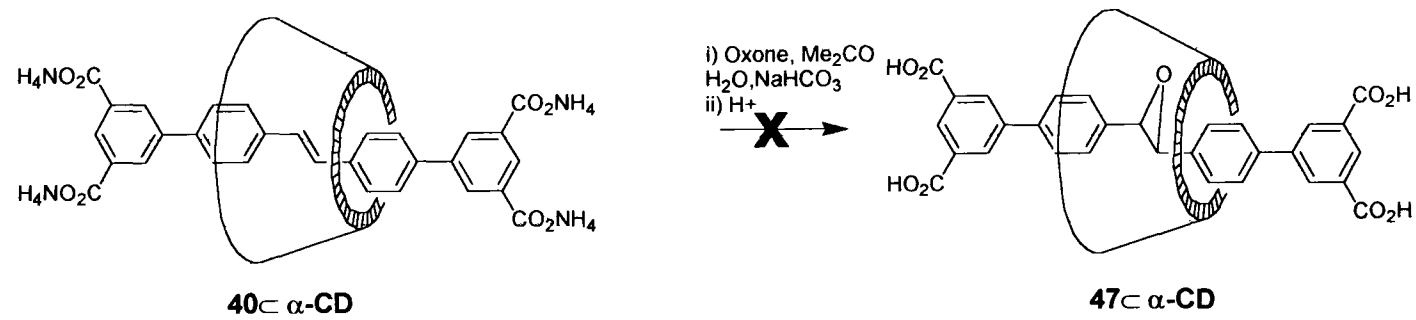

40⊂ α-CD **47⊂ α-CD**

Scheme 3.5. *Attempted epoxidation of the rotaxane* ***40⊂α-CD.***

The rotaxane **40⊂α-CD** was subjected to the same conditions used in the epoxidation of the dumbbell **40** (detailed in Scheme 3.5). In this case, however, no change was seen in the UV/Vis spectrum after 120 hours, despite regular replenishment of the oxidant. Work-up of the reaction yielded only the rotaxane **40⊂α-CD**, characterised by ^{1}H NMR.

Dimethyl dioxirane is a relatively small molecule in comparison to many reactive species, and there can be no doubt that this result proves that a high degree of protection is afforded by encapsulation with α-cyclodextrin.

3.3. Reaction on a surface; hydrogenation

In Vögtle's work[2] on reactivity of rotaxanes *vs.* dumbbells, the macrocycle (a cyclophane) slowed, but did not prevent, the hydrogenation of their stilbenoid chromophore (**16**). The aim of this work is to demonstrate the greater protective ability of cyclodextrins, due to their greater bulk. Hydrogenation on a surface is a common reaction of alkenes, and one which again destroys their conjugation and therefore removes the properties we are interested in.

3.3.1. Hydrogenation of dumbbell

Once again, the conditions of reaction were tested on the dumbbell **40** before attempting reaction with the rotaxane **40⊂α-CD**. The conditions used were typical for this type of reaction, and are shown in Scheme 3.6.

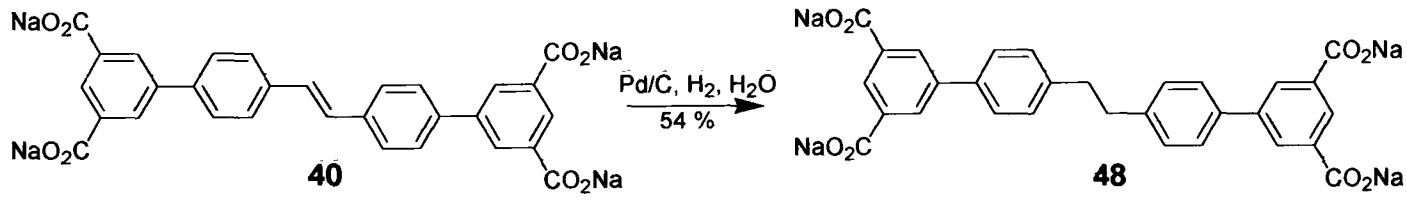

Scheme 3.6. *Hydrogenation of the dumbbell **40** on a surface.*

The sodium salt of the dumbbell **40** was stirred with 5 mol % of the palladium catalyst under a hydrogen atmosphere. The destruction of the chromophore was observed by UV/Vis spectroscopy in a similar manner to previous reactions. In this instance the isolation of the hydrogenation product did prove possible, albeit in a much lower yield than the crude ^{1}H NMR suggested. This was achieved by filtration

to remove the activated carbon, followed by precipitation of the hydrogenation product **48** on addition of acid. This low yield may be due to the increased solubility of the hydrogenated form of the dumbbell over the more conjugated form, causing more to be left in solution during the acidic precipitation stage of the work-up. This experiment demonstrates the suitability of the conditions used for this reaction of the dumbbell unit. We therefore moved on to investigate the hydrogenation of the encapsulated form of the dumbbell.

3.3.2. Attempted hydrogenation of rotaxane

Having ascertained that the dumbbell would react under these conditions, the aim was to prove that the rotaxane was unable to react, or would react more slowly under the hydrogenation conditions.

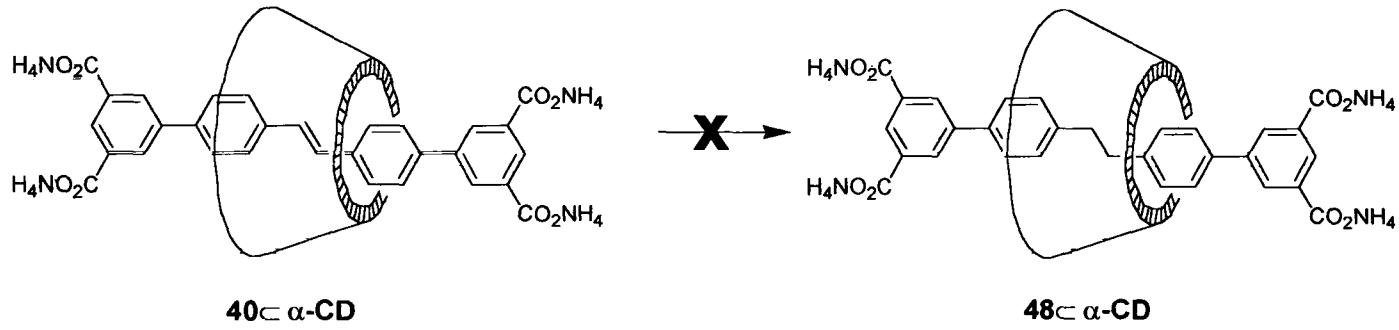

Scheme 3.7. *Attempted hydrogenation of the rotaxane* ***40⊂α-CD****.*

All attempts at hydrogenation of **40⊂α-CD** under these conditions (Scheme 3.7) were unsuccessful. This proves incontrovertibly that the cyclodextrin provides a high degree of protection for the dumbbell component, at least under conditions to which the cyclodextrin itself is stable. Initial attempts stirring the rotaxane under normal laboratory lighting did lead to small changes in the UV/Vis spectrum which appeared similar to the changes expected for chromophore destruction (lowering of absorption at 347 nm and a simultaneous rise at ~265 nm). However, the absorption

was never completely destroyed at 347 nm and work-up of these reactions and subsequent NMR analysis showed that another aromatic system had appeared, without any appearance of hydrogenation product. A suspicion that this might be due to a photo-induced reaction of the stilbene was confirmed by carrying out the same procedure in the dark; on this occasion no change was observed in either UV/Vis or ^{1}H NMR spectra. This interesting observation is further explored in Chapter 5.

The failure to hydrogenate the dumbbell once it had been encapsulated is a success in terms of protection of the chromophore. We have demonstrated the complete protection of the dumbbell from external chemical attack, both under these conditions and in the epoxidation reaction. This protection is naturally limited to reagents which do not destroy the cyclodextrin. However, as the cyclodextrin is considerably different to the dumbbell in its structure and reactivity, the degree of protection afforded is significant. Even in cases where the cyclodextrin does react, there is likely to be some hindrance of the reaction, in the form of sacrificial protection.

3.4. Attempted unthreading of rotaxane

Previous work has been carried out on the 'deslipping' or 'unthreading' of rotaxanes. This involves studies into the exact size of stopper required to hold the dumbbell unit within the macrocycle[11, 12], and investigations into the alteration of environment e.g. solvent[13-15] or temperature[16]. Through working with the rotaxanes it was already obvious that they did not unthread at ambient temperature in any of the limited solvents in which they were soluble (water, aqueous base, DMSO, DMF,

methanol). It was therefore interesting to explore the possibility of unthreading at elevated temperature.

Of the rotaxanes synthesised in Chapter 2, **40⊂α-CD** has the smallest stopper. For this reason, **40⊂α-CD** was chosen as the best rotaxane on which to perform the unthreading experiment initially. It was already known (see Chapter 2) that this dumbbell (**40**) did not form a rotaxane with β-cyclodextrin, which may imply that the stoppers are only just big enough to hold the smaller α-cyclodextrin in place (α-cyclodextrin has an internal diameter of 4.7-5.3 Å, while β-cyclodextrin has a larger diameter of 6.0-6.5 Å[17]). CPK models suggested that, while difficult, it may be possible to unthread the dumbbell from the cyclodextrin, as depicted in Scheme 3.8.

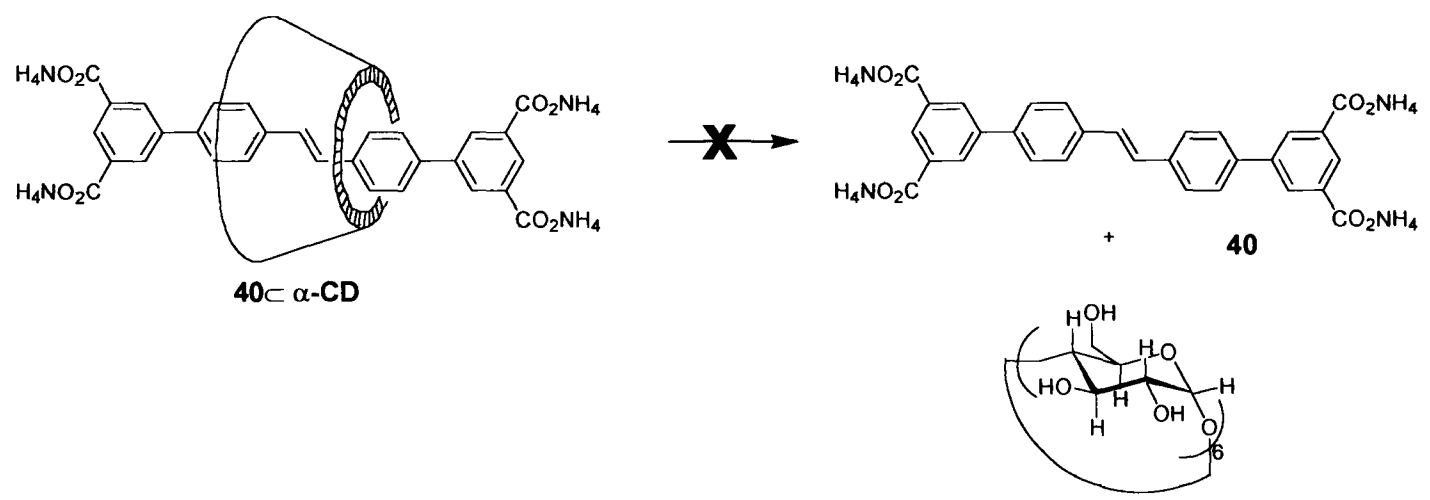

Scheme 3.8. *Attempted unthreading of the rotaxane* ***40⊂α-CD****.*

Extensive attempts were made to unthread the rotaxane **40⊂α-CD**. The samples were observed by ^{1}H NMR, and unthreading was attempted in both heavy water (80 °C) and deutero-DMSO (80 °C and 120 °C). Neither sample showed any signs of unthreading after prolonged periods of heating (several weeks); from this it must be concluded that the stoppers are large enough to prevent unthreading, even at elevated temperature. Therefore, no experiments were undertaken with the larger naphthyl stoppered rotaxanes.

3.5. Methylation of rotaxane

From the evidence of the previous experiments, it is clear that the reactivity of the hydroxyl groups on the cyclodextrin is of some importance in the protective strategy. Masking these reactivities in some way would, therefore, be a useful exercise. If it were possible to synthesise rotaxanes with a less reactive macrocycle, more varied chemistry could be attempted upon the stilbene core (for example, the bromination could be repeated without the complication of the cyclodextrin hydroxyls acting as a nucleophile). However, the protecting group must be small, as CPK models showed that there was not much space around the cyclodextrin. Attempts to synthesise such species directly by substituting permethylated or dimethylated (2,6 permethylated) α-cyclodextrin for α-cyclodextrin in the synthetic route proved unsuccessful; all that could be isolated from these mixtures was free dumbbell. This evidence indicates that the methylated cyclodextrins do not bind the dumbbell well. For this reason, we turned to another approach. If it were not possible to methylate the cyclodextrin and subsequently encapsulate the dumbbell, it may still be viable to encapsulate and then methylate. This method involves methylation of the rotaxane itself, without attacking the double bond. This could be achieved by use of the same conditions required to synthesise permethylated α-cyclodextrin (TM α-cyclodextrin).

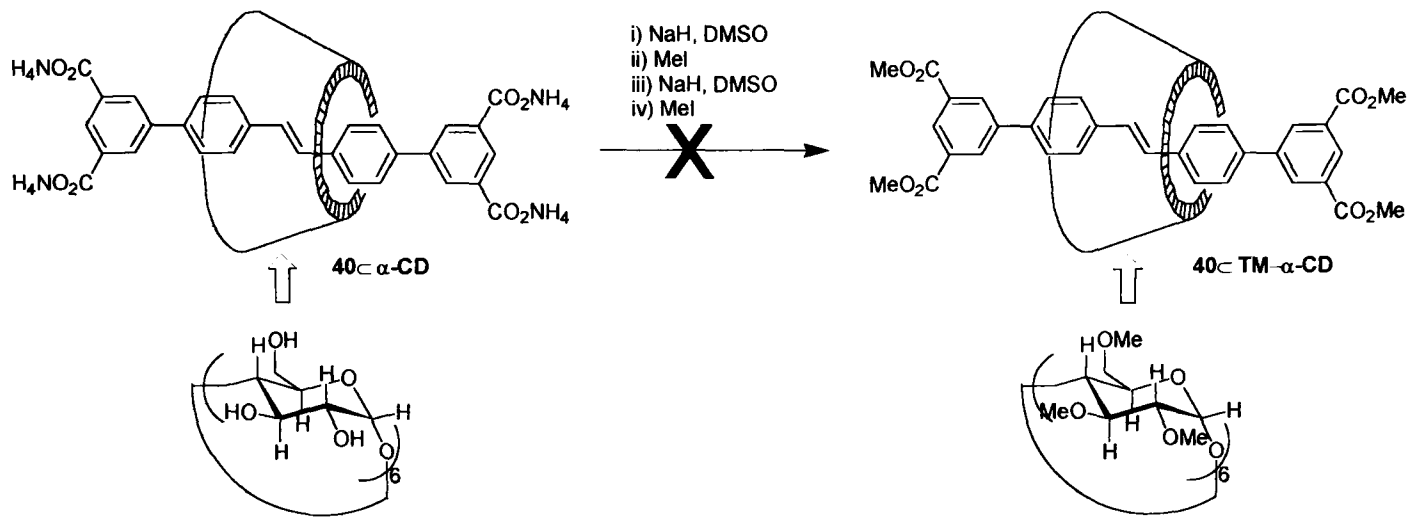

Scheme 3.9. *Methylation of the rotaxane* ***40⊂α-CD****.*

Scheme 3.9 portrays the intended route to the permethylated rotaxane **40⊂TM-α-CD**. The dimsyl anion formed by action of sodium hydride on the DMSO is a strong enough base to deprotonate every hydroxyl on the cyclodextrin. Addition of methyl iodide at this point should methylate every deprotonated site. The procedure was repeated in order to ensure complete methylation. This procedure results in good yields of cleanly methylated product when used on unbound cyclodextrin. However, in this case the crude ^{1}H NMR was extremely complex and the methylation did not appear to have gone to completion. Even after re-subjection to the methylation conditions, there was no improvement. This method is extremely effective at permethylation under normal circumstances, therefore the logical conclusion to be drawn from this result is that there was not enough space around the cyclodextrin once it was non-covalently bound to a guest, and complete methylation could not occur. This is substantiated by the initial result that rotaxanes do not form from these dumbbells and permethylated cyclodextrins. The methyl groups are too bulky or change the structure of the cyclodextrin sufficiently to ensure that binding cannot occur, neither can complete methylation occur if the target molecule is approached from the other direction.

3.6. Conclusions of Chapter 3

This chapter has demonstrated the level of protection for the alkene core of rotaxane **40⊂α-CD** from chemical stimuli afforded by α-cyclodextrin. This has been achieved by comparison of the reactions of the rotaxane **40⊂α-CD** and the dumbbell **40** with various reagents. The range of these reactions encompasses electrophilic bromination (in direct comparison with previous work[2]), epoxidation and hydrogenation. It has been proven that, in the latter two cases, the cyclodextrin does indeed provide complete shielding from the reactive species. In the case of bromination, the cyclodextrin itself becomes an active component of the reaction. We have shown that, unlike other rotaxanes[16], **40⊂α-CD** will not unthread when subjected to extended periods of heating; in fact, no visible changes occurred. Attempts to modify the cyclodextrin *in situ* around the aromatic core were unsuccessful; this was attributed to steric inhibition.

Overall, we have proven that the cyclodextrin provides excellent protection for the aromatic core in some instances, and struggled with the problem of the inherent reactivity of the hydroxyl groups on the cyclodextrin. This is an area which it would be useful and informative to investigate in the future. It would be interesting to find a method of reducing the reactivity of the macrocycle, such that it would provide even more protection for the stilbene core. This cannot, however, be achieved by permethylation of the cyclodextrin, as we have proven that this is too sterically demanding to be possible with the stilbene dumbbell.

References for Chapter 3

[1] J. C. Sherman, *Tetrahedron* **1995**, *51*, 3395.

[2] A. H. Parham, B. Windisch, F. Vögtle, *Eur. J. Org. Chem.* **1999**, 1233 - 1238.

[3] M. R. Craig, M. G. Hutchings, T. D. W. Claridge, H. L. Anderson, *Angew. Chem. Int. Ed.* **2001**, *40*, 1071 - 1073.

[4] D. J. Cram, M. E. Tanner, R. Thomas, *Angew. Chem. Int. Ed. Engl.* **1991**, *30*, 1024.

[5] M. Ziegler, J. L. Brumaghim, K. N. Raymond, *Angew. Chem., Int. Ed.* **2000**, *39*, 4119 - 4121.

[6] S. K. Korner, F. C. Tucci, D. M. Rudkevich, T. Heinz, J. Rebek Jr., *Chem.-Eur. J.* **2000**, *6,* 187 - 195.

[7] A. R. Khan, P. Forgo, K. J. Stine, V. T. D'Souza, *Chem. Rev.* **1998**, *98*, 1977 -1996.

[8] R. Jäger, F. Vögtle, *Angew. Chem. Int. Ed. Engl.* **1997**, *36*, 930 - 944.

[9] R. W. Murray, M. Singh, *Org. Synth.* **1997**, *74*, 91-100.

[10] M. Frohn, Z.-X. Shi, Y. Wang, *J. Org. Chem.* **1998**, *63*, 6425-6426.

[11] G. M. Hübner, G. Nachtsheim, Q. Y. Li, C. Seel, F. Vögtle, *Angew. Chem. Int. Ed.* **2000**, *39*, 1269 - 1272.

[12] F. M. Raymo, K. N. Houk, J. F. Stoddart, *J. Am. Chem. Soc.* **1998**, *120*, 9318 - 9322.

[13] M. Montalti, *Chem. Commun.* **1998**, 1461-1462.

[14] A. l. Credi, V. Balzani, S. J. Langford, J. F. Stoddart, *J. Am. Chem. Soc.* **1997**, *119*, 2679-2681.

[15] A. Harada, J. Li, M. Kamachi, *Nature* **1993**, *364*, 516-518.

[16] M. Craig, DPhil Thesis, Dyson Perrins Laboratory, University of Oxford (Oxford), **2001**.

[17] J. Szejtli, *Chem. Rev.* **1998**, *98*, 1743.

Chapter 4; Photophysical properties

4.1. Factors affecting absorption and emission spectra

There are many factors that may affect absorption and emission spectra of organic chromophores. In this work, we aim to investigate the changes upon encapsulation of a dumbbell-shaped dye molecule inside a macrocycle. In many cases, it has been proven that inclusion of a chromophore can change both absorption and fluorescence characteristics of the complexed species. Changes in absorption can mainly be attributed to the well documented effect of solvatochromism[1, 2], which involves a change in the polarity of the chromophore environment. Changes in aggregation are also important.

There are many reported examples of the alteration in degree of aggregation by encapsulation. Aggregation may be increased, especially in larger cavities[3, 4] such as those of β- or γ-cyclodextrins. More usually it may be decreased, as seen in work by Willner on thionin[5] and Rhodamine B[6]. In these examples, the encapsulation of the chromophores alters both the intensity of absorption and its wavelength. Thionin absorbs at 598 nm, however an increased concentration of thionin normally leads to increased aggregation, and a new absorption peak at 558 nm due to the aggregates. Addition of β-cyclodextrin by Willner caused dispersion of the aggregates, which in turn caused an increase in absorption at 598 nm and a decrease at 558 nm.

The emission spectra of organic molecules may also be affected by aggregation and solvent. In addition, two other considerations may change the emission quantum yield. These are the prevention of solvent quenching by protecting the excited state from solvent molecules (often water), and the stabilisation of the excited state by rigidification.

These effects are more difficult to measure than the previously described effects of aggregation and solvent polarity. The effect of rigidification can be more easily appreciated by comparison of, for example, ring *vs.* open-chain chromophores[7], where rigidification has been shown to enhance fluorescence quantum yield. This is due to a reduction in the number of vibrational non-radiative decay pathways which can be followed by an excited molecule. It seems likely that encapsulation could also rigidify a complexed molecule.

Solvent quenching has been studied alongside solvatochromic effects (which could also play a part here, as the cyclodextrin cavity will be less polar than the surrounding aqueous solvent[8, 9]).

All of these factors could be expected to alter the absorption and emission spectra in some way. This chapter aims to investigate the changes in these properties upon encapsulation, and to rationalise them with respect to the literature.

4.2. Absorption and Emission Spectra

These were measured in aqueous solution (pH ~10 aqueous solution in the case of the carboxylates **40** and **40⊂α-CD**) as this was the best solvent for all compounds. Shown below are the absorption and emission spectra of each series of dumbbell and rotaxane(s). It is particularly interesting to note the changes in the spectra upon encapsulation. All spectra are shown normalised, as intensities will be discussed in Section 4.2.5. The fluorescence spectra are shown PMT-corrected.

4.2.1. Stilbene carboxylates

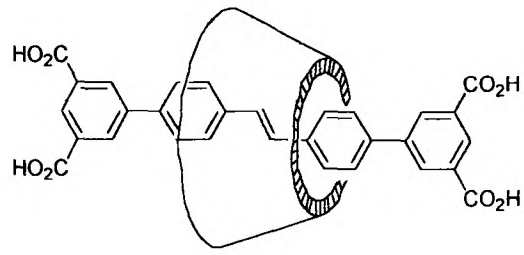

40⊂ α-CD

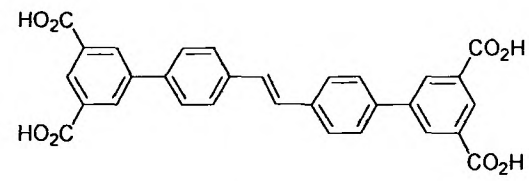

40

Figure 4.1 portrays the absorption spectra of rotaxane **40⊂α-CD** and dumbbell **40**.

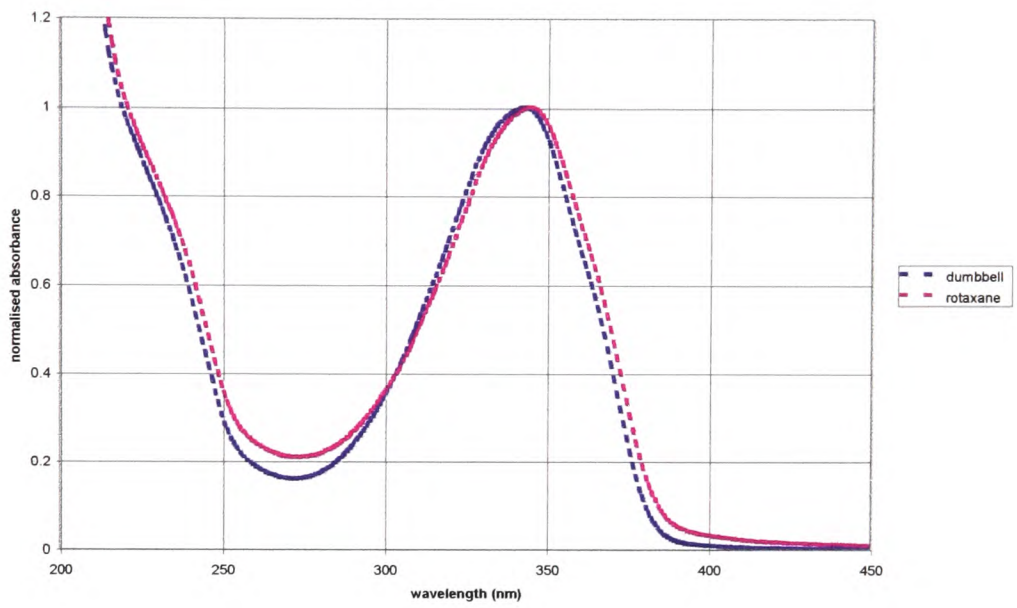

Figure 4.1. *UV absorption spectra of rotaxane* ***40⊂α-CD*** *and dumbbell* ***40****, in pH ~9 NaOH/H_2O, conc. ~0.02 mmol l^{-1}.*

In this case there is little difference between the absorption spectra of the dumbbell **40** and the rotaxane **40⊂α-CD**. The rotaxane shows a slight bathochromic (red) shift with respect to the dumbbell; this may be explained by a solvatochromic effect induced by the less polar environment of the cyclodextrin relative to water.

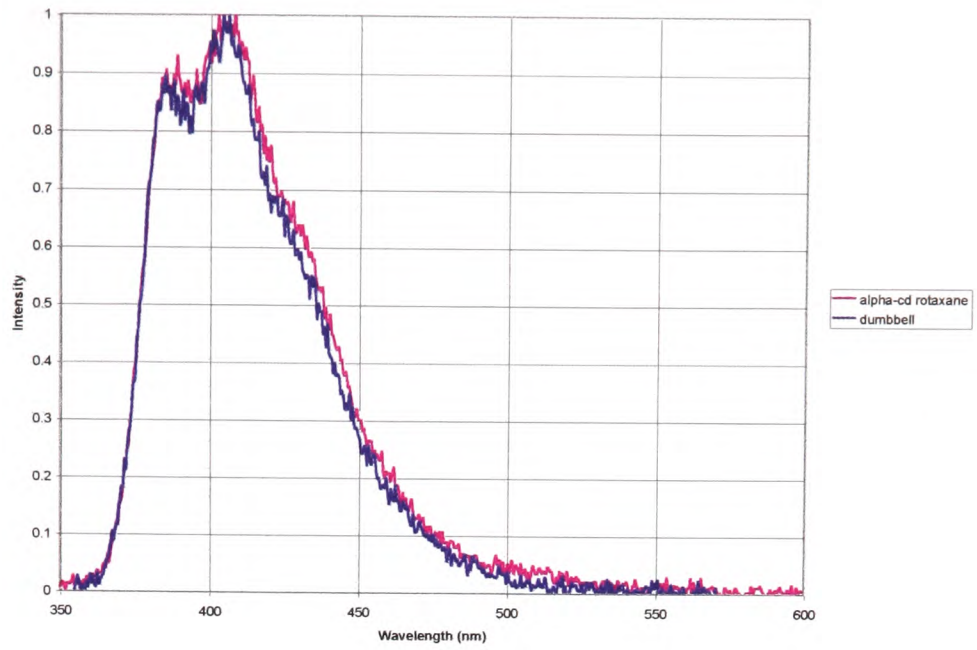

Figure 4.2. *Normalised emission spectra of rotaxane* ***40⊂α-CD*** *and dumbbell* ***40****,* λ_{ex}*=347/340 nm, respectively, conc~1.2 µmol* l^{-1} *in pH ~9* $NaOH/H_2O$*.*

In the emission spectrum (Figure 4.2), there is again little difference between the shapes of the dumbbell **40** and rotaxane **40⊂α-CD** spectra. It would seem that in the case of this dumbbell, neither hydrophobicity nor aggregation play a large part in the shape of the emission spectrum.

4.2.2. Naphthyl stilbenes

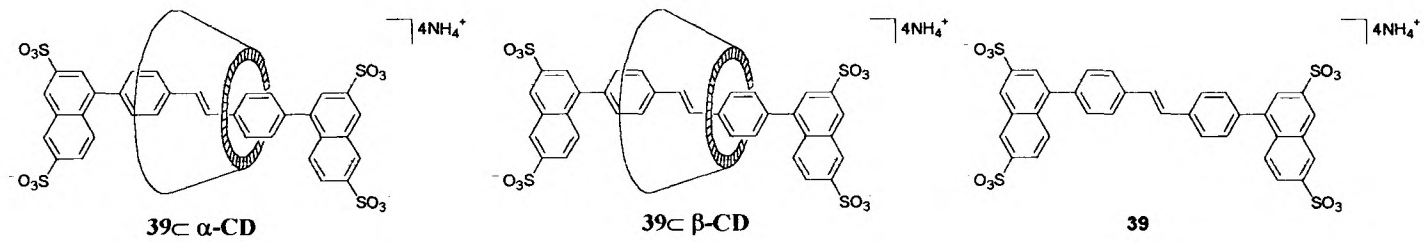

The three napthyl stilbenes under consideration (**39⊂α-CD**, **39⊂β-CD** and **39**) are shown above. In this case again, there is very little difference in the UV/Vis spectra of all three compounds (Figure 4.3), except the relative intensities of the lower wavelength peak (~230 nm) to that at 340 nm.

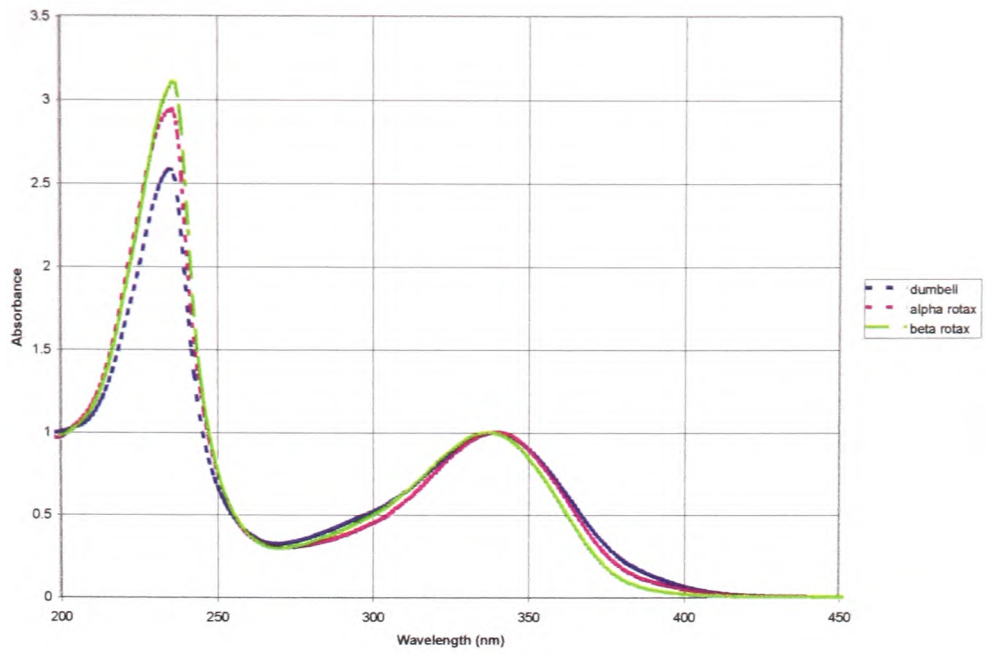

Figure 4.3. *UV absorption spectra of rotaxanes* ***39⊂α-CD*** *and* ***39⊂β-CD,*** *and dumbbell* ***39,*** *in* H_2O*, conc. ~0.02 mmol* l^{-1}.

However, the change in emission upon encapsulation even with the larger β-cyclodextrin is clear to see in Figure 4.4.

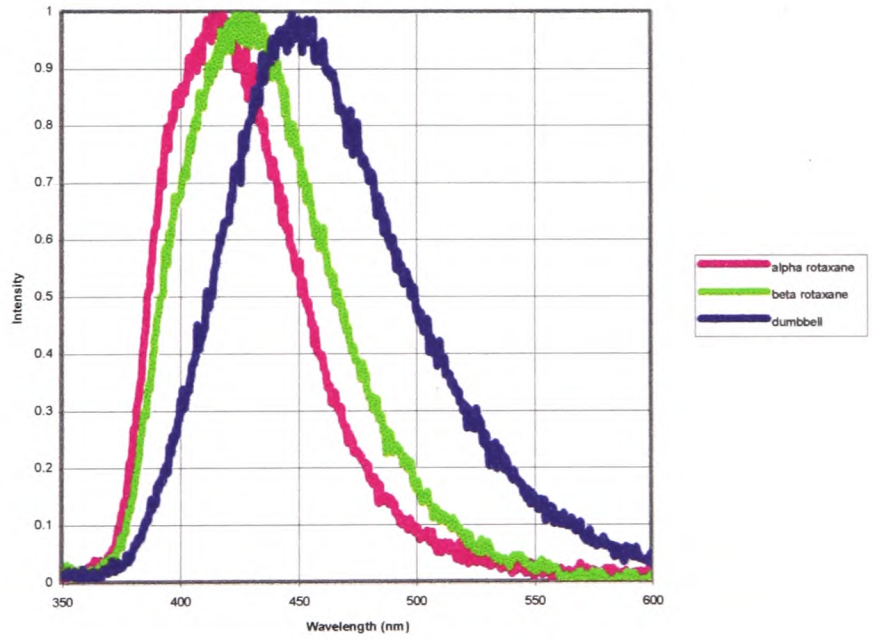

Figure 4.4. *Normalised emission spectra of rotaxanes* ***39⊂α-CD*** *and* ***39⊂β-CD,*** *and dumbbell* ***39,*** λ_{ex}*=341, 331, and 338 nm, respectively, conc~1.2 μmol* l^{-1} *in* H_2O.

The dumbbell emits at a markedly lower wavelength than either of the rotaxanes. If it is assumed that β-cyclodextrin, being larger and less rigid, provides less

protection and a more hydrophilic environment than the smaller α-cyclodextrin which cannot include many water molecules along with the stilbene, then the rotaxanes continue a trend in which encapsulation raises emission wavelength. Encapsulation with α-cyclodextrin causes a hypsochromic shifts (blue shift) in the emission of about 20 nm.

4.2.3. Naphthyl acetylenes

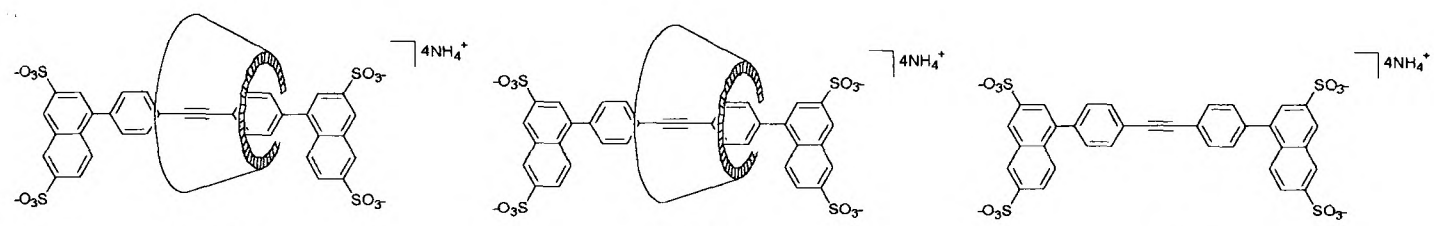

42⊂α-CD **42⊂β-CD** **42**

In this series, (**42**, **42⊂β-CD, 42⊂α-CD**) there is again little difference in the shape of the UV/Vis absorption spectra between the dumbbell and the rotaxanes with α-cyclodextrin and β-cyclodextrin. The absorption spectra are depicted in Figure 4.5.

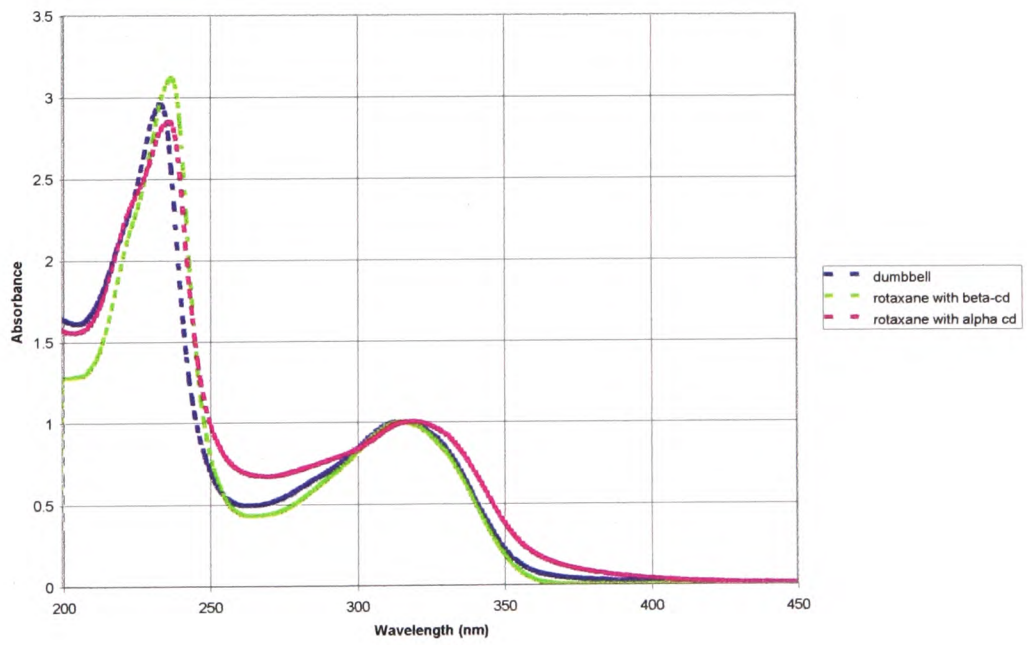

Figure 4.5. *UV absorption spectra of rotaxane* ***42⊂α-CD****, rotaxane* ***42⊂β-CD*** *and dumbbell* ***42****, conc~0.02 mmol* l^{-1} *in* H_2O.

Despite this, differences in the emission spectra (Figure 4.6) are again more pronounced than for the absorption spectra.

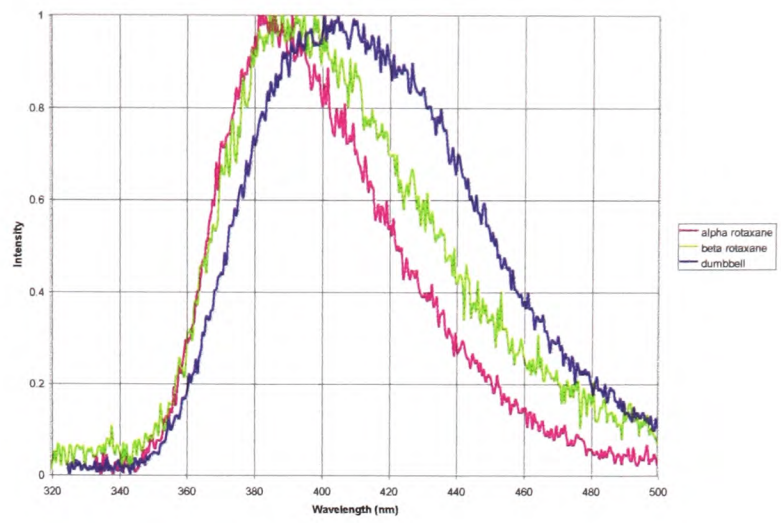

Figure 4.6. *Normalised emission spectra of rotaxane* ***42⊂α-CD****, rotaxane* ***42⊂β-CD*** *and dumbbell* ***42****,* λ_{ex}*=315 nm, conc~1.2 μmol* l^{-1} *in* H_2O*.*

Once again, it is evident that encapsulation exerts more of an influence in the emission spectrum than in the absorption spectrum. Although there is not much difference between the two rotaxanes themselves (size of the macrocycle obviously not being so important in this case where the encapsulated species is smaller than stilbene), there is clearly a significant hypsochromic shift on encapsulation of the dumbbell.

4.2.4. Summary of absorption and emission λ_{max}

Table 4.1. *Wavelengths of absorption and emission maxima for all rotaxanes and dumbbells.*

Compound	Absorption λ_{max} (nm)	Emission λ_{max} (nm)
40⊂α-CD	345	387, 406
40 (Stilbene Isophthalic acid)	343	385, 405
39⊂α-CD	341	416
39⊂β-CD	331	425
39 (Stilbene Naphthyl)	338	445
41⊂α-CD	323	360, 378
41 (Tolan Isophthalic acid)	342.5	359, 378
42⊂α-CD	315	387
42⊂β-CD	315	390
42 (Tolan Naphthyl)	315	409
43⊂β-CD	310	394
43 (Biphenyl Naphthyl)	309	418

Table 4.1 shows the trends seen in both absorption and emission wavelengths. In some cases (particularly the carboxylates **40⊂α-CD** and **40**) the trends are less pronounced than in others but, in general, the rotaxanes emit at lower wavelengths than the dumbbells. β-Cyclodextrin induces less of a shift than that caused by α-cyclodextrin. There is little difference in the absorption spectra of the bound and unbound dumbbells, so the surroundings of the chromophore clearly do not affect the absorption spectra significantly in this work.

A shift to longer wavelengths is to be expected for emission spectra in more polar solvents[10, 11]. This may itself be explained by an expansion of the Franck-Condon principle in which solvent cage relaxation can occur subsequent to excitation, leading to a lower energy ground state than that predicted by Franck-Condon. Emission then occurs to a ground state in which solvent rearrangement again occurs, leading to longer wavelength (lower energy) emissions than predicted. This solvent relaxation will, however, only occur where polar solvents are used, thereby lowering the energy of the transition with solvent polarity. This rationalisation also assumes that the excited state is more polar than the ground state, which is a reasonable assumption for most species. The trends in emission spectra can be rationalised by likening the surroundings of the chromophore to a local solvent; in the case of the unencapsulated dumbbells this is water but becomes increasingly more hydrophobic and less polar on inclusion in the form of the cyclodextrin rotaxanes.

4.2.5. Extinction Coefficients

In addition to the changes in absorption and emission wavelength, encapsulation may have an effect on the intensity of absorption. Marquez and Nau[12] have demonstrated that encapsulation by such macrocycles as cucurbitrils and carcerands may alter the extinction coefficient of an included molecule by affecting the polarisability of the surroundings of the guest molecule. They predict that cyclodextrin cavities have a higher polarisability than water, and thus it is reasonable to expect a slight increase in extinction coefficient of chromophores contained in cyclodextrin cavities. Table 4.2. shows the extinction coefficients of all the rotaxanes and dumbbells described in Chapter 2.

Table 4.2. *Extinction coefficients of all rotaxanes and dumbbells at the peak maxima, in water.*

	Dumbbell	β-rotaxane	α-rotaxane
Stilbene Naphthyl (**39**)	28000	43000	46000
Tolan Naphthyl (**42**)	11500	33000	41000
Biphenyl Naphthyl (**43**)	30000	36000	
Stilbene Isophthalic acid (**40**)*	42000		42500
Tolan Isophthalic acid (**41**)*	35000		48000

*Measured in pH~9 $NaOH/H_2O$.

It can be seen in Table 4.2 that, in every case, the extinction coefficient of the dumbbell is lower than that of the corresponding rotaxanes. Where the core may be encapsulated by either α- or β-cyclodextrin, the extinction coefficient of the more tightly encapsulated α-cyclodextrin rotaxane is always higher than that of the β–cyclodextrin rotaxane. This may be in part due to the de-aggregating effect of encapsulation. As shown by Willner's work on thionin[5], molar absorptivities increase as aggregates are broken up. Encapsulation with either α- or β-cyclodextrin should achieve this and indeed the difference between the extinction coefficients for α- and β-cyclodextrin rotaxanes is much less significant than the difference of rotaxane to dumbbell in most cases. The effect of solvent polarity on extinction coefficients is generally understood[10] to be small relative to overall absorption. This may, however, account for the smaller differences between the extinction coefficients of the α- and β-cyclodextrin rotaxanes.

4.2. Fluorescence Quantum Yields

The fluorescence quantum yield[13, 14] (Φ_F) is the fraction of absorbed light which is re-emitted by the chromophore. Absolute values can be measured directly by the use of rather elaborate apparatus. More usually, such values are obtained by comparision with the quantum yield of a standard having a known fluorescence quantum yield. The standard should be chosen to be emissive in the same area of the spectrum as the substance in question, since the response of most photomulitiplier tubes varies with wavelength (this is corrected in the fluorimeter with a standard correction curve but this correction tends not to be very reliable).

The equation for the calculation of a fluorescence quantum yield is shown in Equation 4.1[13].

$$\Phi_A = \left[\frac{A_B F_A n_A^{\,2}}{A_A F_B n_B^{\,2}}\right]\Phi_B \qquad \textit{Equation 4.1.}$$

where

Φ_B = Fluorescence quantum yield of standard; quinine bisulfate[15, 16]= 0.546 in 0.5 M H_2SO_4(aq.), anthracene[17] = 0.27 in cyclohexane;

A_A = Absorbance of sample in UV/Vis at excitation wavelength;

F_A = Integrated emission (number obtained from spectral integration) cm^{-1} *vs.* counts sec^{-1};

n_A^2 = Square of refractive index of the solvent in which measurement carried out; 0.5 M sulfuric acid = 1.339, cyclohexane = 1.426, water = 1.333.

This method was developed as a result of many refinements of literature methods[10, 13, 14]. The quantum yields were measured as described in the experimental section, and are tabulated in Table 4.3.

Table 4.3. *Fluorescence quantum yields (Φ_F) ± 10 % for all rotaxanes and dumbbells in water.*

	Dumbbell	β-rotaxane	α-rotaxane
Stilbene Naphthyl (**39**)	0.30	0.72	1.03
Tolan Naphthyl (**42**)	0.81	0.98	1.08
Biphenyl Naphthyl (**43**)	0.67	1.04	
Stilbene Isophthalic acid (**40**)*	0.67		0.94
Tolan Isophthalic acid (**41**)*	0.89		0.99

*Measured in pH~9 $NaOH/H_2O$.

We estimate errors of around 10 %, which is in agreement with the generally accepted values[10]. These were estimated by re-integration of the emission peaks to assess the reproducibility of this part of the equation, and by estimation of the errors in measurements such as the microlitre syringes and other equipment used. Table 4.3 demonstrates the high fluorescence of even the unencapsulated dumbbells (**39**, **40**, and **42**). Similar dyes have been used in lasers[18] because of this very property. The dumbbells are all lower in fluorescence quantum yield than the encapsulated forms, and indeed the improvement in quantum yield upon encapsulation of the dumbbells is most marked where the original quantum yield was lowest; the α-cyclodextrin rotaxanes (**39⊂α-CD**, **40⊂α-CD**, and **42⊂α-CD**) have virtually quantitative re-emission of absorbed light. The trend is best highlighted by the series

39 (naphthyl stilbene dumbbell), **39⊂β-CD** (naphthyl stilbene β-cyclodextrin rotaxane) and **39⊂α-CD** (naphthyl stilbene α-cyclodextrin rotaxane), in which the quantum yields range through 0.30, 0.72 and 1.03 respectively. This improvement of fluorescence quantum yield parallels previous work in the Anderson group[19], in which encapsulation increases the fluorescence efficiency in a solvent in which the dye is already fluorescent, although this effect is not observed in water. The enhancement in fluorescence efficiency is also related to a reduction in the quantum yield of photoisomerisation, from the *trans* to the *cis* form of the stilbene core ($\Phi(trans \rightarrow cis)$). This is discussed in Chapter 5.

It is difficult to attribute this fluorescence enhancement to any one factor. Given the large effect that the molecules around the chromophore have upon the emission wavelength (solvatochromism), it is highly likely that this is a consideration in the increase of fluorescence quantum yield with rotaxane formation. This can also be looked upon as a shielding effect. Polar solvent molecules often significantly reduce observed fluorescence quantum yields compared with the yields in other, less polar solvents, by a mechanism known as quenching. Quenching involves radiationless decay of the excited state by interaction with the polar solvent molecules. This was not investigated directly, due to the lack of solubility of the majority of the compounds in solvents other than water. Protection of the chromophore by encapsulation will reduce this quenching effect by preventing the polar solvent molecules from reaching the chromophore to interact with it. However, rigidification of the excited state is unquantifiable and may equally well play a part. It is probable that the results seen in Table 4.3 are a combination of both these causes.

Even allowing for the many explanations for our observations, it is clear that significant enhancement of the fluorescence quantum yield is afforded by encapsulation with cyclodextrins.

4.3. Conclusions of Chapter 4

The absorption and emission spectra of the rotaxanes and dumbbells synthesised in Chapter 2 have been compared and contrasted. Encapsulation does not have much effect upon the shape of the UV spectrum, although the rotaxanes all have slightly higher molar absorptivities than their corresponding dumbbells. However, both the shape of the emission spectra and the fluorescence quantum yields are significantly altered by encapsulation of the dumbbell units. This may be a result of the protective, hydrophobic environment provided by the cyclodextrin cavity.

The results in this chapter show that encapsulation greatly enhances both the intensity of the fluorescence. This is a pleasing justification for the further work in the area of rotaxane synthesis.

References for Chapter 4

[1] D. H. Williams, I. Fleming, *Spectroscopic Methods in Organic Chemistry*, 4 th ed., McGraw-Hill, London, **1989**.

[2] P. F. Gordon, P. Gregory, *Organic Chemistry in Colour*, 1 st ed., Springer Verlag, Berlin, **1987**.

[3] K. Kasatani, M. Ohashi, H. Sato, *Carbohydrate Res.* **1989**, *192*, 197.

[4] H. Hirai, N. Toshima, S. Uenoyama, *Bull. Chem. Soc. Jpn.* **1985**, *58*, 1156.

[5] P. Dan, I. Willner, *J. Chem. Soc., Perkin Trans. 2* **1984**, 455.

[6] Y. Degani, I. Willner, Y. Haas, *Chem. Phys. Lett.* **1984**, *104*, 497.

[7] B. Jousselme, P. Blanchard, P. Frere, J. Roncali, *Tetrahedron Lett.* **2000**, *41*, 5057-5061.

[8] M. Yoon, K. H. Lee, *J. Chem. Soc., Perkin Trans. 2* **1988**, *2*, 1943-1945.

[9] E. J. Bowen, D. M. Stebbens, *J. Chem. Soc.* **1957**, 360-363.

[10] A. Sharma, S. G. Shulman, *Introduction to Fluorescence Spectroscopy*, John Wiley and Sons, New York, **1999**.

[11] N. Strashnikova, V. Papper, P. Parkhomyuk, G. I. Likhtenshtein, V. Ratner, R. Marks, *J. Photochem. Photobiol. A.* **1999**, *122*, 133 - 142.

[12] C. Marquez, W. M. Nau, *Angew. Chem. Int. Ed.* **2001**, *40*, 4387 - 4390.

[13] D. F. Eaton, in *C.R.C. Handbook of Organic Photochemistry* (Ed.: J. C. Scaiano), C.R.C. Press, Florida, **1989**, pp. 231 - 239.

[14] A. G. Szabo, in *Spectrophotometry and Spectrofluorimetry* (Ed.: M. G. Gore), Oxford University Press, Oxford, **2000**, pp. 33 - 60.

[15] S. R. Meech, D. Phillips, *J. Photochem. Photobiol. A.* **1983**, *23*, 193.

[16] W. H. Melhuish, *J. Phys. Chem.* **1961**, *87*, 83.

[17] J. T. Kunjappu, K. N. Rao, *Indian J. Chem. Sect. A* **1988**, *27A*, 1 - 3.

[18] G. Gauglitz, R. Goes, W. Stooss, R. Raue, *Z. Naturforsch. A.* **1985**, *40*, 317.

[19] J. E. H. Buston, J. R. Young, H. L. Anderson, *Chem. Commun.* **2000**, 905 - 906.

Chapter 5; Photoswitching and Photodegradation.

5.1. Introduction

The photochemistry of stilbenes has been well studied in the past[1-6]. Figure 5.1 is reproduced from a recent paper by Meier[7], and summarises the common photochemical reactions from the singlet excited state: [2+2] cycloadditions, *trans*⇆*cis* isomerisation, and dihydrophenanthrene / phenanthrene formation.

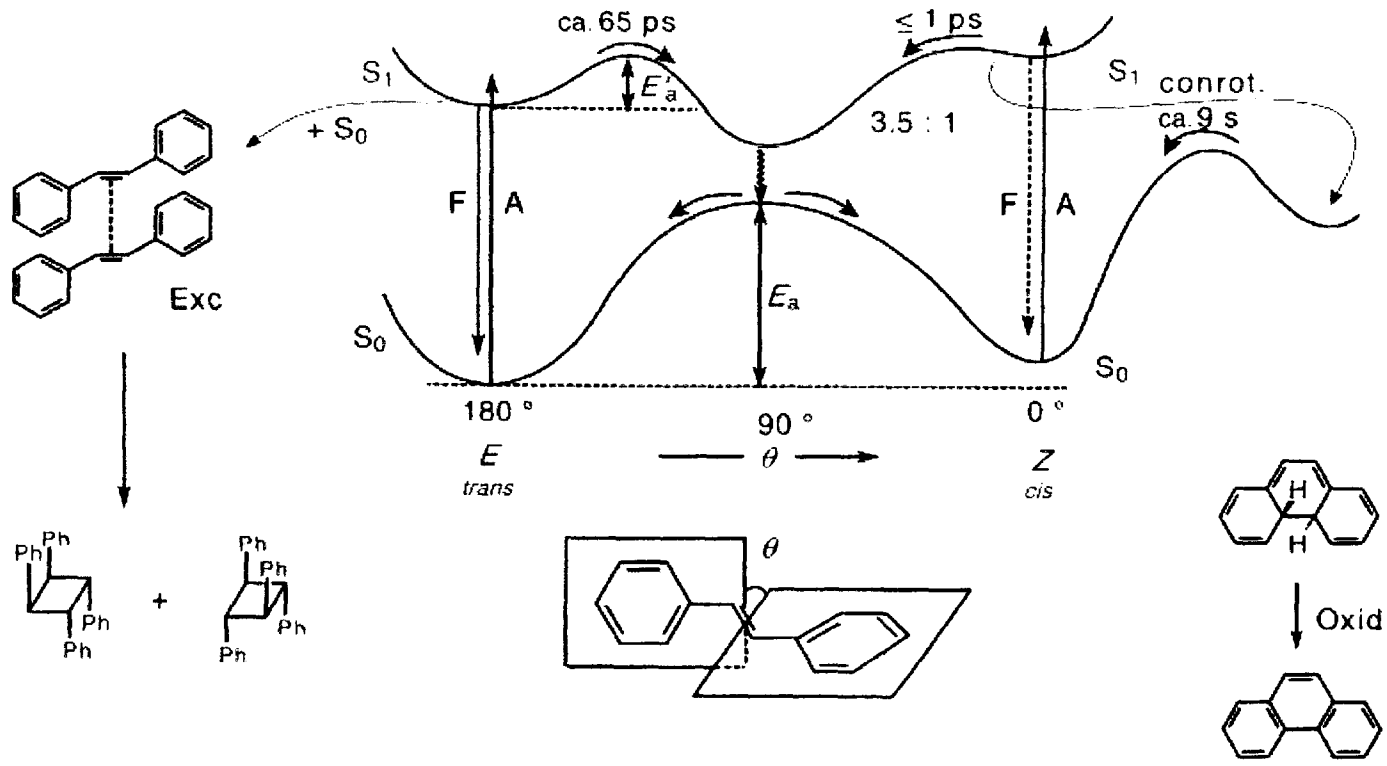

Figure 5.1. *Energetics of stilbene photochemistry[7], showing energy vs. torsional angle of alkene.*

Excitation (A) of stilbene in its ground state by the input of light results in the singlet excited state, S_1. In some cases, intersystem crossing to a triplet state occurs , but less interesting photochemistry results from this. Decay from S_1 can be radiative (as discussed in Chapter 4, stilbenes and their derivatives are often very fluorescent), or non-radiative. A stilbene molecule in its excited S_1 state can react with another, ground state molecule, *via* a [2+2] cycloaddition to form cyclobutanes. This is particularly favourable at high concentrations. If sufficient energy (E'_a) is supplied, the barrier to twisting about the alkene bond may be overcome. This activation

energy is lower in the excited state than in the ground state ($E'_a<E_a$), and from the *cis* form of the excited state, the energy barrier is very small. This results in a high energy intermediate state known as the 'p'-state ('phantom' or 'perpendicular' state), which then decays non-radiatively to the twisted ground state with $\theta \approx 90^o$. This can then form either *cis* or *trans* stilbene in an S_1 state with an approximately equal probability. After prolonged irradiation a photostationary state is formed, in which the proportions of the *cis* and *trans* isomers present in the irradiated mixture depend upon the extinction coefficients of the two isomers at the wavelength used for irradiation and the exact shape of the S_1 and S_0 energy surfaces for that system. The shape of the energy surfaces controls the quantum yields for *trans*→*cis* and *cis*→*trans* isomerisations respectively. *Cis*-stilbenes can reversibly form dihydrophenanthrenes, which can then undergo irreversible oxidation to yield phenanthrenes.

In recent years, work with flash photolysis at picosecond resolution has been used to study the kinetics of stilbene photoisomerisation[8-10], in order to elucidate the shapes of the S_1 and S_0 energy surfaces.

Traditionally, studies of photo-induced switching have focussed around azobenzene derivatives[11, 12], which can be switched by irradiation from *trans*→*cis* form, and both radiatively and thermally from *cis*→*trans*. This isomerisation is depicted in Scheme 5.1. Changes in conformation of a receptor, induced by the isomerisation, have been exploited in these cases to turn binding on and off at will.

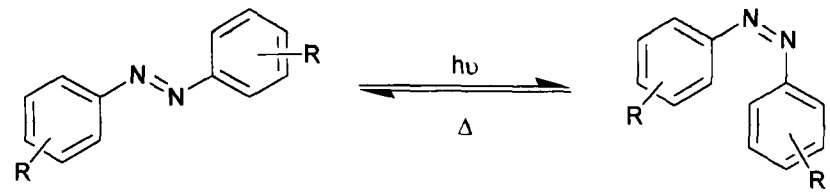

Scheme 5.1. *Switching of azobenzenes.*

Stilbene itself is less useful than the azobenzenes as a molecular switch due to its low *cis→trans* quantum efficiency, and the competing reactions discussed above. These types of reaction do not occur with azobenzenes.

More recently, interest has turned towards stilbene derivatives, which have been exploited in recent years as prototypes for molecular devices[13, 14] such as this molecular rotor by Feringa (Scheme 5.2), which can only move in one direction.

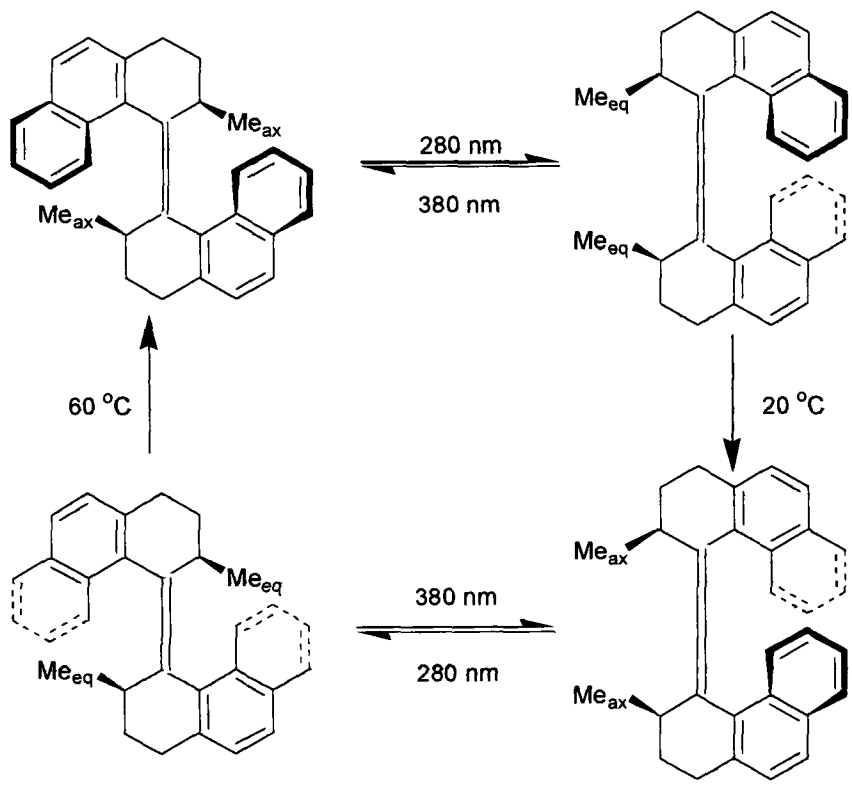

Scheme 5.2. *A light driven molecular rotor*[14]

The advantages of stilbenes in these systems are clear. Stilbenes cannot normally be isomerised by use of heat alone, they do not therefore re-isomerise over time in the dark. Switches and devices produced from these components have a much greater

thermal stability than those produced with azobenzene constituents. They are also pH-stable, unlike azo groups, which may be protonated and form photo-inert hydrazo-groups. This enables the use of protons as a second switching event, thus one can propose the build up to 'AND', 'NAND', 'OR', and 'NOR' logic gates[15].

There are some examples of the use of encapsulation of stilbene-like molecules by cyclodextrins to moderate this switching behaviour[16, 17], as well as the further photochemistry of the encapsulated species[18]. Work to date in this field has been somewhat inconclusive as it is difficult to know if reactions of a host-guest equilibrium, taking place in solution, are occurring as the bound or unbound species. It is therefore important to look at this aspect of reactivity in the rotaxanes.

This work aims to compare and contrast the photochemistry of the stilbene rotaxanes synthesised in Chapter 2 with that of their corresponding dumbbells. We are interested in revealing the effects of encapsulation upon the photochemistry of these particular chromophores. This chapter will thus cover qualitative photoisomerisation experiments, in order to ascertain which rotaxanes and dumbbells can be switched by the action of light on the chromophore. A more in-depth, quantitative study of one of the rotaxanes **40⊂α-CD** and its dumbbell **40** will be described, in which kinetic measurements and deduction of absorption spectra for the photostationary state will be used to arrive at an approximation of the *trans→cis* and *cis→trans* quantum yields (Φ*(trans→cis)* and Φ*(cis→trans)* respectively) for this system. The geometry and spatial structure of a *cis* rotaxane isomer is compared to that of the starting *trans* form by use of NOE spectroscopy. Subsequent photodegradations of both the rotaxane and the dumbbell will also be investigated.

5.2. Qualitative Photoswitching Experiments

This section will address the question of whether the encapsulated chromophore can be photoisomerised. Where this is found to be possible, evidence in the form of UV data will be presented and interpreted. Empirical measurements of rate constants will also be undertaken.

5.2.1. Survey of photoisomerisation in the rotaxanes

A qualitative switching experiment was carried out on the rotaxane **40⊂α-CD** using a monochromatic light from a 150 W Xenon lamp. This provided a source of monochromatic light whose wavelength could be varied easily, and which could be turned on or off at will. This experiment was limited by the scale on which it could be performed; solutions with absorbance of ~1.0 approached a photostationary state in a matter of minutes, however this did not provide enough material for characterisation by ^{1}H NMR. Samples containing sufficient material for NMR analysis could be switched, but the reaction took several days.

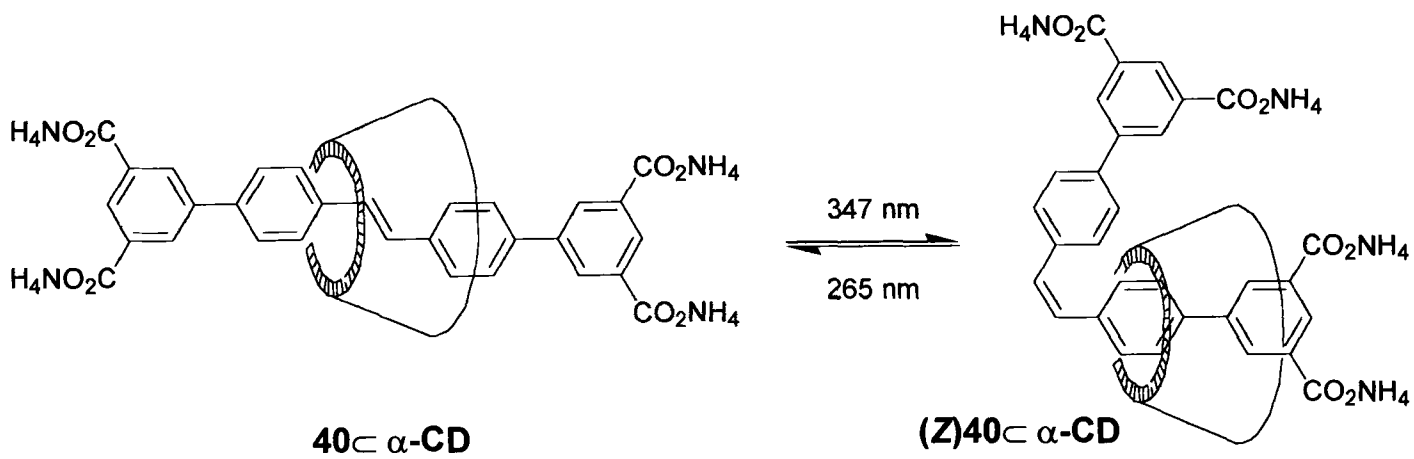

Scheme 5.3. *Photoswitching of the rotaxane* ***40⊂α-CD****.*

Switching between two photostationary states, consisting of different proportions of *cis* and *trans* stilbene, was investigated. This is portrayed in Scheme 5.3. The wavelengths initially chosen for irradiation were 265 and 347 nm. 347 nm was the

absorption maximum for this *trans* rotaxane **40⊂α-CD**, and on irradiation at this wavelength, a new peak appeared at 265 nm (although this was more pronounced in the case of the dumbbell **40**). It was therefore initially surmised that the greatest difference in the UV/Vis spectrum would result from irradiation at around these wavelengths.

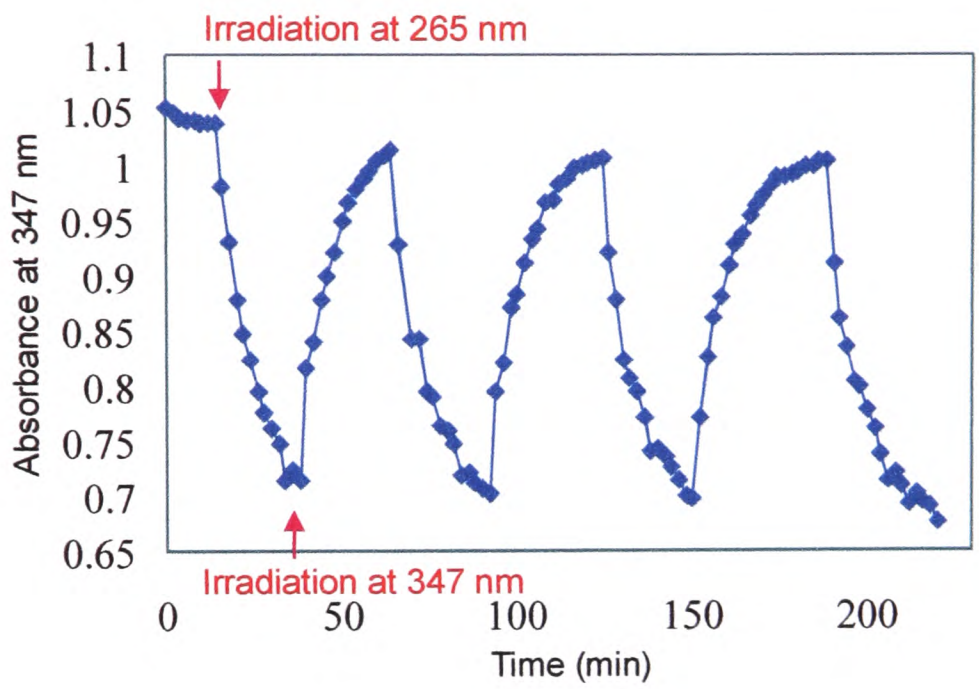

Figure 5.2. *Photoswitching of rotaxane* ***40⊂α-CD****, switching wavelengths 265 nm and 347 nm.*

It can be seen from Figure 5.2, not only that switching between two alternate photostationary states was possible, but also that this switching had good reversibility. The switch was highly fatigue resistant, an observation in agreement with stilbene switches from other sources[13-15]. In the case of the switching of the corresponding dumbbell **40** (Scheme 5.4), it was again possible to plot a switching graph (Figure 5.3). Here, irradiation was again performed at the absorption maximum which was 340 nm.

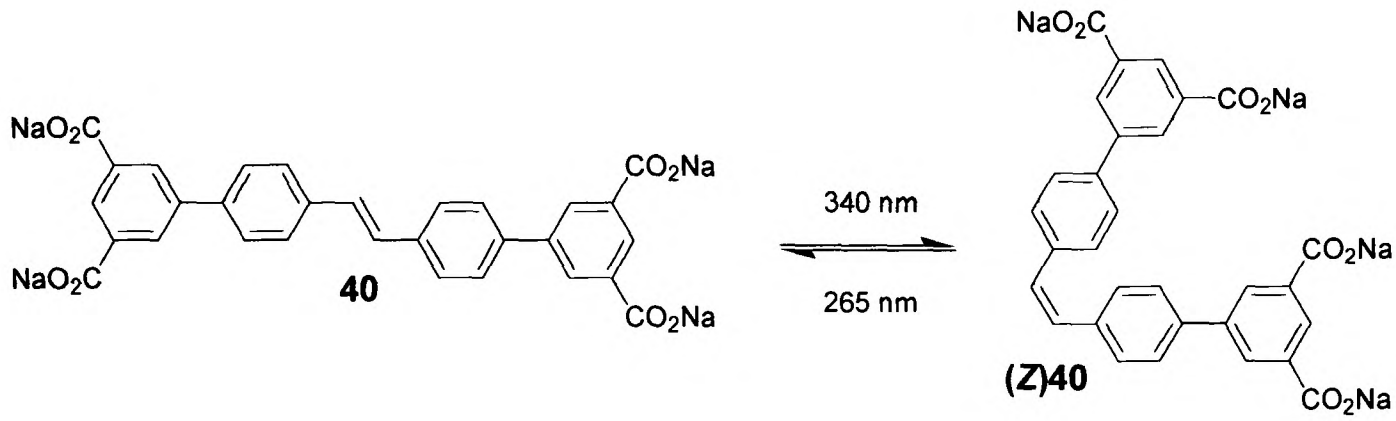

Scheme 5.4. *Trans and cis forms of the dumbbell* ***40****.*

The dumbbell **40** also performed as a functional switch, although it can be seen from the reduced absorbance over time that some photodegradation had occurred over the period in which switching was carried out.

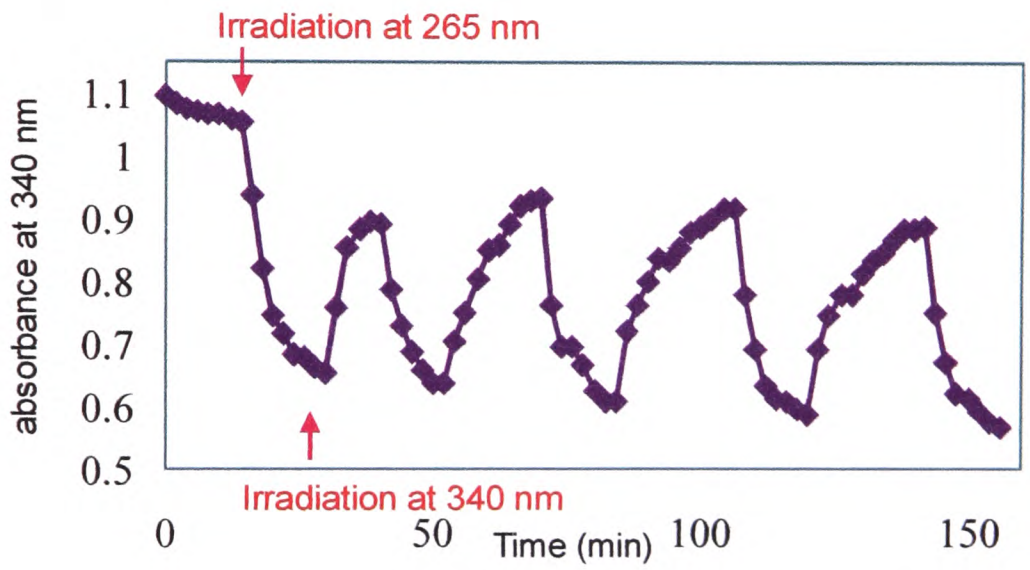

Figure 5.3. *Photoswitching of dumbbell* ***40****; switching wavelengths 265 and 340 nm.*

5.2.2. Empirical rate constant determination

From the information in these plots, it was possible to fit the switching to a first order rate equation of the form

$$A_t = A_F + (A_i - A_F)e^{-kt} \qquad \textbf{Equation 5.1.}$$

where

A_t = observed change in absorption at measured time interval t;

A_F = absorption of the photostationary state at the concentration and wavelength used;

$(A_i - A_F)$ = overall change in absorbance;

k = rate constant (min^{-1}).

The values from all the switching runs performed for the dumbbell **40** and rotaxane **40⊂α-CD** are tabulated in Table 5.1.

Table 5.1. *Constants derived from first-order fits of the photoswitching runs for* ***40*** *and* ***40⊂α-CD****.*

	Event Number†	A_F	$(A_i - A_F)$	k (min^{-1})
Dumbbell **40** irradiation at 265 nm	1	0.913	-0.266	0.330§
	2	0.988	-0.287	0.110
	3	0.955	-0.231	0.091
	4	0.935	-0.237	0.086
Dumbbell **40** irradiation at 340 nm	1	0.655	0.287	0.270
	2	0.613	0.174	0.214
	3	0.540	0.216	0.105§
	4	0.587	0.194	0.329
	5	0.563	0.185	0.262
Rotaxane **40⊂α-CD** irradiation at 265 nm	1	1.050	-0.239	0.082
	2	1.024	-0.233	0.092
	3	1.009	-0.233	0.105
Rotaxane **40⊂α-CD** irradiation at 347 nm	1	0.670	0.310	0.091
	2	0.666	0.258	0.078
	3	0.683	0.236	0.104
	4	0.660	0.247	0.080

§These runs did not give good fits and consequently were not included in the final calculations.

†Event number 1 is the first curve in the switching experiment, etc.

Inspection of the values shows that there is a gradual decrease in projected photostationary state absorption throughout the experiment, and that this is more pronounced in the case of the dumbbell **40**. This can be attributed to a slow photodegradation, which occurs even in the absence of air. For the purpose of attempting to quantify the photoswitching process, the most accurate results are likely to be the initial ones, where little or no degradation has occurred. Example fits of these switching curves are shown below:

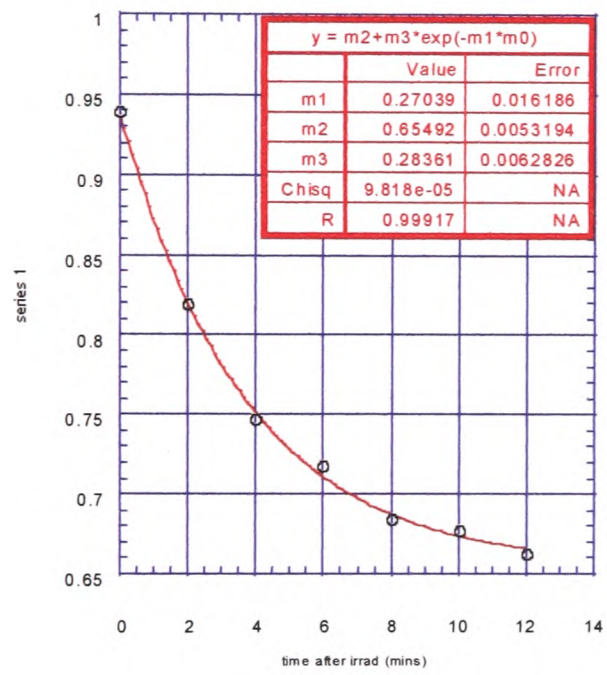

Figure 5.4. *Fitting curve for irradiation of dumbbell* ***40*** *at 340 nm, giving k = 0.27.*

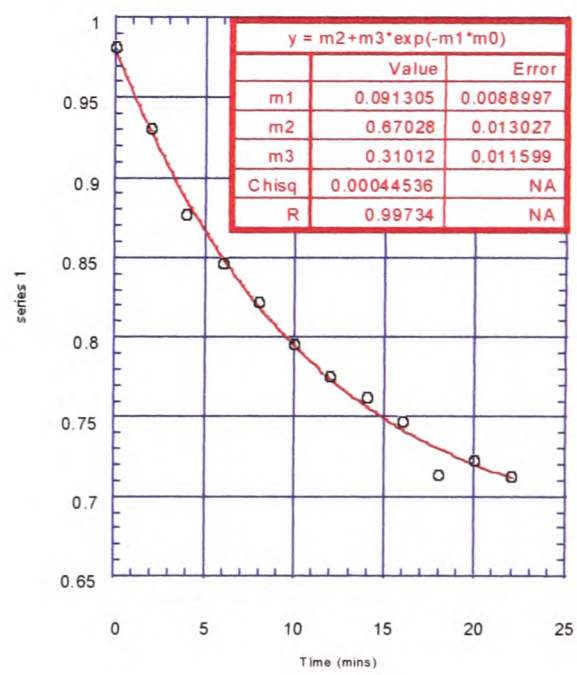

Figure 5.5. *Fitting curve for irradiation of rotaxane* ***40⊂α-CD*** *at 347 nm, giving k = 0.091.*

5.2.3. Switching of bulkier rotaxanes (39⊂α-CD, 39⊂β-CD) and dumbbell (39)

It was clear from these results that the rotaxane is much more reluctant to switch than the dumbbell. The steric demands of the cyclodextrin may account for this. Experiments with the naphthalene-stoppered rotaxanes **39⊂α-CD** and **39⊂β-CD**, and the dumbbell **39** were therefore undertaken to explore this. These compounds

have much bulkier stopper groups and it is easy to envisage a situation in which a combination of the two steric factors could combine to prevent switching altogether. It was initially necessary to confirm that the dumbbell could be isomerised. This was carried out by irradiation at 335 nm, as shown in Scheme 5.5 and Figure 5.6.

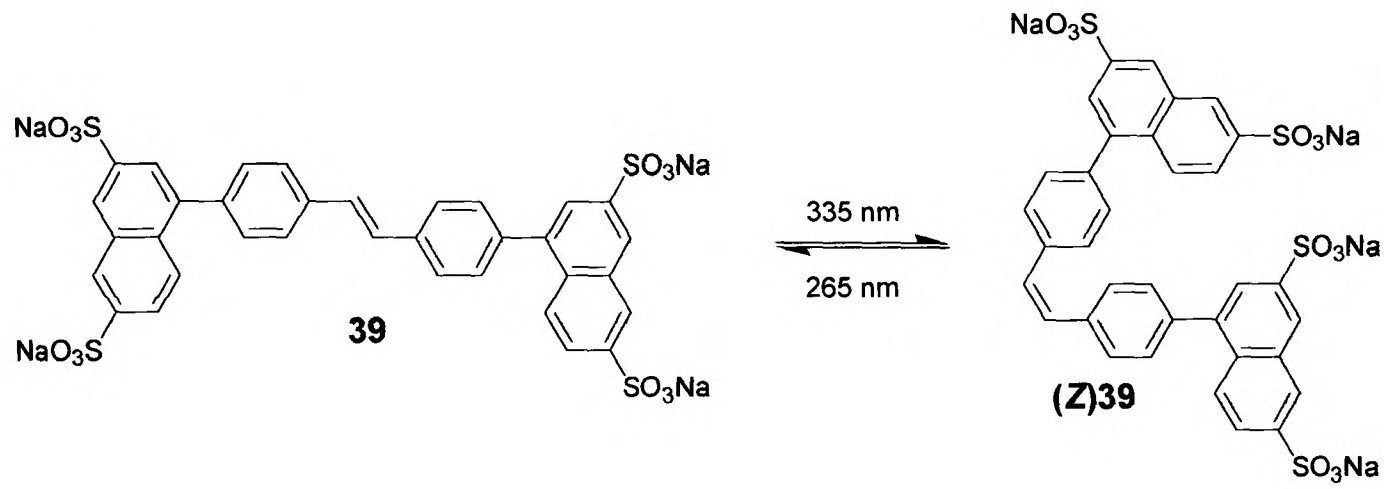

Scheme 5.5. *Photoswitching of dumbbell* ***39****.*

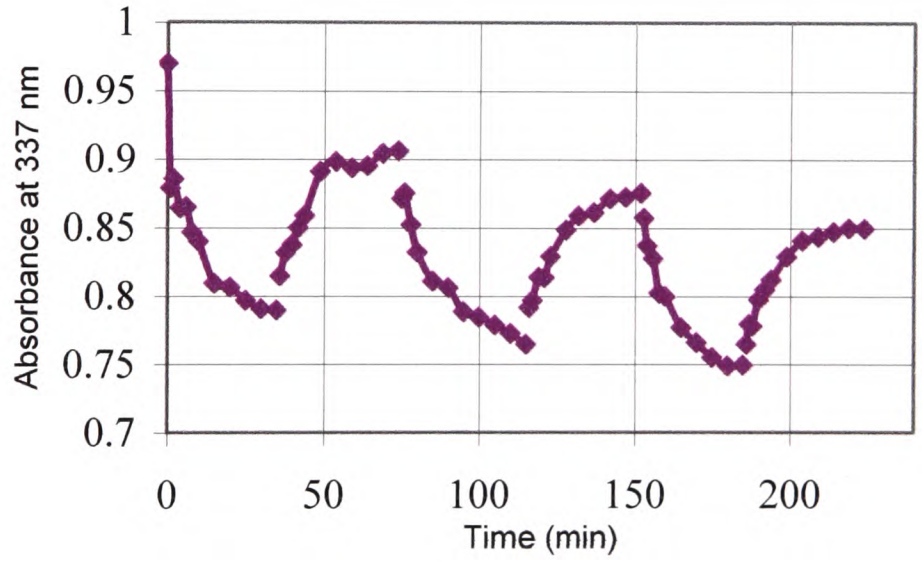

Figure 5.6. *Photoswitching of dumbbell* ***39****.*

This result proves that *cis⇆trans* isomerisation is also possible in the case where the stopper groups are much larger and sterically demanding. The switching of the corresponding rotaxane with α-cyclodextrin **39⊂α-CD** was therefore investigated (shown in Scheme 5.6), by irradiation at 337 nm.

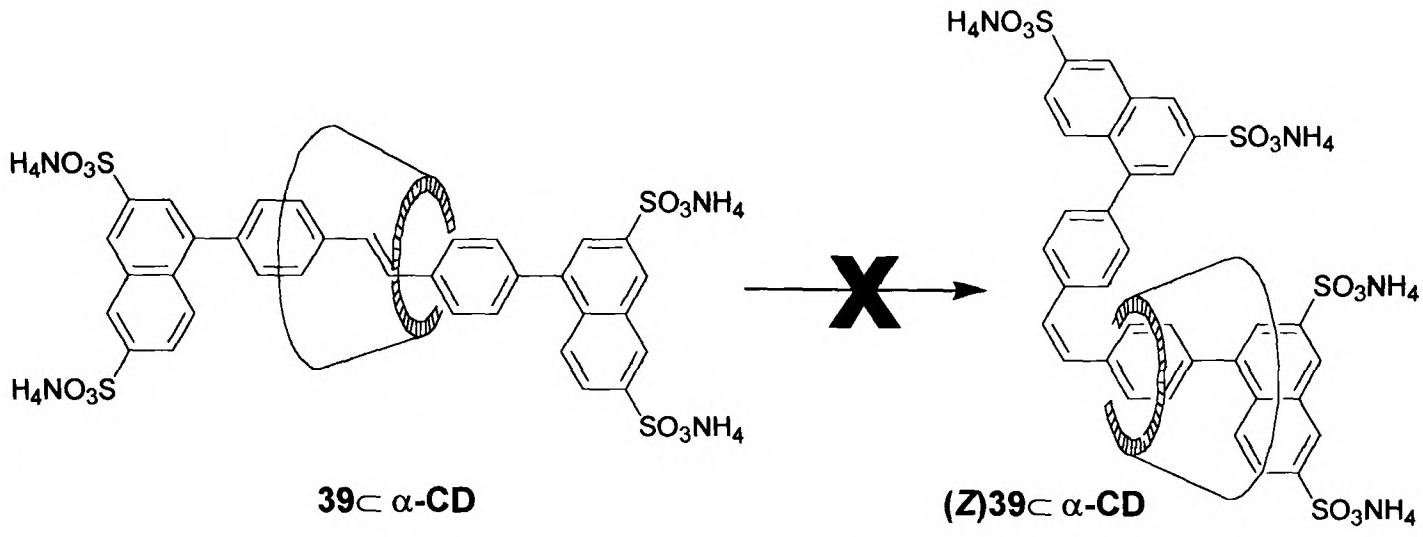

Scheme 5.6. *Photoswitching of rotaxane* ***39⊂α-CD.***

Despite the facile switching action of the dumbbell, this rotaxane **39⊂α-CD** did not appear to switch, as can be seen in Figure 5.7.

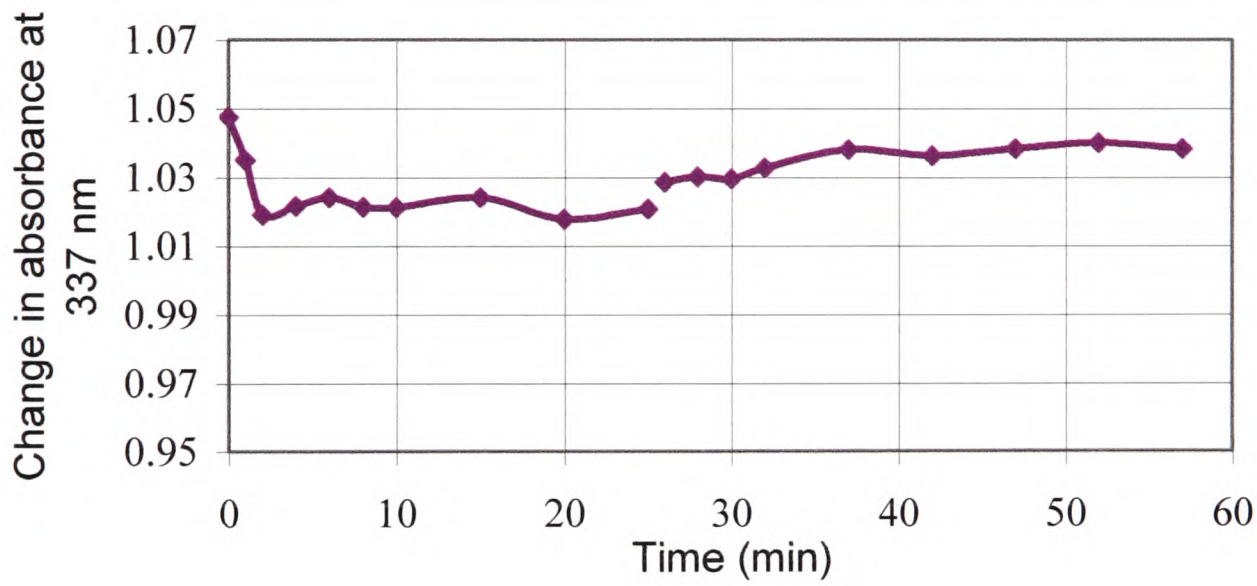

Figure 5.7. *Unsuccessful photoswitching of the rotaxane* ***39⊂α-CD,*** *irradiation wavelength changed from 337 nm to 265 nm at 25 min.*

This was confirmed by a longer, more concentrated irradiation experiment after which no ^{1}H NMR signals attributable to the *cis* isomer or any photoproducts could be found. Indeed, no change whatsoever appeared to have taken place. This may be related to the high fluorescence quantum yield.

Lastly, irradiation of the rotaxane **39⊂β-CD** was undertaken at 329 nm (Scheme 5.7).

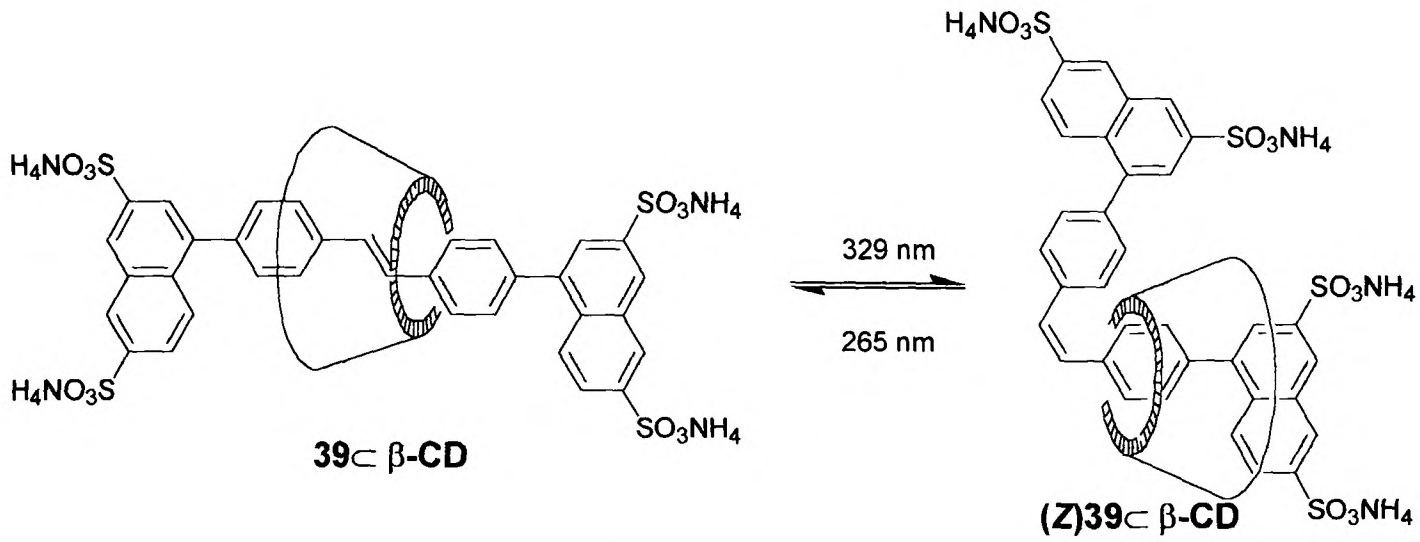

Scheme 5.7. *Photoswitching of rotaxane* ***39⊂β-CD****.*

In this instance, switching did seem to be possible, as Figure 5.8 shows, although possibly to a lesser extent than in the case of its corresponding dumbbell.

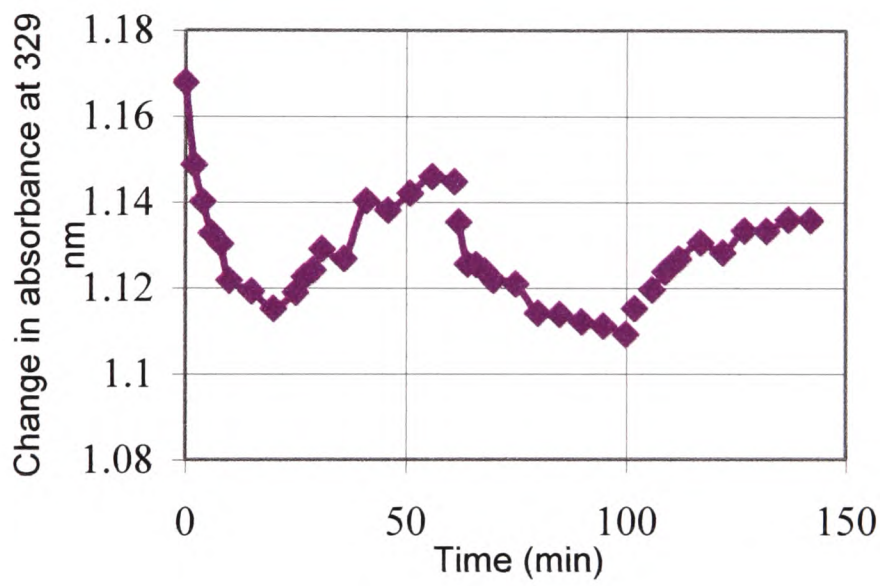

Figure 5.8. *Photoswitching of rotaxane* ***39⊂ β-CD****.*

Although on first inspection, it appears that the extent of switching is **39⊂α-CD** < **39⊂β-CD** < **39**, it is not possible to draw quantitative conclusions from this data without further work to predict or measure the extinction coefficients of the *cis* isomers. Generally, *cis* extinction coefficients are considerably lower than the corresponding *trans* coefficients. However, without exact knowledge of the extinction coefficients, it is impossible to ascertain if the disparity in change of

absorbance on switching of the rotaxane **39⊂β-CD** and dumbbell **39** is due to different proportions of *cis* and *trans* in the photostationary states or simply to vastly different values of *cis* extinction coefficients in the two cases, both of which are possible explanations of the trends in data seen.

5.3. Determination of photoisomerisation quantum yields

5.3.1. General strategy

In order to deduce a quantum yield of photoisomerisation, it is necessary to be able to ascertain the amount of *trans* and *cis* isomers in any sample with a given UV spectrum. Chromatographic separation of the two isomers to obtain pure samples of each proved difficult as the *trans* and *cis* forms of the rotaxane **40⊂α-CD** co-elute in all systems tried. The purified samples, even if such could be prepared, would be subject to re-isomerisation in the presence of light, which would lead to the need for re-purification. For these reasons, we determined the UV spectrum of the *cis* isomer ***(Z)*40⊂α-CD** by extrapolation from a UV spectrum consisting of a known ratio of *trans* to *cis*. The calculated spectrum was then used, in combination with kinetic measurements, to predict the UV spectrum of a photostationary state and subsequently elucidate the ratio of isomers present in the photostationary state. An approximation of the initial rate of switching and use of a 'standard' of known quantum yield enabled us to obtain quantum yields of both switching processes.

5.3.2. Theory

It was first of all necessary to obtain the UV/Vis extinction coefficients of both isomers, which could then be applied to any mixture of the two, to give an

approximation of the relative amounts of each. This can be done by use of Equation 5.2.

$$\frac{A_1}{c_1} = fcis\ \varepsilon_{cis} + ftrans\ \varepsilon_{trans} \qquad \textbf{Equation 5.2.}$$

where

A_1 = measured absorbance of the diluted, irradiated sample, assuming a path length of 1 cm;

c_1 = concentration of the diluted, irradiated sample;

fcis and *ftrans* = fraction of *cis* and *trans* isomer respectively, as determined by ^{1}H NMR.

Here, the only unknown is ε_{cis} as the extinction coefficient of the *trans* isomer may be calculated based on the spectrum of the initial pre-irradiation sample, using Equation 5.3.

$$\varepsilon_{trans} = \frac{A_2}{c_2} \qquad \textbf{Equation 5.3.}$$

where

A_2 = absorbance of all-*trans* solution, assuming a path length of 1 cm;

c_2 = concentration of all-*trans* solution.

ε_{cis} may be calculated by combination of Equation 5.2 and Equation 5.3, as shown in Equation 5.4.

$$\varepsilon_{cis} = \frac{\left(\frac{A_1}{c_1}\right) - ftrans\left(\frac{A_2}{c_2}\right)}{fcis} \qquad \textbf{Equation 5.4.}$$

Once the value of ε_{cis} at all points in the UV/Vis spectrum has been calculated, it is possible to estimate the proportions of *cis* and *trans* isomer in any mixture with a known UV spectrum.

In order to calculate the quantum yields of switching, it is necessary to ascertain the absorbance of the photostationary state and hence the proportions of *cis* and *trans* isomers in that state. Equation 5.5 is of the same form as Equation 5.1, and demonstrates how this stage of the calculation is possible.

$$A_3 = A_F + (A_i - A_F)e^{-kt} \qquad \textbf{Equation 5.5.}$$

where

A_3 = absorbance of the irradiated solution, at concentration (c_3) and time (t);

A_F = projected absorbance of the photostationary state;

A_i = initial absorbance of the solution (when all *trans*);

k = rate constant of the switching process.

It is possible to measure all of these quantities (except A_F) in a kinetic experiment similar to those carried out to determine the empirical rate constants in section 5.2, A_F may therefore be calculated from Equation 5.5. This value is then put to use to determine the composition of the photostationary state in Equations 5.6 and 5.7.

$$\frac{A_F}{c_3} = \frac{\left(\frac{A_3}{c_3}\right) - \varepsilon_{trans}e^{-kt}}{(1 - e^{-kt})} \qquad \textbf{Equation 5.6.}$$

where

c_3 = total concentration;

and hence (in combination with Equation 5.2):

$$\frac{A_F}{c_3} = fcis_F \varepsilon_{cis} + (1 - fcis_F)\varepsilon_{trans}$$

$$\Rightarrow fcis_F = \frac{\left(\frac{A_F}{c_3}\right) - \varepsilon_{trans}}{\varepsilon_{cis} - \varepsilon_{trans}} \qquad \textit{Equation 5.7.}$$

where

$fcis_F$ = fraction of *cis* isomer present in the photostationary state at the irradiation wavelength.

It is now possible to use the known value of $fcis_F$, as well as the previously calculated values of the extinction coefficients, in Equation 5.8 (derived in Appendix 5.1 using the Beer-Lambert Law, assuming that the absorption is small, *i.e.* less than 0.1, and that the path length of the sample is 1 cm).

$$\frac{\Phi(trans \rightarrow cis)}{\Phi(cis \rightarrow trans)} = \frac{\varepsilon_{cis}}{\varepsilon_{trans}} \times \frac{fcis_F}{(1 - fcis_F)} \qquad \textit{Equation 5.8.}$$

where

$\Phi(trans \rightarrow cis)$, $\Phi(cis \rightarrow trans)$ = the respective quantum yields for these processes.

However, Equation 5.8, still contains two unknown quantities: $\Phi(trans \rightarrow cis)$ and $\Phi(cis \rightarrow trans)$. We may approximate relative values of $\Phi(trans \rightarrow cis)$ of the rotaxane and dumbbell by measurement of the initial rate of switching, as this will mostly consist of *trans*→*cis* switching. Equation 5.9 leads to $\Phi(trans \rightarrow cis)$ *via* this approximation.

$$\frac{\Phi(trans \rightarrow cis)_{rotaxane}}{\Phi(trans \rightarrow cis)_{dumbell}} = \frac{(\partial A / \partial t)_{rotaxane}}{(\partial A / \partial t)_{dumbbell}} \times \frac{A_{0\,dumbbell}}{A_{0\,rotaxane}} \times \frac{(\varepsilon_{cis} - \varepsilon_{trans})_{dumbbell}}{(\varepsilon_{cis} - \varepsilon_{trans})_{rotaxane}} \qquad \textit{Equation 5.9.}$$

where

$(\partial A / \partial t)$ = gradient measured from initial few minutes of irradiation;

A_0 = initial absorbance of irradiated sample.

By comparison of the relative quantum yields of rotaxane and dumbbell **40⊂α-CD** and **40** with a known literature value for stilbene ($\Phi(trans \rightarrow cis) = 0.5$[2, 19-21]), it is possible to arrive at absolute values (in the same way that comparison of relative fluorescence quantum yields to a known standard gives 'absolute values') for $\Phi(trans \rightarrow cis)_{rotaxane}$ (**40⊂α-CD**) and $\Phi(trans \rightarrow cis)_{dumbbell}$ (**40**).

These may then be substituted into Equation 5.8 to provide the other quantum yield value $\Phi(cis \rightarrow trans)$ for each species.

5.3.3. Application of the theory to our compounds

The extinction coefficients of the *cis* isomers **(*Z*)40⊂α-CD** and **(*Z*)40** could not be measured directly as there is no wavelength at which the photostationary state consists of 100 % *cis*. Estimates for ε_{cis} were therefore obtained *via* extrapolation from a mixture of *trans* and *cis*, where the extinction coefficient of the *trans* isomer (ε_{trans}) and the ratio of *cis* : *trans* were known. Since photodegradation competes with switching, the samples were irradiated for the shortest time possible to produce an accurately measurable proportion of *cis* isomer in the mixture.

The rotaxane **40⊂α-CD** and dumbbell **40** were irradiated in water at their respective absorption maxima (347 nm and 340 nm) until a significant amount of the *cis* isomer had formed. ^{1}H NMR integrals, measured in D_2O with a 90° pulse width, gave a proportion of 0.75 : 0.25 of *trans* : *cis* in the rotaxane **40⊂α-CD** solution and 0.62 : 0.38 of *trans* : *cis* in the solution of dumbbell **40**.

The extinction coefficient of the *cis* isomer (ε_{cis}) for both the rotaxane **40⊂α-CD** and the dumbbell **40** was then derived according to Equation 5.4, by calculations performed in an Excel spreadsheet at every point on the spectrum from 200 – 500 nm with a data interval of 1 nm.

The results of this calculation are shown in Figure 5.9 and 5.10.

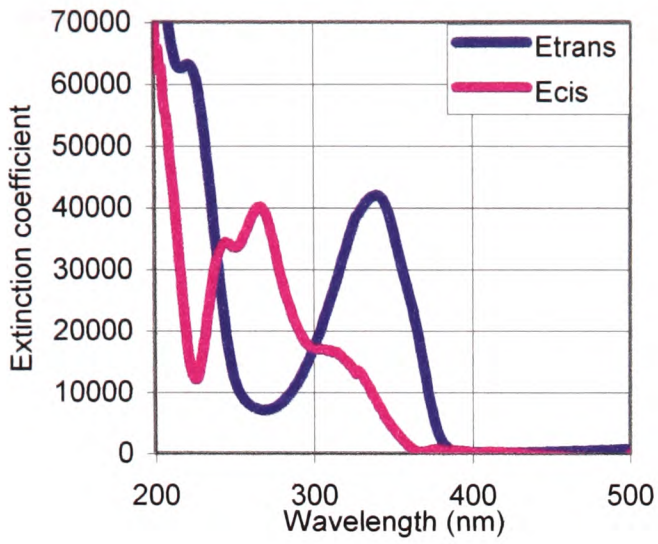

Figure 5.9. *Spectrum of ε_{cis} and ε_{trans} of dumbbell* ***40****.*

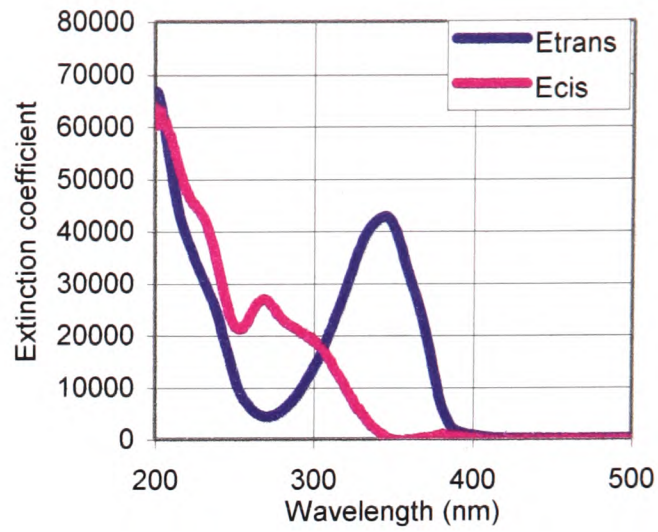

Figure 5.10. *Spectrum of ε_{cis} and ε_{trans} of rotaxane* ***40⊂α-CD****.*

For the purposes of these calculations, quantitative kinetic photoswitching experiments were carried out with irradiation at the isosbestic point in the case of both rotaxane **40⊂α-CD** and dumbbell **40**. This wavelength was chosen in order to reduce the error introduced by the previous approximations as $\varepsilon_{cis} = \varepsilon_{trans}$ at this point. The irradiation wavelength was 307 nm and 300 nm for the rotaxane **40⊂α-CD** and the dumbbell **40** respectively. Irradiation was ceased when the incremental changes in absorption became small. In the case of the dumbbell **40**, identification of the exact isosbestic point was difficult, due to the competing process of photodegradation, as well as the changing proportions of *cis* and *trans* isomers. These experiments gave the rate constant (k) and projected proportions of *cis* and *trans* isomers in the photostationary state ($fcis_F$ and $ftrans_F$ respectively).

As seen in Equations 5.5. and 5.6, the kinetic experiments enable the determination of the ratio of *cis* : *trans* isomers in the photostationary state. The rate constants were calculated in a similar way to that in Section 5.3, by fitting the curve obtained

to an empirical first order exponential equation. These curves are shown in Figure 5.11 and 5.12.

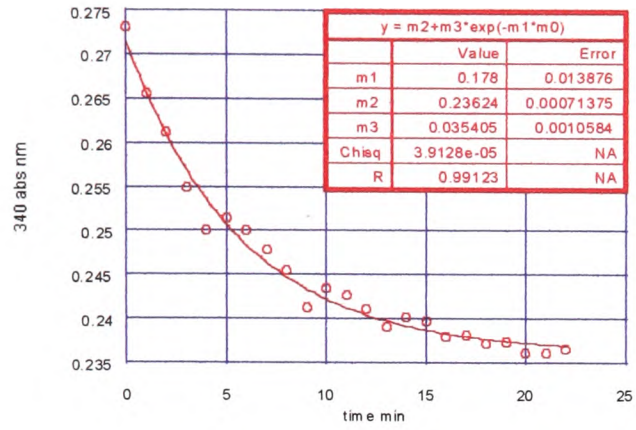

Figure 5.11. *Fitting curve for irradiation of dumbbell* ***40*** *at 300 nm.*

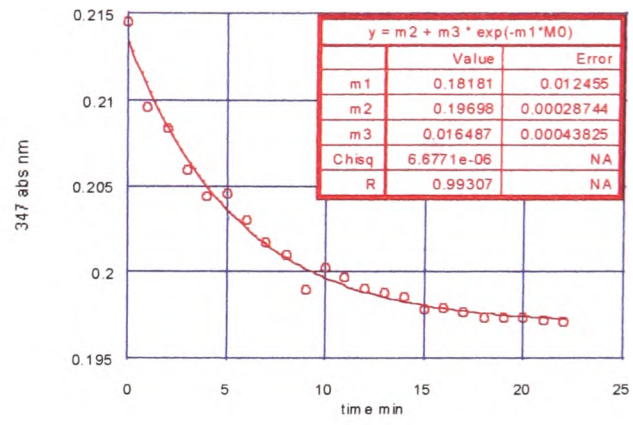

Figure 5.12. *Fitting curve for irradiation of rotaxane* ***40⊂α-CD*** *at 307 nm.*

In this case, the rate constants were found to be 0.175 min^{-1} (**40⊂α-CD**) and 0.191 min^{-1} (**40**). These are average values from repeated switching experiments.

The calculations to determine $fcis_F$, the fraction of *cis* isomer in the photostationary state, were then carried out for several different time points in the kinetic switching runs. Figures 5.13 and 5.14 show the results at t=17 min for dumbbell **40** and the rotaxane **40⊂α-CD** respectively.

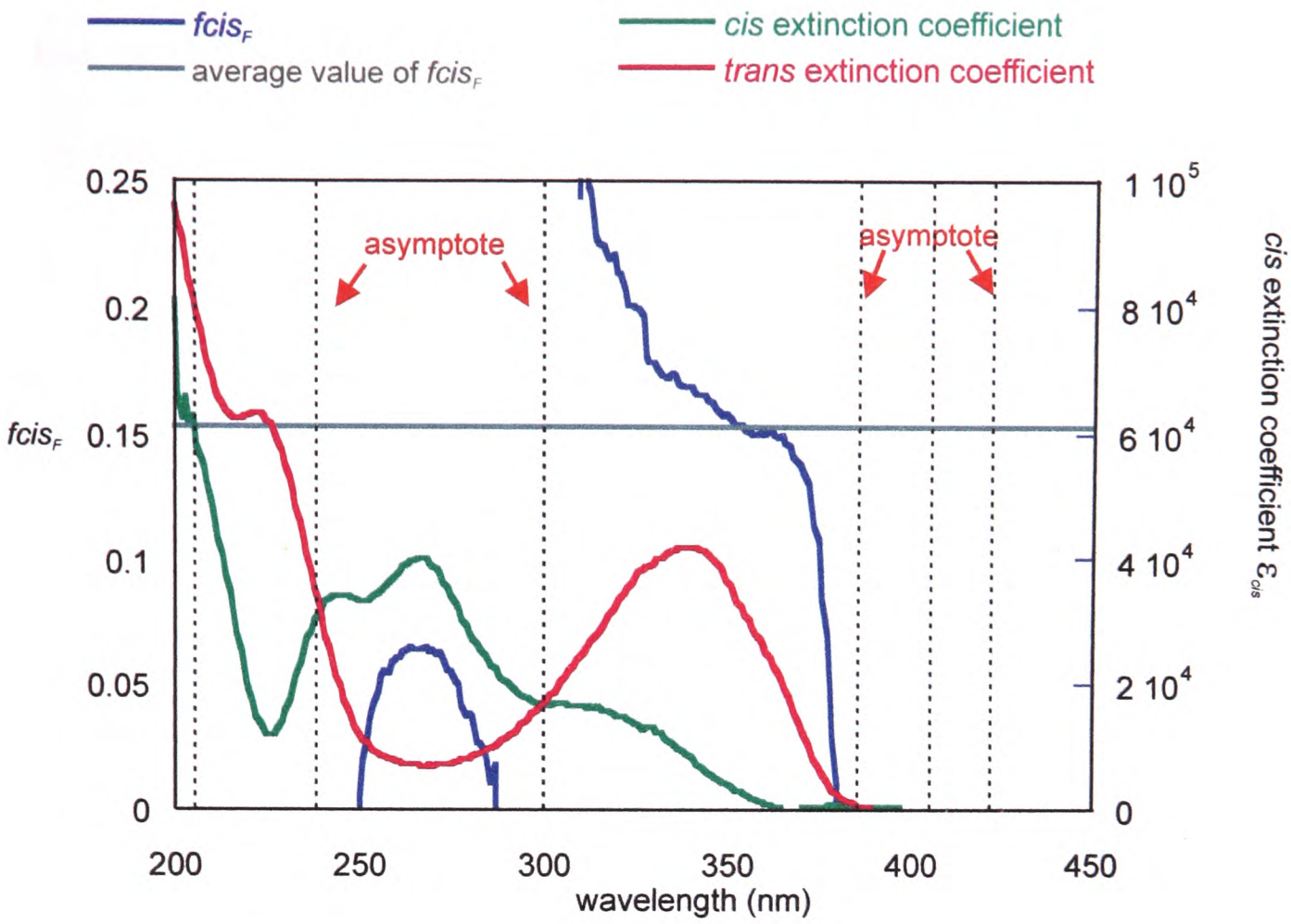

Figure 5.13. *Plot of $fcis_F$ vs. wavelength for dumbbell* ***40****. The extinction coefficient graphs are superimposed.*

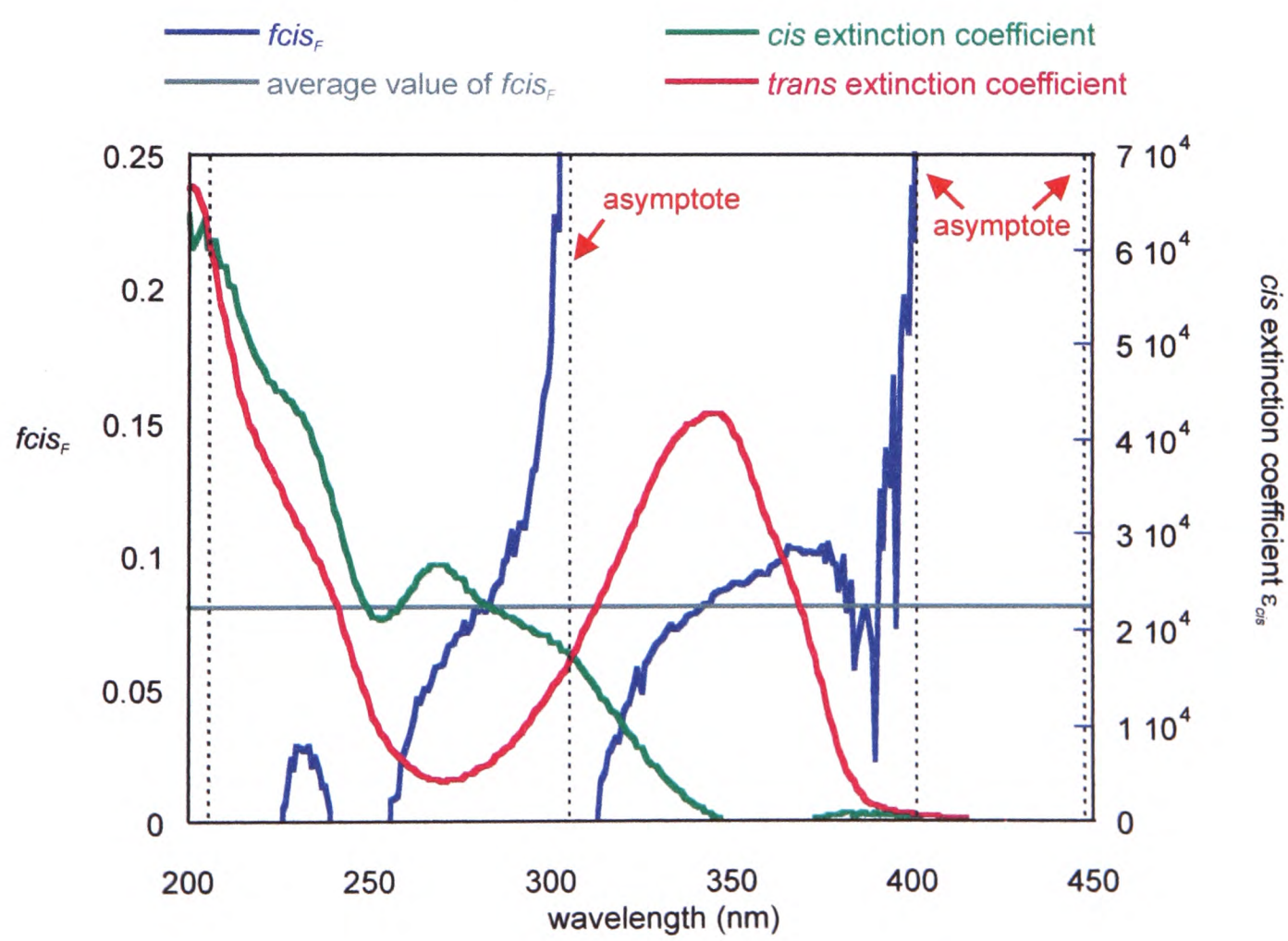

Figure 5.14. *Plot of $fcis_F$ vs. wavelength for rotaxane* ***40⊂α-CD****. The extinction coefficient graphs are superimposed.*

Values taken for $fcis_F$ were 0.15 for the dumbbell **40** and 0.08 for the rotaxane **40⊂α-CD**. These were the average values for the two graphs respectively (shown in grey). The extinction coefficients curves are superimposed in order to explain the seemingly erratic behaviour of the $fcis_F$ curves. At the points at which $\varepsilon_{cis} = \varepsilon_{trans}$, the result $fcis_F$ becomes infinite, as the denominator in Equation 5.8 is 0. At points in which neither isomer absorbs greatly, the calculation also becomes inaccurate. Thus the points chosen to use as the final value for $fcis_F$ (which is theoretically a straight line, as shown by the grey line) must be carefully selected in the region of 340 nm, far from the isosbestic points and where both isomers absorb strongly.

However, unless $\Phi(trans \rightarrow cis)$ or $\Phi(cis \rightarrow trans)$ is known, it is only possible to calculate a ratio from Equation 5.8. We therefore calculated $\Phi(trans \rightarrow cis)$ relative to that of stilbene (**49**). The initial rate of switching can be well approximated by fitting a straight line through the initial data points of a plot of time *vs.* absorbance (in the case where the rate fits well to an exponential curve).

In all cases 325 nm was chosen as the irradiation wavelength, in order to ensure that the intensity of light provided by the fluorimeter was the same for each sample (the response of the fluorimeter has been found to vary slightly with wavelength). As the derivation of Equation 5.8 in Appendix 5.1 shows, the calculations depend on this assumption, as well as the condition that the experiment is carried out at high dilution. Scheme 5.8 shows the photoswitching of stilbene (**49**).

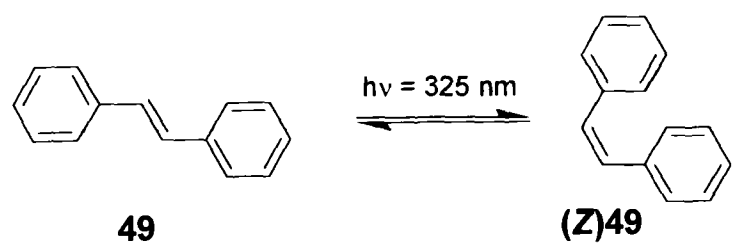

Scheme 5.8. *Irradiation of trans-stilbene at 325 nm.*

Reproducible values for *Φ(trans → cis)* of rotaxane **40⊂α-CD**, dumbbell **40** and *trans* stilbene **49** were obtained *via* this route.

The calculated values of the quantum yields are shown in Scheme 5.9.

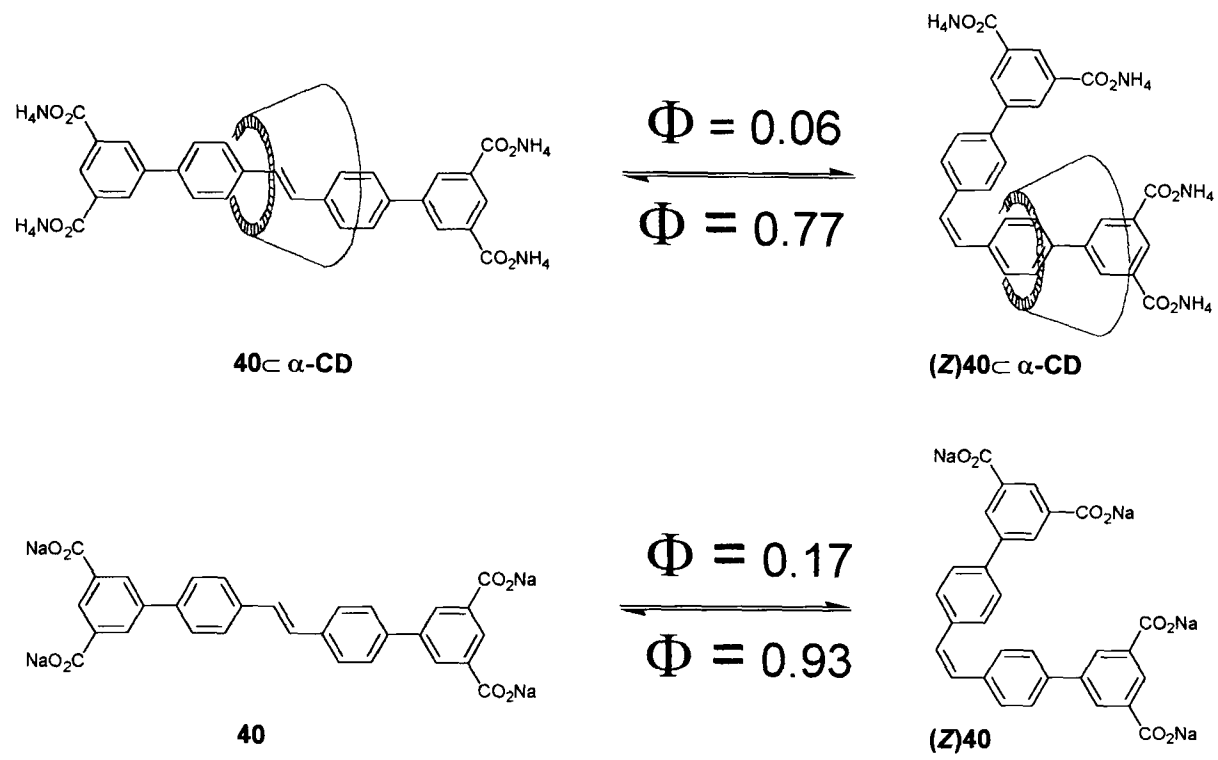

40⊂ α-CD **(Z)40⊂ α-CD**

40 **(Z)40**

Scheme 5.9. *Quantum yields of trans⇆cis switching for dumbbell **40** and rotaxane **40⊂α-CD**.*

For both rotaxane and dumbbell, *Φ(trans → cis)* is considerably lower than that of stilbene **49** (0.50). This indicates that even the dumbbell **40** is much less susceptible to photoswitching than unsubstituted stilbenes, probably due to the electron withdrawing effect of the additional phenyl group. This is substantiated by work performed on a range of biaryl stilbenes[22], in which such species demonstrated lowered *trans→cis* quantum yields, though not to the extent seen here. Indeed, we had expected these numbers to be small, given the high fluorescence quantum yields which clearly indicate that the majority of the singlet excited species decays in a radiative fashion, losing the excitation energy *via* fluorescence. Comparison of these calculated quantum yields shows clearly that the encapsulation of the stilbene unit, although it does not prevent photochemistry from occurring, does considerably

influence the outcome of the irradiation. The *Φ(trans→cis)* value for the rotaxane **40⊂α-CD** is much smaller than that for the corresponding dumbbell (**40**) (0.06 *vs.* 0.17). This implies that either the 'p'-state collapse has been affected by the encapsulation, or the attainability of the 'p'-state itself has been altered *i.e.* the energy barrier to achieve a twisted intermediate has been raised. The quantum yields for the reverse process, *Φ(cis→trans)*, are both large (0.77 *vs.* 0.93) and as such indicate that encapsulation of the *cis* form does not greatly alter its ability to switch. This may be explained if we assume that the *trans* isomer may only switch when the cyclodextrin adopts a specific position on the dumbbell. The cyclodextrin is more locked in position in the case of the *cis* isomer (expanded in Section 5.4) and thus most positions of the cyclodextrin may result in *cis→trans* isomerisation. These results are in partial agreement with the work by Stoddart *et al.*[23] in which the quantum yield for *trans→cis* is halved upon encapsulation, as is the reverse quantum yield of *cis→trans* (shown in Figure 5.15).

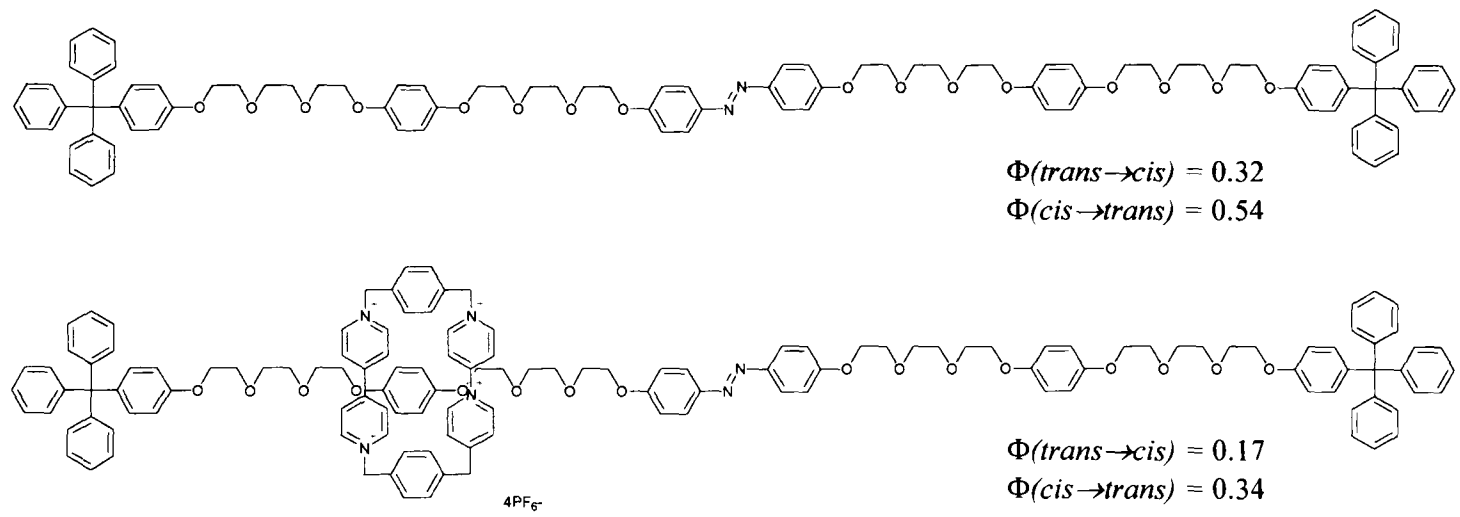

Figure 5.15. *Stoddart's work on switching of azobenzenes, and the quantum yields for the switching processes.*

Unlike the present study, the work of Stoddart involves switching of an azobenzene unit, which could well explain the differences in the trends seen here, as

azobenzenes may also isomerise in this direction *via* a thermal mechanism, whereas the efficiency of the *cis→trans* isomerisation of stilbenes is virtually unaffected by temperature. Furthermore, the component macrocycle and dumbbell units are different in nature compared to those under investigation here. However, it is interesting to note the agreement of the trends in the quantum yield of the light-induced isomerisations.

5.4. Structural studies of the *cis* rotaxane (*Z*)40⊂α-CD

From space-filling (CPK) models of the rotaxane, it was unclear whether or not the *trans→cis* isomerisation would be possible. For this reason, and to characterise the new *cis* form of **(*Z*)40⊂α-CD** more fully, detailed NOE studies were carried out on the mixture previously used to calculate the proportions of *cis* : *trans*. It was possible to distinguish NOEs that were due to both isomers in the mixture and to use these in the assignment of the *cis* isomer (NOEs present in the *trans* form have been discussed in Chapter 2).

40⊂ α-CD

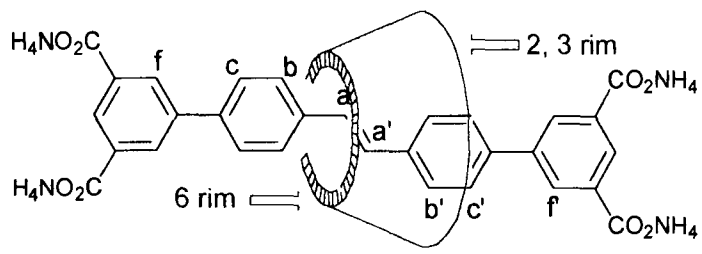

(*Z*)40⊂ α-CD

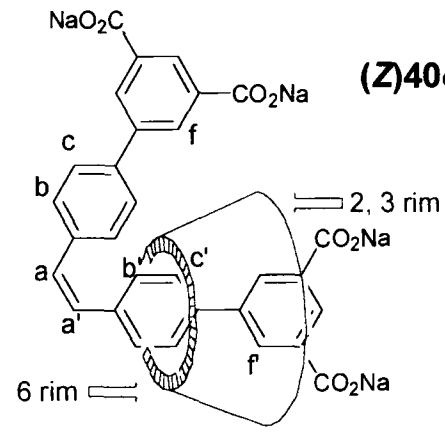

Table 5.2. *Tabulated NOEs visible in both isomers of* ***40⊂α-CD****.*

(*E*)40⊂α-CD

	f	c	b	a	a'	b'	c'	f'
3				W	W	W	S	W
4								
5		M	W	M	M	S	S	
6/6'		M	W	W	W	W	W	

(*Z*)40⊂α-CD

	f	c	b	a	a'	b'	c'	f'
3							S	S
4		W						
5					W	S	S	
6/6'						S	S	

S = strong interaction, M = medium strength interaction, W = weak interaction.

The following points stand out from Table 5.2: first of all, the *trans* isomer has many NOEs, from the protons of cyclodextrin to many different protons on the dumbbell backbone. Although it does seem to sit preferentially over one of the benzene rings, there is no single position for the cyclodextrin which could account for all of the observed NOEs. This implies a degree of mobility along the dumbbell. In the case of the *cis* isomer a few strong NOEs are observed. These can be attributed to a less mobile, more locked position of the cyclodextrin on the dumbbell core. All of the NOEs seen can be attributed to a structure similar to the one shown, in which the cyclodextrin sits permanently over the stopper unit. This idea is reinforced by the NOE seen, unusually, from the unencapsulated portion of the

dumbbell to the 4-H on the outside of the cyclodextrin ring. This work improves upon the attempts by Vögtle[24] to prove the reduction of translational motion of a macrocycle along the axle of his rotaxane system, on switching of an azobenzene unit. The NOE evidence has proven invaluable in our elucidation of this structure.

The whole ^{1}H spectrum of the *cis/trans* mixture was assigned by use of HSQC, COSY, and the NOESY (the 2D NOESY is depicted in Appendix 5.2). The assigned spectrum is shown below in Figures 5.16 and 5.17.

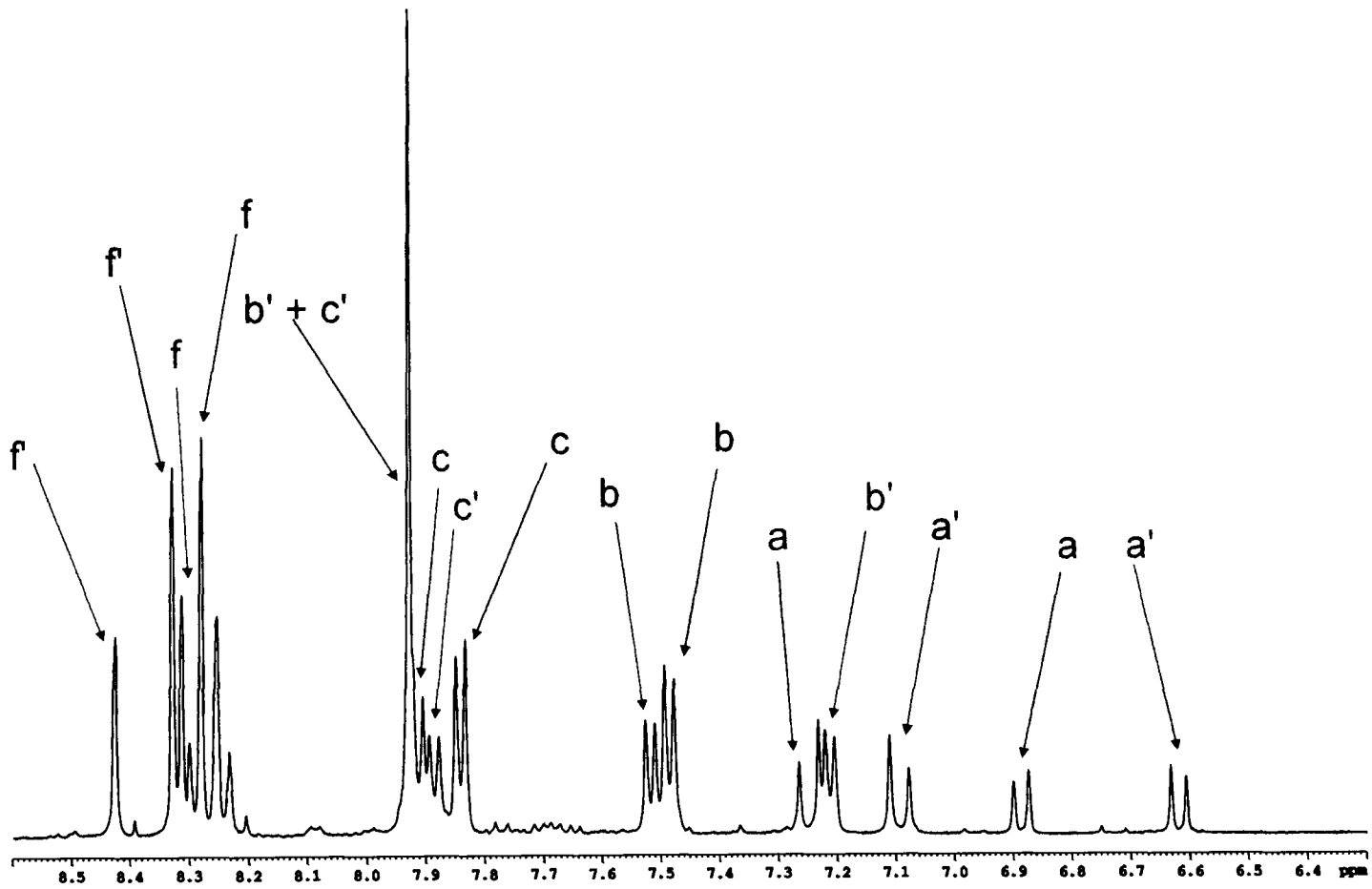

Figure 5.16. *Aromatic region of the cis/trans mixture of rotaxane* ***40⊂α-CD****, recorded in D_2O on a 500 MHz instrument. The assignments of the cis isomer* ***(Z)40⊂α-CD*** *are shown in blue, and the trans isomer* ***40⊂α-CD*** *in red.*

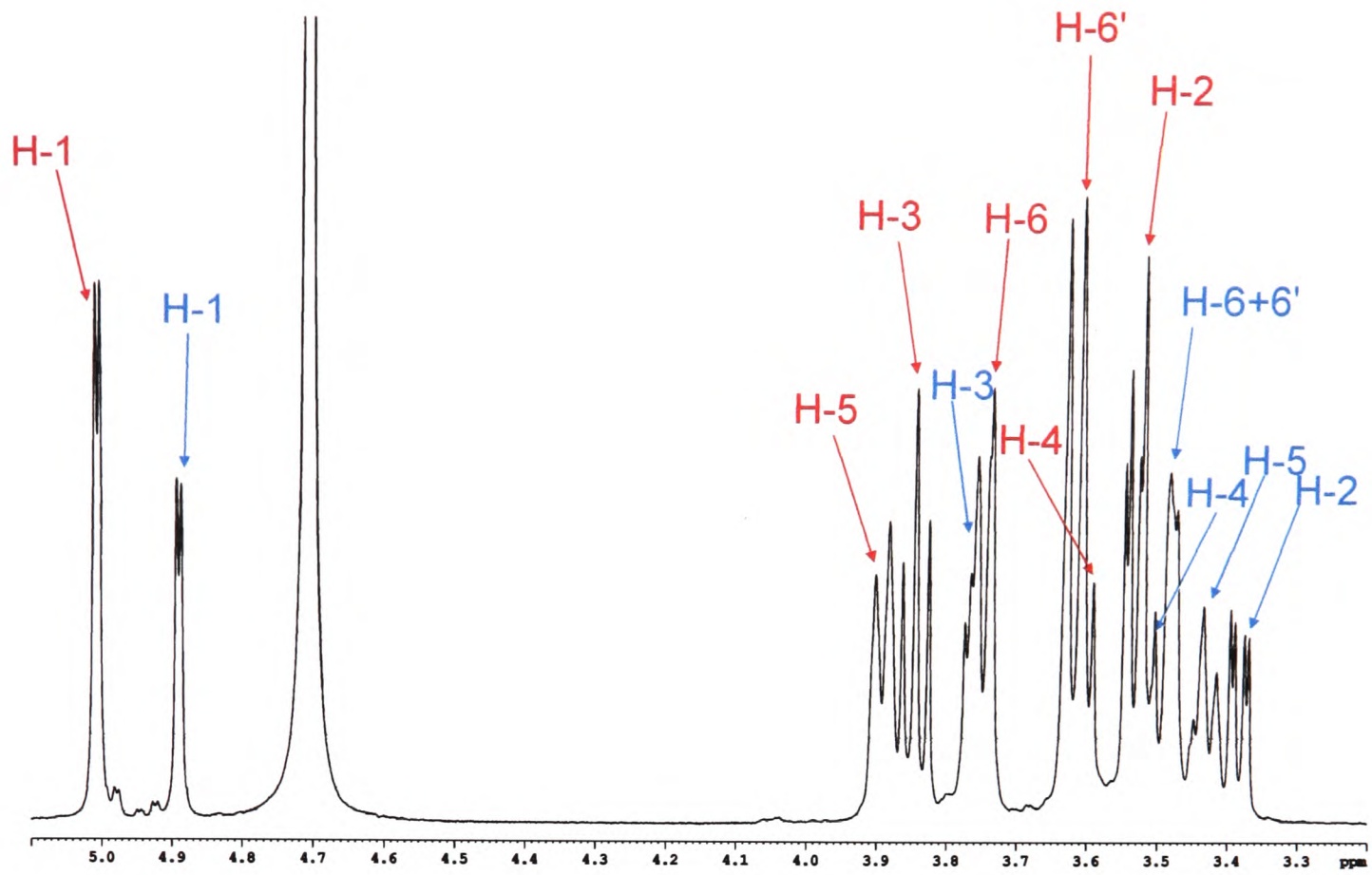

Figure 5.17. *Aliphatic region of the cis/trans mixture of rotaxane* ***40⊂α-CD****, recorded in D_2O on a 500 MHz instrument. The assignments of the cis isomer* ***(Z)40⊂α-CD*** *are shown in blue, and the trans isomer* ***40⊂α-CD*** *in red..*

The anomeric atoms (H-1 and C-1) could be identified by their characteristic chemical shifts. The HSQC was then used to assign all the cyclodextrin protons by the typical ordering of ^{13}C chemical shifts (C-6<C-2<C-5<C-3<C-4<C-1) and by the splitting patterns of the ^{1}H peaks. The C-6 was the only carbon peak in the cyclodextrin region which coupled to two distinct protons (H6 and H6'). The COSY was then utilised to assign the cyclodextrin protons undistinguishable using the HSQC, by following the correlations around the glucose ring. The aromatic portions were then separated into the contributions from the *cis* and *trans* isomers by distinguishing those peaks with NOEs to one of the cyclodextrins environments and by the differing coupling constants of the two alkenes. The COSY spectrum was then used to assign the remaining protons by correlations to those which had already been identified as *cis* or *trans* isomers. The pure *trans* isomer had previously been

fully assigned (in Chapter 2) which aided the assignment of this rather complex system.

Modelling using CACHE, with minimisation of the distances between protons showing strong to moderate NOEs, gives a space-filling picture of the *cis* isomer, shown in Figure 5.18.

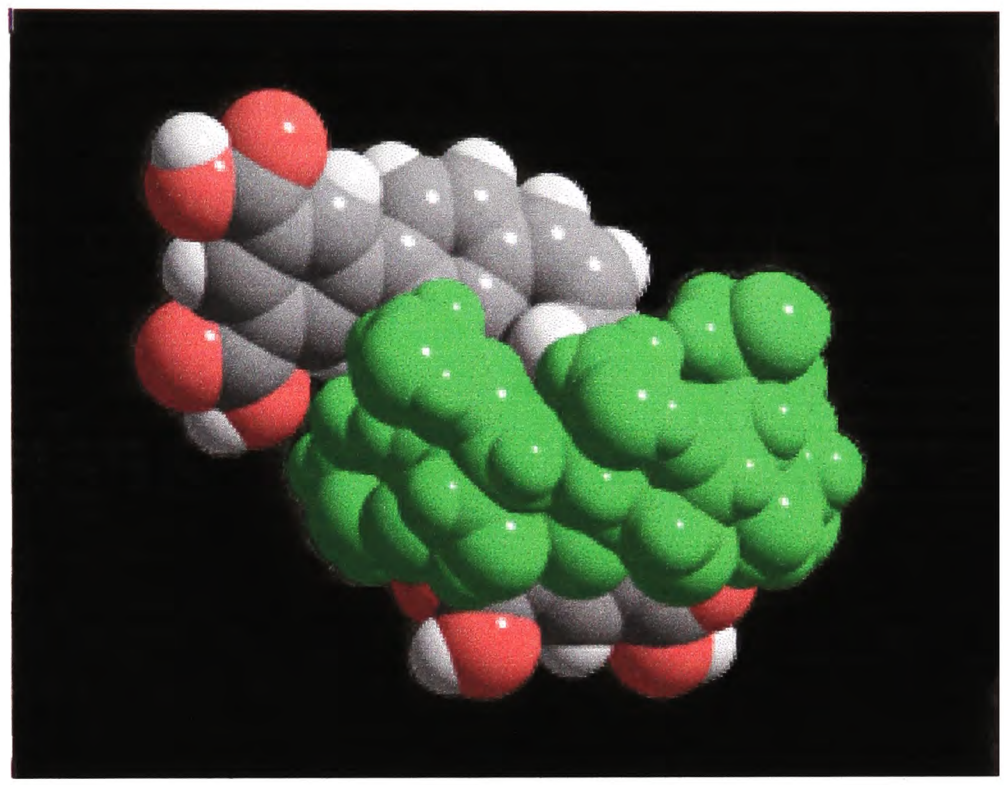

Figure 5.18. *Space-filling representation of predicted low-energy conformation of cis isomer* ***(Z)40⊂α-CD****.*

It is important to note that this isomer is the only one formed from the isomerisation process. It could be envisaged that an alternative isomer (shown in Figure 5.19) could also be produced by the switching of **40⊂α-CD**.

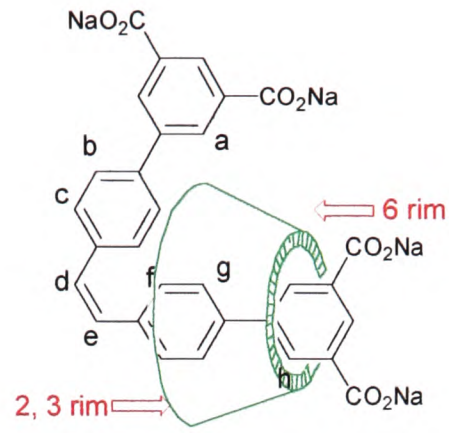

Figure 5.19. *Proposed alternative isomer of the isomerised rotaxane* ***(Z)40⊂α-CD****, not formed in the photoisomerisation.*

However, the only product of irradiation here is the isomer shown in Figure 5.18, with the wide rim (the 2, 3 rim) of the cyclodextrin exclusively pointing towards the stopper units. Previous work carried out within the Anderson group has investigated the orientation of the cyclodextrin upon an asymmetrical dumbbell unit[25], and in some cases[26] has demonstrated preference in orientation of binding. However, it must be stressed that the trends seen in previous work do not bear much relevance to the situation seen here, where the conformation adopted is under thermodynamic rather than kinetic control. In this case, the conformation assumed must be due, at least in part, to the steric demands placed upon the molecule on switching. Hydrophobic interactions and the solvation shells of the carboxylate groups may also contribute to produce the results seen. Rudimentary calculations using the CACHE program suggest that the alternative (not seen) isomer does indeed have a higher energy (2 *vs.* 12 kCal mol^{-1}). This is an area in which it would be possible to expand upon this work by use of longer, asymmetrical dumbbell units.

It is obvious from the loss of cyclodextrin mobility that the *cis* isomer is more constrained than the more mobile *trans* isomer. This effect could be exploited in

many ways, for example in the design of molecular switches, or the enhancement of the conductive properties of organic polymers, by hindering the isomerisation process and subsequent loss of conductivity.

5.5. Elucidation of the photodegradation processes

Although it was clear from the photoswitching experiments that a small amount of degradation was occurring, it was not possible within the constraints of those investigations to examine this in any great depth. It was anticipated that the eventual photoproducts would be cyclobutanes[18, 27, 28] (in the case of the dumbbell; the rotaxane probably being too sterically hindered to allow [2+2] addition to occur) and dihydrophenanthrenes / phenanthrenes[29-31]. These have been documented on numerous occasions in the past.

5.5.1. Complete photodegradation and identification of photoproducts

In order to investigate this more fully, both the rotaxane **40⊂α-CD** and the corresponding dumbbell **40** were irradiated at their respective maxima (347 nm for **40⊂α-CD** and 340 nm for **40**), both in the presence and absence of air. Figures 5.20 and 5.21 show the result of the irradiations.

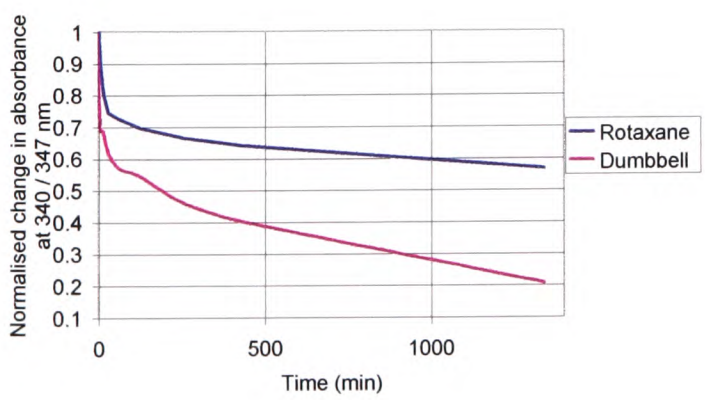

Figure 5.20. *Anaerobic photodegradation of* ***40⊂α-CD*** *and* ***40****, plot of changing absorbance at maximum vs. time.*

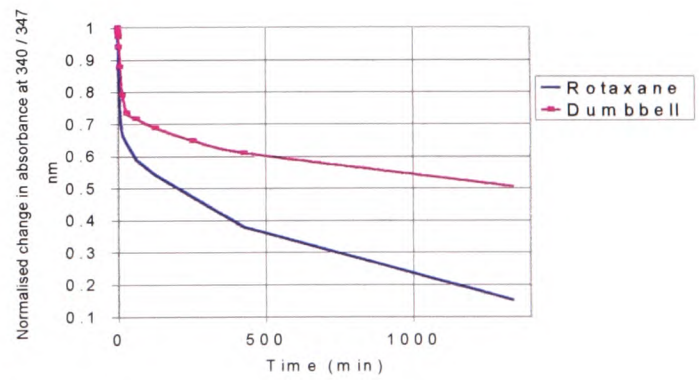

Figure 5.21. *Aerobic photodegradation of* ***40⊂α-CD*** *and* ***40****, plot of changing absorbance at maximum vs. time*

The majority of the published literature suggested that degradation would produce a phenanthrene (or dihydrophenanthrene) or cyclobutane. The irradiations were performed on a preparative scale (by use of two 300 W lamps) to ascertain which photoproducts had been formed. Irradiation in the presence of air proved to be quite messy, giving a complex mixture of products, including evidence of aldehydes in the ^{1}H NMR, probably formed by photo-oxidation[32] of the stilbene. For this reason, it was decided to concentrate on the anaerobic degradation, as this appeared to be cleaner.

In the case of the rotaxane, no evidence was found to point to either of these possible photodegradation products (phenanthrene or cyclobutane). The crude ^{1}H NMR was complex, however the use of mass spectrometry did reveal a possible identity for this photoproduct. Addition of a unit of mass 18 a.m.u. to the starting material pointed towards a light induced hydration. Scrutiny of the literature[33-35] then suggested a rather unusual reaction, not normally observed in stilbenes, because of the greater rate of the other potential reactions relative to the addition of water, as well as the fact that stilbenes are generally quite insoluble in water. This possibility was photohydration (shown in Scheme 5.10). It is possible, according to a recent paper by Miranda[36], that inclusion in a cyclodextrin cavity increases the likelihood of photohydration. Miranda's work investigated the hydration of various small, non-conjugated alkenes in the presence of β-cyclodextrin and found that photohydration, and not the expected cyclisations to which such alkenes are normally susceptible, was the major reaction occurring in his system.

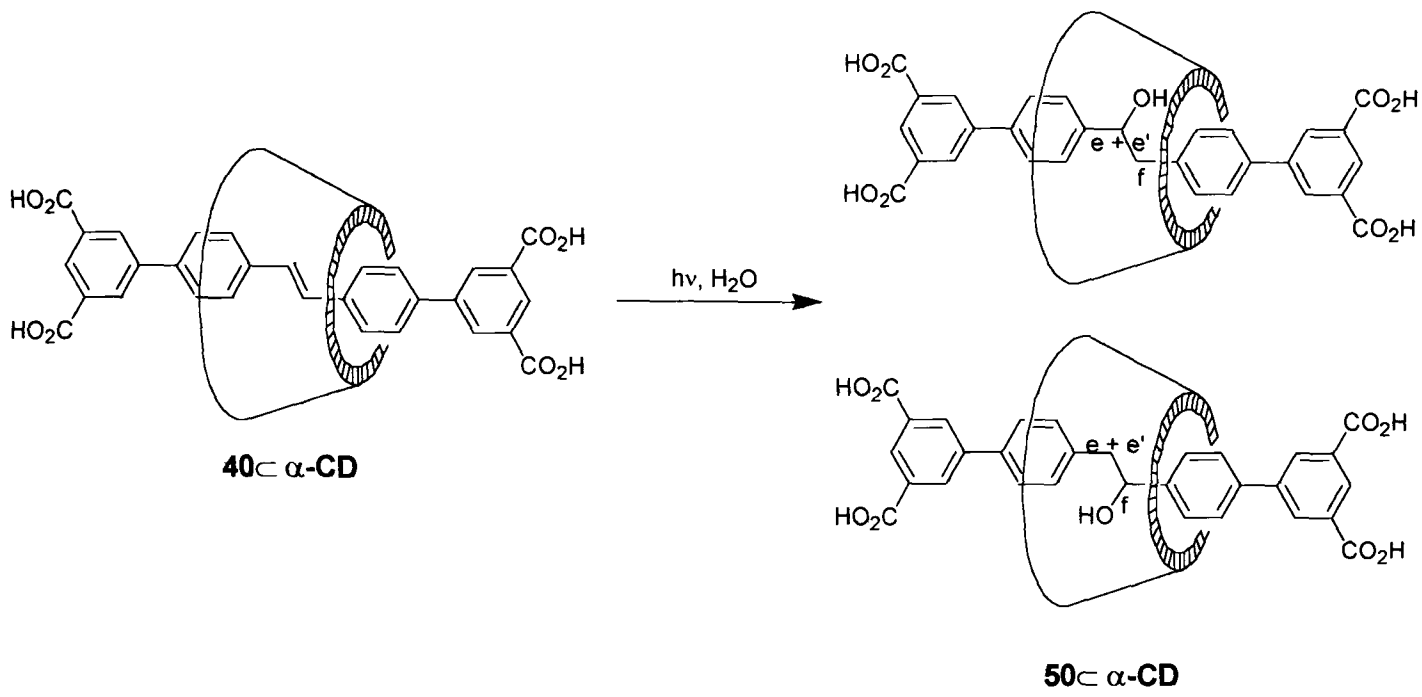

Scheme 5.10. *Photohydration of rotaxane* ***40⊂α-CD.***

Inspection of the ^{1}H NMR in the light of this knowledge still showed the presence of four species of this form (**50⊂α-CD**), two orientational isomers and two enantiomers; the hydration creates a chiral centre, albeit in varied proportions. All species showed disruption of the previously symmetrical aromatics, resulting in more complex aromatic signals in the 8.06 – 7.20 ppm envelope. These were consistent with at least three species of the form shown. A double doublet at 5.05 ppm indicated a single proton, *f*, coupling to two adjacent, inequivalent ones (*e* and *e'*). These were more difficult to locate; at 3.11 ppm and 3.03 ppm, they were dwarfed by the wide cyclodextrin envelope (3.95 – 3.25 ppm). However, COSY correlations to the *f* protons enable these signals to be incontrovertibly assigned. Presence of four distinct species indicates that the stereochemistry of the stereocentre formed in this desymmetrisation of the dumbbell core is not greatly affected by the presence of the cyclodextrin. This is perhaps slightly unexpected as, although water is a symmetrical molecule, α-cyclodextrin itself is chiral. It would therefore be reasonable to expect that it might influence the stereochemistry of the

attack by water. However, studies of this photohydration have shown that this reaction occurs *via* the excited singlet state[37] or *via* the 'p'-state, and there is no direct way of pinpointing the position of the cyclodextrin upon the backbone when in an excited state. It may be that in the excited states the cyclodextrin does not in fact sit anywhere near the alkene and is thus unable to prevent the excited state from reaction, as it does in the ground state. The existence and conformation of the *cis* isomer **(*Z*)40⊂α-CD** is a good indication that this could be true; although it does not prove that the cyclodextrin also adopts this position in the excited state, it does prove that such a conformation could also be possible in the singlet excited state.

5.5.2. Photohydration of dumbbell 40

The dumbbell **40** was subjected to similar conditions as above, in the hope of discovering whether the photohydration reaction was the favoured one for this dumbbell unit, or simply the only one which could occur in the case of the rotaxane, as all other reactivity had been blocked by encapsulation. The photohydration of **40** is depicted in Scheme 5.11.

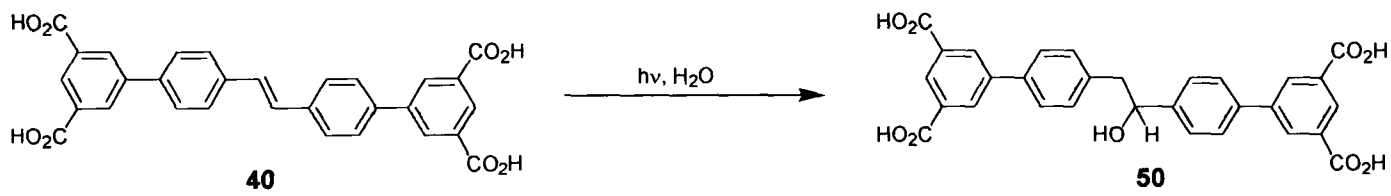

Scheme 5.11. *Photohydration of the dumbbell* ***40****.*

A mixture of the photohydration product (**50**) and another species was detected by mass spectrometry and ^{1}H NMR. The minor species had a mass that could only correspond to a combination of two dumbbell units in some manner, and the aromatic ^{1}H NMR signals were symmetrical, indicating one of the two structures shown below as the likely assignment for this side product.

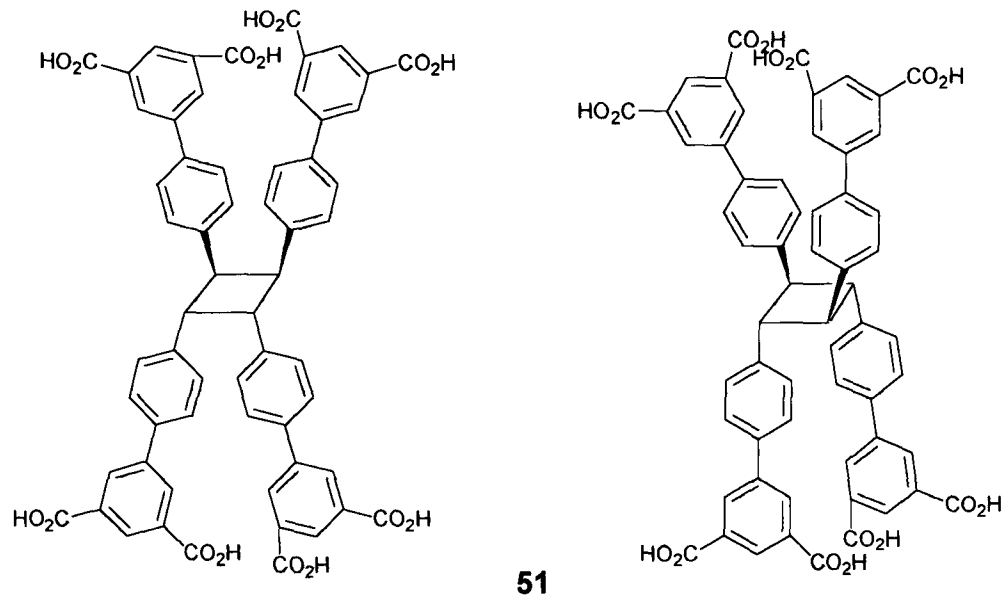

51

Figure 5.22. *Potential structures for the minor product (**51**) in the photohydration reaction.*

Formation of cyclobutanes in water has been reported previously[27], the surprising result perhaps being that this is not the major product but in fact constitutes around only 20 % of the degradation. This may indicate a pre-disposition of the dumbbell towards photohydration, possibly due to the highly electron withdrawing effects of the biphenyl groups on the alkene, rendering it very open to nucleophilic attack by water. The other possible explanation for the low proportion of [2+2] adduct formed is simply that, unlike 'normal' stilbenes, these water-solubilised stilbenes do not aggregate so readily in water and thus are less able to come together to undergo the [2+2] addition. One conclusion which is clear from this work, however, is the extent of protection which can be afforded by encapsulation. Although some cyclobutane is formed in the irradiation of the dumbbell, none is seen in the case of the rotaxane. This may account for the lower rate of degradation seen in the rotaxane in 5.5.1.

Attempts to fit the rate data for the degradation (shown in Figure 5.20) suggested that the degradation fits well to a pseudo bi-exponential, in which one set of parameters corresponds to those from the pseudo-first order switching process. The second set of parameters (assuming that the possibility of dimerisation is negligible at the concentrations at which these experiments were conducted), corresponds to

the rate of photohydration. This was found to be five times faster in the case of the dumbbell than that of the rotaxane, thus providing further evidence for the protective ability of the cyclodextrin.

5.5.3. Attempted phenanthrene syntheses

In an extension of the work on photodegradation, we decided to attempt to force the expected reaction to form phenanthrenes. Although it has been shown that the dihydrophenanthrenes can be oxidised simply by the action of air, we decided to use a more controllable oxidant, since initial irradiations in the presence of air appeared to have produced mainly aldehydes (see Section 5.5.1). The oxidising agent employed in this case was iodine, and the HI formed was scavenged by an excess of propylene oxide, which could subsequently be easily removed under vacuum. The reaction scheme is shown in Scheme 5.12.

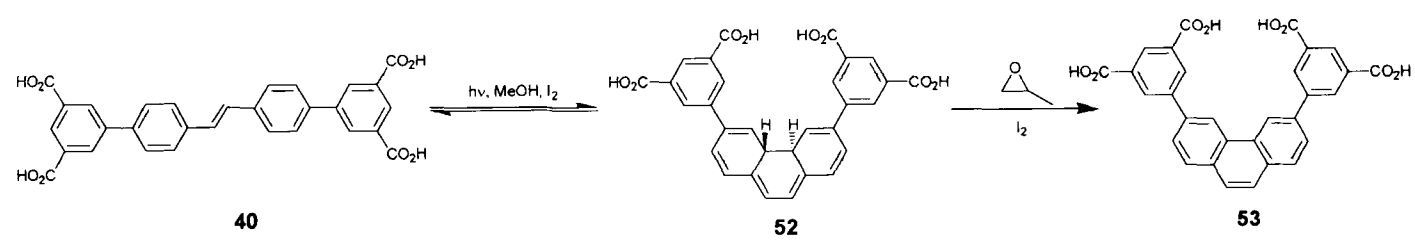

40 52 53

Scheme 5.12. *Phenanthrene formation from dumbbell* ***40*** *in methanol*[38].

The reaction was monitored by UV/Vis spectroscopy and destruction of the stilbene chromophore, along with increased absorbance at 265 nm, was observed. However, the crude ^{1}H NMR and mass spectrum did not show the presence of the target phenanthrene (**53**), or even the reversible formation of a dihydrophenanthrene (**52**). The ^{1}H NMR appeared to point towards the formation of an asymmetrical species, possibly **54**.

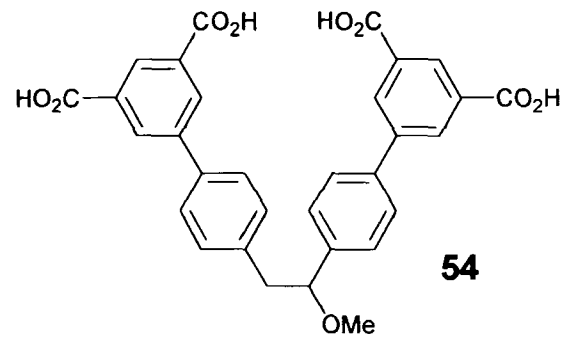

54

Mass spectrometry also confirmed this as a possibility, with a mass ion corresponding to **54**. This could be formed in a similar mechanism to the photohydration products, **50** and **50⊂α-CD**, by nucleophilic attack of the solvent, in this case methanol. The methanol adduct proved difficult to purify but, as it was not our target molecule, the reaction was attempted again. This time, we chose acetonitrile as the reaction solvent, in an attempt to prevent the possibility of nucleophilic attack by the solvent.

In acetonitrile, destruction of the chromophore was again seen, which appeared quite promising in our efforts to form the phenanthrene. However, crude NMRs again showed a more complex pattern of signals than that expected for the symmetrical phenanthrene **53**, and the spectrum did not correspond to any of the photoproducts previously isolated. Crude electrospray and FAB mass spectra also showed none of the known photoproducts. It seems unlikely that the phenanthrene **53** was formed at all, however it is difficult to elucidate the exact nature of this reaction. There is some precedent for a non-nucleophilic molecule such as acetonitrile adding to an alkene upon irradiation, in a photo-induced Ritter-style[39, 40] reaction, though intermolecular reaction is unusual. Amines[41], amides[42], and a thioisoindole[43] have also been added in this way. In the case that such an addition has indeed taken place, this would confirm the conclusions which can be drawn from the photohydration and methanol additions: this particular stilbene type is much more prone to nucleophilic attack than any other photoreaction of the alkene.

Despite this seeming failure, the rotaxane was subjected to the conditions for phenanthrene formation in acetonitrile. This is portrayed in Scheme 5.13.

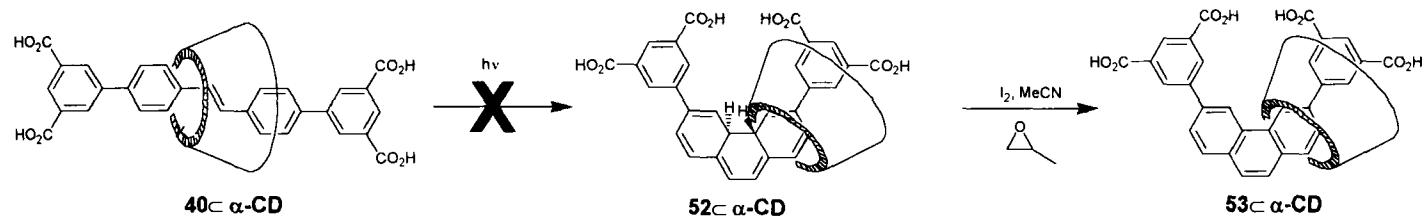

Scheme 5.13. *Attempted phenanthrene formation from rotaxane* ***40⊂α-CD****.*

There appeared to be no reaction. However, solubility of the rotaxane in acetonitrile was poor and consequently the attempt was also carried out in DMF. There is no reason to suppose that phenanthrene formation could not take place in DMF, although it is not the usual solvent for such reactions. Again, no change was observed after prolonged irradiation. Unfortunately, it is impossible to completely explain these results without further work, including attempts in many different solvents. Time constraints rendered this impossible within the limits of this thesis. It is possible to conclude, however, that phenanthrene formation does not appear to be favourable either in the case of the dumbbell **40** or rotaxane **40⊂α-CD**, and that the rotaxane does not undergo the destruction of the chromophore seen in the case of the dumbbell. Although it is unclear what was formed in the dumbbell irradiation, the fact that it does not happen when the rotaxane is subjected to similar conditions upholds the idea that encapsulation can significantly protect the encapsulated molecule from both chemically and photochemically reactive encounters.

5.6. Conclusions of Chapter 5

This chapter has illustrated the versatile photochemistry of stilbenes, both encapsulated and unencapsulated, whilst underlining the differences in reactivity

upon this encapsulation. All the tested rotaxanes and their corresponding dumbbells could be switched between *trans* and *cis* isomers to varied extents, with the exception of **39⊂α-CD** which could not form the *cis* isomer. This was ascribed to steric considerations. The complete prevention of *trans*→*cis* isomerism is an important result, as this has not previously been achieved by encapsulation.

The other rotaxanes all showed a better reversibility than their dumbbell counterparts, degrading much more slowly and to a different mixture of species. The degradation products of one rotaxane **40⊂α-CD** and one dumbbell **40** have been analysed and partially characterised; it was found that photohydration was the major degrading reaction in both cases, although the dumbbell **40** also undergoes [2+2] cycloaddition. The degradation is approximately five times faster in the case of the rotaxane **40⊂α-CD** than that of its corresponding dumbbell **40**.

Experiments were undertaken to calculate the proportions of *cis* and *trans* isomers in a photostationary state, and the extinction coefficients of these unisolable *cis* isomers. By use of these and an approximation involving comparison of the initial switching rates of **40⊂α-CD** and **40** with *trans*-stilbene→*cis*-stilbene (**49**→**(*Z*)49**), values of the quantum yields for Φ*(trans→cis)* and Φ*(cis→trans),* of **40⊂α-CD** and **40** respectively, were calculated. These show that encapsulation does indeed affect the efficiency of the switching process by a factor of around 3, but only in the *trans*→*cis* direction.

The new *cis* isomer of the rotaxane **(*Z*)40⊂α-CD** was further characterised by NOE analysis, showing a significant reduction in the mobility of the cyclodextrin upon the axle, once in the more constrained *cis* form.

Further photoreactivity of the rotaxane **40⊂α-CD** and dumbbell **40** was also investigated, and it has been proven that the encapsulation again has a limiting effect upon reactivity of the contained molecule.

Although encapsulation does not completely prohibit the inherent photochemistry of the dumbbell in most cases, it does alter the response in an interesting and significant way, and opens up new possibilities for use of these compounds in switching devices and opto-electronics.

References for Chapter 5

[1] H. Görner, H. J. Kuhn, in *Adv. Photochem., Vol. 19* (Eds.: D. C. Neckers, D. H. Volmen, G. v. Bünau), John Wiley and Sons, New York, **1995**, pp. 1 - 117.

[2] D. H. Waldeck, *Chem. Rev.* **1991**, *91*, 415.

[3] J. Saltiel, *J. Am. Chem. Soc.* **1967**, *89*, 1036-1037.

[4] R. Searle, J. L. R. Williams, D. E. DeMeyer, J. C. Doty, *Chem. Commun.* **1967**, 1165.

[5] R. A. Caldwell, R. P. Gajewski, *J. Am. Chem. Soc.* **1971**, *93*, 532-534.

[6] H. Meier, *Angew. Chem., Int. Ed. Engl.* **1992**, *31*, 1437 - 1456.

[7] H. Meier, *Angew. Chem. Int. Ed.* **2001**, *40*, 1851-1853.

[8] C. Warmuth, F. Milota, H. F. Kauffmann, H. Wadi, E. Pollak, *J. Chem. Phys.* **2000**, *112*, 3938-3941.

[9] M. Sumitani, K. Yoshihara, *Bull. Chem. Soc. Jpn.* **1982**, *55*, 85-89.

[10] G. Gershinsky, E. Pollak, *J. Chem. Phys.* **1997**, *107*, 812-824.

[11] S. Shinkai, Y. Honda, K. Ueda, O. Manabe, *Bull. Chem. Soc. Jpn.* **1984**, *57*, 2144-2149.

[12] A. M. Caamano, M. E. Vazquez, J. Martinez-Costas, L. Castedo, J. L. Mascarenas, *Angew. Chem. Int. Ed.* **2000**, *39*, 3104-3107.

[13] L. Gobbi, P. Seiler, F. Diederich, V. Gramlich, *Helv. Chim. Acta* **2000**, *83*, 1711-1723.

[14] N. Koumura, R. W. J. Zijlstra, R. A. v. Delden, N. Harada, B. L. Feringa, *Nature* **1999**, *401*, 152-154.

[15] L. Gobbi, P. Seiler, F. Diederich, V. Gramlich, C. Boudon, J.-P.Gisselbrecht, M. Gross, *Helv. Chim. Acta* **2001**, *84*, 743-777.

[16] W. Herrmann, S. Wehrle, G. Wenz, *Chem. Commun.* **1997**, 1709-1710.

[17] H. S. Banu, A. Lalitha, K. Pitchumai, C. Srinivasan, *Chem. Commun.* **1999**, 607-608.

[18] W. Herrmann, M. Schneider, G. Wenz, *Angew. Chem. Int. Ed. Engl.* **1997**, *36*, 2511-2514.

[19] D. Gegiou, K. A. Muszkat, E. Fischer, *J. Am. Chem. Soc.* **1968**, *90*, 12.

[20] J. Saltiel, A. Marinari, D. W. L. Chang, J. C. Mitchener, E. D. Megarity, *J. Am. Chem. Soc.* **1979**, *101*, 2982.

[21] T.-I. Ho, T.-M. Su, T.-C. Hwang, *J. Photochem. Photobiol., A.* **1988**, *41*, 293-298.

[22] G. Gauglitz, R. Goes, W. Stooss, R. Raue, *Z. Naturforsch. A.* **1985**, *40*, 317.

[23] M. Asakawa, P. R. Ashton, V. Balzani, C. L. Brown, A. Credi, O. A. Matthews, S. P. Newton, F. M. Raymo, A. N. Shipway, N. Spencer, A. Quick, J. F. Stoddart, A. J. P. White, D. J. Williams, *Chem. - Eur. J.* **1999**, *5*, 860 - 875.

[24] C. Kaufmann, W. M. Muller, F. Vogtle, S. Weinman, S. Abramson, B. Fuchs, *Synthesis* **1999**, 849-853.

[25] J. E. H. Buston, J. R. Young, H. L. Anderson, *Chem. Commun.* **2000**, 905-906.

[26] M. R. Craig, T. D. W. Claridge, M. G. Hutchings, H. L. Anderson, *Chem. Commun.* **1999**, 153 -1538.

[27] M. S. Syamala, V. Ramamurthy, *J. Org. Chem.* **1986**, *51*, 3712-3715.

[28] S. Y. Jon, Y. H. Ko, S. H. Park, H.-J. Kim, K. Kim, *Chem. Commun.* **2001**, *1938*, 1938.

[29] F. B. Mallory, C. S. Wood, J. T. Gordon, *J. Am. Chem. Soc.* **1964**, *86*, 3094-3102.

[30] F. B. Mallory, K. E. Butler, A. C. Evans, E. J. Brondyke, C. W. Mallory, C. Yang, A. Ellenstein, *J. Am. Chem. Soc.* **1997**, *119*, 2119-2124.

[31] L. Liu, B. Yang, T. Katz, M. K. Poindexter, *J. Org. Chem.* **1991**, *56*, 3769-3775.

[32] L. E. Manning, J. Eriksen, C. S. Foote, *J. Am. Chem. Soc.* **1980**, *102*, 4275-4257.

[33] J. B. Kramer, S. Canonica, J. Hoigné, J. Kaschig, *Environ. Sci. Technol.* **1996**, *30*, 2227-2234.

[34] J. W. Happ, M. T. McCall, D. G. Whitten, *J. Am. Chem. Soc.* **1971**, *93*, 5496-5498.

[35] P. Wan, K. Yates, *J. Org. Chem.* **1983**, *48*, 869-876.

[36] O. Benali, M. C. Jiménez, M. A. Miranda, R. Tormos, *Chem. Commun.* **2001**, 2328 - 2329.

[37] M. T. McCall, D. G. Whitten, *J. Am. Chem. Soc.* **1969**, 5681-5682.

[38] M. T. Reetz, S. Sostman, *Tetrahedron* **2001**, *57*, 2515-2520.

[39] S. J. Cristol, W. A. Dickenson, M. K. Stanko, *J. Am. Chem. Soc.* **1983**, *105*, 1218 - 1220.

[40] H. Ishii, T. Hirano, S. Maki, H. Niwa, M. Ohashi, *Tetrahedron Lett.* **1998**, *39*, 2791 - 2972.

[41] F. D. Lewis, T. J. Simpson, *J. Am. Chem. Soc.* **1980**, *102*, 7593-7595.

[42] C. Bosman, A. D'Annibale, S. Resta, C. Trogolo, *Tetrahedron* **1994**, *50*, 13847.

[43] J. D. Coyle, P. A. Rapley, *J. C. S., Perkin Trans. 1* **1986**, 2273-2278.

Chapter 6; Attempts at rotaxane formation *via* triazine chemistry

6.1. Introduction to 1,3,5-triazine chemistry

1,3,5-Triazines such as **55** (cyanuric chloride) are used in the dye industry[1, 2] primarily to introduce a reactive group which can be covalently bonded to a substrate surface, thereby improving their wash-fastness properties, or to link more than one chromophore together to form a new colour (for example, mixing a blue and a yellow chromophore to yield a green dye or pigment).

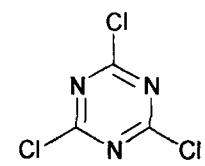

55; cyanuric chloride

Most commonly, the chlorine atoms are substituted in a stepwise fashion by nucleophilic attack of an amine or amines to give reactive dyes or pigments of the form **56** or **57**.

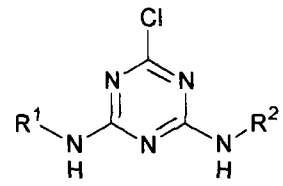

56

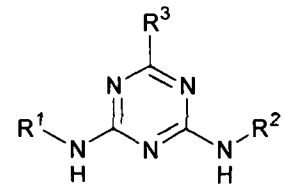

57

where at least one of R^1 and R^2 is a chromophore
and R^3 may be a chromophore or any unreactive group such as -OH, taurine, or morpholine

Figure 6.1. *General structure of triazinyl dyes and pigments*

Previous work within the Anderson group[3-5] and elsewhere[6] has shown that such dyes are suitable for rotaxane formation. The disubstituted triazine group was proven to be a large enough stopper to non-covalently bond permethylated α-cyclodextrin (TM-α-cyclodextrin) onto an aromatic core. The emphasis was on the formation of an encapsulated reactive dye. TM-α-cyclodextrin was chosen in order that free hydroxyls from the sugar should not react with the reactive chlorine

of another molecule of the rotaxane-encapsulated dye. It appears unlikely, however, that reaction between the bound cyclodextrin and the dumbbell to which it is bound could occur in this case (unlike the bromination reaction in Chapter 3) as the reactive chlorine does not appear to be correctly aligned according to CPK models. The current work therefore encompasses studies using α-cyclodextrin in addition to the permethylated macrocycle.

The aim in this section of work was to explore how transferable the previously discovered route to rotaxane synthesis and stability enhancement of azo dyes by encapsulation[3] was to other dyes, in particular those used in ink-jet printing rather than as reactive dyes for cotton.

6.2. Binding studies by UV/Vis spectroscopy

The free amine **58** was kindly provided by Avecia plc.

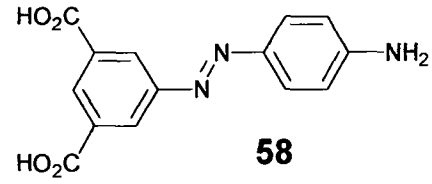

58

CPK models suggest that this is an ideal shape for binding within α-cyclodextrin. It was known from previous work (see Chapter 2) that the isophthalic acid stopper unit would act as a stopper for α-cyclodextrin, and induces good aqueous base solubility, essential for the formation of rotaxanes *via* the hydrophobic effect. In addition, this amine is already used by Avecia to form a triazine-based dye **59** (marketed as Projet Fast Yellow 2), which proves the ability of **58** to react in this way.

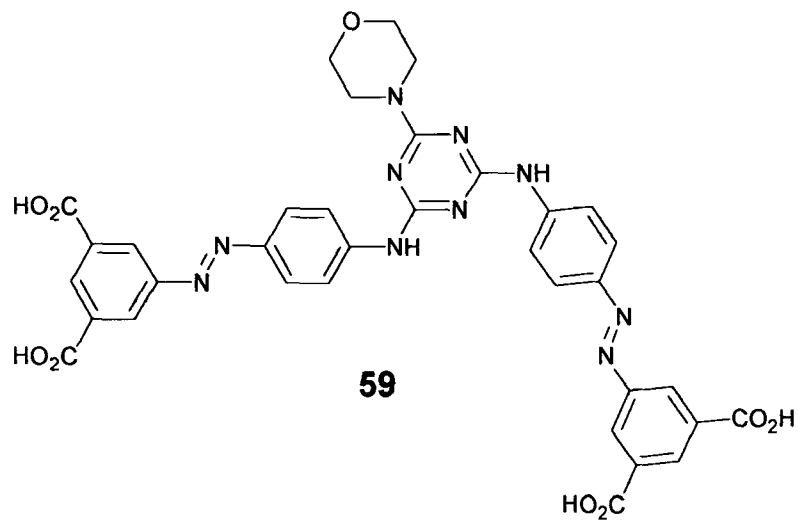

59

It was necessary to confirm that the CPK models were correct in predicting the formation of a 1:1 inclusion complex between **58** and either α-cyclodextrin or TM-α-cyclodextrin. To this end, a series of binding titrations was undertaken by UV/Vis spectroscopy. Both titrations were carried out in pH 7.0 buffer (aqueous sodium orthophosphate and citric acid), to ensure the solubility of all species throughout the titration.

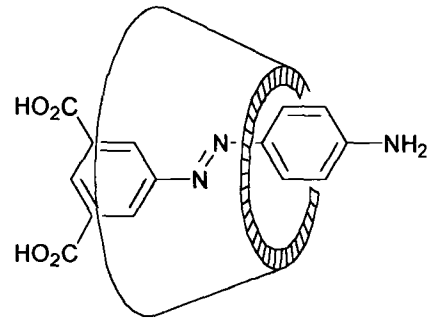

Figure 6.2. *Suggested form of complex between* ***58*** *and α-cyclodextrin or TM-α-cyclodextrin .*

The results of the titration against α-cyclodextrin suggested a 1:1 complex was formed, with the possibility of some 2:1 complexation (2 cyclodextrins to one molecule of **58**) at higher concentrations ($k_1 = 4.0 \times 10^3$, $k_2 = 400$).

The results of the titration performed against TM-α-cyclodextrin also suggested a 1:1 complex was formed, and did not fit to 2:1 complexation. The binding constant ($k = 1.8 \times 10^4$) was a factor of 10 higher for 1:1 binding with TM-α-cyclodextrin than for α-cyclodextrin. In both titrations, the absorbance of the complex appeared

to be less than that of the free dye, with a lowering in absorbance at 350 nm throughout the titration. The spectra both appeared to have isosbestic points at around 200 and 400 nm, and the λ_{max} did not appear to change greatly during the binding process. The binding curves were analysed and binding constants obtained by the use of Specfit Global Analysis software.

Both these binding constants should be sufficient to enable rotaxane formation, given a good coupling reaction.

6.3. Attempts at rotaxane formation

With the knowledge of the magnitude of binding constants and the best reaction conditions for coupling the amine and cyanuric chloride in hand, we set about the synthesis of some rotaxanes. The first target molecule was simply an encapsulated version of the commercial dye, chosen for ease of the comparison of properties with a known material. The reaction is shown in Scheme 6.1.

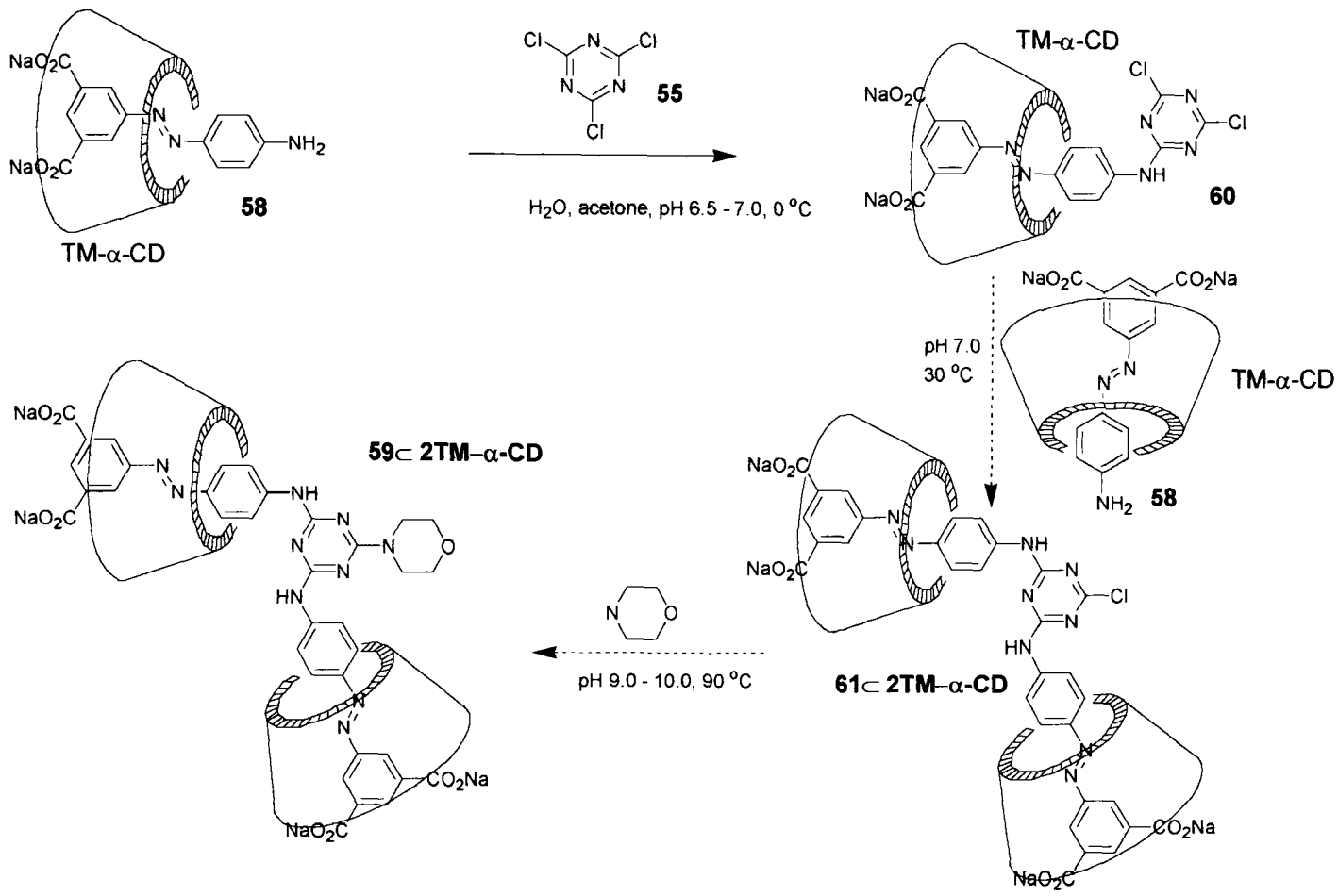

Scheme 6.1. *Attempted formation of the [3]rotaxane* ***59⊂2TM-α-CD*** *from* ***58*** *and TM-α-cyclodextrin.*

The conditions used were similar to those in use on a preparative scale in industry, so no necessity for optimisation was anticipated. However, despite the use of an excess of TM-α-cyclodextrin, a mixture of [2] and [3]rotaxane (portrayed in Figure 6.3) was formed.

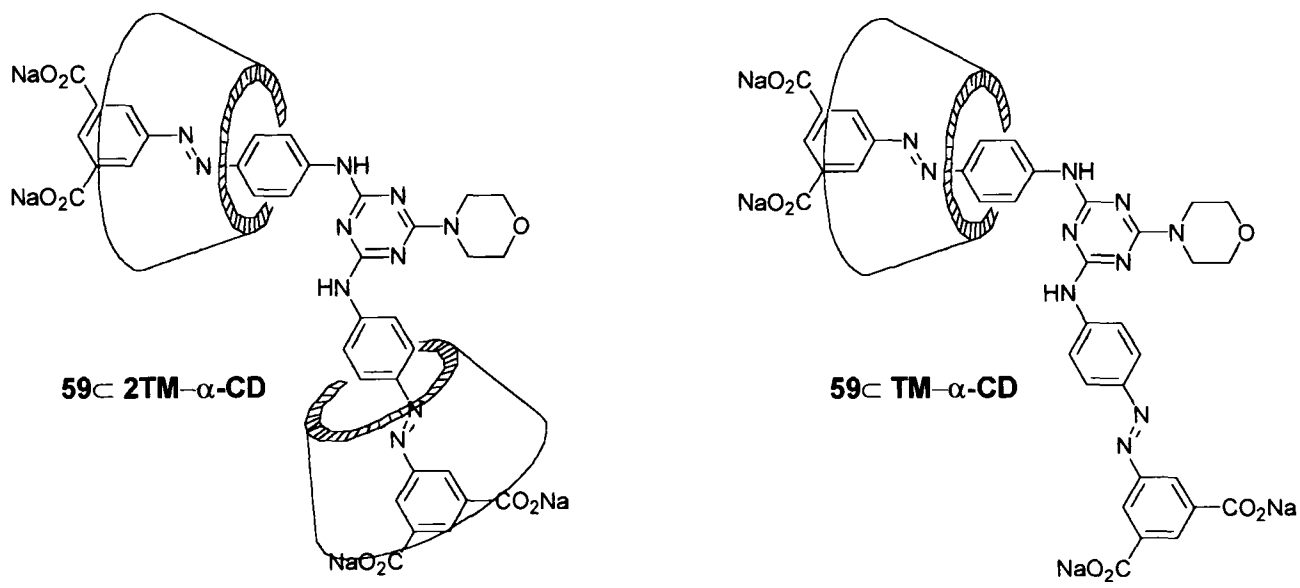

Figure 6.3. *[2] and [3]rotaxanes formed from the reaction shown in Scheme 6.1.*

This was indicated both by electrospray mass spectrometry and by TLC. All attempts to separate the rotaxane species were unsuccessful. For this reason, we decided to attempt the synthesis of the simpler [2]rotaxane **63⊂TM-α-CD**.

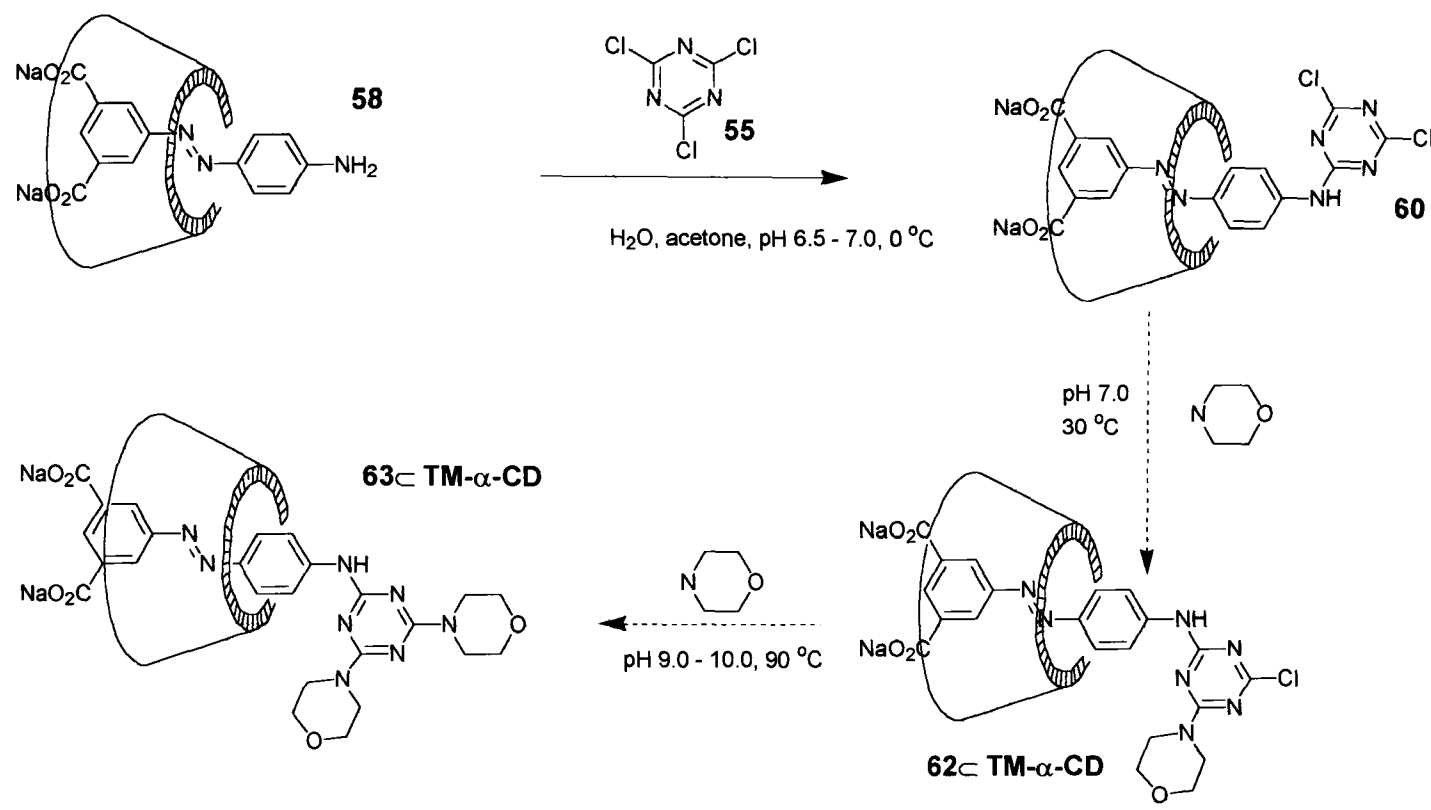

Scheme 6.2. *Attempted formation of the [2]rotaxane* ***63⊂TM-α-CD*** *from* ***58*** *and TM-α-cyclodextrin*

Problems with solubility dogged this synthetic route, shown in Scheme 6.2, the morpholine cap being rather insoluble in the aqueous conditions used, and apparently conveying this insolubility also onto the coupling reaction products. It was difficult to positively identify any of the desired species in the crude mixture; ^{1}H NMR and mass spectrometry were inconclusive.

We decided to attempt the synthesis of a similar rotaxane, using solubilising capping groups instead of the problematic morpholine. Two approaches to this were investigated. Isophthalic acid and diiminoacetic acid were used as capping groups in syntheses with both α-cyclodextrin and TM-α-cyclodextrin as the macrocycle. From one of these experiments (shown in Scheme 6.3), the dumbbell could be positively identified and characterised.

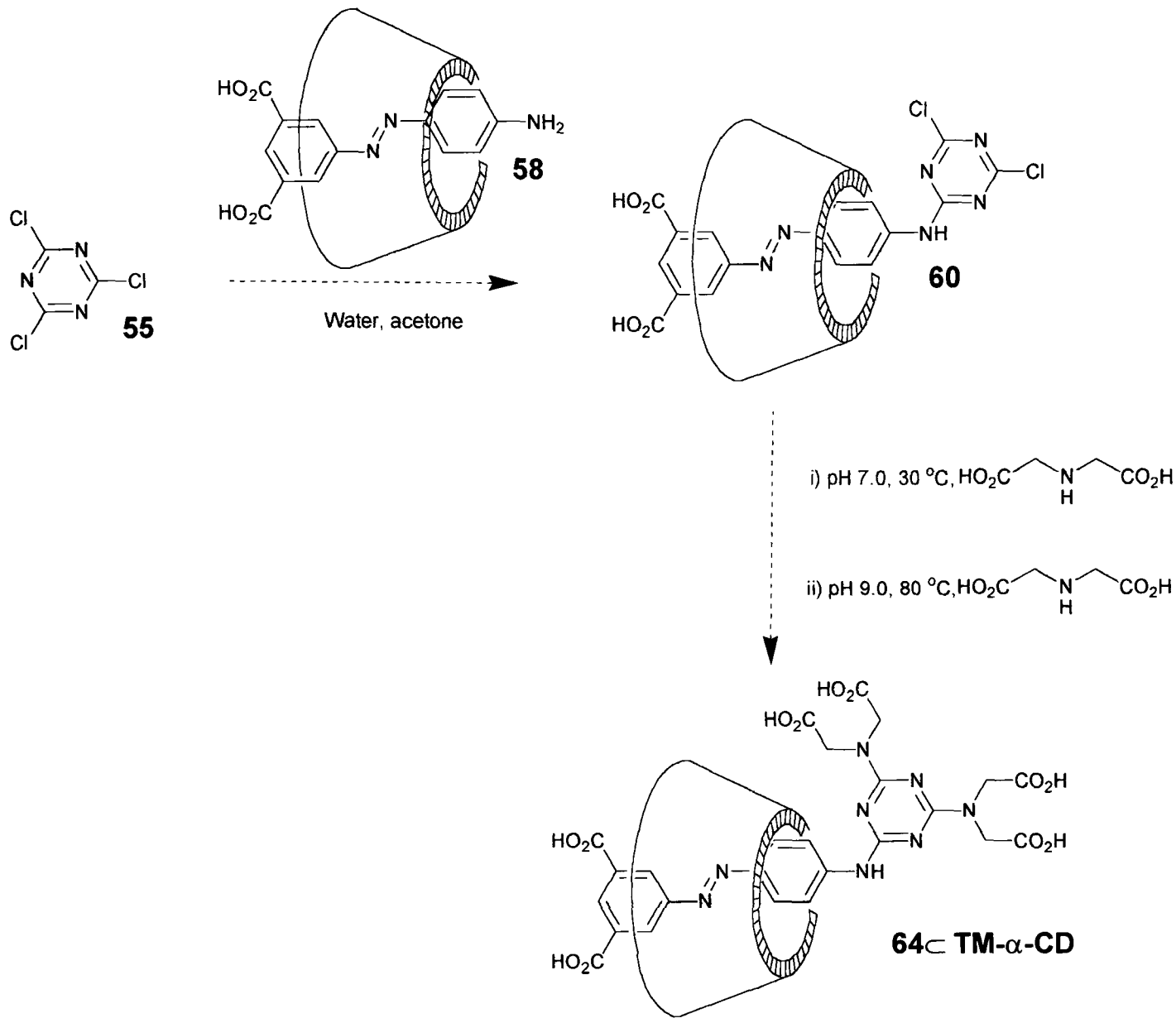

Scheme 6.3. *Attempted synthesis of 1-{4-[4-(bis-carboxymethyl-amino)-6-hydroxy-[1,3,5]triazin-2-ylamino]-phenylazo}-benzene 3,5-carboxylic acid TM-α-cyclodextrin [2]rotaxane* ***64⊂TM-α-CD****.*

The only component of the reaction mixture which could be isolated and characterised was **65**.

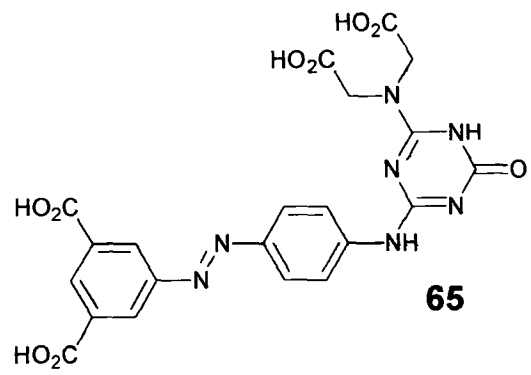

This is probably formed from the hydrolysis of the monocapped intermediate. The fact that no cyclodextrin-based equivalent of this dumbbell could be isolated,

together with inconclusive NMR and mass spectra, lead to a possible conclusion that the desired rotaxanes could not be formed easily.

This is a conclusion that appears to be at odds with our previous findings. It was known that the coupling reaction worked well (and indeed this is confirmed by the presence of dumbbell in the crude mixture), and it was known from the UV/Vis titrations that the binding constants are also favourable. The only explanation left for this was that the cyclodextrin must be binding to the dye in such a way as to disfavour rotaxane formation. This might be a mode of binding of the dye to the outside of the cyclodextrin rather than through the cavity. Alternatively, the cyclodextrin may simply be binding over the reactive site of the dye. These potential forms are shown in Figure 6.4.

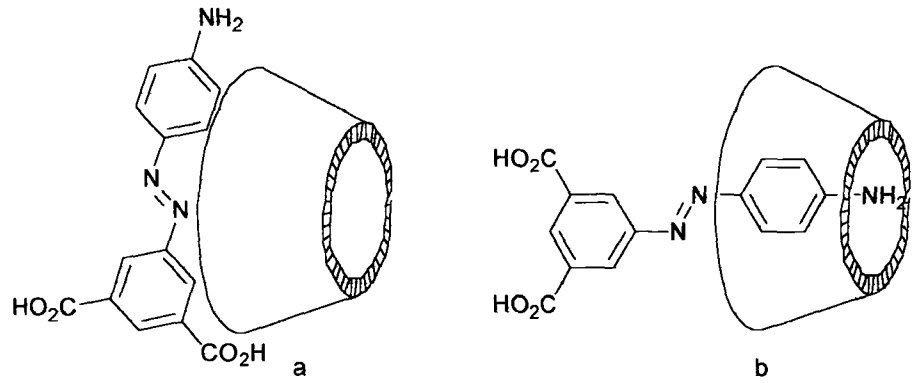

Figure 6.4. *Potential modes of binding of* ***58*** *to cyclodextrins; a) facial and b) over the reactive group.*

In order to ascertain which, if any, of these proposed binding modes is correct, it was necessary to perform some NMR experiments.

6.4. Binding studies by ^{1}H NMR

These were carried out at a dye concentration of approximately 2.5 mM, with approximately 2 eq. cyclodextrin per dye molecule. All NMR binding experiments were performed by Dr T.D.W. Claridge on a 500 MHz NMR instrument, in

Na_2CO_3/D_2O (~pD 9). The NOE spectra with α-cyclodextrin were inconclusive, probably due to the lower binding constant of **58** with this macrocycle. However, some information was gleaned from the analysis of ROESY spectra of a mixture of the dye **58** and TM-α-cyclodextrin. The aromatic peaks were irradiated, and correlations to the cyclodextrin protons observed. The cyclodextrin ^1H spectrum had previously been completely assigned by use of an HSQC experiment. The results of the binding experiment are shown in Figure 6.5.

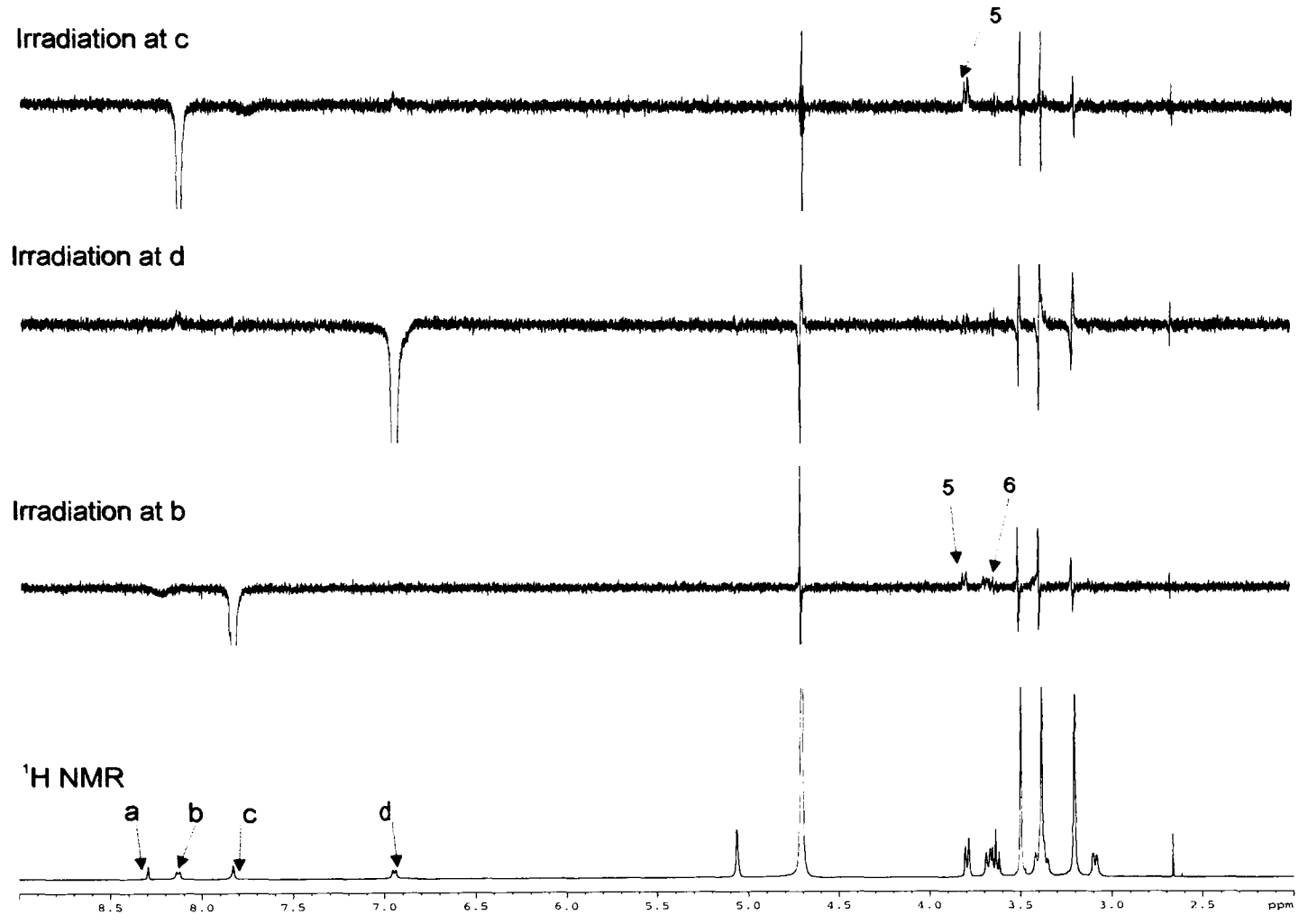

Figure 6.5. *Through-space experiments run on 500 MHz in D_2O, in order to distinguish the position of the TM-α-cyclodextrin relative to the dye,* ***58****.*

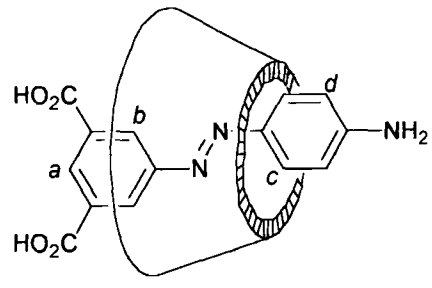

Figure 6.6. *Assignment system for the irradiations of* ***58*** *in Figure 6.5.*

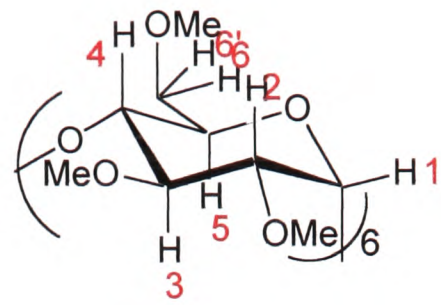

Figure 6.7. *Numbering system for the TM-α-cyclodextrin glucose unit.*

The fact that all correlations observed for the cyclodextrin are to the 5 and/or 6 positions implies that the cyclodextrin is threading over the dye, the mode suggested in Figure 6.4.b. *i.e.* over the amine may be somewhat extreme. However, use of this information in conjunction with CPK models indicated that some steric interference is afforded by the cyclodextrin when these NOEs hold true. The macrocycle may not sit directly over the amine, but it may well inhibit the reaction of it to a certain extent, slowing the bound *vs.* unbound rate of reaction and thus giving mainly dumbbell as the reaction product. This information does not conclusively exclude the possibility of any rotaxane formation, but it appears that the rotaxane formation is at best difficult to achieve and purify, and at the worst, it does not happen at all.

6.5. Conclusions of Chapter 6

This chapter has been a foray into a different field of rotaxane chemistry to that of the previous chapters. Despite the failure to synthesise any pure rotaxanes by the strategy of triazine chemistry with the amine **58**, it is known that rotaxane formation in general by this route is possible[3, 5]. The chosen amine would therefore appear to be the source of the problem in this instance. Binding titrations by UV/Vis indicated that a complex was indeed formed between **58** and both α- and TM-α-cyclodextrin. However, NMR work suggested that the complex was not a potentially useful one for formation of rotaxanes. Future attempts at rotaxane synthesis *via* this route (or

indeed any route involving hydrophobic binding as opposed to a more specific templated interaction) should take into consideration the possibility that inclusion in a macrocycle may actually hinder the coupling reaction. The amine may not be long enough to allow both binding and reaction to occur; previous work has prepared rotaxanes such as **66⊂TM-α-CD**[5] and **67⊂TM-α-CD**[4] (depicted in Figure 6.8), which both contain an extra aryl ring to provide more space for binding.

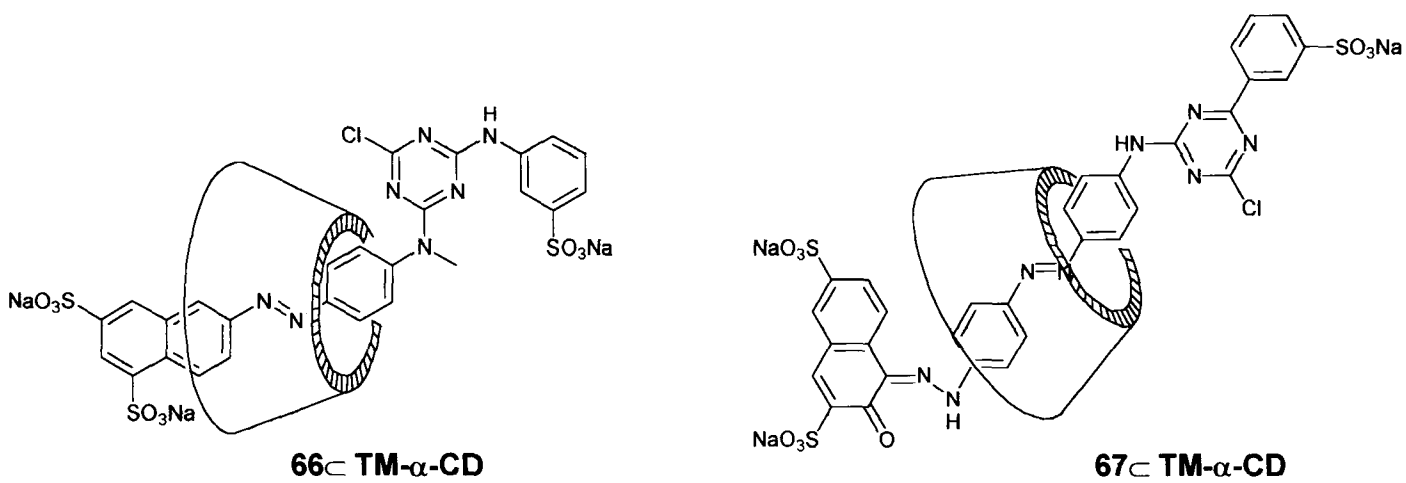

Figure 6.8. *Examples of previous azo-dye rotaxanes which have been successfully prepared by use of triazine chemistry.*

This explanation could be further tested by conversion of the amine into a Suzuki substrate *via* a route such as that outlined in Scheme 6.4. The amine could be converted into an iodide *via* a Sandmeyer-type reaction, and then reacted with a boronate ester under Suzuki conditions and in the presence of the appropriate cyclodextrin.

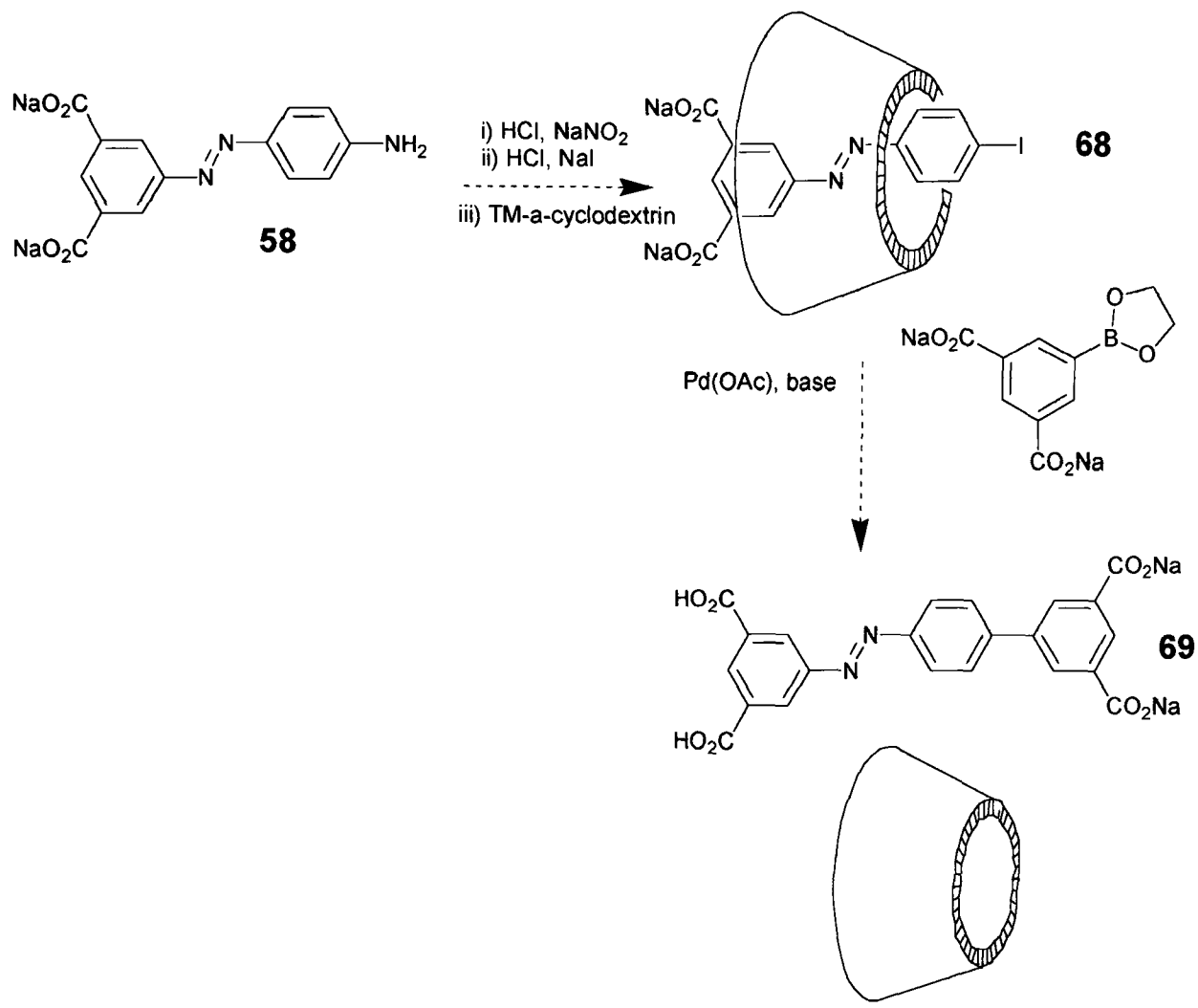

Scheme 6.4. *Suggested route for testing the hypothesis that the position of binding or length of dumbbell inhibits the reaction of the included species.*

However, if the explanation that complexation prevents reaction is true, the dumbbell **69** should also be the only product of this reaction, coupling being possible only when the cyclodextrin is not binding. This would be an interesting extension of the work carried out with this amine. It appears that another amine must be investigated if rotaxanes are to be made using triazine chemistry.

This chapter emphasises the need for a good understanding of the mechanism of binding, in addition to the knowledge of the magnitude of binding strength and the testing of an efficient coupling reaction, before successful attempts to synthesise a rotaxane can be made.

References for Chapter 6

[1] H. Zollinger, *Colour Chemistry*, 2nd ed., VCH Gmbh, Weinheim, 1991.

[2] P. F. Gordon, P. Gregory, *Organic Chemistry in Colour*, 1st ed., Springer Verlag, Berlin, 1987.

[3] M. R. Craig, M. G. Hutchings, T. D. W. Claridge, H. L. Anderson, *Angew. Chem. Int. Ed.* 2001, *40*, 1071 - 1074.

[4] S. J. Alderman, Part II Thesis, Dyson Perrins Laboratory, University of Oxford (Oxford), 2001.

[5] M. R. Craig, DPhil Thesis, Dyson Perrins Laboratory, University of Oxford (Oxford), 2001.

[6] M. Kunitake, K. Kotoo, O. Manabe, T. Muramatsu, N. Nakashima, *Chem. Lett.* 1993, 1033 - 1036.

Chapter 7; Experimental Details

7.1. Techniques

All manipulations of air or water sensitive compounds were performed using standard Schlenk techniques, under an inert atmosphere. THF was distilled from sodium/fluorene under nitrogen, and DMF, DMSO and iodomethane were distilled from calcium hydride under nitrogen prior to use. TM-α-cyclodextrin (2,3,6-tri-O-methyl-α-cyclodextrin) was prepared by a standard method[1]. 5-Iodo-1,3-benzenecarboxylic acid (**31**) was kindly prepared by Mr J. Kelly[2]. All other reagents were used as commercially supplied.

Petroleum ether refers to the fraction boiling between 60 – 80 °C unless otherwise stated.

R_f values are accurate to ~0.05.

NMR spectra were recorded at ambient probe temperature using either Brüker AMX500, DRX500, 400, DPX250 or 200 as stated in the text. *J* values are accurate to ~0.5 Hz.

Mass spectra were carried on an Electrospray (ESI) or Electron ionisation (EI) BioQ-II-ZS Micromass instrument or a Matrix assisted laser desorption ionisation instrument (MALDI) Tof Spec 2E Micromass instrument from a 2,4,6-trihydroxyacetophenone matrix in Oxford by Dr R. Aplin, or on an APCI Platform I instrument. FAB Spectra were carried out by the EPSRC Service staff at the University of Wales, Swansea. Accurate mass ESI spectra were recorded on an LCT Micromass spectrometer by Dr R. Aplin.

Elemental analyses were carried out by Elemental Microanalysis Limited of Okehampton.

Infrared spectra were recorded as KBr discs on a Perkin-Elmer 1750 FT-IR spectrometer.

UV/Vis spectra were recorded on a Perkin-Elmer Lambda 20 spectrophotometer. Extinction coefficients are quoted in M cm^{-1}.

Fluorescence spectra were recorded on an ISA Fluoromax-2 fitted with a 150 W Xenon arc lamp and a red-sensitive R928P photomultiplier tube detector (accurate between 290 – 850 nm). The data was processed using the Datamax software. All emission spectra were recorded with a correction curve supplied by the manufacturer.

Ultrafiltration was carried out at a pressure of 4.5 atm in a stirred cell with an Amicon 500 or 1000 NMWCO (nominal molecular weight cut-off) cellulose membrane as indicated.

TLCs were performed using Merck self-indicating aluminium backed (60-F_{254}) silica plates with visualisation by UV.

Flash column chromatography was performed under 4.5 atm air or nitrogen, using Merck silica.

Melting points were measured on a Griffin melting point apparatus.

New compounds are designated by italicising the full name in the text.

Alkaline β-naphthol test:

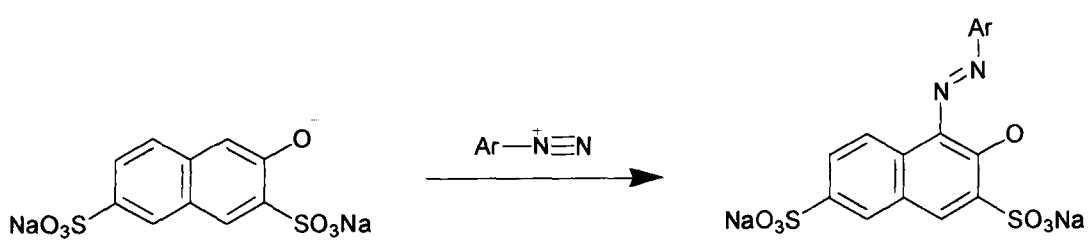

pale yellow

70

red / purple

Scheme 7.1. *Alkaline β-napthol test.*

A small amount (~5 mg) of **70** was dissolved in NaOH (2 M, ~3 cm^3). This solution was applied in stripes to a filter paper *via* pasteur pipette. The sample to be tested was then applied in a similar manner, in a line at right angles across the stripes. In cases where the diazonium ion was present, a colour change from pale yellow to red or purple was observed where the sample line crossed the stripes.

Ion-exchange chromatography was performed using BioRad AG 4 × 4 resin under 4.5 atm N_2. A column of volume 6 – 8 cm^3 was packed in pH 5 aq. acetic acid. The mixture to be ion-exchanged was acidified before loading onto the column. Excess cyclodextrin was washed off with pH 5 aq. acetic acid (~500 cm^3). The salts were removed by washing with water (500 – 750 cm^3), and the ammonium salt of the required compound finally eluted by washing with 1 % aqueous ammonia (~750 cm^3). The column was regenerated by a washing cycle of water and pH 5 aq. acetic acid, and re-used up to 4 times for the same compound only.

7.2. Experimental procedures for Chapter 2

Synthesis of 4-bromobenzyl phosphonate (34)[3]

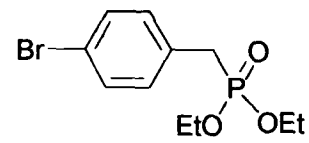

34

4-Bromobenzyl bromide (10 g, 40 mmol) was dissolved in triethyl phosphite (70 cm^3, 400 mmol) and heated at 100 °C for 15 h under a nitrogen atmosphere. Excess triethyl phosphite and volatile side products were removed *via* short path distillation under vacuum to give a yellow oil. This was further purified by flash column chromatography using a gradient of 1:1 petroleum ether : ethyl acetate to pure ethyl acetate. This yielded the phosphonate **34** as a yellow oil. (9.57 g, 78 %); R_f= 0.17 (1:1 petroleum ether : ethyl acetate); δ_H (400 MHz, $CDCl_3$) 7.44 (2H, d, J_H 7.7, aryl *ortho* to Br), 7.18 (2H, d, J_H 7.7, J_P 2.5, aryl *meta* to Br), 4.02 (4H, q, J_H 7.0, -OCH_2-), 3.10 (2H, dd, J_P 22, PCH_2Ar), 1.25 (6H, t, J_H 7,-CH_3); δ_C (100 MHz, $CDCl_3$) 131.6 (d, J_P 2.8, Ar-H), 131.4 (d, J_P 6.4, Ar-H), 130.7 (d, J_P 9.4, C-Br), 120.9 (d, J_P unresolved, aryl *para* to Br), 62.2 (d, J_P 6.7, -OCH_2-), 33.2 (d, J_P 138.7, PCH_2Ar), 16.4 (d, J_P 5.8, -CH_3); *m/z* (APCI$^+$) 329, 331 (5 %, M^+), 307, 309 (100, M^+ - Et), 279, 281 (5).

Synthesis of 4,4',α,α'-tetrabromodiphenylethane (35)[4]

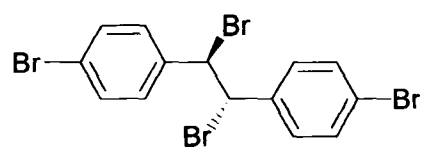

35

Diphenylethane (78 g, 0.48 mol) was dissolved in a mixture of acetic acid (930 cm^3) and water (35 cm^3). Bromine (284.5 g, 91.7 cm^3, 1.78 mol) was added dropwise with stirring. The evolving HBr was trapped with NaOH (aq). The mixture was

refluxed for 75 min and an off-white precipitate was formed. The solid was filtered and washed with hot acetic acid, ethanol and finally diethyl ether, and dried *in vacuo* to give **35** as a fine white powder (68.16 g, 31.9 %); mp 235 - 240 °C (lit.[4] 235 – 245 °C dec.); ν_{max} (KBr)cm^{-1} 1587 (aryl C-C), 832 (aryl C-H), 715 (C-Br); δ_H (200 MHz, $CDCl_3$) 7.57 (4H, d, J_H 8.0, aryl), 7.38 (4H, d, J_H 8.0, aryl), 5.38 (2H, s, ArC*H*Br); δ_C (125 MHz, d_6-DMSO) 140.9, 132.5, 131.1, 122.8, 55.1; *m/z* (EI^+) 497.7, (M^+, 25 %), 416.8 (35), 337.9 (93), 258.0 (32), 178.1 (100), 89.1 (59).

A white precipitate later formed in the filtrate was found to be mostly the 2,4 substituted tetrabromodiphenylethane.

Synthesis of *trans*-4,4'-dibromostilbene (32)[5]

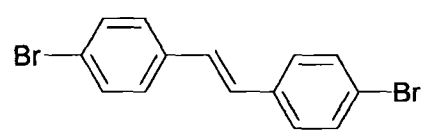

32

Method A:

LDA was prepared as follows:

Diisopropylamine (0.218 cm^3, 1.56 mmol) was dissolved in THF (15 cm^3) and cooled under anhydrous conditions to -78 °C. To the stirred solution, *n*-BuLi (1.04 cm^3, 1.3 mmol, 1.25 M in hexanes) was added. The brown solution was then warmed to 0 °C for 30 min before recooling to -78 °C.

The phosphonate **34** (0.40 g, 1.3 mmol) was dissolved in THF (10 cm^3) and this solution was added to the solution of LDA at -78 °C. The temperature was allowed to rise to 0 °C over a period of 30 min. 4-Bromobenzaldehyde (0.130 g, 0.70 mmol) was added in THF (20 cm^3), and the reaction allowed to warm to room temperature

over a period of 15 h. The reaction was quenched by addition of saturated aqueous $NaHCO_3$ (2 cm^3) and extraction carried out with dichloromethane (3 × 25 cm^3). The organic extracts were combined and solvent removed *in vacuo* to give a brown solid which was purified by recrystallisation from hot toluene (alternatively by extraction with ether and recrystallisation from petroleum ether (30 - 40) and dichloromethane) to give dibromostilbene **32** as cream-white flaky crystals (0.165 g, 55 %); mp 207 - 210 °C (lit.[4] 215 – 216 °C); R_f = 0.5 in 5 % dichloromethane / petroleum ether; δ_H (500 MHz, $CDCl_3$) 7.49 (4H, d, J_H 7.5, aryl), 7.38 (4H, d, J_H 7.5, aryl), 7.03 (2H, s, alkene); δ_C (125 MHz, $CDCl_3$) 136.2 (aryl *para* to Br), 132.1 (aryl *meta* to Br), 128.4 (alkene), 128.2 (aryl *ortho* to Br), 121.9 (aryl C-Br); *m/z* ($APCI^+$) 338 (8 %, M^+), 337 (3, M^+), 315 (4), 313 (9), 259 (3), 257 (11), 255 (5), 213 (3), 200 (8), 199 (12), 198 (20), 197 (22), 160 (4), 158 (63), 156 (100), 139 (9), 122 (20), 116 (11).

Method B:[4]

4,4', α, α'-tetrabromodiphenylethane **35** (15 g, 0.03 mol), copper (I) chloride (7.56 g, 0.076 mol) and pyridine (30 cm^3) were thoroughly mixed and then refluxed for 1 h. The mixture was cooled to 0 °C and concentrated hydrochloric acid (120 cm^3, 1.2 mol) was added carefully. The resulting solid was collected and washed with hydrochloric acid and water before recrystallisation from toluene to give **32** as a white crystalline solid (5.33 g, 52.7 %).

Synthesis of 4,4'-bis(1,3,2-dioxaborol-2-yl)-(*E*)-1,2-diphenylethene (28)[6-8]

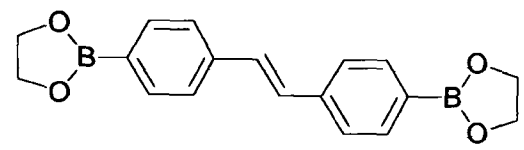

28

4,4'-Dibromo-(*E*)-1,2-diphenylethene **32** (0.5 g, 1.5 mmol) was dissolved in THF (20 cm^3) under anhydrous conditions and cooled to -78 °C. To this solution was added *n*-BuLi (3.26 cm^3, 6.5 mmol, 2 M in hexanes). The mixture was allowed to warm to 0 °C over a period of 1 h, then recooled to -78 °C. Triisopropylborate (2.1 cm^3, 18 mmol) was added, and the mixture stirred at -78 °C for 1 h before being allowed to warm to room temperature for 3 h. Aqueous HCl (2 cm^3, 2 M) was added and the mixture stirred for a further 15 h. THF was removed *in vacuo* and the residue dissolved in aq. NaOH (100 cm^3, 2 M). This was stirred for 30 min before filtering and reacidification of the filtrate to pH 1 with HCl (conc.). The resulting suspension was centrifuged (4500 rpm, 10 min) and the dried white gel-like solid **36** used unpurified in the next step.

Ethanediol (0.2 g, 3.2 mmol) was added to the 4,4'-bis(boronic acid)-(*E*)-1,2-diphenylethene in toluene (25 cm^3). The mixture was refluxed for 15 h with removal of water by means of a Dean-Stark trap. Solvent was removed *in vacuo* and the cream residue dissolved in toluene, filtered, then recrystallised from hot toluene to yield fine off-white needles of *4,4'-bis(1,3,2-dioxaborol-2-yl)-(E)-1,2-diphenylethene* **28** (0.15 g, 31 %); mp 272 - 274 °C; found C 67.6, H 5.7 %, $C_{18}H_{18}O_4B_2$ requires C 67.6, H 5.7 %; ν_{max} (KBr)/cm^{-1} 2963 (=C-H conjug.), 2911 (Ar-H), 1606 (C=C), 1596 (Ar-C=C), 1365 (C-O), 1328 (B-O); λ_{max} ($CHCl_3$)/nm 327 (ε 28,000); δ_H (200 MHz, $CDCl_3$) 7.82 (4H, d, J_H 8.0, aryl), 7.55 (4H, d, J_H 8.0, aryl), 7.20 (2H, s, stilbene), 4.40 (8H, s, $-OCH_2CH_2O-$); δ_C (125 MHz, $CDCl_3$) 140.1

(quaternary), 135.3 (aryl), 129.7 (alkene), 128.3 (quaternary), 126.1 (aryl), 66.1 (-OCH_2CH_2O-); *m/z* (EI^+) 320.2 (M^+, 100 %), 205.2 (44), 191.2 (31), 178.2 (91).

Synthesis of 4,4'-dibromo(diphenyl acetylene) (33)[9]

33

Sodium ethoxide was freshly prepared by addition of clean sodium metal (4.55 g, 0.20 mol) to dry ethanol under nitrogen. 4,4', α,α'-Tetrabromodiphenylethane **35** (5 g, 0.01 mol) was added when all solid had dissolved, and the reaction was refluxed with stirring for 30 min. The mixture became orange-brown and contained a solid. The mixture was cooled to 0 °C and poured into ice-water (200 cm^3). The solid was removed by vacuum filtration and the filtrate was extracted with chloroform (3 × 50 cm^3). Extracts were combined and the solvent removed to give a white solid. This was combined with the solid filtered off and then recrystallised from hot chloroform to give **33** as small off-white crystals (2.0 g, 60 %); mp 181 – 183 °C (lit.[9] 182 – 184 °C); δ_H (500 MHz, $CDCl_3$) 7.50 (4H, d, J_H 8.3, aryl), 7.39 (4H, d, J_H 8.3, aryl); δ_C (125 MHz, $CDCl_3$) 133.2 (aryl), 131.9 (aryl), 123.0 (quaternary), 122.1 (quaternary), 89.6 (acetylene), *m/z* (EI^+) 335.9 (M^+,100 %), 256.0 (7), 176.1 (75), 150.1 (25).

Synthesis of 4,4'-bis(1,3,2-dioxaborol-2-yl)-1,2-diphenylethyne (29)

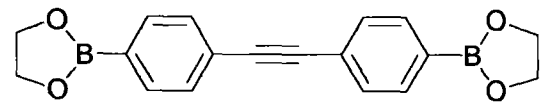

29

The 4,4'-dibromo-1,2-diphenylethyne **33** (0.326 g, 0.97 mmol) was dissolved in THF (15 cm^3) under anhydrous conditions and cooled to -78 °C. To this solution was added *n*-BuLi (2.43 cm^3, 4.8 mmol, 2 M in hexanes). The mixture was allowed to warm to 0 °C over a period of 1 h, then recooled to -78 °C. Triisopropylborate (1.3 cm^3, 5.6 mmol) was added, and the reaction stirred at -78 °C for 1 h before being allowed to warm to room temperature for 3 h. Aqueous HCl (1 cm^3, 2 M) was added and the reaction stirred for a further 15 h. THF was removed *in vacuo* and the residue dissolved in aq. NaOH (300 cm^3, 2 M). This was stirred for 30 min before filtering and reacidification of the filtrate to pH 1 with HCl (conc.). The resulting suspension was centrifuged and the dried, white gel-like solid **37** was used unpurified in the next step.

Ethanediol (0.12 g, 1.9 mmol) was added to the 4,4'-bis(boronic acid)-1,2-diphenylethyne in toluene (25 cm^3). The mixture was refluxed for 15 h with removal of water by means of a Dean-Stark trap. The solvent was removed *in vacuo* and the cream residue dissolved in toluene, filtered and recrystallised from hot toluene to yield fine off-white needles of *4,4'-bis(1,3,2-dioxaborol-2-yl)-1,2-diphenylethyne* **29** (0.171 g, 55 % over two steps); mp 254 - 255 °C; found C 68.1, H 5.1 %, $C_{18}H_{16}O_4B_2$ requires C 68.0 H 5.0 %; ν_{max} (KBr)/cm^{-1} 2906 (C-H), 1334 (B-O), 1090 (C-O), 830 (*p*-Ar); λ_{max} ($NaOH/H_2O$)/nm 295 (ε 27,000), 313 (ε 27,000); δ_H (250 MHz, D_2O/NaOH) 7.43 (4H, d, J_H 7.8, aryl), 7.33 (4H, d, J_H 7.8, aryl), 3.51 (8H, s, $-OCH_2CH_2O-$); δ_C (125 MHz, D_2O/NaOH) 131.8 (quaternary + aryl), 130.4

(aryl), 119.6 (quaternary), 63.0 (-OCH_2CH_2O-); *m/z* (EI^+) 318.1 (M^+, 100), 248.1 (17).

Synthesis of 1-iodonaphthalene-3,6-disulfonate, disodium salt (30)

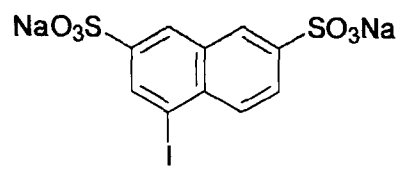

30

To a solution of 1-amino-3,6-naphthalenedisulfonate disodium salt (Freund's acid) **38** (5 g, 14.4 mmol) in water (11 cm^3), conc. hydrochloric acid (3.6 cm^3, 0.36 mmol) was added dropwise. The solution was cooled to 0 °C and a cooled solution of sodium nitrite (0.99 g, 14.4 mmol) in water (9 cm^3) was added dropwise. The mixture was stirred for 1 h at 0 °C, monitoring the formation of the diazonium salt by use of the alkaline β-naphthol test. A mixture of sodium iodide (6.95 g, 46 mmol) in water (7 cm^3) and conc. hydrochloric acid (3.6 cm^3, 36 mmol) was added slowly to the diazonium salt solution, which was heated to 80 °C for 1 h. This was also tested with the alkaline β-naphthol to check for destruction of all diazonium salt. The mixture was cooled and filtered to give a brown solid which contained much excess iodine. This was heated to 50 °C under vacuum until no further iodine sublimed off, and recrystallised three times from water to give *1-iodonaphthalene-3,6-disulfonate, disodium salt* **30** as a light brown solid (2.15 g, 33 %); mp >300 °C; ν_{max} (KBr)/cm^{-1} 524 (Ar-I); λ_{max} (H_2O)/nm 232 (ε 58,000); δ_H (400 MHz, d_6-DMSO) 8.28 (1H, d, J_H 1), 8.18 (1H, s,), 8.14 (1H, d, J_H 1), 7.95 (1H, d, J_H 8), 7.86 (1H, dd, J_H 8, 1); δ_C (100 MHz, d_6-DMSO) 146.8 (2C), 135.5, 133.2,

132.1, 131.0, 126.6, 125.5 (2C), 98.9(C-I); *m/z* (HR ESI$^-$) 412.8653 (20 %, M$^-$), 206 (M^{2-}, 100), $C_{10}H_6O_6S_2{}^{127}I$ requires 412.8651.

Synthesis of 4,4'-bis(naphth-1-yl-3,6-disulfonate)-(*E*)-1,2-diphenylethylene, tetra ammonium salt, α-cyclodextrin [2]rotaxane (39⊂α-CD)

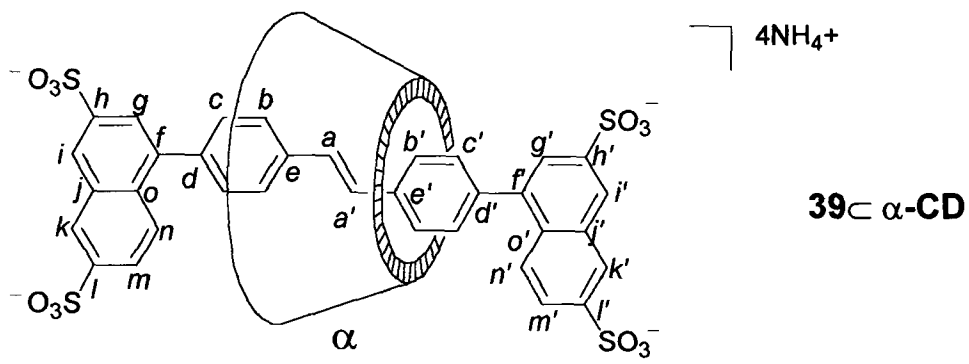

Degassed water (12 cm^3) was added to a mixture of the boronate ester **28** (100 mg, 0.31 mmol), α-cyclodextrin (2.0 g, 2.05 mmol), stopper **30** (287 mg, 0.62 mmol), sodium bicarbonate (0.18 g, 2.14 mmol), sodium carbonate (0.24 g, 2.26 mmol) and palladium (II) acetate (1.0 mg, 1.5 mol %). The mixture was heated for 18 h at 45 °C. The cooled mixture was filtered through cotton wool, acidified with acetic acid to pH ~4, and converted to the ammonium salt on an ion exchange resin. The crude rotaxane was purified by repeated water / 2-propanol recrystallisations until pure by ^{1}H NMR, to give *4,4'-bis(naphth-1-yl-3,6-disulfonate)-(E)-1,2-diphenylethylene, tetra ammonium salt, α-cyclodextrin [2]rotaxane* **39⊂α-CD** (138 mg, 25 %); mp 190 °C (dec.); ν_{max}(KBr)/cm^{-1} 3391 (OH), 2361 (NH_4^+), 1636 (C=C), 1403 (C-O), 1151 (SO_3^-); λ_{max} (H_2O)/nm 236 (ε 135,000), 341 (ε 46,000); δ_H (500 MHz, D_2O) 8.48 (2H, d, J_H 1.5, *k* + *k'*), 8.45 (2H, s, *i* + *i'*), 8.04 (1H, d, J_H 9.0, *n'*), 7.97 - 7.80 (6H, m, *g, m, n , g', m', b'*), 7.70 (2H, d, J_H 8.0, *c'*), 7.61 (2H, d, J_H 7.3, *c*), 7.51 (2H, d, J_H 7.3, *b*), 7.27 (1H, d, J_H 16.5, *a'*), 7.13 (1H, d, J_H 16.5, *a*), 4.95

(6H, d, J_H 2.4, CD H1), 3.90 (6H, bd, J_H 9.4, CD H5), 3.84 (6H, t, J_H 9.6, CD H3), 3.74 (6H, dd, J_H 11.8, 3.5, CD H6), 3.61 (6H, d, J_H 11.8, CD H6'), 3.55 (6H, t, J_H 9.4, CD H4), 3.50 (6H, dd, J_H 9.6, 2.4, CD H2); δ_C (125 MHz, D_2O) 141.35, 141.28, 141.25, 141.15, 140.99, 140.89 (2C), 140.07, 139.86, 135.88 (*e'*), 135.38 (*e*), 133.66, 133.42, 132.43, 132.35, 131.20 (*c*), 130.68 (*c'*), 129.31 (*a'*), 128.27 (*a*), 127.95 (*n'*), 127.77, 127.54 (*b'*), 127.33, 127.20 (2C), 127.00, 126.75, 126.65, 126.43 (*b*), 125.08, 124.99, 124.95, 124.79, 124.51, 102.37 (C-1), 81.65 (C-4), 74.03 (C-3), 73.07 (C-5), 72.57 (C-2), 60.31 (C-6); *m/z* (ES, CV = -30V) 628 (20%), 471 (10), 250 ($[M-3H]^{3-}$, 45), 187 ($[M-4H]^{4-}$, 100); found C 43.1, H 5.6 %, $C_{70}H_{84}O_{42}S_4.13.8(H_2O).(C3H8O)$, requires C 43.1, H 5.9 %;

Synthesis of 4,4'-bis(naphth-1-yl-3,6-disulfonate)-(*E*)-1,2-diphenylethylene, tetra ammonium salt, β-cyclodextrin [2]rotaxane (39⊂β-CD)

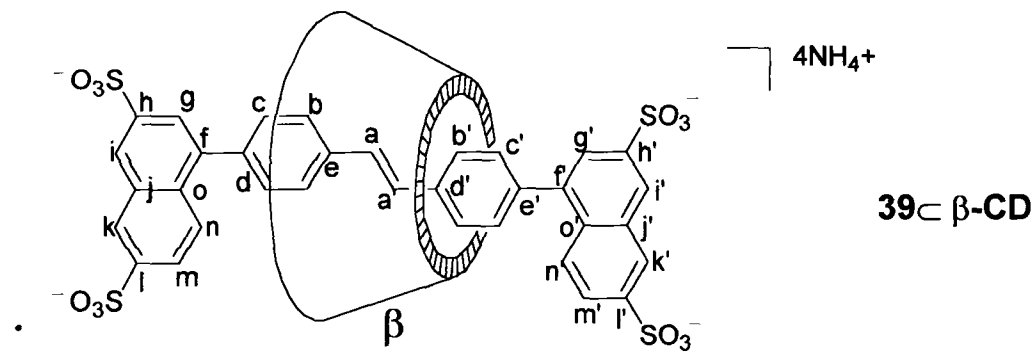

Degassed sodium bicarbonate solution (9 cm^3, 0.1 M, 0.9 mmol) and degassed sodium carbonate solution (9 cm^3, 0.2 M, 1.8 mmol) were added to a mixture of the boronate ester **28** (150 mg, 0.47 mmol), β-cyclodextrin (3.57 g, 3.14 mmol), stopper **30** (0.65 g, 1.42 mmol), and palladium (II) acetate (1.1 mg, 1.05 mol %). The mixture was heated for 18 h at 85 °C. The cooled mixture was filtered through Celite, acidified with acetic acid to pH ~4, and converted to the ammonium salt on

ion exchange resin. The crude rotaxane was purified by flash column chromatography (conc. ammonia : ethanol : THF; 1 : 1 : 2) followed by repeated water / 2-propanol recrystallisations until pure by ^{1}H NMR, to yield the rotaxane *4,4'-bis(naphth-1-yl-3,6-disulfonate)-(E)-1,2-diphenylethylene, tetra ammonium salt, β-cyclodextrin [2]rotaxane* **39⊂β-CD** as a pale orange powder (128 mg, 14 %); mp 200 °C (dec); R_f = 0.1 (conc. ammonia : ethanol : THF; 1 : 1 : 2); $\lambda_{max}(H_2O)$/nm 236.5 (ε 130,000), 337.6 (43,000); ν_{max} 3396 (OH), 2364 (NH_4^+), 1636 (C=C), 1405 (C-O), 1155 (SO_3^-); δ_H (500 MHz, D_2O) 8.64 (1H, s, *i*, *i'*, *k*, or *k'*), 8.63 (1H, s, *i*, *i'*, *k*, or *k'*), 8.60 (1H, s, *i*, *i'*, *k*, or *k'*), 8.56 (1H, s, *i*, *i'*, *k*, or *k'*), 8.14 (1H, d, J_H 2.2, *g* or *g'*), 8.08 (1H, d, J_H 2.2, *g* or *g'*), 7.99 - 7.95 (4H, m, *m*, *m'*, *n* + *n'*) 7.80 (2H, d, J_H 7.7, *b*, *b'*, *c*, or *c'*), 7.77 (2H, d, J_H 7.7, *b*, *b'*, *c*, or *c'*), 7.70 (2H, d, J_H 7.7, *b*, *b'*, *c*, or *c'*), 7.66 (2H, d, J_H 7.7, *b*, *b'*, *c*, or *c'*), 7.39 (1H, d, J_H 16.6, *a* or *a'*), 7.35 (1H, d, J_H 16.6, *a* or *a'*), 5.05 (7H, d, J_H 2.9, CD H1), 3.88 - 3.81 (14H, m, CD), 3.77 - 3.74 (7H, m, CD), 3.68 - 3.66 (7 H, m, CD), 3.61 - 3.56 (14H, m, CD); δ_C (125 MHz, DMSO) 145.85, 145.55, 145.19 (2C), 144.12 (2C), 139.50, 139.20, 138.90, 138.82, 136.18 (2C), 135.79 (2C), 132.11, 131.92, 131.97, 130.48, 129.90 (2C), 128.28, 127.38, 126.55 (2C), 126.23, 125.82, 125.80, 125.30 (2C), 125.23, 125.14, 124.99, 124.74, 124.47, 101.89, 81.16, 73.09, 72.45, 71.99, 59.68; *m/z* (ESI$^-$, CV = -20 V) 628 (40 %, $[M-3H]^{3-}$), 470 (100, $[M-4H]^{4-}$).

Synthesis of 4,4'-bis(naphth-1-yl-3,6-disulfonate)-1,2-diphenylethyne, tetra ammonium salt, α-cyclodextrin [2]rotaxane (42⊂α-CD)

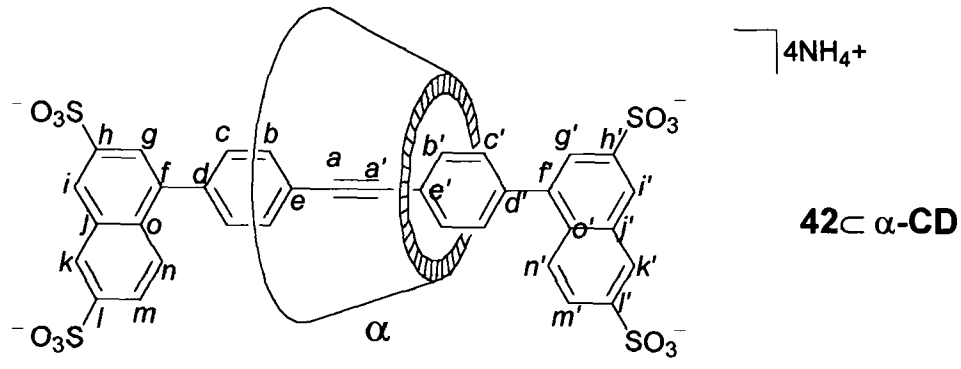

Degassed water (12 cm^3) was added to a mixture of the boronate ester **29** (100 mg, 0.31 mmol), α-cyclodextrin (1.53 g, 1.55 mmol), stopper **30** (287 mg, 0.63 mmol), sodium bicarbonate (0.16 g, 1.88 mmol), sodium carbonate (0.20 g, 1.88 mmol) and palladium (II) acetate (1 mg, 1.2 mol %). The mixture was heated for 18 h at 45 °C. The cooled mixture was filtered through paper, acidified with acetic acid to pH ~4, and converted to the ammonium salt on ion exchange resin. Aqueous ultrafiltration through a 500 NMWCO membrane followed by several recrystallisations from water / 2-propanol yielded the rotaxane *4,4'-bis(naphth-1-yl-3,6-disulfonate)-1,2-diphenylethyne, tetra ammonium salt, α-cyclodextrin [2]rotaxane* **42⊂α-CD** as an off-white powder (23 mg, 31 %); mp 204 °C (dec); ν_{max}(KBr)/cm^{-1} 3400 (O-H, b, vs), 2000 (C≡C, w), 1638 (NH_4^+), 1152 (C-O), 1031 (C-O); λ_{max}(H_2O)/nm 319.9 (ε 41,000), 236.4 (ε 117,000); δ_H (500 MHz, D_2O) 8.49 (2H, s, *i* and *i'* or *k* and *k'*), 8.47 (2H, s, *i* and *i'* or *k* and *k'*), 8.05 (2H, d, J_H 7.5), 7.94 - 7.87 (6H, m), 7.74 (2H, d, J_H 7.5, *b*, *b'*, *c* or *c'*), 7.65 (2H, d, J_H 7.7, *b*, *b'*, *c* or *c'*), 7.53 (2H, d, J_H 7.7, *b*, *b'*, *c* or *c'*), 4.98 (6H, d, J_H 2.5, CD H1), 4.07 (6H, d, J_H 9), 3.89 (6H, d, J_H 10.5), 3.76 - 3.72 (12H, m), 3.60 - 3.50 (12H, m); δ_C (125 MHz, D_2O) 141.2, 141.0, 140.8, 140.5, 133.5, 133.3, 132.8, 132.4, 132.4, 131.7, 130.9, 130.0, 127.6, 127.5, 127.3, 127.2, 126.9, 125.1, 124.8, 121.4, 121.4, 102.3 (CD C1), 90.6 (*a* or *a'*), 90.4 (*a* or

a'), 81.5 (CD), 74.0 (CD), 72.5 (CD), 72.1 (CD), 60.4 (CD); *m/z* (ESI, CV = -30 V) 580.7 ($[M-4H+Na]^{3-}$, 15 %), 573.4 ($[M-3H]^{3-}$, 35), 429.8 ($[M-4H]^{4-}$,100).

Synthesis of 4,4'-bis(naphth-1-yl-3,6-disulfonate)-1,2-diphenylethyne, tetra ammonium salt, β-cyclodextrin [2]rotaxane (42⊂β-CD)

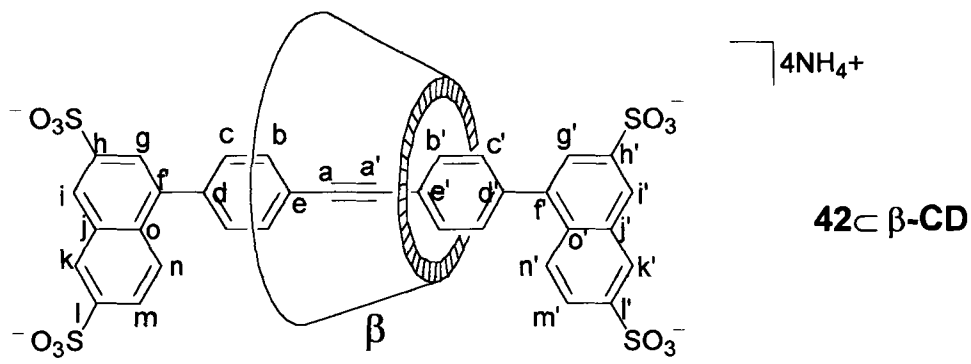

42⊂β-CD

Degassed sodium bicarbonate solution (9 cm^3, 0.1 M, 0.9 mmol) and degassed sodium carbonate solution (9 cm^3, 0.2 M, 1.8 mmol) were added to a mixture of the boronate ester **29** (150 mg, 0.47 mmol), β-cyclodextrin (3.57 g, 3.2 mmol), stopper **30** (0.65 g, 1.41 mmol), and palladium (II) acetate (1.1 mg, 1 mol %). The mixture was heated for 18 h at 80 °C. The cooled mixture was filtered through paper, acidified with acetic acid to pH ~4, and converted to the ammonium salt on ion exchange resin. The crude rotaxane was purified by flash column chromatography eluting with ethanol : ethyl acetate : conc. ammonia solution 1 : 2 : 1. Acetamide formed by the eluant was then removed by sublimation, leaving pale brown granules. This was purified by repeated recrystallisation from water / acetone and water / 2-propanol until pure by ^1H NMR, to afford the rotaxane *4,4'-bis(naphth-1-yl-3,6-disulfonate)-1,2-diphenylethyne, tetra ammonium salt, β-cyclodextrin [2]rotaxane* **42⊂β-CD** (150 mg, 16 %) as an off-white powder; mp 211 °C (dec.); R_f = 0.3 (ethanol : ethyl acetate : conc. ammonia; 1 : 2 : 1); ν_{max}(KBr)/cm^{-1} 3400 (O-

H, b, vs), 2000 (C≡C, w), 1654 (NH_4^+), 1156 (C-O), 1031 (C-O); $\lambda_{max}(H_2O)$/nm 237 (ε 100,000), 314 (33,000); δ_H (500 MHz, D_2O) 8.55 (2H, bs, *i*, *k*, *i'* or *k'*), 8.51 (1H, d, J_H 1.5, *i*, *k*, *i'* or *k'*), 8.48 (1H, d, J_H 1.5, *i*, *k*, *i'* or *k'*), 8.01 - 7.98 (2H, m), 7.88 - 7.87 (2H, m), 7.85 (1H, dd, J_H 9, 1.5), 7.80 (1H, d, J_H 9), 7.70 (2H, d, J_H 8), 7.69 (2H, d, J_H 8), 7.63 (2H, d, J_H 8), 7.59 (2H, d, J_H 8), 4.95 (7H, d, J_H 4, CD H1), 3.90 - 3.78 (14H, m, CD), 3.65 - 3.60 (14H, m, CD), 3.53 - 3.47 (14H, m, CD); δ_C (125 MHz, D_2O) 141.4, 141.2 ,140.9, 140.8, 140.7, 140.5 (2C), 140.3, 133.4, 133.3, 132.6, 132.5, 132.0, 131.5, 130.9, 130.3, 127.8, 127.6, 127.4, 127.4, 126.9, 126.6, 125.5, 125.0, 124.7, 124.6, 122.5, 121.9, 102.2, 90.3, 89.2, 80.9, 73.7, 72.4, 72.3, 60.3; *m/z* (ESI^-, = -40 V) 627 (100 %, $[M-3H]^{3-}$), 470 (25, $[M-4H]^{4-}$), 249 (5, dumbbell $[M-3H]^{3-}$).

Synthesis of 4,4'-bis(phenyl-2,4-dicarboxylate)-(*E*)-1,2-diphenylethene, tetra ammonium salt, α-cyclodextrin [2]rotaxane (40⊂α-CD)

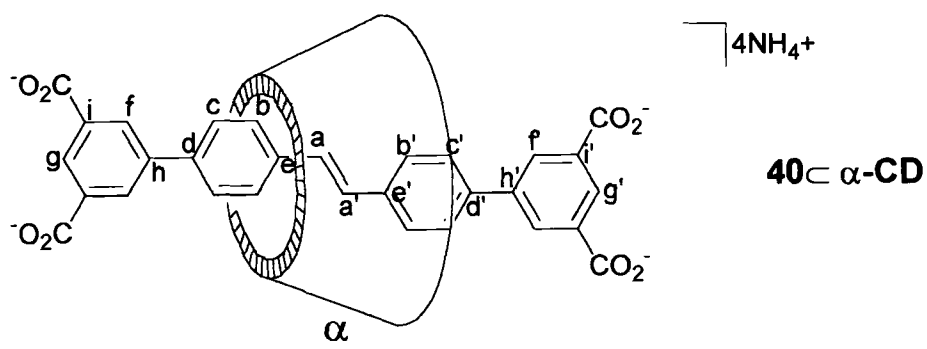

Degassed water (8 cm^3) was added to a mixture of 4,4'-bis(1,3,2-dioxaborol-2-yl)-(E)-1,2-diphenylethene (**28**) (100 mg, 0.31 mmol), α-cyclodextrin (1.6 g, 1.64 mmol), 5-iodo-1,3-benzenecarboxylic acid (**31**) (151 mg, 0.63 mmol), sodium carbonate (0.41 g, 3.9 mmol) and palladium (II) acetate (1.6 mg, 4 mol %). The mixture was heated for 18 h at 45 °C. The volume was made up to 120 cm^3 with

sodium carbonate solution (0.2 M) and the cooled mixture was filtered through paper. The pH was brought to ~1 with conc. HCl, forming a suspension of fine white precipitate. The suspension was centrifuged and supernatant liquid removed. The precipitate was redissolved in sodium carbonate solution (100 cm^3, 0.2 M) and the precipitation/centrifugation repeated. Finally, the precipitate was resuspended twice in water and centrifuged to remove salts. The resultant white solid was dissolved in conc. NH_3 solution and the solvent removed to give the dry ammonium salt of the rotaxane *4,4'-bis(phenyl-2,4-dicarboxylate)-(E)-1,2-diphenylethene, tetra ammonium salt, α-cyclodextrin [2]rotaxane* **40⊂α-CD** (312 mg, 73 %) as white powder; mp 205 °C (dec); ν_{max}(KBr)/cm^{-1} 3369 (vb, OH and NH_4^+), 2930 (C-H), 1610 (Ar-C=C), 1558 and 1405 (s, CO_2^-), 1152 (C-O); λ_{max}(H_2O)/nm 344 (ε 42,500); δ_H (500 MHz, D_2O) 8.45 (2H, s, *f'*), 8.40 (2H, s, *f*), 8.29 (1H, s, *g* or *g'*), 8.27 (1H, s, *g* or *g'*), 8.06 (4H, bs, *b'* and *c'*), 7.83 (2H, d, J_H 6.5, *c*), 7.48 (2H, d, J_H 6.5, *b*), 7.23 (1H, d, J_H 15.5, *a*), 7.08 (1H, d, J_H 15.5, *a'*), 4.99 (6H, d, J_H 3.5, CD H1), 3.93-3.89 (6H, m, CD H5), 3.89-3.84 (6H, m, CD H3), 3.77 (6H, dd, J_H 12.5 and 3, CD H6), 3.68-3.60 (12H, m, CD H6' and H4), 3.57 (6H, dd, J_H 10 and 3.5, CD H2); δ_C (125 MHz, D_2O) 174.5 (CO_2^-), 174.4 (CO_2^-), 140.4 (*d'*), 140.2 (*d* or *h'*), 140.2 (*d* or *h'*), 139.9 (*h*), 136.7 (*i*), 136.6 (*i'*), 135.6 (*e'*), 135.0 (*e*), 130.4 (*f'*), 130.1 (*f*), 128.5 (*a'*), 128.2 (*g* or *g'*), 128.2 (*g* or *g'*), 127.9 (*c*), 127.8 (*a*), 127.8 (*b'*), 127.5 (*c'*), 126.7 (*b*),102.2 (CD 1-C), 81.3 (CD 4-C), 73.8 (CD 3-C), 72.4 (CD 5-C), 71.9 (CD 2-C), 59.8 (CD 6-C); *m/z* (ESI CV = -15 V); 739.4 ($[M-2H]^{2-}$, 5 %), 492.8 ($[M-3H]^{3-}$, 32 %), 369.3 ($[M-4H]^{4-}$, 60 %); free acid **40⊂α-CD**, requires $C_{66}H_{80}O_{38}.4H_2O$ C 51.0 H 5.7 %, found C 51.3 H 5.7 %.

Synthesis of 4,4'-bis(phenyl-2,4-dicarboxylic acid)-(*E*)-1,2-diphenylethene (40)

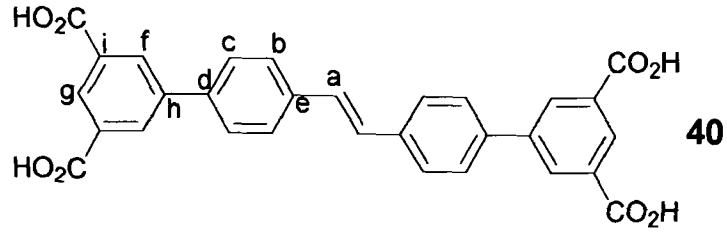

40

Degassed water (17 cm^3) was added to a mixture of 4,4'-bis(1,3,2-dioxaborol-2-yl)-(*E*)-1,2-diphenylethene (**28**) (150 mg, 47 mmol), 5-iodo-1,3-benzenecarboxylic acid (**31**) (206 mg, 70.5 mmol), sodium carbonate (398 mg, 3.8 mmol) and palladium (II) acetate (5 mg, 5 mol %). The mixture was heated for 18 h at 50 °C. The volume was made up to 100 cm^3 with sodium carbonate solution (0.2 M) and the cooled mixture was filtered under gravity. The pH was brought to ~1 with conc. HCl, forming a suspension of fine white precipitate. The suspension was centrifuged and supernatant liquid removed. The precipitate was redissolved in sodium carbonate solution (5 cm^3, 0.2 M) and the precipitation/centrifugation repeated. Finally, the precipitate was resuspended in water and centrifuged to remove salts. Drying *in vacuo* yielded the *4,4'-bis(phenyl-2,4-dicarboxylic acid)-(E)-1,2-diphenylethene* **40** (127 mg, 71 %) as a brown powder, mp >250 °C; λ_{max} (H_2O)/nm 342.5 (ε 42,000); ν_{max} (KBr)/cm^{-1} 3500 (C-H), 3027 (CO_2H), 1696 (Ar-CO_2H), 1599 (Ar C=C); δ_H (250 MHz, NaOD/D_2O) 8.20-8.43 (6H, m, *f* + g), 7.77 (4H, d, J_H 8.4, *b* or *c*), 7.68 (4H, d, J_H 8.4, *b* or *c*), 7.26 (2H, s, *a*); δ_C (125 MHz, NaOD/D_2O) 175.3, 140.3, 139.3 137.5, 137.1, 129.8, 128.7, 128.4, 127.7, 127.6; *m/z* (ESI CV = -20 V) 507 ($[M-H]^-$, 5 %), 253 ($[M-2H]^{2-}$, 100 %), 182 ($[M-4H+Na]^{3-}$, 40 %), 168 ($[M-3H]^{3-}$, 94 %), 153 ($[M-3H-CO_2H]^{3-}$, 80 %).

Synthesis of 4,4'-bis(naphth-1-yl-3,6-disulfonate)-1,2-diphenylethyne, tetra sodium salt (42)

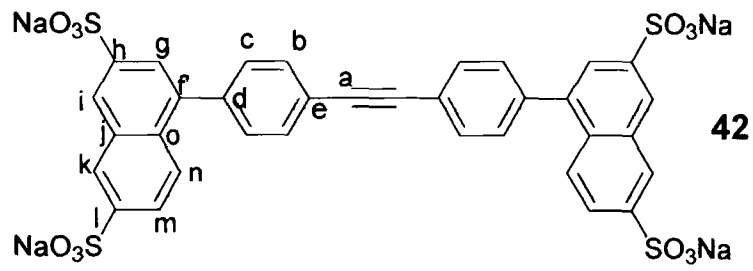

42

Degassed water (14 cm^3) was added to a mixture of the boronate ester **29** (100 mg, 0.314 mmol), stopper **30** (260 mg, 0.566 mmol), sodium carbonate (133 mg, 1.256 mmol), and palladium (II) acetate (3.5 mg, 5 mol %). The mixture was heated for 18 h at 50 °C. The cooled mixture was filtered through paper, and the water removed *in vacuo*. The mixture was redissolved in methanol (20 cm^3), and precipitation with 2-propanol yielded a solid, which was collected by centrifugation and dried. This was purified by flash column chromatography (1-propanol : ethyl acetate : water : acetic acid 40 : 31 : 28 : 1), followed by two further water / 2-propanol recrystallisations to give *4,4'-bis(naphth-1-yl-3,6-disulfonate)-1,2-diphenylethyne, tetra sodium salt* **42** (5 mg, 2 %) as a white powder; R_f = 0.7 (1-propanol : ethyl acetate : water : acetic acid 40 : 31 : 28 : 1); λ_{max} (H_2O)/nm 315.0 (ε 11,500), 233.4 (ε 34,000); δ_H (500 MHz, D_2O) 8.48 (2H, d, J_H 1.5, *i* or *k*), 8.44 (2H, s, *i* or *k*), 8.05 (2H, d, J_H 9, *g*), 7.86 (2H, d, J_H 9, *n*), 7.84 (2H, dd, J_H 9 and 1.5, *m*), 7.73 (4H, d, J_H 8.3, *c* or *b*), 7.57 (4H, d, J_H 8.3, *c* or *b*); δ_C (125 MHz, D_2O) 141.1 (2C, *h* + *l*), 140.8, 139.6, 133.3, 132.4, 132.1 (*b* or *c*), 130.6 (*b* or *c*), 127.6, 127.4, 126.7, 125.0, 124.6, 122.5, 90.3 (*a*); *m/z* (ESI CV = -30 V) 186.5 ($[M-4H]^{4-}$, 100 %), 249.1 ($[M-3H]^{3-}$, 70 %).

Synthesis of 4,4'-bis(naphth-1-yl-3,6-disulfonate)-(*E*)-1,2-diphenylethene, tetra sodium salt (39)

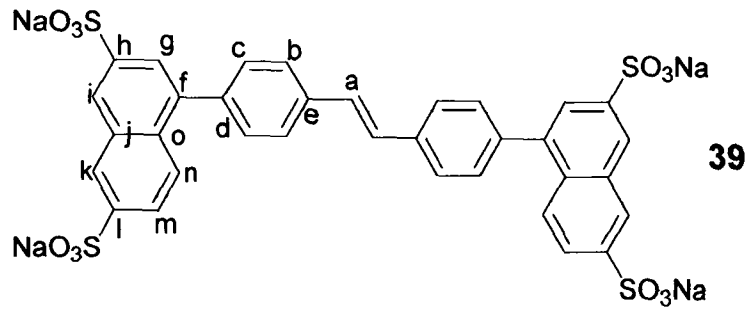

39

Degassed water (4 cm^3) was added to a mixture of the boronate ester **28** (30 mg, 0.094 mmol), stopper **30** (78 mg, 0.169 mmol), sodium carbonate (40 mg, 0.376 mmol), and palladium (II) acetate (1.0 mg, 5 mol %). The mixture was heated for 18 h at 50 °C. The cooled mixture was filtered through paper, and the water removed *in vacuo*. The mixture was redissolved in methanol (8 cm^3), and precipitation with 2-propanol yielded a solid which was collected by centrifugation and dried to give *4,4'-bis(naphth-1-yl-3,6-disulfonate)-(E)-1,2-diphenylethene, tetra sodium salt* **39** as a pale yellow powder (25 mg, 35 %); mp >300 °C; λ_{max} (H_2O)/nm 339.1 (ε 28,000), 235.5 (ε 73,000); ν_{max}(KBr)/cm^{-1} 1636 (C=C trans, conjug.), 1515 (C=C aryl), 1106 (R-SO_3^-); δ_H (500 MHz, D_2O) 8.30 (2H, s, *i* or *k*), 8.24 (2H, s, *i* or *k*), 7.93 (2H, d, J_H 8.7, *m* or *n*), 7.87(2H, d, J_H 8.7, *m* or *n*), 7.83 (2H, s, *g*), 7.28 (4H, d, J_H 7.5, *b* or *c*), 7.17 (4H, d, J_H 7.5, *b* or *c*), 6.72 (2H, s, *a*); δ_C (125 MHz, D_2O) 141.3, 141.0, 140.8, 138.0, 136.7, 133.1, 132.4, 130.6, 128.4, 127.6, 127.3, 126.8, 126.3, 124.9, 124.5; *m/z* (ESI CV = -15 V) 257.2 ($[M-4H+Na]^{3-}$, 8 %), 249.8 ($[M-3H]^{3-}$, 10 %), 187.0 ($[M-4H]^{4-}$, 100%).

7.3. Experimental procedures for Chapter 3

Bromination of dumbbell (40)

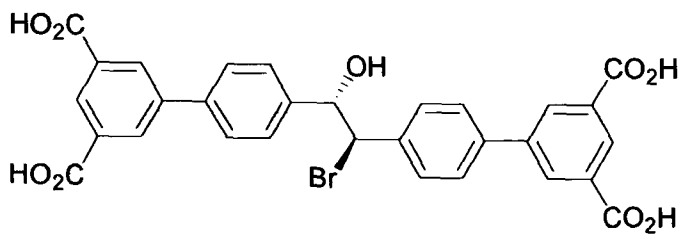

44

Bromine (0.1 ml, 1.9 mmol) was dissolved in water (5 cm^3), in the presence of sodium bromide (6 mg, 0.059 mmol). The resulting solution was added dropwise to the dumbbell sodium salt **40** (30 mg, 0.059 mmol) in water (5 cm^3) at 0 – 5 °C. Aqueous sodium bicarbonate was added as necessary to prevent precipitation. The mixture was stirred for 8 h at room temperature, with monitoring by UV/Vis spectroscopy. After this time, no absorbance at 340 nm could be detected, but the absorbance at 265 nm had increased relative to the starting material. The product (**44**) was not isolated. *m/z* (ESI CV = - 30) 561 ([M-CO_2H], 6 %), 347 (4), 91 (100); λ_{max} 265 nm.

Bromination of rotaxane (40⊂α-CD)

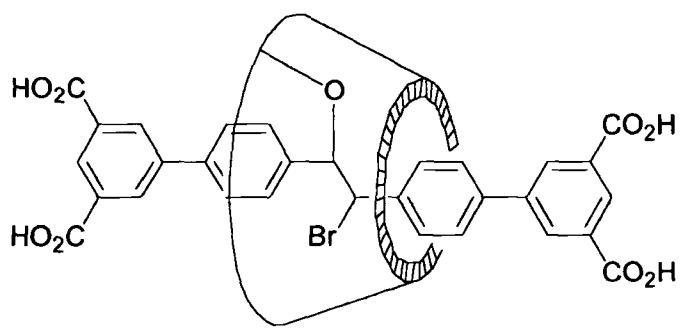

45

Bromine (0.12 ml, 2.3 mmol) in the presence of sodium bromide (0.32 g, 3.1 mmol) was dissolved in water (4 cm^3). The resulting solution was added dropwise to the rotaxane **40⊂α-CD** ammonium salt (15 mg, 0.0095 mmol) in water (4 cm^3) at 0 – 5 °C. Aqueous sodium bicarbonate was added as necessary to prevent precipitation.

The mixture was stirred for 15 h at room temperature, then filtered. Addition of conc. HCl to the orange solution gave a yellow precipitate that was collected and washed with water *via* centrifugation. This solid was redissolved in aqueous sodium bicarbonate and subjected to ultrafiltration through a 500 NMWCO membrane using *ca.* 1 litre water. The solvent was removed and the residue suspended in methanol and filtered. The solvent was removed from the filtrate to yield an orange solid (6 mg, 40 % based on target molecule **45**); selected *m/z* (ESI CV = -25 V) 779.2 ($[M-2H]^{2-}$, 60 %) 519.1 ($[M-3H]^{3-}$, 100), 389.1 ($[M-4H]^{4-}$, 45); δ_H (500 MHz, D_2O) 8.52 – 8.51 (sm), 8.34 (apparent s), 8.32 – 8.22 (sm), 8.03 (d, J_H 7.0), 7.90 – 7.70 (sm), 7.74 (d, J_H 8.0), 7.58 (d, J_H 8.0), 7.40 (d, J_H 7.0), 5.43 – 4.60 (sm), 4.50 – 2.50 (bm); Key HSQC correlations between H at 5.65 – 5.33 and C at 50; λ_{max} 268, 238 nm.

Epoxidation of dumbbell[10, 11]

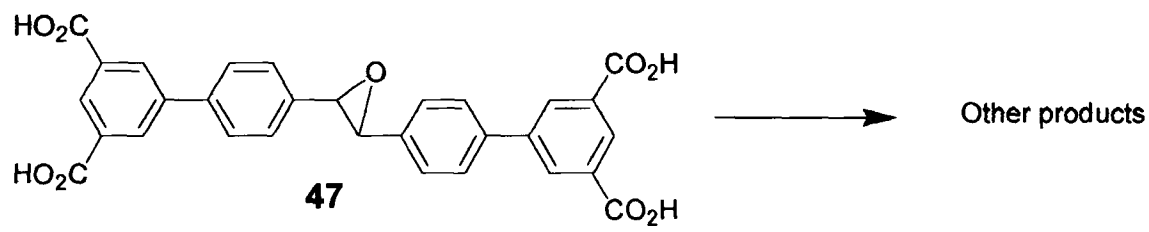

47

Solid oxone ($2KHSO_5.KHSO_4.K_2SO_4$)(181 mg, 0.295 mmol) was added in 3 portions over 10 min to a solution of dumbbell **40** sodium salt (50 mg, 0.098 mmol) in a mixture of aqueous sodium bicarbonate (10 cm^3, 0.05 M) and acetone (6 cm^3) at 0 °C. The reaction was monitored by means of UV/Vis spectroscopy and testing with starch-iodide paper for presence of oxidant. After 6 h at 0 °C, further oxone (11.9 mg, 0.019 mmol) was added. The temperature was allowed to rise to room temperature. After 15 h, oxidant was still present and UV spectroscopy indicated complete destruction of the chromophore at 340 nm. The product **47** was not

isolated; *m/z* (Maldi-Tof-ve mode), 563.3 ($[M+K]^{3-}$, 100 %), 547.3 ($[M+Na]^{3-}$, 95), 541.3 ($[M-H]^{-}$,60) 523.3 (40); δ_H (500 MHz, D_2O) 9.87 (s), 8.5 – 7.2 (complex multiplets), 4.20 (s), 1.84 (s); δ_C (125 MHz, D_2O) 196.6, 175.4, 175.3, 175.1, 165.1, 139.6, 137.7, 137.6, 131.2, 130.5, 130.53, 130.1, 130.0, 129.4, 128.8, 128.5, 128.1, 127.7, 127.3, 127.1, 63.1, 23.7; λ_{max} ~260 nm.

Attempted epoxidation of rotaxane[10, 11]

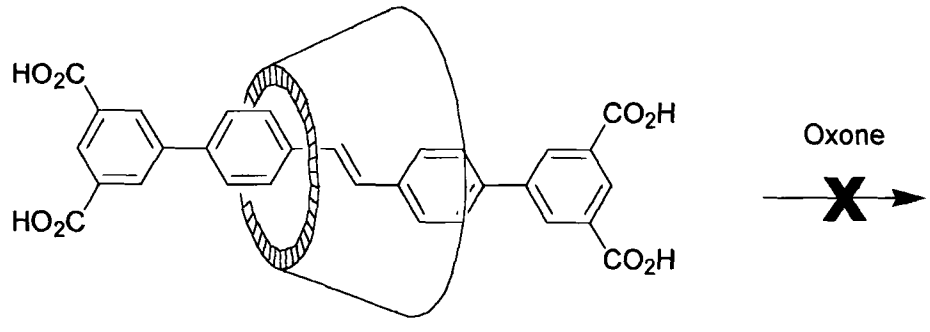

40⊂α-CD

Solid oxone (11.9 mg, 0.019 mmol) was added in 3 portions over 10 min to a solution of rotaxane **40⊂α-CD** (10 mg, 0.0065 mmol) in a mixture of aqueous sodium bicarbonate (3 cm^3, 0.05 M) and acetone (2 cm^3) at 0 °C. The reaction was monitored by means of UV/Vis spectroscopy and testing with starch-iodide paper for the presence of oxidant. After 6 h at 0 °C, further oxone (11.9 mg, 0.019 mmol) was added. The temperature was allowed to rise to room temperature but after 10 h recooled and further oxone added (11.9 mg, 0.019 mmol). This cycle was repeated for 120 h, adding oxone each time no oxidant was observed. No change in UV/Vis or ^1H NMR spectra was observed after this time.

Hydrogenation of dumbbell (40)

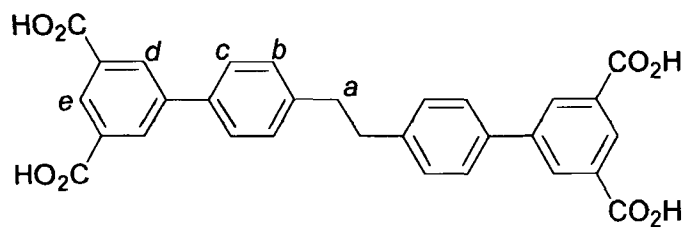

48

Palladium on carbon (2.1 mg, 10 % Pd/C, 5 mol %) and dumbbell **40** sodium salt (20 mg, 0.040 mmol) in water (4 cm^3) were stirred vigorously under a hydrogen atmosphere in the dark. The reaction was monitored by UV/Vis spectroscopy over 20 h, after which time UV showed no further change. Subsequent filtration of the mixture through Celite and removal of solvent, followed by precipitation of the product from a small volume of water by addition of conc. HCl and washing with water, gave the hydrogenated dumbbell **48** as a brown powder (10.8 mg, 54 %); δ_H (250 MHz, D_2O/NaOH) 8.13 (2H, d, J_H 1.5, *e*), 8.12 (4H, d, J_H 1.5, *d*), 7.57 (4H, d, J_H 8.2, *b* or *c*), 7.28 (4H, d, J_H 8.2, *b* or *c*), 2.92 (4H, s, *a*); δ_C (125 MHz, D_2O/NaOH) 175.4, 142.3, 140.7, 137.7, 137.5, 129.9, 129.8, 128.1, 127.3, 36.9; λ_{max}(H_2O/NaOH)/nm 263 (ε 66,500), 233 (ε 80,900); *m/z* (ESI CV = - 30 V) 509.2 ($[M-H]^-$, 10 %), 375.3 (4), 347.3 (8), 254.2($[M-2H]^{2-}$, 100)

Attempted hydrogenation of rotaxane (40⊂α-CD)

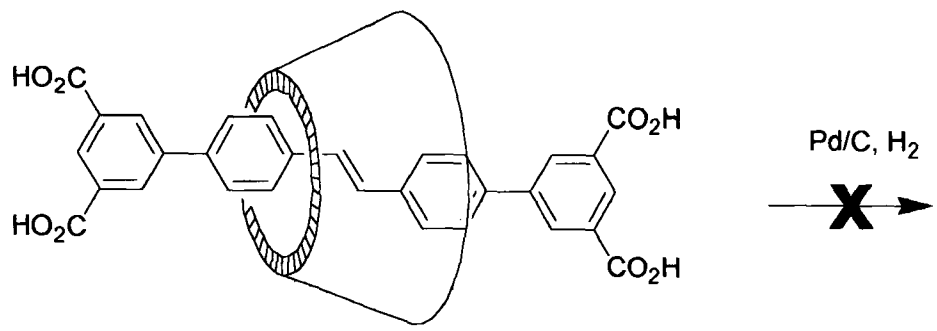

40⊂ α-CD

Palladium on carbon (0.3 mg, 10 % Pd/C, 5 mol %) and rotaxane **40⊂α-CD** ammonium salt (10 mg, 0.0063 mmol) in water (2 cm^3) were stirred vigorously under a hydrogen atmosphere in the dark. The reaction was monitored by UV/Vis spectroscopy over 96 h, after which time there was no change in the UV spectrum. Subsequent filtration of the mixture through Celite and removal of solvent showed no change by ^1H NMR.

Attempted unthreading of rotaxane (40⊂α-CD)

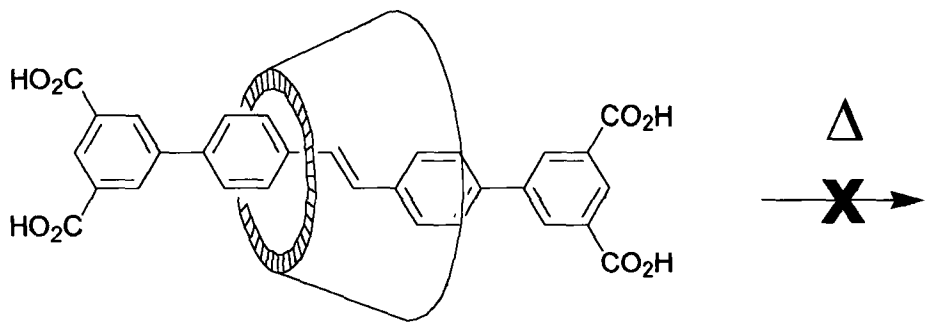

40⊂ α-CD

In D_2O:

Rotaxane **40⊂α-CD** ammonium salt (12.5 mg, 0.0079 mmol) was dissolved in degassed D_2O (4.5 cm^3) and placed in an NMR tube. The tube was heated to 80 °C for 70 h with monitoring by ^1H NMR. No significant change was observed after this time.

In d_6-DMSO:

Rotaxane **40⊂α-CD** ammonium salt (12.5 mg, 0.0079 mmol) was dissolved in degassed d_6-DMSO (4.5 cm^3) and heated as above. Again, no change observed after 70 h. After this time the temperature was raised to 120 °C and the sample heated for a further 168 h. No change in ^1H NMR spectrum was observed after this time.

Methylation of rotaxane (40⊂α-CD)

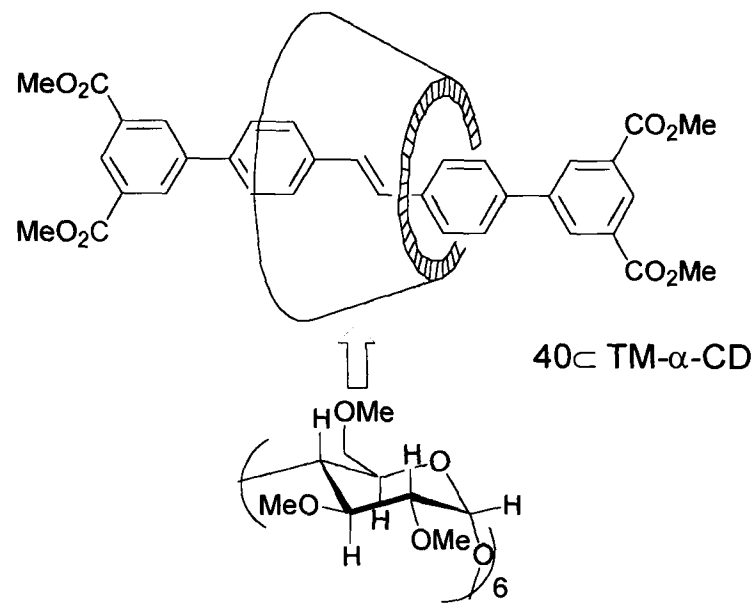

Base prepared as follows:

Sodium hydride (0.25 g, 60 % dispersion in paraffin oil, 6.3 mmol) was dissolved in dry DMSO (2 cm^3) under an inert atmosphere. The mixture was stirred at 65 °C (N.B. Danger of explosion at temperatures above 80 °C[12, 13]) until no further gas was evolved (*ca.* 2 h).

Methylation procedure:

The dry rotaxane ammonium salt **40⊂α-CD** (100 mg, 0.063 mmol) was dissolved in DMSO (2 cm^3). To this mixture was added half of the base solution (above). The resulting thick mixture was stirred at 65 °C for 30 min, then cooled to 0 °C before addition of iodomethane (0.2 cm^3, 3.15 mmol) *via* syringe. This mixture was stirred

for 3 h at ambient temperature, then the remaining base solution was added. Heating to 65 °C for 15 h was followed by cooling to 0 °C and addition of further iodomethane (0.8 cm^3, 12.6 mmol). The mixture was stirred for 6 h at ambient temperature. After this time, the mixture was poured into water (50 cm^3) and extracted with chloroform (3 x 25 cm^3). The organic extracts were dried over sodium sulfate and the solvent removed *in vacuo* to give yellow DMSO-containing residues (~5 cm^3). Precipitation of a sticky solid occurred upon addition of water to this mixture. The solid was washed with further water and dried to give a yellowish gum which had a complex ^1H NMR with multiple anomeric signals. Re-subjection to the methylation conditions did not improve the purity of the mixture.

7.4. Experimental procedures for Chapter 4

Measurement of Fluorescence Quantum Yields[14, 15]

All quantum yields were measured relative to quinine bisulfate in 0.5 M sulfuric acid (aq.) and to anthracene in cyclohexane, with a subsequent solvent correction according to the following:

$$\Phi_A = \left[\frac{(A_B F_A n^2)}{A_A F_B n^2}\right] \Phi_B \qquad \textit{Equation 7.1.}$$

where

$\mathbf{\Phi_B}$ = Fluorescence quantum yield of standard; quinine bisulfate[16, 17] = 0.546, anthracene = 0.27[18].

$\mathbf{A_A}$ = Absorbance of sample in UV/Vis at excitation wavelength

$\mathbf{F_A}$ = Integrated emission (number obtained from spectral integration) cm^{-1} *vs.* counts sec^{-1}.

$\mathbf{n_A^2}$ = Square of refractive index of the solvent in which measurement carried out; 0.5 M sulfuric acid = 1.339, cyclohexane = 1.426, water = 1.333

A UV/Vis spectrum of the sample was first recorded, with an absorbance of ~0.5. The exact concentration was not calculated. A known volume of the UV sample (normally 20 μl) was then removed and added to a known volume of the same solvent (normally 3 ml) in a fluorescence cuvette. This was to ensure that the absorbance of the fluorescence sample was below 0.1 (thus avoiding problems with

reabsorption), whilst enabling a more accurate determination of the exact absorbance. The absorbance of the sample in the fluorescence cuvette was then calculated from the dilution used.

An excitation spectrum was performed of each sample before emission measurements were commenced. This was in order to check that the calibration of UV and fluorescence spectrometers was in agreement, giving the same absorbance maximum. In some cases, a small correction was required here as it was not possible to recalibrate the UV spectrometer manually.

A fluorescence spectrum was then recorded at 1 nm bandpass, choosing a point for excitation where both standard and sample had absorbance and, where possible, neither was changing rapidly with respect to wavelength (*i.e.* the top or shoulder of a broad peak). A series of emission spectra was then run with incremental increases in concentration. This was performed for every sample and standard, re-measuring the standard if the measurements were not carried out on the same day.

The spectra were then integrated using the Datamax software, and the quantum yields calculated according to Equation 7.1. (a plot for each substance of absorbance *vs.* emission integral gave a straight line where the gradient was the fluorescence quantum yield, less any necessary solvent corrections). Example experimental data can be found in Appendix 7.1.

7.5. Experimental procedures for Chapter 5

Photoswitching of rotaxane (40⊂α-CD)

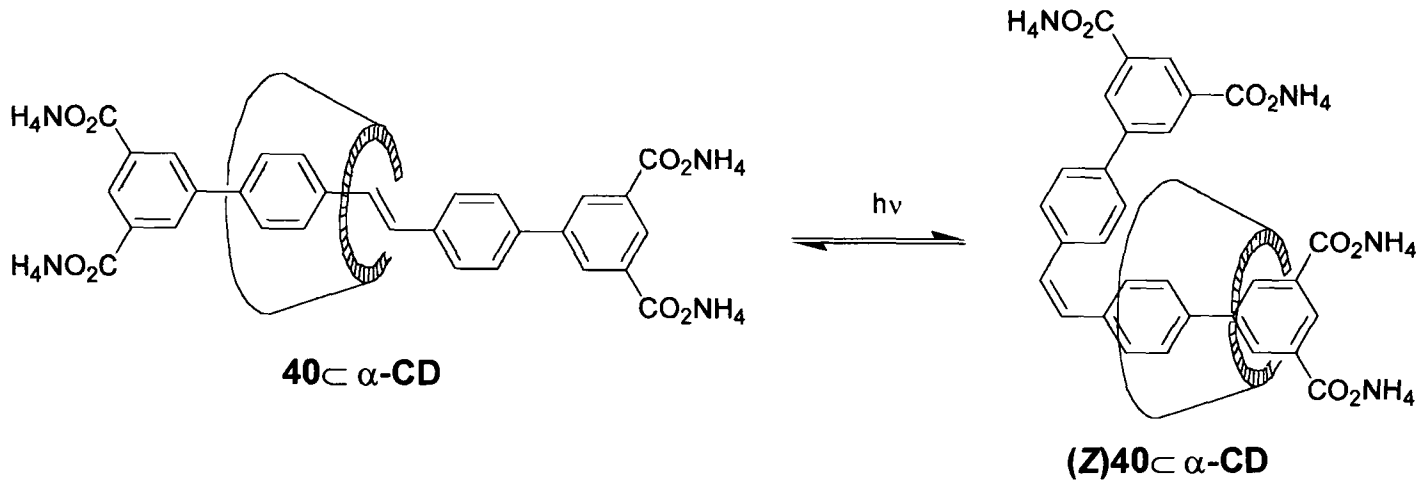

40⊂ α-CD **(*Z*)40⊂ α-CD**

Rotaxane (**40⊂α-CD**) was dissolved in degassed water to give a solution of absorbance ~1.0 a.u. and placed in a 4 cm^3 fluorescence cuvette. An initial UV spectrum was recorded, followed by timed intervals of irradiation at 265 nm in the Fluoromax-2 (slits at 5 nm bandpass). At each time point, a further UV spectrum was recorded. Once a stable photostationary state appeared to have been reached, the irradiation wavelength was altered to 347 nm, and the process repeated until a second photostationary state had been reached. The irradiation wavelength was switched back to 265 nm, and the cycle was repeated a further three times. Data can be found in Appendix 7.2.

Photoswitching of dumbbell (40)

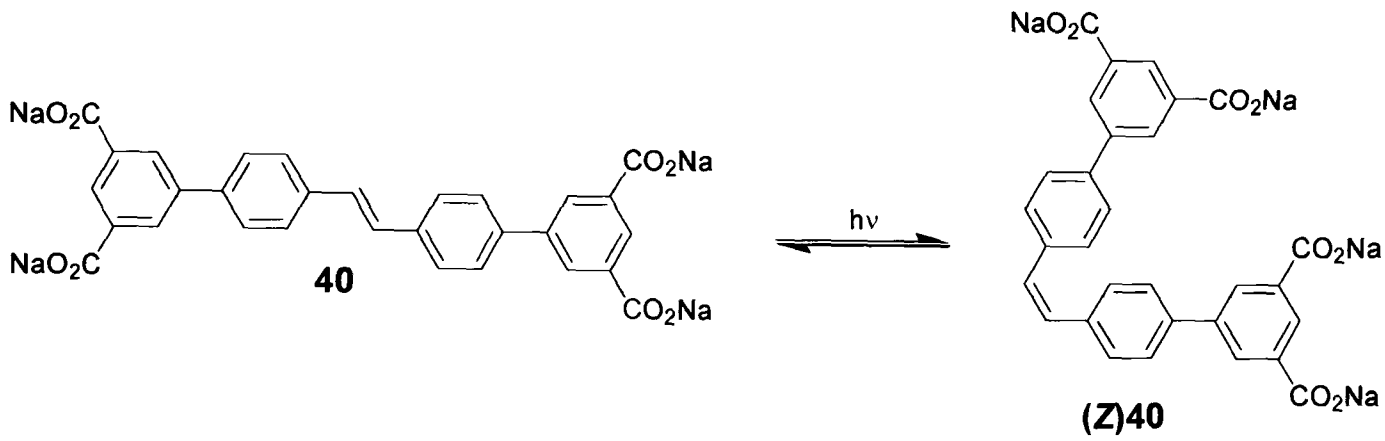

Dumbbell (**40**) was dissolved in degassed water to give a solution of absorbance ~1.0 a.u. and placed in a 4 cm^3 fluorescence cuvette. An initial UV spectrum was recorded, followed by timed intervals of irradiation at 265 nm in the Fluoromax-2 (slits at 5 nm bandpass). At each time point, a further UV spectrum was recorded. Once a stable photostationary state appeared to have been reached, the irradiation wavelength was altered to 340 nm, and the process repeated until a second photostationary state had been reached. The irradiation wavelength was switched back to 265 nm, and the cycle was repeated a further three times. Data can be found in Appendix 7.3.

Photoswitching of dumbbell (39)

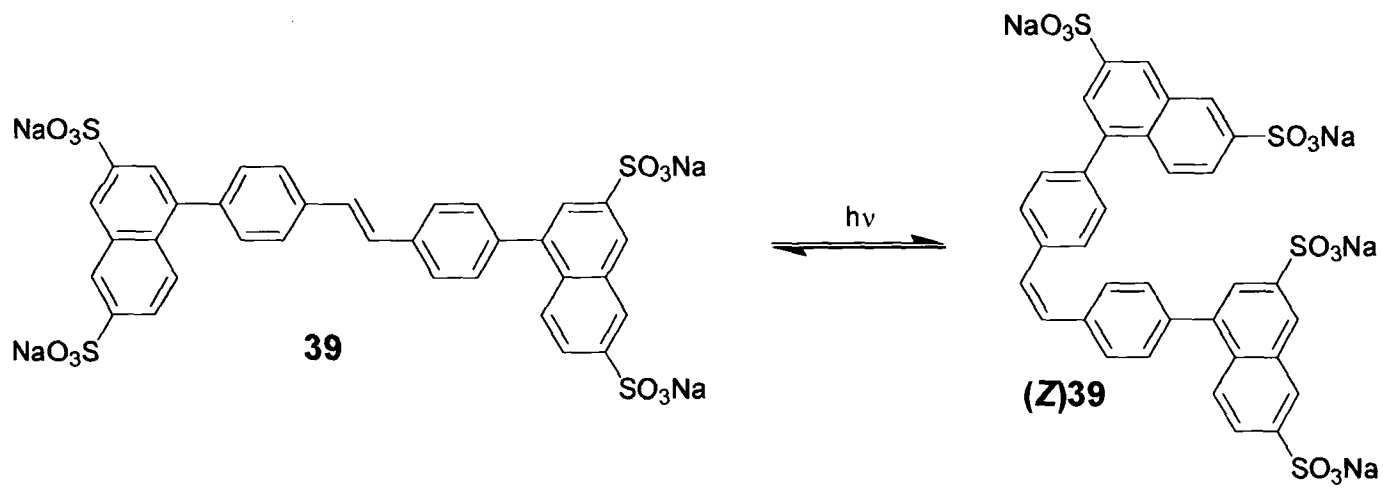

As for 'photoswitching of dumbbell **40**' above, with the alteration that irradiation was at 335 nm. Data can be found in Appendix 7.4.

Photoswitching of α rotaxane (39⊂α-CD)

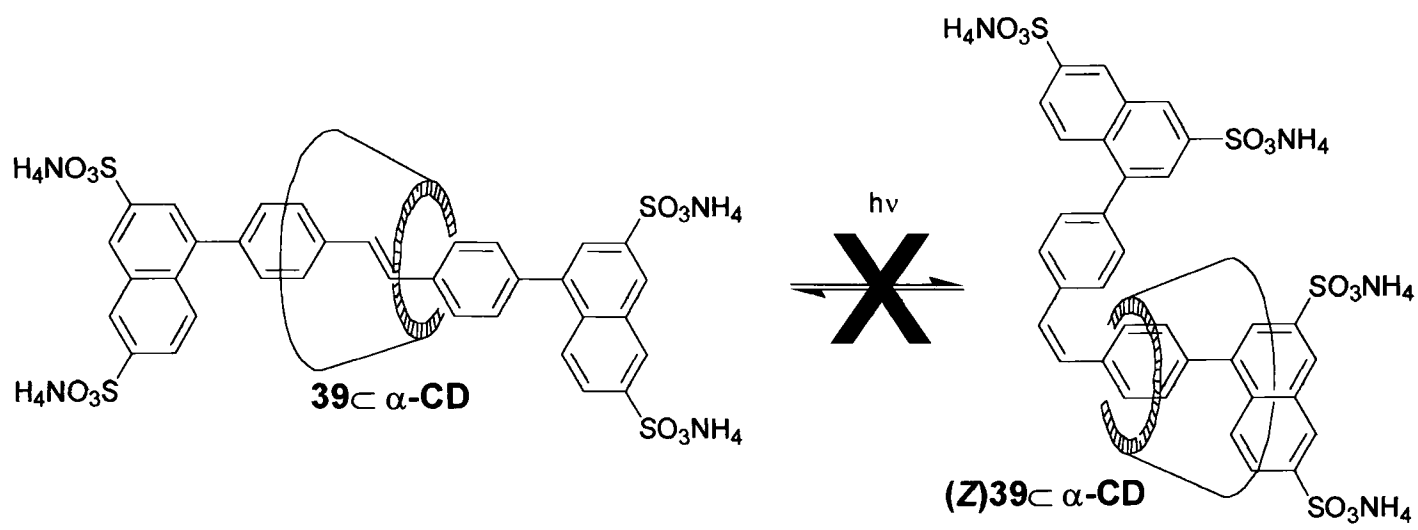

As for 'photoswitching of rotaxane **40⊂α-CD**' above, with the alteration that irradiation was at 337 nm. The rotaxane did not appear to switch. Data can be found in Appendix 7.5.

Photoswitching of β rotaxane (39⊂β-CD)

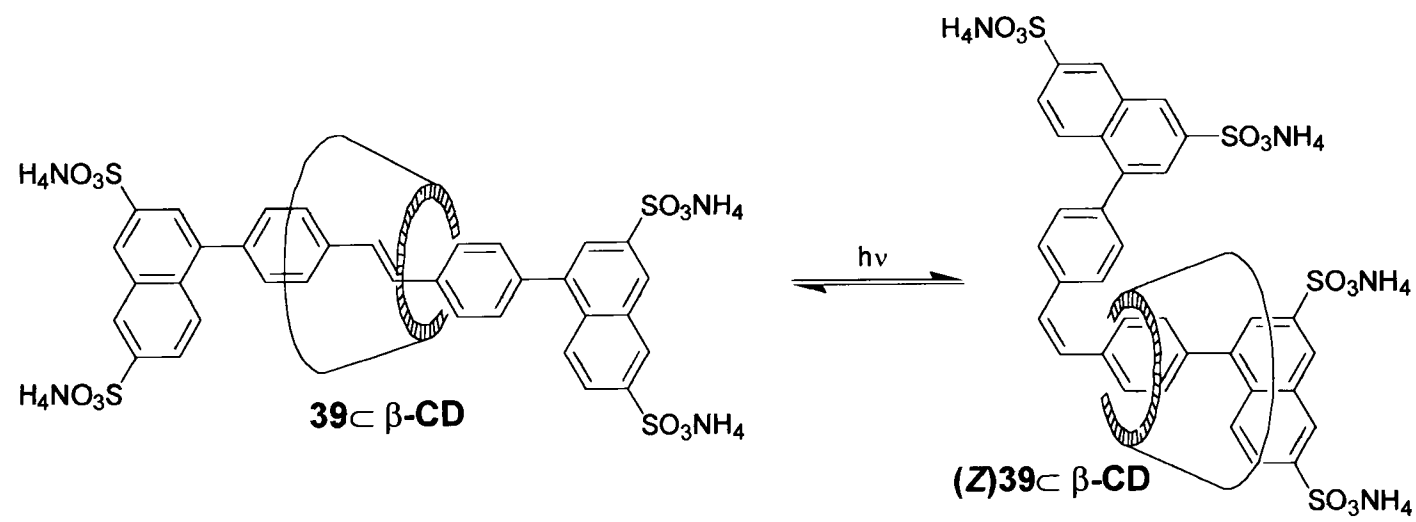

As for 'photoswitching of rotaxane **40⊂α-CD**' above, with the alteration that irradiation was at 329 nm. Data can be found in Appendix 7.6.

Photoswitching of the rotaxane (40⊂α-CD) for calculation of ε_{cis}

Rotaxane **40⊂α-CD** ammonium salt (8.9 mg, 5.74 μmol) was dissolved in degassed water (4.4 cm^3). and placed in a 4.5 cm^3 fluorescence cuvette. An initial UV spectrum of a diluted aliquot was recorded, and the sample was irradiated at 347 nm in the Fluoromax-2 (slits at 5 nm bandpass). The absorbance of diluted samples was monitored by UV/Vis spectroscopy. Irradiation was undertaken for *ca.* 72 h. A further UV spectrum was recorded and water was removed from the sample, which was analysed by ^1H NMR in D_2O, measured on a 500 MHz spectrometer with a 90° pulse width to give accurate integrals of the ethene protons. The UV spectra were normalised at 306 nm to enable a correction for concentration measurements to be undertaken. The calculations for ε_{cis} were based on a ratio of 0.746 : 0.254 for *trans* : *cis*.

Photoswitching of the dumbbell (40) for calculation of ε_{cis}

Dumbbell **40** ammonium salt (3.0 mg, 5.95 μmol) was dissolved in degassed water (4.25 cm^3). and placed in a 4.5 cm^3 fluorescence cuvette. Procedure as for the rotaxane **40⊂α-CD** above, but spectra normalised at 300 nm. The calculations for ε_{cis} were based on a ratio of 0.617 : 0.383 for *trans* : *cis*.

Isosbestic photoswitching of the rotaxane (40⊂α-CD)

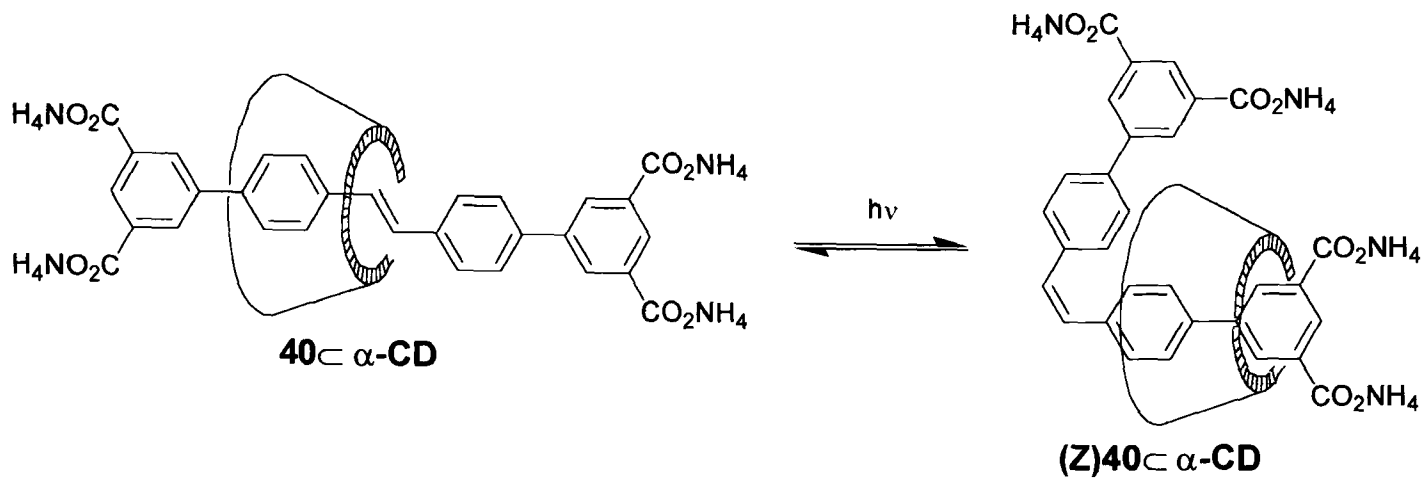

40⊂ α-CD **(Z)40⊂ α-CD**

As 'photoswitching of the rotaxane **40⊂α-CD**' above, but with the following alterations: irradiation wavelength was 307 nm and irradiation was ceased when the change in absorbance became insignificant. The solution was made of a concentration giving an absorbance of 0.1 rather than 1.0.

Isosbestic photoswitching of the dumbbell (40)

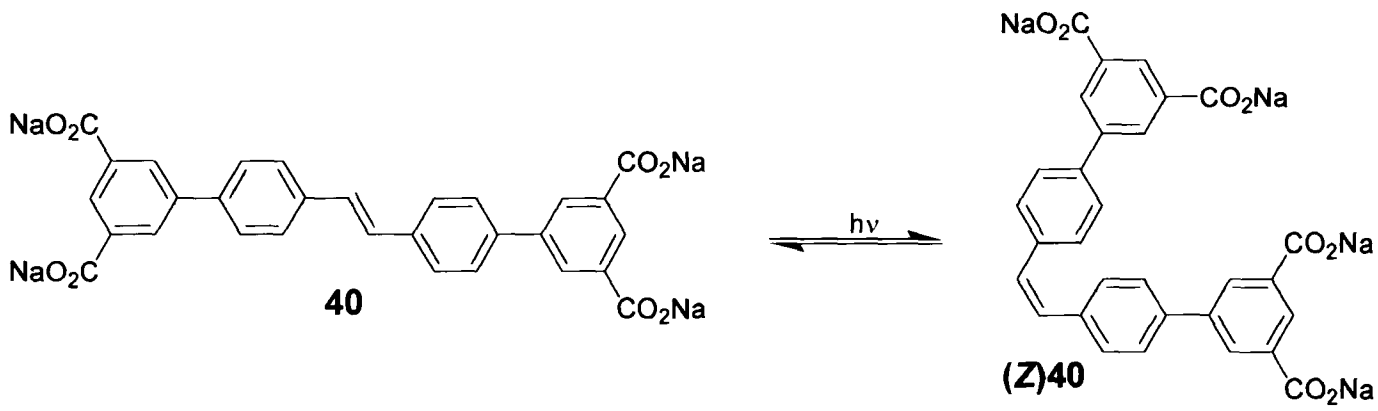

40 **(Z)40**

As 'photoswitching of the dumbbell **40**' above but with the following alterations: irradiation wavelength was 300 nm and irradiation was ceased as soon as the initial photostationary state had been reached. The solution was made up of a concentration giving an absorbance of 0.1 rather than 1.0.

Photoswitching of dumbbell (40), rotaxane (40⊂α-CD) and stilbene (49) for initial rates

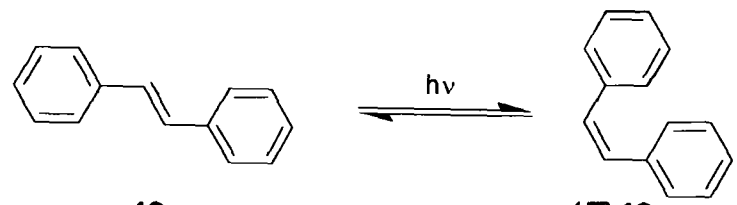

49 **(*Z*)49**

As 'photoswitching of the dumbbell and rotaxane **40** and **40⊂α-CD**' above, but with the alterations that the irradiation wavelength for all species was 325 nm, also that irradiation was carried out with a narrower slit width of 1 nm bandpass, to reduce the intensity of light and therefore slow the switching process. Data can be found in Appendix 7.7.

Aerobic photodegradation of rotaxane (40⊂α-CD)

Rotaxane (**40⊂α-CD**) was dissolved in undegassed water to give a solution of absorbance ~1.0 a.u. and placed in a 4 cm^3 fluorescence cuvette. An initial UV spectrum was recorded, followed by timed intervals of irradiation at 347 nm in the Fluoromax-2 (slits at 5 nm bandpass). At each time point, a further UV spectrum was recorded. After the initial switching period, the changes in absorbance were much smaller. The irradiation was left for over 22 h. Data can be found in Appendix 7.8.

Anaerobic photodegradation of rotaxane (40⊂α-CD)

As for the aerobic degradation, except that the water was degassed *via* a nitrogen purge cycle. Data can be found in Appendix 7.9.

Aerobic photodegradation of dumbbell (40)

Dumbbell (**40**) was dissolved in undegassed water to give a solution of absorbance ~1.0 a.u. and placed in a 4 cm^3 fluorescence cuvette. An initial UV spectrum was recorded, followed by timed intervals of irradiation at 340 nm in the Fluoromax-2 (slits at 5 nm bandpass). At each time point, a further UV spectrum was recorded. After the initial switching period, the changes in absorbance were much smaller. The irradiation was left for over 22 h. Data can be found in Appendix 7.10.

Anaerobic photodegradation of dumbbell (40)

As for the aerobic degradation, except that the water was degassed *via* a nitrogen purge cycle. Data can be found in Appendix 7.11.

Photohydration of rotaxane (40⊂α-CD)

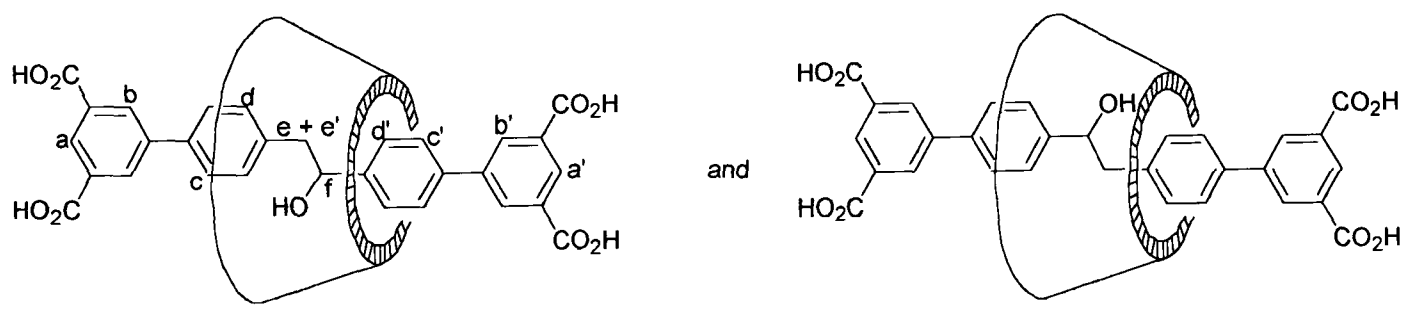

50⊂α-CD

The rotaxane (**40⊂α-CD**) ammonium salt (40 mg, 0.032 mmol) was placed under nitrogen in a flask fitted with a water-cooled cold-finger, and dissolved in degassed water (36 cm^3). The mixture was irradiated for 96 h with two 300 W UV/Vis

tungsten filament lamps and monitored by UV/Vis spectroscopy. Solvent was the removed and the residue re-dissolved in the minimum amount of water (*ca.* 4 cm^3). Addition of conc. HCl (1 drop) resulted in precipitation of an off-white solid which was collected by centrifugation and repeatedly washed with water, followed by drying *in vacuo* to yield the free acid (**50⊂α-CD**) as an off-white solid (25 mg, 65 %); λ_{max} (H_2O)/nm 265; ν_{max} (KBr)/cm^{-1}; δ_H (500 MHz, D_2O) 8.51 – 8.15 (several m, all J_H ~2, *a*, *b*, *a'*, *b'*), 8.06 – 7.20 (~14 d, all J_H ~8, *c*, *d*, *c'*, *d'*), 5.05 (dd, J_H 7.4, 12.9, *f*), 5.00 – 4.80 (3 or more d, J_H ~3.5, *H-1* of CD), 3.95 – 3.25 (m, *H-2* - *H-6* of CD), 3.11 (dd, J_H 12.9, 5.8, *e*), 3.03 (dd, J_H 7.4, 5.8, *e'*); Key COSY correlation *f* ↔ *e'*, *e* ↔ *e'*; δ_C (125 MHz, D_2O) 175.3, 175.1, 175.0, 145.8 – 126.4 (complex, at least 38 C), 102.3, 101.8, 81.8, 81.6, 74.0, 73.8, 73.7, 72.5, 72.4, 72.3, 72.1, 69.9, 62.9, 60.7, 60.3, 60.1, 43.2, 42.8, 42.6; *m/z* (ESI CV = - 30 V) 748.4 ($[M-2H]^{2-}$, 65 %), 498.9 ($[M-2H]^{2-}$, 34).

Photohydration / photodimerisation of dumbbell (40)

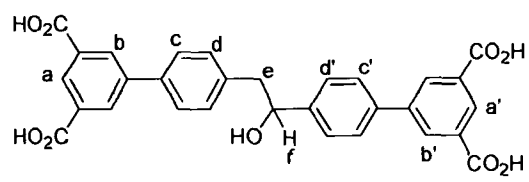

50

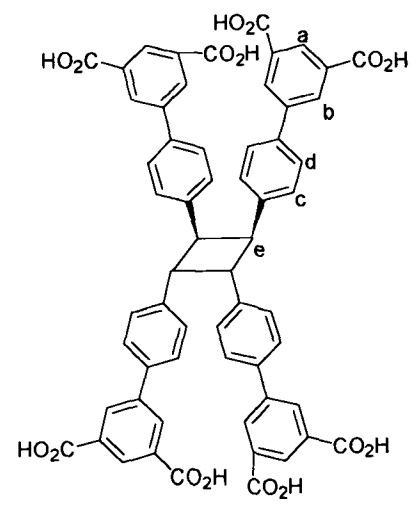

51

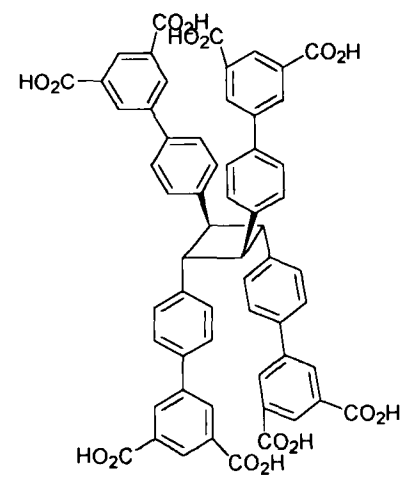

The dumbbell (**40**) (16 mg, 0.032 mmol) was placed under nitrogen in a flask fitted with a water-cooled cold-finger, and dissolved in degassed water (45 cm^3) with

addition of sodium hydroxide (5.2 mg, 0.131 mmol). The mixture was irradiated for 72 h with two 300 W UV/Vis tungsten filament lamps and monitored by UV/Vis spectroscopy. Solvent was removed and the residue re-dissolved in the minimum amount of water (*ca.* 2 cm^3). Addition of conc. HCl (1 drop) resulted in precipitation of an off-white solid which was collected by centrifugation and repeatedly washed with water, followed by drying *in vacuo* to yield the free acid (**50** + **51**) as a grey solid (3.1 mg, 19 % based on **50**); δ_H (500 MHz, D_2O) 8.23 (s, *b* + *b'* of **50** +**51**), 8.21 (s, *a* + *a' of* **50** +**51**), 7.75 (d, J_H 8.3, *c'* of **50**), 7.67 (d, J_H 8.7, *c* of **50**), 7.64 (d, J_H 8.0, *c* of **51**), 7.53 (d, J_H 8.3, *d'* of **50**), 7.39 (d, J_H 8.7, *d* of **50**) 7.35 (d, J_H 8.0, *d* of **51**), 5.06 (dd, J_H 8.1, 6.0, *f* of **50**), 3.20 – 3.08 (m, *e*+*e'* of **50**), 2.35 (s, *e* of **51**), integration gives ratio of **50** : **51** ~4 :1; Key NOEs in **50**: *f* ↔ *e,e'* (medium), *e* ↔ *d* (strong), *e* ↔ *d'* (weak), *f* ↔ *d* (weak), *f* ↔ *d'* (strong); Key COSY correlations in **50**: *c* ↔ *d*, *c'* ↔ *d'*, *f* ↔ *e*, *e'*; δ_C (125 MHz, D_2O) 175.4, 175.3, 168.8, 145.0 - 127.2 (complex, at least 17 C), 75.0, 63.5; *m/z* (Na salt M=**51**) (FAB^+) 1103.2 ($[MNa_4H_3]^+$, 76 %), 1079.2 ($[MNa_3H_3]^+$, 45), 1057.4 ($[MNa_2H_3]^+$, 20), 1033.3 ($[MNaH]^+$, 23).

Attempted phenanthrene formation from dumbbell (40) in methanol[19]

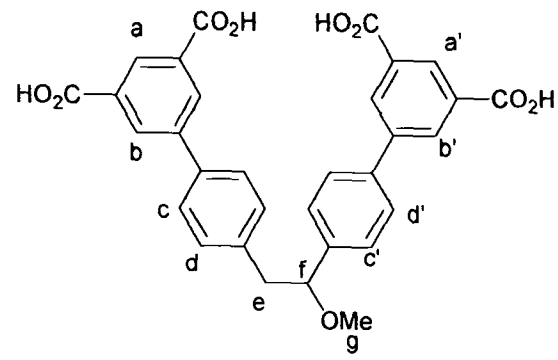

54

The dumbbell **40** (15 mg, 0.030 mmol) and iodine (8.3 mg, 0.033 mmol), were dissolved in degassed methanol (20 cm^3), in a round bottomed flask fitted with a water-cooled cold-finger. Propylene oxide (0.21 cm^3, 2.98 mmol) was added to the mixture *via* syringe, and the mixture irradiated by means of two 300 W UV/Vis lamps for 20 h. The reaction was monitored by UV/Vis spectroscopy. After 20 h the mixture was degassed for 5 min to remove excess propylene oxide, filtered and solvent removed *in vacuo* to yield a brown solid. This was purified by dissolving in aq. sodium hydroxide (1 cm^3, 2.5 M), precipitation by addition of conc. HCl, and repeated washing with water. The precipitate was dried under vacuum to afford a brown powder (5.9 mg, 37 %); *m/z* for methanol adduct **54** (ESI CV = -20 V) 539 ($[M-H]^-$, 100 %); δ_H (250 MHz, d_6-DMSO) 9.37 (1H, s), 8.70 – 8.25 (~10 H, several m, *a*, *a'*, *b*, *b'*), 8.23 (8H,~4 d, *c*, *d*, *c'*, *d'*) 4.75 (1H, s, *f*), 3.52 (3H, s, *g*) 3.15 (1H, s, *e* or *e'*), 2.80 (1H, s, *e* or *e'*).

Attempted phenanthrene formation from dumbbell (40) in acetonitrile[19]

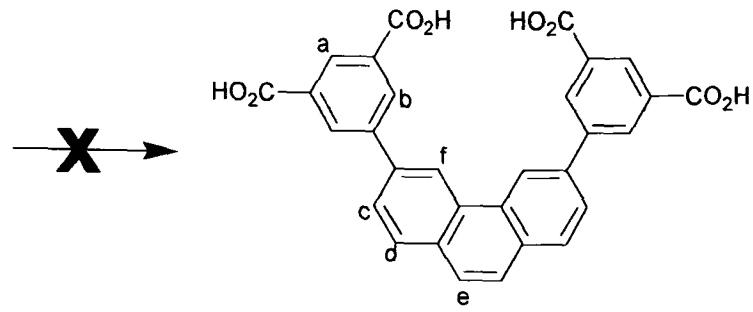

53

The dumbbell **40** (15 mg, 0.030 mmol) and iodine (8.3 mg, 0.033 mmol) were dissolved in degassed acetonitrile (15 cm^3), in a round bottomed flask fitted with a water-cooled cold-finger. Propylene oxide (0.21 cm^3, 2.98 mmol) was added to the mixture *via* syringe, and the mixture irradiated by means of two 300 W UV/Vis lamps for 24 h. After 16 h further acetonitrile (10 cm^3) was added to dissolve all of the solid. The reaction was monitored by UV/Vis spectroscopy. After 24 h the mixture was degassed for 5 min to remove excess propylene oxide, filtered and solvent removed *in vacuo* to yield a brown solid. This was purified by dissolving in aq. sodium hydroxide (1 cm^3, 2.5 M), precipitation by addition of conc. HCl, and repeated washing with water. The precipitate was dried under vacuum to afford a brown powder which still contained some salt (25 mg). This did not appear to be either the target molecule **53**, or a photohydrated species; δ_H (250 MHz, D_2O) 8.35 – 8.25 (6H, m, a +b), 8.02 (H, d, J_H 8.2,), 7.95 (H, d, J_H 8.3,), 7.90 (H, d, J_H 8.2,), 7.79 (H, d, J_H 8.2,). *m/z* (FAB^+) 406.8 (8 %), 331.9 (10), 257.0 (15), 254.0 (38), 157.0 (58).

Attempted phenanthrene formation from rotaxane (40⊂α-CD)[19]

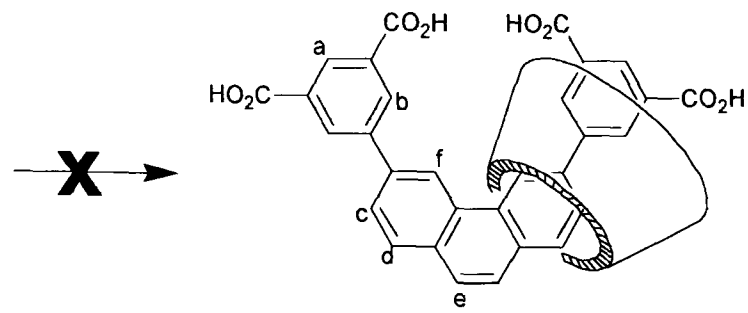

53⊂ α-CD

The rotaxane ammonium salt **40⊂α-CD** (80 mg, 0.052 mmol) and iodine (14.4 mg, 0.057 mmol) were dissolved in degassed acetonitrile (50 cm^3), in a round bottomed flask fitted with a water-cooled cold-finger. Propylene oxide (0.36 cm^3, 5.20 mmol) was added to the mixture *via* syringe, and the mixture irradiated by means of two 300 W UV/Vis lamps for 48 h. The reaction was monitored by UV/Vis spectroscopy, showing no change either by UV/Vis or by ^1H NMR after 48 h.

The procedure was repeated with DMF as solvent but no further alterations. This also showed no change by UV/Vis or ^1H NMR after 48 h.

7.6. Experimental procedures for Chapter 6

Attempted synthesis of 1-{4-[4-(bis-carboxymethyl-amino)-6-hydroxy-[1,3,5]triazin-2-ylamino]-phenylazo}-benzene 3,5-carboxylic acid TM-α-cyclodextrin [2]rotaxane (64⊂TM-α-CD)

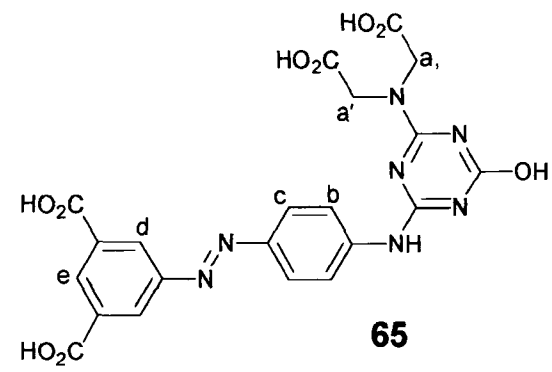

65

Cyanuric chloride (63 mg, 0.342 mmol) (**55**) was dissolved in hot acetone (3 cm^3) and re-precipitated as a fine suspension by addition of ice (1 cm^3). This solution was maintained at 0 - 5 °C. 1-(4-Amino-phenylazo)-benzene 3,5-carboxylic acid disodium salt **58** (70 mg, 0.170 mmol) and TM-α-cyclodextrin (0.625 g, 0.51 mmol) were dissolved in the minimum amount of water (~7 cm^3), and this solution added dropwise to the cyanuric chloride solution, maintaining the pH between 6.5 – 7.0 by careful monitoring with a pH meter. After all the dye / cyclodextrin solution had been added, the mixture was stirred for 2 h, allowing the pH to rise to 7.0 but maintaining the temperature at 0 °C throughout. After this time, the mixture was filtered through glass wool to remove any cyanuric acid formed by hydrolysis of the chloride. The temperature was allowed to rise to room temperature for the reaction of the 2nd chlorine. Iminodiacetic acid (25 mg, 0.188 mmol) was added, with maintenance of the pH at 7.0. The mixture was stirred for 15 h at 30 °C, after which time further iminodiacetic acid (30 mg, 0.225 mmol) was added, the pH raised to 9.0, and the temperature raised to 80 °C. Most of the solvent was removed to leave ~5 cm^3 of a concentrated basic solution, to which conc. HCl was added until

precipitation of a dark brown solid occurred. The precipitate was collected and washed with water by means of centrifugation, followed by redissolving in base and repeating the precipitation twice. The orange solid was then dried to afford the dumbbell **65** as a dark orange powder (13 mg, 15 %) which contained no cyclodextrin signals by ^{1}H NMR or mass spectrometry (supernatant did contain TM-α-CD by ^{1}H NMR but no rotaxane by ESI); mp >350 °C; λ_{max} (H_2O)/nm 371 (ε 9,800); ν_{max} (KBr)/cm^{-1} 3294 (H-bonding *HO*-C-NH-), 2930 (CO*OH*), 1714 (C=O), 1626, 1592, 1561, 1500 (all aryl CH), 921 (*m*-sub aryl), 845 (*p*-sub aryl), 761 (*m*-sub aryl); δ_H (500 MHz, D_2O/NaOH) 8.30 (1H, d, J_H 1.1, *e*), 8.25 (2H, d, J_H 1.1, *d*), 7.83 (2H, d, J_H 8.9, *b* or *c*), 7.7 (2H, d, J_H 8.9, *b* or *c*), 4.04 (1H, s, *a* or *a'*), 4.00 (1H, s, *a* or *a'*); δ_C (125 MHz, D_2O/NaOH) 178.8, 178.6, 174.7, 172.4, 167.6, 165.7, 152.7, 147.2, 144.0, 138.3, 131.2, 124.9, 124.4, 124.2, 120.4, 52.5, 52.0; *m/z* (ESI CV = -30 V) 510.2 ([M-H]$^-$, 45 %), 395.1 (25), 377.2 (65), 309.1 (35), 265.2 (75), 254.5 ([M-2H]$^{2-}$, 100).

Binding Titration of 1-(4-amino-phenylazo)-benzene 3,5-carboxylic acid disodium salt (58) *vs.* α-cyclodextrin

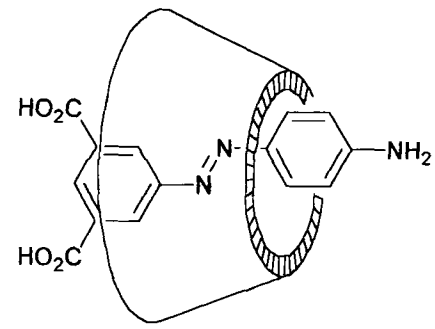

58

α-cyclodextrin

pH 7.0 buffer:

Sodium orthophosphate (Na_2HPO_4) aq. (82 cm^3, 0.2 M), citric acid aq. (18 cm^3, 0.1 M)

Solution A:

1-(4-Amino-phenylazo)-benzene 3,5-carboxylic acid disodium salt **58** (5.1 mg, strength 412 g/mol, 0.015 mmol) was dissolved in pH 7.0 buffer (exactly 25 cm^3), and filtered through glass wool to remove insoluble material. 2.5 cm^3 of this solution was dissolved in 50 cm^3 buffer to give Solution A (0.0248 mmol l^{-1}).

Solution B:

A solution of host was made by dissolving α-cyclodextrin (13.9 mg, 14.3 μmol) in 2.5 cm^3 of Solution A to give Solution B (8.88 mmol l^{-1}).

An initial UV spectrum of Solution A (2 cm^3) was recorded, and aliquots of Solution B were added, recording a UV spectrum at 298 K after each addition. This procedure was repeated three times and the data analysed using Specfit Global Analysis Software and Associate. Data can be found in Appendix 7.12.

Log *k* for 1:1 fit was found to be 3.64, 3.57 and 3.60 respectively. Log *k* for 2:1 fit was found to be 2.85, 0, and 2.35.

Binding Titration of 1-(4-amino-phenylazo)-benzene 3,5-carboxylic acid disodium salt (58) *vs.* TM-α-cyclodextrin

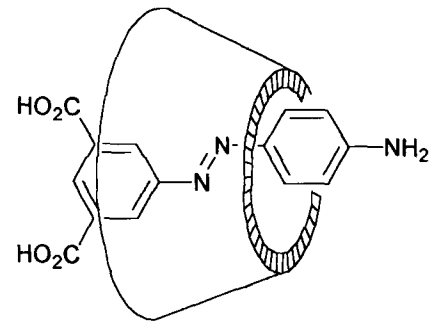

58

TM–α-cyclodextrin

Solution A:

1-(4-amino-phenylazo)-benzene 3,5-carboxylic acid disodium salt **58** (6.3 mg, strength 412 g/mol, 0.015 mmol) was dissolved in pH 7.0 buffer (exactly 25 cm^3), and filtered through glass wool to remove insoluble material. 2.5 cm^3 of this solution was dissolved in 50 cm^3 buffer to give Solution A (0.0153 mmol l^{-1}).

Solution B:

A solution of host was made by dissolving TM-α-cyclodextrin (11.0 mg, 8.98 μmol) in 2.5 cm^3 of Solution A to give Solution B (3.59 mmol l^{-1}).

An initial UV spectrum of Solution A (2 cm^3) was recorded, and aliquots of Solution B were added, recording a UV spectrum at 298 K after each addition. This procedure was repeated three times and the data analysed using Specfit Global Analysis Software and Associate. Data can be found in Appendix 7.13.

Log *k* for 1:1 fit was found to be 4.24, 4.43 and 4.10 respectively. The curve did not fit to a 2:1 model.

Refererences for Chapter 7

[1] M. Craig, DPhil Thesis, Dyson Perrins Laboratory, University of Oxford (Oxford), **2001**.

[2] A. Grahl, *Chem. Ber.* **1895**, *28*, 85.

[3] S. D. Taylor, C. L. Kotoris, A. N. Dinaut, M. J. Chen, *Tetrahedron* **1998**, *54*, 1691 - 1714.

[4] J. I. G. Cadogan, P. W. Inward, *J. Chem. Soc.* **1962**, 4170 - 4178.

[5] R. S. Mali, P. G. Jagtap, *Synth. Commun.* **1991**, 841.

[6] M. J. Hall, Part II Thesis, Dyson-Perrins Laboratory, University of Oxford (Oxford),**1999**.

[7] K. Nakashima, K. R. A. S. Sandanayake, S. Shinkai, *J. Chem. Soc., Chem. Commun.* **1994**, 1621.

[8] H. Suenaga, K. Nakashima, M. Mikami, H. Yamamoto, T. D. James, K. R. A. S. Sandanayake, S. Shinkai, *Recl.Trav. Chim. Pays-Bas* **1996**, *115*, 44 - 48.

[9] H. J. Barber, R. Slack, *J. Chem. Soc.* **1944**, 612 - 614.

[10] R. W. Murray, M. Singh, *Org. Synth.* **1997**, *74*, 91-100.

[11] M. Frohn, Z.-X. Shi, Y. Wang, *J. Org. Chem.* **1998**, *63*, 6425-6426.

[12] F. A. French, *Chem. Eng. News* **1966**, *44*, 48.

[13] G. A. Olson, *Chem. Eng. News* **1966**, *44*, 7.

[14] D. F. Eaton, in *C.R.C. Handbook of Organic Photochemistry, Vol. I* (Ed.: J. C. Scaiano), C.R.C. Press, Florida, **1989**, pp. 231 - 239.

[15] A. G. Szabo, in *Spectrophotometry and Spectrofluorimetry* (Ed.: M. G. Gore), Oxford University Press, Oxford, **2000**, pp. 33 - 60.

[16] S. R. Meech, D. Phillips, *J. Photochem.* **1983**, *23*, 193.

[17] W. H. Melhuish, *J. Phys. Chem.* **1961**, *87*, 83.

[18] J. T. Kunjappu, K. N. Rao, *Indian J. Chem. Sect. A* **1988**, *27A*, 1 - 3.

[19] M. T. Reetz, S. Sostman, *Tetrahedron* **2001**, *57*, 2515 - 2520.

Appendix 2.1. Crystal Data for Rotaxane 40⊂α-CD

Crystals of **40⊂α-CD** were grown over 2 weeks from aqueous solution in a 5 mm NMR tube by warming the lower region to 40 °C while the upper region was cooled to 20 °C. Data was obtained on a Siemens SMART CCD diffractometer and using a silicon 111 monochromator.The structure was solved using synchrotron X-rays at Daresbury Station 9.8. Data was obtained and solved by Professor W. Clegg of University of Newcastle and Daresbury Laboratory. Methods and programs are described elsewhere[1]. Refinement included application of SHELXL-97 and the SQUEEZE procedure (A. L. Spek, PLATON program, University of Utrecht, The Netherlands, 2000) to model diffuse electron density in two substantial voids per unit cell, presumably occupied by highly disordered solvent molecules. No H atoms were included, as they did not appear clearly in difference syntheses and those attached to oxygen atoms cannot be unambiguously placed from purely geometrical considerations. These limitations of the structural model and the weak diffraction due to disorder and crystal size and quality are reflected in the relatively high crystallographic residual factors, as is often found for cyclodextrin-containing materials. The full file (CCDC 156256) in .cif format can be found in the supplementary data of Stanier *et al.*[2].

Table A2.1. *Crystal data and structure refinement for* ***40⊂α-CD****, 4,4'-bis(phenyl-2,4-dicarboxylate)-(E)-1,2-diphenylethene, tetra ammonium salt, α-cyclodextrin [2]rotaxane.*

Empirical formula	C66 H80 O38
Formula weight	1481.30
Temperature (K)	160
Wavelength (Å)	0.69420 (Synchrotron radiation)
Crystal system	Monoclinic
Space group	*I*2 (alternative setting of *C*2)
Unit cell dimensions	a = 20.767(5) Å α = 90.00
	b = 13.960(3) Å β = 107.479(3)
	c = 28.085(7) Å γ = 90.00
Volume (Å^3)	77663(3)
Z	4
Absorption coefficient μ (mm^{-1})	0.105
F(000)	3120
Crystal size (mm^3)	0.10 × 0.15 × 0.20
Theta range for data collection(^{o})	1.74 to 22.50
Index ranges	-22 ≤ h 22, -15≤ k ≤15, -30 ≤ l ≤ 30
Observed reflections	9681
Unique reflections	10443
Goodness-of-fit on F	1.060
R indices (all data)	R1 = 0.164 wR2 = 0.394

[1] W. Clegg, M. R. J. Elsegood, S. J. Teat, C. Redshaw and V. C. Gibson, *J. Chem. Soc., Dalton Trans.* **1998**, 3037.

[2] C. A. Stanier, M. J. O'Connell, W. Clegg, H. L. Anderson, *Chem. Commun.* **2001**, 493 – 494.

Appendix 5.1; Derivation of Equations for Photoisomerisation Quantum Yields

Photostationary state analysis

If the process of isomerisation is assumed to be reversible

$$trans \leftrightarrows cis$$

we can represent the rate of change of each isomer with time in terms of the absorption

$$\frac{d[trans]}{dt} = -Iabs_{trans}.\Phi(trans \rightarrow cis) \qquad \textit{Equation A5.1.}$$

$$\frac{d[cis]}{dt} = -Iab_{cis}.\Phi(cis \rightarrow trans) \qquad \textit{Equation A5.2.}$$

$Iabs_{trans,cis}$ = incident light absorbed by the *trans* and *cis* isomers respectively.

$\Phi(trans \rightarrow cis)$, $\Phi(cis \rightarrow trans)$= quantum yield of *trans*→*cis* isomerisation and *cis*→*trans* isomerisation respectively.

At the photostationary state, no net change is occurring:

$$Iabs_{trans}.\Phi(trans \rightarrow cis) = Iabs_{cis}.\Phi(cis \rightarrow trans) \qquad \textit{Equation A5.3.}$$

We know from the Beer Lambert Law that

$$\frac{Io - Iabs}{Iabs} = 10^{-\varepsilon cl} \qquad \textit{Equation A5.4.}$$

Io = incident light
c = concentration of solution in mol l^{-1}
l = path length of cell in cm, =1 in all our experiments
ε = extinction coefficient

$$Iabs = Io\left(1 - 10^{-\varepsilon c}\right) \qquad \textit{Equation A5.5.}$$

$$Iabs = Io\left(1 - e^{-(\ln 10)\varepsilon c}\right)$$

By use of the approximation

$$1 - e^{-x} \approx x$$

where x is small

$$Iabs \approx Io \ln 10 \varepsilon c \qquad \textit{Equation A5.6.}$$

only where

$$Io \ln 10 \varepsilon c < 0.1$$

By applying this to the equation for the photostationary state we obtain:

$$\varepsilon_{trans}.\Phi(trans \rightarrow cis)[trans]_{SS} = \varepsilon_{cis}.\Phi(cis \rightarrow trans)[cis]_{SS} \qquad \textit{Equation A5.7.}$$

where $[trans]_{SS}$, $[cis]_{SS}$ = concentration of *trans* and *cis* isomers at the photostationary steady-state.

ε_{cis} and ε_{trans} are the extinction coefficients of the *cis* and *trans* isomers at the wavelength of irradiation.

which can be re-arranged to:

$$\frac{\Phi(trans \rightarrow cis)}{\Phi(cis \rightarrow trans)} = \frac{\varepsilon_{cis}}{\varepsilon_{trans}} \times \left(\frac{[cis]}{[trans]} \right)_{SS} \qquad \textit{Equation A5.8.}$$

We can define a fraction $fcis_F$, which is the fraction of *cis* isomer present in the photostationary state at the irradiation wavelength.

$$fcis_F = \left(\frac{[cis]}{[trans]+[cis]} \right)_{SS} \qquad \textit{Equation A5.9.}$$

This leads to the final expression:

$$\frac{\Phi(trans \rightarrow cis)}{\Phi(cis \rightarrow trans)} = \frac{\varepsilon_{cis}}{\varepsilon_{trans}} \times \frac{fcis_F}{(1 - fcis_F)} \qquad \textit{Equation A5.10.}$$

This simplified form of the equation only works if the assumption that $Io \ln 10 \varepsilon c < 0.1$ is true. This is because it becomes more difficult to account for the *cis* molecules which are shielded from the light by molecules of *trans*. For this reason, the experiment should be carried out under dilute conditions.

Initial rate analysis

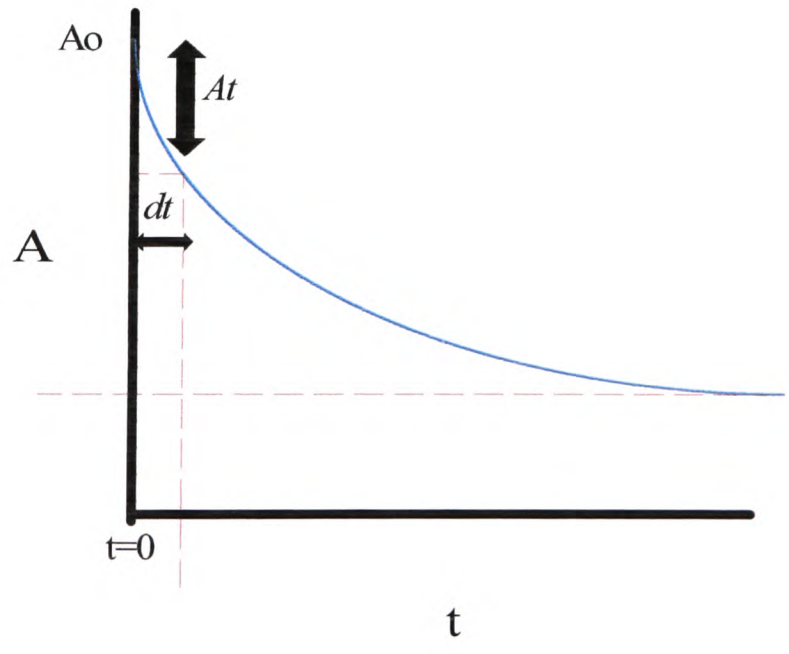

During a short time δt from the start of irradiation, when the bulk material is essentially all *trans*, the changes in the system can be described in terms of concentration or absorption:

$$\frac{d[trans]}{dt} = -Iabs_{trans} \cdot \phi_{t \rightarrow c} \qquad \textit{Equation A5.1.}$$

$$d[trans] = -Io \ln 10 Ao.\Phi(trans \rightarrow cis) \text{ where } Ao < 0.1$$

$$\delta[trans] = -Io \ln 10 Ao \Phi(trans \rightarrow cis)\delta t$$

$$\delta A = \delta[trans](\varepsilon_{trans} - \varepsilon_{cis}) \qquad \textbf{\textit{Equation A5.11.}}$$

combination of these two expressions gives us:

$$\delta A = Io \ln 10 Ao \Phi(trans \rightarrow cis)(\varepsilon_{cis} - \varepsilon_{trans})\delta t \qquad \textbf{\textit{Equation A5.12.}}$$

The mathematics may be simplified because the same intensity light was used for both dumbbell, rotaxane and stilbene irradiation experiments. This gives us:

$$\frac{(\partial A/\partial t)_{rotaxane}}{(\partial A/\partial t)_{dumbbell}} = \frac{\Phi(trans \rightarrow cis)_{rotaxane}}{\Phi(trans \rightarrow cis)_{dumbell}} \times \frac{A_{0\,rotaxane}}{A_{0\,dumbbell}} \times \frac{(\varepsilon_{cis} - \varepsilon_{trans})_{rotaxane}}{(\varepsilon_{cis} - \varepsilon_{trans})_{dumbbell}} \qquad \textbf{\textit{Equation A5.13.}}$$

or, in the form shown in the the text:

$$\frac{\Phi(trans \rightarrow cis)_{rotaxane}}{\Phi(trans \rightarrow cis)_{dumbell}} = \frac{(\partial A/\partial t)_{rotaxane}}{(\partial A/\partial t)_{dumbbell}} \times \frac{A_{0\,dumbbell}}{A_{0\,rotaxane}} \times \frac{(\varepsilon_{cis} - \varepsilon_{trans})_{dumbbell}}{(\varepsilon_{cis} - \varepsilon_{trans})_{rotaxane}}$$

Appendix 5.2; NOESY of the rotaxane 40⊂α-CD

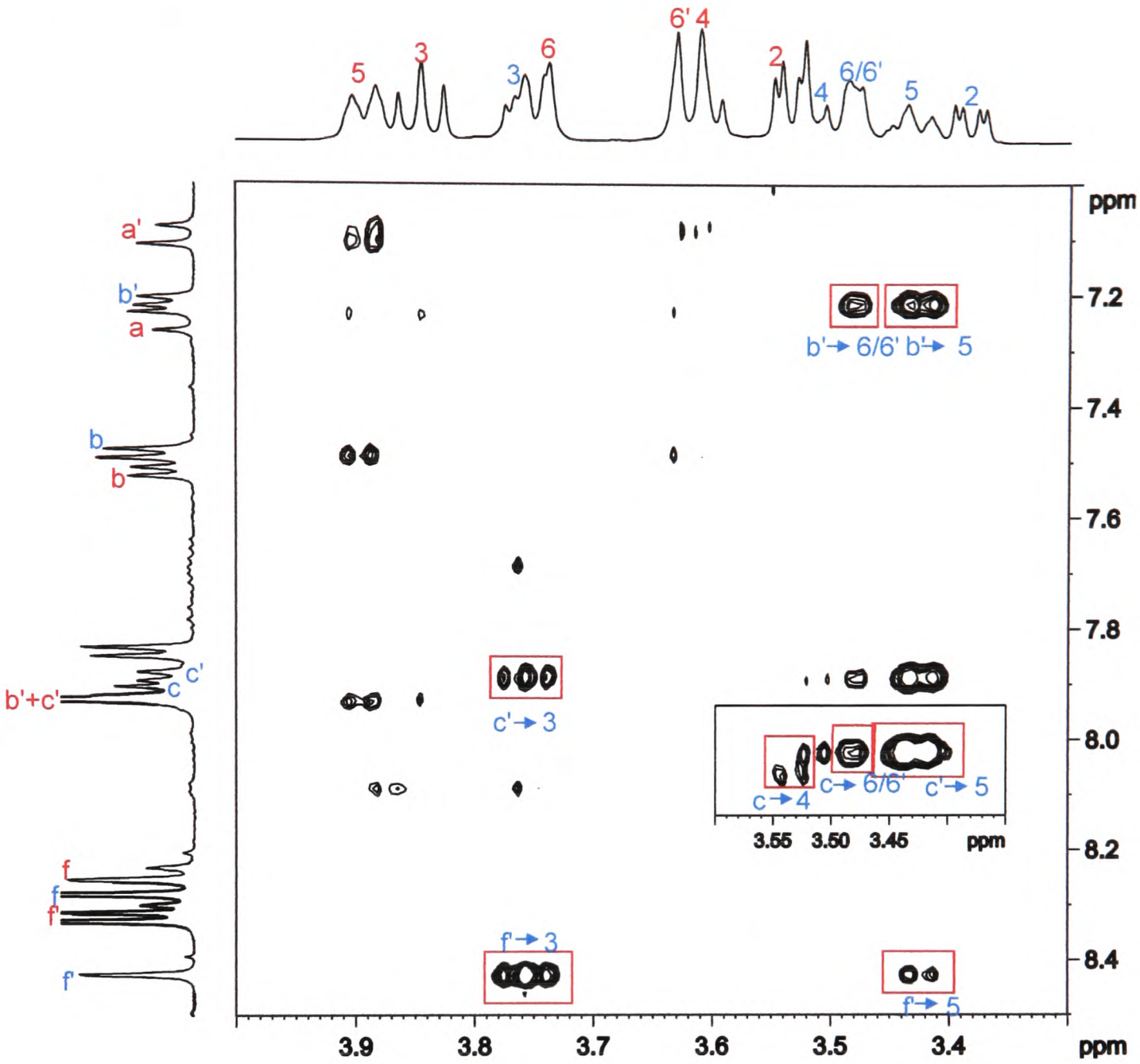

Figure A5.1. *NOESY of the cis/trans mixture of rotaxane* ***40⊂α-CD****, recorded in* D_2O *on a 500 MHz instrument. The assignments of the cis isomer* ***(Z)40⊂α-CD*** *are shown in blue, and the trans isomer in red.*

Appendix 7.1; Fluorescence Quantum Yields; example data

Compound	Excitation wavelength (nm)	Abs of solution (calc)	Integral of emission peak
Quinine bisulfate	317	0.00433477	2928000000
		0.01073030	5527000000
		0.01906450	8999000000
		0.02718570	11950000000
		0.03705000	15620000000
42	317	0.00602762	3547000000
		0.01197590	9137000000
		0.01784640	13460000000
		0.02364070	19580000000
		0.02672280	21350000000
42⊂β-**CD**	315	0.0116049180	12090000000
		0.0161410420	15850000000
		0.0206184460	19880000000
		0.0250382630	24410000000
		0.0294015970	28690000000
		0.0337095230	32330000000
		0.0379630910	36020000000
		0.0421633220	40100000000
		0.0463112140	43600000000
		0.0504077390	46510000000
		0.0544538460	50540000000
		0.0584304580	54460000000
		0.0623984800	58130000000
		0.0720616760	65390000000
		0.0814398230	75410000000
		0.0905453480	81180000000
		0.0993899710	88440000000
		0.1079847450	94060000000
42⊂α-**CD**	317	0.00335172	3697000000
		0.00665934	7100000000
		0.01314570	13320000000
		0.01946570	20030000000
		0.02562580	25970000000
39	340	0.01650550	5292000000
		0.03375260	8986000000
		0.04995130	12660000000
		0.06519440	16020000000
		0.07956390	18490000000
39⊂β-**CD**	331	0.00914295	5847000000
		0.01799090	11380000000
		0.02655800	16240000000
		0.03485750	20160000000

		0.04290150	25270000000
39⊂α-CD	341	0.005689205	4845000000
		0.0195879	16750000000
		0.0250214	21650000000
		0.03038510	25680000000
		0.03565802	29690000000
40	317	0.00391093	2904000000
		0.01157940	8311000000
		0.01905000	12230000000
		0.02633020	16610000000
		0.03342730	20300000000
40⊂α-CD	317	0.00480146	4659000000
		0.01421600	12480000000
		0.02338770	21050000000
		0.03232570	28670000000
		0.04103880	35900000000
41	317	0.00576589	4820000000
		0.01145590	8743000000
		0.01707150	13810000000
		0.02261420	18510000000
		0.03348650	28580000000
41⊂α-CD	317	0.00422709	4112000000
		0.00839855	7755000000
		0.01657890	15470000000
		0.02454960	22470000000
		0.03231840	29730000000

Appendix 7.2; Qualitative photoswitching of 40⊂α-CD

Time (mins)	Absorbance (a.u.) @ 347 nm	Absorbance @ Baseline (500 nm)	Difference in Absorbance	
0	1.0532	0.00064	1.05256	Irrad at 265
2	1.0469	0.00046	1.04644	
4	1.0442	0.0002	1.044	
6	1.0417	0.00005	1.04165	
8	1.0395	0	1.0395	
10	1.0389	0.00015	1.03875	
12	1.0384	0.00021	1.03819	
14	1.0379	0.00033	1.03757	
16	0.98199	-0.0001	0.98209	Irrad at 347
18	0.93137	-0.00003	0.9314	
20	0.87768	0.00008	0.8776	
22	0.84668	0.00018	0.8465	
24	0.82257	-0.00006	0.82263	
26	0.79635	0.00006	0.79629	
28	0.77614	-0.00011	0.77625	
30	0.76296	0.0002	0.76276	
32	0.74754	0.00012	0.74742	
34	0.71386	0.00002	0.71384	
36	0.72358	0	0.72358	
38	0.71349	0.00012	0.71337	
40	0.81747	0.00004	0.81743	Irrad at 265
42	0.8409	-0.00007	0.84097	
44	0.87925	0.00007	0.87918	
46	0.89985	0	0.89985	
48	0.92225	0.00015	0.9221	
50	0.94997	-0.00008	0.95005	
52	0.96727	0.00008	0.96719	
54	0.97754	0.00005	0.97749	
56	0.98699	-0.00005	0.98704	
58	0.99559	0.00004	0.99555	
60	1.0043	-0.00004	1.00434	
62	1.0089	0.00002	1.00888	
64	1.015	-0.00008	1.01508	
66	0.92758	0	0.92758	Irrad at 347
70	0.84292	0.0003	0.84262	
72	0.84222	-0.00021	0.84243	
74	0.79586	0.00005	0.79581	
76	0.78993	0.00035	0.78958	

78	0.76555	0.00035	0.7652	
80	0.75901	0.0004	0.75861	
82	0.74852	-0.00016	0.74868	
84	0.71977	0.00028	0.71949	
86	0.71993	-0.00036	0.72029	
88	0.7112	0.00018	0.71102	
90	0.70641	0.00026	0.70615	
92	0.70329	0.00032	0.70297	
94	0.79658	0.00018	0.7964	Irrad at 265
96	0.82274	0.00035	0.82239	
98	0.87129	0.0003	0.87099	
100	0.88364	-0.00039	0.88403	
102	0.91252	-0.00009	0.91261	
104	0.93365	0.00042	0.93323	
106	0.9436	0.0005	0.9431	
108	0.96643	0.00023	0.9662	
110	0.97033	0.0004	0.96993	
112	0.98317	0.00029	0.98288	
114	0.98836	0.00037	0.98799	
116	0.99879	0.00035	0.99844	
118	0.99996	0.00038	0.99958	
120	1.0019	0.0003	1.0016	
122	1.0056	0.00052	1.00508	
124	1.0069	0.00047	1.00643	
126	0.92294	0.00055	0.92239	Irrad at 347
128	0.87791	0.00043	0.87748	
130	0.82484	0.0001	0.82474	
132	0.80721	0.00045	0.80676	
134	0.79524	0.00038	0.79486	
136	0.77068	0.00041	0.77027	
138	0.73993	0.00048	0.73945	
140	0.7439	0.00048	0.74342	
142	0.73511	0.00021	0.7349	
144	0.725	-0.00028	0.72528	
146	0.71429	0.00036	0.71393	
148	0.69999	-0.00003	0.70002	
150	0.69884	0.00036	0.69848	
152	0.77078	0.00045	0.77033	Irrad at 265
154	0.82705	-0.00021	0.82726	
156	0.86349	0.00041	0.86308	
158	0.88216	0.00041	0.88175	
160	0.90983	0.00026	0.90957	

162	0.92922	0.00022	0.929	
164	0.93936	0.00029	0.93907	
166	0.9544	0.0004	0.954	
168	0.96457	0.00048	0.96409	
170	0.97465	0.0004	0.97425	
172	0.98293	0.00043	0.9825	
174	0.9898	-0.00016	0.98996	
176	0.992	0.00053	0.99147	
178	0.99392	0.00038	0.99354	
180	0.99583	0.00047	0.99536	
182	1.0011	0.0005	1.0006	
184	1.0007	0.00032	1.00038	
186	1.0034	-0.00027	1.00367	
188	1.0061	0.00048	1.00562	
190	0.9131	0.00019	0.91291	Irrad at 347
192	0.86373	0.00083	0.8629	
194	0.83719	0.00073	0.83646	
196	0.80486	0.0006	0.80426	
198	0.79947	0.00066	0.79881	
200	0.779	0.00093	0.77807	
202	0.76251	0.00069	0.76182	
204	0.73885	0.00064	0.73821	
206	0.71582	0.00074	0.71508	
208	0.72329	0.0012	0.72209	
210	0.71009	0.00078	0.70931	
212	0.69291	0.00051	0.6924	
214	0.70324	0.00089	0.70235	
216	0.69613	0.0011	0.69503	
218	0.69195	0.00095	0.691	
220	0.67736	0.00102	0.67634	

Appendix 7.3; Qualitative photoswitching of 40

Time (mins)	Absorbance (a.u.) @ 340 nm	Absorbance @ Baseline (500 nm)	Difference in Absorbance	
0	1.0865	-0.00755	1.09405	Irrad at 265
2	1.0753	-0.00781	1.08311	
4	1.0683	-0.00792	1.07622	
6	1.0626	-0.00803	1.07063	
8	1.0606	-0.00768	1.06828	
10	1.0576	-0.00796	1.06556	
12	1.0502	-0.00835	1.05855	
14	1.0464	-0.00801	1.05441	
16	0.93126	-0.00808	0.93934	Irrad at 340
18	0.81067	-0.00816	0.81883	
20	0.7391	-0.00826	0.74736	
22	0.70989	-0.00824	0.71813	
24	0.67643	-0.0083	0.68473	
26	0.6678	-0.00932	0.67712	
28	0.65283	-0.00969	0.66252	
30	0.64232	-0.00986	0.65218	Irrad at 265
32	0.74732	-0.00985	0.75717	
34	0.84604	-0.00961	0.85565	
36	0.87495	-0.00987	0.88482	
38	0.88624	-0.00979	0.89603	
40	0.88269	-0.00948	0.89217	
42	0.77668	-0.00972	0.7864	Irrad at 340
44	0.71898	-0.00992	0.7289	
46	0.67883	-0.00979	0.68862	
48	0.64998	-0.00997	0.65995	
50	0.62933	-0.00992	0.63925	
52	0.62865	-0.00982	0.63847	
54	0.69541	-0.01015	0.70556	Irrad at 265
56	0.7397	-0.01008	0.74978	
58	0.79252	-0.00994	0.80246	
60	0.84124	-0.01005	0.85129	
62	0.84919	-0.01005	0.85924	
64	0.88021	-0.01005	0.89026	
66	0.91098	-0.01007	0.92105	
68	0.91832	-0.01	0.92832	
70	0.92287	-0.01019	0.93306	
72	0.75153	-0.01091	0.76244	Irrad at 340
74	0.6837	-0.01073	0.69443	

76	0.6838	-0.01085	0.69465	
78	0.65546	-0.01073	0.66619	
80	0.61553	-0.01072	0.62625	
82	0.59608	-0.01075	0.60683	
84	0.59604	-0.01078	0.60682	
86	0.71137	-0.01057	0.72194	Irrad at 265
88	0.75015	-0.01065	0.7608	
90	0.78969	-0.01062	0.80031	
92	0.82637	-0.01062	0.83699	
94	0.82173	-0.0108	0.83253	
96	0.84172	-0.01082	0.85254	
98	0.8686	-0.01091	0.87951	
100	0.87679	-0.01118	0.88797	
102	0.8882	-0.01104	0.89924	
104	0.90522	-0.01101	0.91623	
106	0.90672	-0.01113	0.91785	
108	0.76984	-0.01111	0.78095	Irrad at 340
110	0.6806	-0.01111	0.69171	
112	0.62326	-0.01095	0.63421	
114	0.6012	-0.01092	0.61212	
116	0.59798	-0.01112	0.6091	
118	0.58288	-0.01093	0.59381	
120	0.57728	-0.01106	0.58834	
122	0.68003	-0.01104	0.69107	Irrad at 265
124	0.73282	-0.01109	0.74391	
126	0.7692	-0.01108	0.78028	
128	0.76862	-0.01127	0.77989	
130	0.80069	-0.01099	0.81168	
132	0.82207	-0.01165	0.83372	
134	0.83495	-0.01178	0.84673	
136	0.85499	-0.01165	0.86664	
138	0.87189	-0.01182	0.88371	
140	0.8724	-0.01261	0.88501	
142	0.87565	-0.01236	0.88801	
144	0.7373	-0.01282	0.75012	Irrad at 340
146	0.65809	-0.01303	0.67112	
148	0.60854	-0.01213	0.62067	
150	0.59848	-0.01212	0.6106	
152	0.58	-0.01235	0.59235	
154	0.56327	-0.0124	0.57567	
156	0.55346	-0.01245	0.56591	

Appendix 7.4; Qualitative photoswitching of 39

Cumulative time (mins)	Time (mins)	Absorbance (a.u.) @ 335.4 nm	Absorbance @ Baseline (500 nm)	Difference in Absorbance	
0	0	0.99694	0.02706	0.96988	Irrad at 335.4
1	1	0.90568	0.02677	0.87891	
2	2	0.91234	0.02682	0.88552	
4	4	0.89091	0.0267	0.86421	
6	6	0.89186	0.02686	0.865	
8	8	0.87304	0.02688	0.84616	
10	10	0.86657	0.02673	0.83984	
15	15	0.83568	0.02679	0.80889	
20	20	0.83393	0.0276	0.80633	
25	25	0.82302	0.0266	0.79642	
30	30	0.81698	0.02653	0.79045	
35	35	0.81618	0.02651	0.78967	
36	1	0.84193	0.02737	0.81456	Irrad at 265
38	3	0.85842	0.02685	0.83157	
40	5	0.86399	0.02673	0.83726	
42	7	0.87638	0.02653	0.84985	
44	9	0.88552	0.0269	0.85862	
49	14	0.91781	0.02685	0.89096	
54	19	0.92522	0.027	0.89822	
59	24	0.92062	0.02692	0.8937	
64	29	0.92217	0.02701	0.89516	
69	34	0.93156	0.02705	0.90451	
74	39	0.93301	0.02673	0.90628	
75	1	0.89814	0.02697	0.87117	Irrad at 335.4
76	2	0.90189	0.0264	0.87549	
78	4	0.87846	0.02647	0.85199	
80	6	0.85843	0.02656	0.83187	
85	11	0.83699	0.02646	0.81053	
90	16	0.83064	0.0246	0.80604	
95	21	0.8145	0.02629	0.78821	
100	26	0.81081	0.02637	0.78444	
105	31	0.80548	0.02675	0.77873	
110	36	0.79926	0.02681	0.77245	
115	41	0.7915	0.02679	0.76471	
116	1	0.81817	0.02686	0.79131	Irrad at 265
117	2	0.82309	0.02651	0.79658	
119	4	0.83986	0.02628	0.81358	

121	6	0.83985	0.02663	0.81322	
123	8	0.85558	0.02671	0.82887	
128	13	0.87407	0.02575	0.84832	
132	17	0.88339	0.02473	0.85866	
137	22	0.88585	0.02467	0.86118	
142	27	0.89565	0.02441	0.87124	
147	32	0.89668	0.02443	0.87225	
152	37	0.90008	0.02453	0.87555	
153	1	0.8813	0.02423	0.85707	Irrad at 335.4
154	2	0.86102	0.02434	0.83668	
156	4	0.8515	0.02431	0.82719	
158	6	0.82644	0.02442	0.80202	
160	8	0.82408	0.02437	0.79971	
165	13	0.80112	0.02429	0.77683	
170	18	0.7901	0.02429	0.76581	
175	23	0.77918	0.02441	0.75477	
180	28	0.77294	0.02428	0.74866	
185	33	0.77348	0.02414	0.74934	
186	1	0.78871	0.02408	0.76463	Irrad at 265
187	2	0.80619	0.02691	0.77928	
188	3	0.80435	0.02627	0.77808	
190	5	0.82362	0.02643	0.79719	
192	7	0.83062	0.0262	0.80442	
194	9	0.83806	0.02637	0.81169	
199	14	0.85491	0.02637	0.82854	
204	19	0.8668	0.02644	0.84036	
209	24	0.86942	0.02636	0.84306	
214	29	0.87309	0.02628	0.84681	
219	34	0.87563	0.02607	0.84956	
224	39	0.87563	0.02632	0.84931	
229	44	0.88	0.2631	0.6169	

Appendix 7.5; Qualitative photoswitching of 39⊂α-CD

Cumulative time (mins)	Time (mins)	Absorbance (a.u.) @ 337.3nm	Absorbance @ Baseline (500 nm)	Difference in Absorbance	
0	0	1.0487	0.00119	1.04751	Irrad at 337.3
1	1	1.0362	0.00124	1.03496	
2	2	1.0203	0.00134	1.01896	
4	4	1.023	0.00149	1.02151	
6	6	1.0253	0.00118	1.02412	
8	8	1.0223	0.00102	1.02128	
10	10	1.0233	0.00212	1.02118	
15	15	1.0252	0.00109	1.02411	
20	20	1.0189	0.00112	1.01778	
25	25	1.0218	0.00109	1.02071	
26	1	1.0296	0.00107	1.02853	Irrad at 265
28	3	1.0311	0.00103	1.03007	
30	5	1.0305	0.00108	1.02942	
32	7	1.0337	0.00104	1.03266	
37	12	1.039	0.00095	1.03805	
42	17	1.0373	0.00117	1.03613	
47	22	1.0393	0.00105	1.03825	
52	27	1.0408	0.00085	1.03995	
57	32	1.0392	0.001	1.0382	

Appendix 7.6; Qualitative photoswitching of 39⊂β-CD

Cumulative time (mins)	Time (mins)	Absorbance (a.u.) @ 328.9 nm	Absorbance @ Baseline (500 nm)	Difference in Absorbance	
0	0	1.176	0.00811	1.16789	Irrad at 328.9
2	2	1.1553	0.0066	1.1487	
4	4	1.1465	0.00639	1.14011	
6	6	1.1407	0.00795	1.13275	
8	8	1.1365	0.00622	1.13028	
10	10	1.1278	0.00604	1.12176	
15	15	1.1261	0.00686	1.11924	
20	20	1.122	0.00688	1.11512	
25	25	1.1251	0.00619	1.11891	
27	2	1.1279	0.0054	1.1225	Irrad at 265
29	4	1.1298	0.00565	1.12415	
31	6	1.135	0.00594	1.12906	
36	11	1.1328	0.00599	1.12681	
41	16	1.1457	0.00537	1.14033	
46	21	1.1429	0.00487	1.13803	
51	26	1.1465	0.00448	1.14202	
56	31	1.15	0.00411	1.14589	
61	36	1.1492	0.00448	1.14472	
62	1	1.1397	0.00433	1.13537	Irrad at 328.9
64	3	1.1301	0.00454	1.12556	
66	5	1.1296	0.00421	1.12539	
68	7	1.1282	0.00421	1.12399	
70	9	1.1257	0.00393	1.12177	
75	14	1.1249	0.00403	1.12087	
80	19	1.1188	0.00468	1.11412	
85	24	1.118	0.00421	1.11379	
90	29	1.1163	0.00426	1.11204	
95	34	1.1153	0.0042	1.1111	
100	39	1.1133	0.0042	1.1091	
102	2	1.1193	0.0042	1.1151	Irrad at 265
104	4	1.1336	0.00411	1.12949	
106	6	1.1238	0.00424	1.11956	
109	9	1.1278	0.00415	1.12365	
112	12	1.1309	0.00423	1.12667	
117	17	1.1344	0.00396	1.13044	
122	22	1.1321	0.00391	1.12819	

127	27	1.1374	0.00411	1.13329
132	32	1.1374	0.00421	1.13319
137	37	1.1397	0.00387	1.13583
142	42	1.1397	0.00394	1.13576

Appendix 7.7; Initial rate of switching experiments of dumbbell (40), rotaxane (40⊂α-CD) and *trans*-stilbene (49).

Dumbbell 40.

Time (mins)	Absorbance (a.u.) @ 325 nm	Abs at 340	Absorbance @ Baseline (500 nm)	Difference in 325Absorbance	Diff in 347 abs
0	0.1183	0.13238	0.00087	0.11743	0.13151
1	0.11364	0.12914	0.00003	0.11361	0.12911
2	0.11331	0.12821	0.00006	0.11325	0.12815
3	0.11143	0.12566	0.00023	0.1112	0.12543
4	0.11223	0.12624	0.00011	0.11212	0.12613
5	0.11115	0.12466	0.00001	0.11114	0.12465
6	0.10806	0.12052	0.00008	0.10798	0.12044
7	0.10823	0.12109	0.0001	0.10813	0.12099
8	0.10707	0.12019	0.00004	0.10703	0.12015
9	0.10812	0.1204	0.00031	0.10781	0.12009
10	0.10613	0.11829	0.00013	0.106	0.11816
11	0.10619	0.11792	0.00016	0.10603	0.11776
12	0.10543	0.11693	0.00016	0.10527	0.11677
13	0.10274	0.11396	0.00012	0.10262	0.11384
14	0.10304	0.11357	0.00025	0.10279	0.11332
15	0.10342	0.1141	0.00014	0.10328	0.11396
16	0.10282	0.11351	0.0002	0.10262	0.11331
17	0.10102	0.11102	0.00009	0.10093	0.11093
18	0.1015	0.112	0.00023	0.10127	0.01073
19	0.10106	0.11153	0.00027	0.10079	0.01074
20	0.10121	0.11054	0.00054	0.10067	0.00987
0	0.10943	0.1252	0.0003	0.10913	0.1249
1	0.10808	0.12273	0.00009	0.10799	0.12264
2	0.10664	0.12129	0.00011	0.10653	0.12118
3	0.10615	0.12	0.00001	0.10614	0.11999
4	0.10576	0.11912	0.00004	0.10572	0.11908
5	0.10455	0.11816	0.00004	0.10451	0.11812
6	0.10382	0.11678	-0.00001	0.10383	0.11679
7	0.10354	0.11584	-0.00003	0.10357	0.11587
8	0.10254	0.11497	-0.00019	0.10229	0.11516
9	0.1021	0.11394	-0.00013	0.10139	0.11407
10	0.10126	0.11347	-0.00011	0.10027	0.11358
11	0.10016	0.11178	-0.00011	0.1003	0.11189
12	0.10019	0.11157	0.00002	0.099269	0.11155
13	0.099289	0.11023	-0.00013	0.098569	0.11036
14	0.098439	0.10958	-0.00023	0.098669	0.10981

Rotaxane 40⊂α-CD.

Time (mins)	Absorbance (a.u.) @ 325 nm	Abs at 347	Absorbance @ Baseline (500 nm)	Difference in 325Absorbance	Diff in 347 abs
0	0.10528	0.12302	0.00083	0.10445	0.12219
1	0.10495	0.12239	0.00066	0.10429	0.12173
2	0.1043	0.12189	0.00075	0.10355	0.12114
3	0.10334	0.12118	0.00068	0.10266	0.1205
4	0.10419	0.12133	0.00073	0.10346	0.1206
5	0.10278	0.12	0.00033	0.10245	0.11967
6	0.10231	0.11951	0.0003	0.10201	0.11921
7	0.10179	0.11916	0.00044	0.10135	0.11872
8	0.10176	0.1189	0.00061	0.10115	0.11829
9	0.10087	0.11799	0.0003	0.10057	0.11769
10	0.10092	0.11793	0.00018	0.10074	0.11775
11	0.10023	0.11739	0.00006	0.10017	0.11733
12	0.10012	0.11683	0.00042	0.0997	0.11641
13	0.099759	0.11653	0.00052	0.099239	0.11601
14	0.099809	0.11666	0.00056	0.099249	0.1161
15	0.099629	0.11574	0.00015	0.099479	0.11559
				0	0
0	0.098529	0.12181	0.00004	0.098489	0.12177
1	0.097679	0.12035	-0.00022	0.097899	0.12057
2	0.095959	0.11845	-0.00046	0.096419	0.11891
3	0.096119	0.11866	-0.00047	0.096589	0.11913
4	0.095899	0.11806	-0.0004	0.096299	0.11846
5	0.094728	0.11604	-0.00069	0.095418	0.11673
6	0.094849	0.11715	-0.00043	0.095279	0.11758
7	0.094669	0.1166	-0.0006	0.095269	0.1172
8	0.094259	0.11631	-0.00055	0.094809	0.11686
9	0.093579	0.11567	-0.00055	0.094129	0.11622
10	0.093259	0.11498	-0.00062	0.093879	0.1156
11	0.092679	0.11456	-0.00079	0.093469	0.11535
12	0.092419	0.11472	-0.00067	0.093089	0.11539
13	0.092199	0.1137	-0.0005	0.092699	0.1142
14	0.091699	0.11349	-0.00058	0.092279	0.11407
15	0.091618	0.1133	-0.0007	0.092318	0.114
16	0.090459	0.11212	-0.00077	0.091229	0.11289
17	0.090379	0.11194	-0.00072	0.091099	0.11266

Trans-stilbene (49)

Time (mins)	Absorbance (a.u.) @ 325 nm	Abs at 308	Absorbance @ Baseline (500 nm)	Difference in 325Absorbance	diff in 308 abs
0	0.11009	0.23879	0.00295	0.10714	0.23584
1	0.10721	0.23386	0.00152	0.10569	0.23234
2	0.10494	0.23048	0.00013	0.10481	0.23035
3	0.10366	0.22824	0.00016	0.1035	0.22808
4	0.10345	0.22755	0.00069	0.10276	0.22686
5	0.101	0.22336	-0.00032	0.10132	0.22368
6	0.10147	0.22236	0.00037	0.1011	0.22199
7	0.097915	0.21858	-0.00069	0.098605	0.21927
8	0.096375	0.21638	-0.00086	0.097235	0.21724
9	0.095175	0.21282	-0.00105	0.096225	0.21387
10	0.094745	0.21353	-0.00096	0.095705	0.21449
11	0.094094	0.21203	-0.00105	0.095144	0.21308
0	0.12425	0.27435	-0.00198	0.12623	0.27633
1	0.12035	0.2696	-0.00201	0.12236	0.27161
2	0.12031	0.26857	-0.00204	0.12235	0.27061
3	0.11779	0.26567	-0.00184	0.11963	0.26751
4	0.11689	0.26207	-0.00192	0.11881	0.26399
5	0.11565	0.25941	-0.00195	0.1176	0.26136
6	0.11463	0.25735	-0.00201	0.11664	0.25936
7	0.11355	0.25533	-0.00197	0.11552	0.2573
8	0.11245	0.2529	-0.00184	0.11429	0.25474
9	0.11236	0.2512	-0.00191	0.11427	0.25311
10	0.11001	0.2479	-0.0019	0.11191	0.2498
11	0.10954	0.24582	-0.00176	0.1113	0.24758
12	0.10718	0.2426	-0.00179	0.10897	0.24439
13	0.10658	0.24214	-0.00187	0.10845	0.24401
14	0.10547	0.23995	-0.00186	0.10733	0.24181

Appendix 7.8; Aerobic photodegradation of rotaxane 40⊂a-CD.

Time (mins)	Absorbance (a.u.) @ 347 nm	Absorbance @ Baseline (500 nm)	Difference in Absorbance
0	1.2678	0.00099	1.26681
1	1.2479	0.00146	1.24644
2	1.2316	0.00171	1.22989
4	1.1896	0.00118	1.18842
8	1.1114	0.00109	1.11031
16	0.99993	0.00091	0.99902
32	0.92788	0.00078	0.9271
64	0.90625	0.00096	0.90529
128	0.86952	0.00097	0.86855
256	0.8193	0.00115	0.81815
430	0.77087	0.00112	0.76975
1340	0.63556	-0.00264	0.6382

Appendix 7.9; Anaerobic photodegradation of rotaxane 40⊂α-CD

Time (mins)	Absorbance (a.u.) @ 347 nm	Absorbance @ Baseline (500 nm)	Difference in Absorbance
0	0.98617	0.00215	0.98402
1	1.0341	0.0026	1.0315
4	0.91928	0.00268	0.9166
8	0.83855	0.00312	0.83543
16	0.76064	0.00344	0.7572
32	0.7026	0.00327	0.69933
64	0.68295	0.00331	0.67964
128	0.65664	0.00343	0.65321
256	0.62769	0.00309	0.6246
430	0.6036	0.00244	0.60116
1340	0.53913	0.00645	0.53268

Appendix 7.10; Aerobic photodegradation of dumbbell 40.

Time (mins)	Absorbance (a.u.) @ 340 nm	Absorbance @ Baseline (500 nm)	Difference in Absorbance
0	1.1476	-0.00231	1.14991
1	0.99737	-0.00213	0.9995
2	0.99297	-0.00201	0.99498
4	0.94893	-0.00208	0.95101
8	0.82735	-0.00201	0.82936
16	0.76295	-0.0019	0.76485
32	0.72711	-0.00212	0.72923
64	0.67271	-0.00196	0.67467
128	0.61807	-0.002	0.62007
256	0.53717	-0.00251	0.53968
430	0.43049	-0.00238	0.43287
1340	0.17298	0.00137	0.17161

Appendix 7.11. Anaerobic photodegradation of dumbbell 40

Time (mins)	Absorbance (a.u.) @ 340 nm	Absorbance @ Baseline (500 nm)	Difference in Absorbance
0	0.92636	0.00348	0.92288
1	0.80224	0.00295	0.79929
2	0.78251	0.00213	0.78038
4	0.72066	0.00253	0.71813
8	0.63505	0.00254	0.63251
16	0.63426	0.00241	0.63185
32	0.57278	0.00241	0.57037
64	0.52773	0.0031	0.52463
128	0.50735	0.00695	0.5004
256	0.43365	0.00933	0.42432
430	0.37982	0.00924	0.37058
1340	0.19091	0.00088	0.19003

Appendix 7.12; Titration data for 58 *vs.* α-CD

Aliquot added (ml)	Cumulative vol. added (ml)	Total Volume (ml)	Concentration of macrocycle (Mol)	Absorbance at 450 nm
0	0	2	0	0.12641
0.01	0.01	2.01	3.79E-05	0.19135
0.02	0.03	2.03	0.000112	0.17426
0.04	0.07	2.07	0.000257	0.15768
0.08	0.15	2.15	0.000531	0.14333
0.16	0.31	2.31	0.001021	0.13244
0.32	0.63	2.63	0.001823	0.12813
0.64	1.27	3.27	0.002955	0.12574
0.5	1.77	3.77	0.003572	0.20671

Aliquot added (ml)	Cumulative vol. added (ml)	Total Volume (ml)	Concentration of macrocycle (Mol)	Absorbance at 450 nm	Absorbance at 350 nm
0	0	2	0	0.20469	0.30592
0.01	0.01	2.01	3.79E-05	0.19399	0.30007
0.01	0.02	2.02	7.53E-05	0.18724	0.29637
0.02	0.04	2.04	0.000149	0.1754	0.28907
0.03	0.07	2.07	0.000257	0.16615	0.2855
0.05	0.12	2.12	0.000431	0.15309	0.27761
0.1	0.22	2.22	0.000754	0.1409	0.26795
0.1	0.32	2.32	0.00105	0.13578	0.26503
0.1	0.42	2.42	0.001321	0.13331	0.26412
0.1	0.52	2.52	0.00157	0.13152	0.26339
0.1	0.62	2.62	0.001801	0.12996	0.26334
0.1	0.72	2.72	0.002014	0.12996	0.26341
0.1	0.82	2.82	0.002213	0.12812	0.2627
0.1	0.92	2.92	0.002397	0.12828	0.26321
0.1	1.02	3.02	0.00257	0.12597	0.26108
0.1	1.12	3.12	0.002731	0.1287	0.26435
0.1	1.22	3.22	0.002883	0.12745	0.26367
0.2	1.42	3.42	0.003159	0.12668	0.26353
0.2	1.62	3.62	0.003405	0.12686	0.26462
0.2	1.82	3.82	0.003625	0.12619	0.2645

Aliquot added (ml)	Cumulative vol. added (ml)	Total Volume (ml)	Concentration of macrocycle (Mol)	Absorbance at 450 nm	Absorbance at 268 nm
0	0	2	0	0.19742	0.21657
0.01	0.01	2.01	4.42E-05	0.18628	0.22131
0.01	0.02	2.02	0.000088	0.17843	0.22797
0.02	0.04	2.04	0.000174	0.16636	0.2346
0.03	0.07	2.07	0.000301	0.15385	0.23931
0.05	0.12	2.12	0.000503	0.14346	0.24535
0.05	0.17	2.17	0.000696	0.13375	0.24677
0.1	0.27	2.27	0.001057	0.13142	0.25358
0.1	0.37	2.37	0.001388	0.12795	0.25708
0.1	0.47	2.47	0.001691	0.124	0.25945
0.1	0.57	2.57	0.001971	0.12521	0.26144
0.1	0.67	2.67	0.00223	0.124	0.26319
0.1	0.77	2.77	0.002471	0.12297	0.26316
0.2	0.97	2.97	0.002903	0.1229	0.26539
0.1	1.07	3.07	0.003098	0.12308	0.26602
0.1	1.17	3.17	0.00328	0.12173	0.26752
0.2	1.37	3.37	0.003613	0.12158	0.26896
0.2	1.57	3.57	0.003909	0.12137	0.27187
0.2	1.77	3.77	0.004173	0.12123	0.27315

Appendix 7.13; Titration data for 58 *vs.* TM-α-CD

Abs at 600 nm	Abs at 350 nm	Abs difference	Abs at 450 nm	Abs difference	Amt added	Total amt added	cumulative vol	Conc of macrocycle
0.04698	0.41426	0.36728	0.29994	0.25296	0	0	2	0
0.03929	0.3803	0.34101	0.28683	0.24754	0.01	0.01	2.01	1.79E-05
0.03818	0.36073	0.32255	0.28174	0.24356	0.01	0.02	2.02	3.55E-05
0.03058	0.33149	0.30091	0.26952	0.23894	0.02	0.04	2.04	7.04E-05
0.0153	0.29511	0.27981	0.24866	0.23336	0.04	0.08	2.08	0.000138
0.00374	0.26547	0.26173	0.23226	0.22852	0.08	0.16	2.16	0.000266
0.00274	0.25628	0.25354	0.22896	0.22622	0.16	0.32	2.32	0.000495
0.00781	0.25454	0.24673	0.22921	0.2214	0.2	0.52	2.52	0.000741
0.00931	0.25435	0.24504	0.22978	0.22047	0.2	0.72	2.72	0.00095
0.00541	0.25259	0.24718	0.23028	0.22487	0.4	1.12	3.12	0.001289
0.00843	0.25262	0.24419	0.23093	0.2225	0.4	1.52	3.52	0.00155

Abs at 600 nm	Abs at 350 nm	Abs difference	Abs at 450 nm	Abs difference	Amt added	Total amt added	cumulative vol	Conc of macrocycle
0.04354	0.40868	0.36514	0.29672	0.25318	0	0	2	0
0.03878	0.39472	0.35594	0.28956	0.25078	0.01	0.01	2.01	6.33E-06
0.03802	0.38676	0.34874	0.28708	0.24906	0.01	0.02	2.02	1.26E-05
0.02394	0.35809	0.33415	0.26983	0.24589	0.02	0.04	2.04	2.5E-05
0.01287	0.32079	0.30792	0.25206	0.23919	0.05	0.09	2.09	5.48E-05
0.00615	0.29829	0.29214	0.24069	0.23454	0.05	0.14	2.14	8.33E-05
0.00491	0.28001	0.2751	0.23461	0.2297	0.1	0.24	2.24	0.000136
0.00373	0.27336	0.26963	0.23314	0.22941	0.1	0.34	2.34	0.000185
0.00463	0.27063	0.266	0.23251	0.22788	0.1	0.44	2.44	0.00023
0.00429	0.26779	0.2635	0.23283	0.22854	0.1	0.54	2.54	0.000271
0.004	0.26651	0.26251	0.23218	0.22818	0.1	0.64	2.64	0.000309
0.00452	0.26791	0.26339	0.23153	0.22701	0.15	0.79	2.79	0.00036
0.00678	0.26799	0.26121	0.23247	0.22569	0.15	0.94	2.94	0.000407
0.00459	0.26934	0.26475	0.23209	0.2275	0.15	1.09	3.09	0.000449
0.00589	0.26803	0.26214	0.23184	0.22595	0.15	1.24	3.24	0.000487
0.00703	0.2665	0.25947	0.23258	0.22555	0.15	1.39	3.39	0.000522

Abs at 600 nm	Abs at 350 nm	Abs difference	Abs at 450 nm	Abs difference	Amt added	Total amt added	cumulative vol	Conc of macrocycle
0.04605	0.3452	0.29915	0.25675	0.2107	0	0	2	0
0.04454	0.33595	0.29141	0.25046	0.20592	0.01	0.01	2.01	7.47E-06
0.04072	0.32635	0.28563	0.24599	0.20527	0.01	0.02	2.02	1.49E-05
0.02646	0.29847	0.27201	0.22703	0.20057	0.02	0.04	2.04	2.95E-05
0.02075	0.28548	0.26473	0.21918	0.19843	0.02	0.06	2.06	4.37E-05
0.01031	0.25688	0.24657	0.20672	0.19641	0.05	0.11	2.11	7.83E-05
0.00369	0.24034	0.23665	0.19481	0.19112	0.05	0.16	2.16	0.000111
0.00465	0.22846	0.22381	0.19124	0.18659	0.1	0.26	2.26	0.000173
0.00345	0.22463	0.22118	0.19108	0.18763	0.1	0.36	2.36	0.000229
0.00457	0.22087	0.2163	0.19019	0.18562	0.1	0.46	2.46	0.000281
0.00497	0.21975	0.21478	0.19122	0.18625	0.1	0.56	2.56	0.000329
0.006	0.21812	0.21212	0.19019	0.18419	0.1	0.66	2.66	0.000373
0.00474	0.21744	0.2127	0.19077	0.18603	0.1	0.76	2.76	0.000414
0.00808	0.21745	0.20937	0.191	0.18292	0.1	0.86	2.86	0.000452
0.00735	0.2166	0.20925	0.19064	0.18329	0.1	0.96	2.96	0.000487
0.01818	0.22266	0.20448	0.19619	0.17801	0.1	1.06	3.06	0.00052